

Synchronous Rhythms in Coronary Heart Disease:
An Hypothesis Concerning the Anomalous
Nature of Some Common Ventricular
Arrhythmias - Investigation with
an Electronic Analogue

by

Alexander Maurice Solomons

Ph.D.



University of Edinburgh, 1974

ACKNOWLEDGEMENTS

My sincere thanks are due

to Dr. J. M. M. Neilson of the Department of Medical Physics, Edinburgh as my supervisor and teacher of science. I am particularly grateful for the opportunity of participating in the ongoing research at Edinburgh into cardiac arrhythmias. It has been a privilege to be able to use the very special equipment devised and built by Dr. Neilson whose foresight and skill made this and much other work possible.

to Dr. C. W. Vellani of the Department of Medicine, Edinburgh Royal Infirmary for many useful discussions of the physiological aspects of this study. It has been my good fortune to have worked alongside Dr. Vellani building upon the solid foundations which he has laid down. I also appreciate having access to much of his electrocardiographic material.

ABSTRACT

Various temporal aspects of arrhythmias containing frequent, single ventricular ectopic complexes are investigated using 24 hour tape recordings of ECGs. High-speed electronic analysis of records containing such complexes reveal characteristics difficult to reconcile with existing theories of the origin of these beats.

A general hypothesis (posed by Vellani and Neilson) is investigated in order to explain these arrhythmias. The general hypothesis assumes that a ventricular parasystolic pacemaker, although protected by entrance block, is not totally impervious to sinus excitation of the surrounding ventricular myocardium. The action of sinus excitation on the ectopic focus is graded with respect to its time of arrival in the ectopic pacemaker cycle and this may cause synchronization between the otherwise separate sinus and ectopic rhythms.

Divers experimental evidence and various reported arrhythmias are cited in support of the general hypothesis.

Four particular hypotheses, whereby the action of sinus excitation affects the ectopic rhythm, are formulated on the basis of existing knowledge of cardiac electrophysiology. These are simulated on purpose-built electronic analogues in order to investigate their arrhythmic properties which are compared to the characteristics seen earlier in ECGs. It is concluded that two of these particular hypotheses contain the most likely explanation of the ECGs investigated, and that these hypotheses may account for many arrhythmias containing single ventricular ectopic complexes.

It is pointed out that much of cardiac electrical activity, both normal and abnormal, may be viewed in terms of coupled relaxation oscillations, and that the proposed hypotheses emanate naturally from such thinking.

TABLE OF CONTENTS

Page	
i	Title Page
ii	Acknowledgements
iii	Abstract
iv	Table of Contents

1 INTRODUCTION

PART I

Some Inadequacies of Accepted Accounts of the Origin of Single Ventricular Ectopic Complexes

4	Chapter I	Theories of the Origin of Single Ventricular Ectopic Complexes
4		Origin of Cardiac Arrhythmias: Abnormal Impulse Formation and Conduction
5		The Type of Arrhythmia Investigated - Terminology
7		Theories of the Origin of Single V.E.Cs
8		i) Sinus-Locked Hypotheses
		ii) Pure Parasystole
9		Summary and Concluding Remarks
10	Chapter II	Temporal Characteristics Expected in the Electrocardiogram from the Accepted Theories
10		Preliminary: Outline of the Characteristics Investigated and of Their Anomalous Behaviour
10		i) Coupling Interval Histogram
11		ii) Scattergram of Coupling Interval versus the Preceding Sinus Period (X-Y plot)
12		iii) Histogram of Inter-Ectopic Numbers (N)
14		Derivation of the Expected Characteristics.
		a) Sinus-Locked Hypotheses
14		i) Coupling Interval Histogram
16		ii) Scattergram of CI versus Sinus Period
18		iii) Histogram of Inter-Ectopic Numbers (N)
21		b) Pure Parasystole
23		i) CI Histogram

Page	
27	ii) Scattergram of CI versus Sinus Period
30	iii) Histogram of Inter-Ectopic Numbers (N)
33	Concluding Remarks
34	Chapter III Methods of Measuring Temporal Characteristics in the Electrocardiogram
34	Measurement Procedure
37	Assessment of Errors and Some Further Details
39	i) Detection of Sinus Complexes and V.E.Cs
41	ii) Timing Errors
	iii) Effect of Errors on the Interpretation of the Data
43	Chapter IV The Anomalous Nature of Frequent, Single Ventricular Ectopic Complexes Observed in Patients in a Coronary Care Unit
43	Tests and Criteria for the Comparison of Expected to Observed Characteristics
44	i) Inspection of the Coupling Interval Histogram
45	ii) Inspection of the Scattergram of CI versus Sinus Period
47	iii) Inspection of the Histogram of Inter-Ectopic Numbers
48	The Anomalous Nature of Arrhythmias Containing Single V.E.Cs
	Selection and Presentation of Cases
64	Concluding Remarks

PART II

A General Hypothesis - "Pulling" of Ventricular Ectopic Pacemakers

66	Chapter V The Essential Attributes of a Mechanism Capable of Explaining these Arrhythmias - "Pulled" Parasystole versus Re-Entry with Wenkebach Conduction
67	A General Hypothesis Based on Parasystole
69	Hypotheses Based on Re-Entry - Difficulties
72	Concluding Remarks

Page

73	Chapter VI	Divers Reported Evidence Supporting the Hypothesis of a Pulling Mechanism
73		Experimental Evidence of Pulling in Mammalian Heart Fibres
76		Arrhythmias Indicative of Pulling in the Human Heart
		i) Some Aspects of Arrhythmias Showing Fixed and Variable Coupling of Single V.E.Cs
78		ii) Some Aspects of Clinical Parasystole
78		iii) Some Aspects of A-V Arrhythmias
79		The Successes of Models and Ideas Related to the Pulling Hypothesis
79		The Work of Vellani and Neilson on Ventricular Ectopic Rhythms
80		Concluding Remarks

PART III

Investigation of Some Possible
Electrophysiological Pulling Mechanisms

81	Chapter VII	A Preliminary Hypothesis of Electrotonic Pulling of Ventricular Pacemakers During Parasystole - Some Theoretical Behaviour of a Simplified Model - Investigation with an Electronic Analogue
81		The Preliminary Pulling Hypothesis: An Hypothesis Proposed by C. W. Vellani
83		Mathematical Analysis of Some Consequences of the Preliminary Pulling Hypothesis
84		i) Synchrony Under a Slowly Changing Sinus Rhythm - the Static Theory
91		ii) Synchrony Under a Rapidly Changing Sinus Rhythm - the Dynamic Theory
92		Testing of the Preliminary Hypothesis with an Electronic Analogue
		i) Description of the Simulator
94		ii) Mathematical Check of the Simulator's Performance
96		iii) Comparison of the Simulator's Performance with the Data Measured from ECGs

Page	
98	Chapter VIII Testing of Further Pulling Hypotheses with the Simulator
98	The Three Hypotheses and an Outline of Their Electronic Simulation
101	i) Phase 4 Cathodal Extension
102	ii) Phase 4 Anodal Shortening
103	iii) Action Potential Extension
103	A Quantitative Check on the Static Performance of the Three Simulators
104	Comparison of the Simulators' Performances with the Data Measured from ECGs
104	i) Phase 4 Cathodal Extension
105	ii) Phase 4 Anodal Shortening
106	iii) Action Potential Extension
106	Concluding Remarks

PART IV

Applicability of the General Hypothesis

109	Chapter IX	Conclusions and Further Suggestions
109		Particular Pulling Mechanisms
111		Suggestion for a Further Test of the General Hypothesis of Pulled Ventricular Parasystole
112		Some Reported Arrhythmias that may be Explained by the General Hypothesis of Pulled Ventricular Parasystole
113		Concluding Remarks
115	Appendix I	An Outline Proof that for Independent Pacemakers the CIs are, in the Long Term, Uniformly Distributed
117	Appendix II	Examination of the X-Y Plots
121	Appendix III	The Dynamic Theory - Behaviour Predicted by the Preliminary Pulling Hypothesis under a Rapidly Changing Sinus Rhythm in the Presence of Constant E, P and c

Page

126	Appendix IV	The Electronic Analogue of the Mechanism of the Preliminary Pulling Hypothesis
132	Appendix V	The Electronic Analogues of Post Cathodal Extension and Post Anodal Shortening
134	Appendix VI	The Electronic Analogue of Action Potential Extension
136	Appendix VII	A Quantitative Check of the Static Performance of the Electronic Simulators for Phase 4 Cathodal Extension and Action Potential Extension
140	REFERENCES	

SYNCHRONOUS RHYTHMS IN CORONARY HEART DISEASE:

AN HYPOTHESIS CONCERNING THE ANOMALOUS NATURE OF SOME COMMON VENTRICULAR ARRHYTHMIAS - INVESTIGATION WITH AN ELECTRONIC ANALOGUE

INTRODUCTION

The normal heart beat consists of a highly complex sequence of events which, when continually repeated, give rise to a most efficient pumping action. Each sequence is initiated by an electrical impulse formed within the sino-atrial node, an automatic pacemaker situated high in the right atrium. This initial excitation is communicated to the rest of the heart by an elaborate electrophysiological distribution system. Different parts of the system have their own characteristic conduction properties, and as a result excitation reaches the various parts of the heart at appropriately timed intervals. This variegated spread of excitation causes a sequence of mechanical contractions which result in non-turbulent, pulsatile blood-flow between the upper and lower chambers of the heart, and the surrounding vessels. Alterations in the electrical activity of even a few heart fibres may disrupt this smooth repetitive sequence and reduce the normal flow of blood. The danger associated with such arrhythmic activity depends on the extent to which blood-flow is reduced and varies a great deal from one arrhythmia to another. For example, if electrical excitation begins in the ventricles instead of in the usual sino-atrial node, then the pumping action of the resulting beat is not particularly effective. Such abnormal beats will be designated as ventricular ectopic complexes (V.E.Cs). On the other hand, the electrical (and hence mechanical) activity in fibrillation is totally fragmented and disorganised, hence if this arrhythmia occurs in the ventricles the residual blood-flow is reduced to virtually nothing. Ven-

tricular tachycardia represents a similarly dangerous arrhythmia in that there is insufficient time for proper filling of the ventricles between contractions, and again the result is poor blood-flow.

In coronary care units the most frequently seen disturbance of cardiac rhythm arises from non-consecutive, ventricular ectopic complexes (V.E.Cs)^{26 33 37 77}, yet of all arrhythmic phenomena the origin of these complexes is perhaps least understood^{66 84}. Furthermore, the prognosis associated with these arrhythmias is highly variable in the presence of coronary heart disease: frequent, non-consecutive V.E.Cs (more than 5 per minute) can continue harmlessly for many hours or days, or even longer - several cases have been observed where frequent, single V.E.Cs persisted over a period of years with the 'patient' leading an active life^{75 77 84}. On the other hand occasional V.E.Cs may suddenly develop into ventricular tachycardia or fibrillation via the 'R-on-T' phenomenon^{37 66 72 73 77}. Hence it is clear that the mere quantity of V.E.Cs is insufficient as a guide to their clinical significance. The present investigation was carried out in the belief that an understanding of the underlying arrhythmic mechanisms may help towards estimating prognosis, and may also help to put treatment of these arrhythmias, when necessary, on a firmer basis.

Recent work in this laboratory^{48 81} has shown the value of examining the quantitative behaviour of single V.E.Cs continuously over many hours. This is facilitated by automatic, high-speed analysis of pre-recorded ECGs. The present study continues this work and falls into four parts. Part I elucidates some of the inadequacies of accepted accounts of the origin of single V.E.Cs in diseased hearts - characteristics measured from many ECGs show anomalous behaviour when interpreted in terms of presently accepted theories. In Part II a general hypothesis (posed by Vellani and Neilson) is enunciated to explain this behaviour, and divers evidence is cited from the literature in support of it. The general hypothesis is concerned with the coupling

of sinus and ectopic rhythms in ventricular parasystole. In Part III, particular forms of the hypothesis are formulated on the basis of existing knowledge of cardiac electrophysiology. Purpose built electronic analogues are used to establish the characteristics of arrhythmias that would be expected from these mechanisms, and it is found that the behaviour of some of them compares favourably with the characteristics measured in Part I. Part IV uses this investigation in discussing the applicability of the general hypothesis. In addition, various arrhythmias reported in the literature are explained in terms of the hypothesis, and a further way of testing it is also suggested.

Finally, an alternative theory, not based on parasystole, is indicated as a possible explanation for some of the arrhythmias investigated. It is suggested that the implications of this second general hypothesis need to be established in order to determine which, if either, hypothesis is tenable as the mechanism generally responsible for single V.E.Cs. In conclusion it is pointed out that both hypotheses have an essential element in common, namely that they may be cast in terms of relaxation oscillators with incomplete coupling - the only difference between them lies in the 'configuration' of their respective oscillators. Similar reasoning has been applied to the A-V conduction system with considerable success^{3 53}, hence it may be that the notion of coupled relaxation oscillators will serve as a unifying concept for a great deal of both normal and abnormal cardiac electrophysiology.

PART I

Some Inadequacies of Accepted Accounts
of the Origin of Single Ventricular
Ectopic Complexes

CHAPTER I Theories of the Origin of Single
Ventricular Ectopic Complexes

Origin of Cardiac Arrhythmias: Abnormal Impulse Formation
and Conduction

The specialized fibres of the heart are primarily responsible for establishing and maintaining normal cardiac rhythm⁷⁷, hence abnormal formation and/or conduction of impulses within these automatic fibres is a primary source of arrhythmias^{4 25 61 77 83}. In addition, certain arrhythmic mechanisms may also involve 'ordinary' myocardial fibres, the archetype being continuous circus movement¹⁷ which need not necessarily use the specialized conduction system at all⁴⁰. The re-entry hypothesis of ventricular extrasystoles may also be regarded as a circus movement involving 'ordinary' myocardial fibres in that the ectopic impulse re-enters the Purkinje system via the myocardium, thus forming a closed loop of excitation.

The reduced conduction velocity or uni-directional block necessary for such re-entry may occur in either specialized or ordinary myocardial fibres, although there is good reason to believe that automatic fibres are the more susceptible to these conduction disturbances. Certain other abnormalities may also arise in both types of cardiac tissue, but some disorders of impulse formation clearly are peculiar to automatic fibres. Hence ectopic impulse formation responsible for cardiac arrhythmias may involve abnormalities in either or both kinds of fibre. This is true of some of the hypotheses frequently proposed to explain the type of arrhythmia investigated in this thesis. All these hypotheses are considered following a preliminary discussion of the type of

arrhythmia included in this study and the terminology used.

The Type of Arrhythmia Investigated - Terminology

The term "ventricular ectopic complex" (V.E.C.) is adopted to refer to any complex or 'wave' in the ECG which represents ventricular excitation initiated from within the ventricles. Here the 'ventricles' are taken as starting immediately after the bifurcation of the Bundle of His into the left and right bundle branches, hence A-V junctional beats are specifically excluded from the category 'V.E.C.'. In other words, for a V.E.C. to occur, the abnormality of impulse formation or conduction must lie at or beyond the distal end of the Bundle of His. This results in aberrant ventricular excitation and a complex of bizarre shape in the ECG. According to this definition, most heart block and certain types of A-V dissociation (i.e. enhanced automaticity within the A-V junction, junctional escape, and junctional parasystole) do not cause V.E.Cs.

On the other hand, ventricular extrasystoles, whatever their cause, come within the category of V.E.C. and at one time these two terms were synonymous. The term 'ventricular extrasystole' is insufficient here because it has taken on a connotation of a 'fixed coupling' between the ectopic ventricular complex and the immediately preceding sinus QRS complex^{61 66 77 83}. Apart from the fact that 'fixed coupling' is not a well defined entity (see Chapter II, p.15), such a restriction on the meaning of extrasystole assumes that the origin of all V.E.Cs has been established as either truly 'fixed coupled' (ventricular extrasystoles) or as 'freely' coupled (parasystoles). There has long been evidence to show that this is not the case and that arrhythmias with uniformly shaped V.E.Cs may show variation in the coupling interval too great to be regarded as 'fixed' but not great enough to be regarded as 'free' (i.e. parasystolic)^{29 34 44 59 77}. This behaviour may take the form of an apparently "spontaneous" movement between 'fixed' and variable coupling⁶⁶ (e.g. p.369)²⁹, but as Soloff rightly points out, such descriptions are unscientific and only serve to "mask a lack of knowledge"⁷⁵.

Indeed, the well known phenomenon of intermittent parasystole characterized by "constant coupling of the first ectopic to the preceding sinus beat"^{66 (p.297)} is reminiscent of such behaviour and remains unexplained^{66 (p.1025)}.

The aim of the first part of this thesis is to elucidate some inadequacies of presently accepted accounts of the origin of single V.E.Cs. An a priori acceptance of the dichotomy between 'fixed' and 'free' coupling (implied by the term 'extrasystole') would pre-empt the present investigation, and would also thwart any attempt at explaining these uniformly shaped complexes on the basis of a single theory. The term V.E.C. is adopted since it does not lay any restriction on the behaviour of the coupling interval and does not pre-judge the origin of these beats. This term will remain useful so long as it does not become associated with concepts more specific than those stated earlier in this section.

This thesis is only concerned with ECGs having episodes of frequent (i.e. more than 10 per minute), non-consecutive V.E.Cs of uniform shape. Between V.E.Cs only sinus rhythm is manifest. The coupling interval is measured from some specified point on the QRS complex preceding the V.E.C. to some specified point on the V.E.C., and this quantity is abbreviated to 'CI'. Measured in this way, the CI may not be equal to the coupling interval as taken from the start of the QRS complex to the start of the V.E.C. However, these measurements only differ by a constant providing the marker points remain unchanged. The reason for using this measurement is made clear in Chapter III.

Single V.E.Cs are thought to arise in a variety of ways^{4 25 61 66 77 83}. For convenience, these hypotheses are divided into two groups according to the theoretical behaviour of the CI, a procedure advocated by Scherf and Schott^{66 (p.361)}, Stock⁷⁷, Schamroth^{61 (p.139)}, and others.

In the first group of hypotheses the ectopic mechanism is driven or triggered by sinus excitation in the ventricles. Such sinus-locked V.E.Cs tend to be 'fixed-coupled' to the preceding sinus beat. For the second group the ectopic

mechanism is autonomous and self driven. The only member of this group is parasystole. These two types of hypothesized mechanisms will be designated as 'sinus-locked' and 'pure parasystole' respectively.

Theories of the Origin of Single V.E.Cs

i) Sinus-Locked Hypotheses

There are three sinus-locked hypotheses. The first depends on the re-entry phenomenon or circus movement^{4 17 61 66 77 83} in which sinus excitation effectively gives rise to a double beat, the second of which is a V.E.C. If the conduction velocity through a ventricular fibre is abnormally low, then sinus excitation may not emerge from its distal portion until after surrounding fibres have recovered. These fibres are then re-excited in a retrograde direction. This second excitation may in turn spread to the whole of the ventricles thereby forming a V.E.C. Alternatively, re-entry may arise from uni-directional block in a ventricular fibre so that it is activated from its distal end in a retrograde direction. Again, a double beat is seen so long as the re-entrant impulse emerges after the surrounding fibres have recovered from the initial sinus excitation - if the re-entrant path is not sufficiently long to allow time for these fibres to recover, then the re-entrant impulse meets refractory tissue and is not propagated. The constancy of the CI associated with this hypothesis is a reflection of the constancy of the time taken for the re-entrant impulse to enter, traverse, and emerge from its pathway.

The second sinus-locked hypothesis involves focal enhancement and impulse formation within an ectopic centre. This could depend on several mechanisms^{4 25 61 66 77 83} which again result in sinus excitation initiating a double beat. Perhaps the most obvious mechanism is that of after-potentials following sinus excitation of the ectopic fibre. The after-potential, which is 'fixed' to the sinus excitation, may become supra-threshold and thereby initiate a V.E.C.²⁵ Other

mechanisms cited as possibly contributing to focal enhancement and impulse formation include the Wedensky effect⁸ and Wedensky facilitation¹⁵, and oscillatory behaviour^{4 5 25 61 66 77 83}.

Finally, in the third hypothesis of sinus-locked V.E.Cs the ectopic site initiates an impulse of its own volition, either as a consequence of slow sinus rhythm (giving rise to an escape beat) or as a result of enhanced automaticity within the ventricles. In both cases the ventricular ectopic site is re-set during every QRS complex, hence the ectopic rhythm is locked to the sinus rhythm. If a V.E.C. is to appear it must do so before a sinus excitation can re-set the ectopic site. The CI is purely a measure of the automaticity of the ectopic site.

ii) Pure Parasystole

In parasystole the ectopic focus is protected from sinus excitation by entrance block and so proceeds with its own automaticity^{4 9 25 61 66 77 83 84}. From time to time the fibres protecting this ectopic pacemaker allow impulses to emanate from it and initiate a V.E.C. The break down of entrance block is considered in Part IV.

In this thesis the term 'pure parasystole' is used to refer to the form of the hypothesis where the sinus and ectopic pacemakers have truly independent rhythms. This concept is elucidated in the next chapter, but for the moment it suffices to say that the rhythms are not the same. Pure parasystole arises when there is no inter-action between the two competing rhythms, and it seems that this condition is generally implied by most authors⁸⁴: the three criteria universally adopted to identify parasystole assume independence of the rhythms. These are^{9 25 44 61 66 77}: varying CIs; a simple arithmetical relationship between the size of inter-ectopic intervals such that they all are multiples of the basic ectopic period; the possible presence of fusion beats which show the sinus and ectopic impulses invading the myocardium nearly simultaneously from different points. Although not always stated explicitly, it is clearly implied that the

basic ectopic period must not be the same as the sinus period if the V.E.Cs are to be regarded as parasystolic. It is interesting to note that the parasystolic rhythm may be a good deal faster than the sinus rhythm^{56 64} even though the automaticity of specialized ventricular fibres is normally lower than that of the S-A node.

Summary and Concluding Remarks

The term 'V.E.C.' is adopted throughout this thesis in preference to the term 'extrasystole' since the former does not prejudge the issue of fixation of the CI. Theories of the origin of single V.E.Cs are considered under the headings of sinus-locked hypotheses and of pure parasystole. The mechanisms discussed involving abnormal impulse conduction have all been demonstrated under plausible physiological or pathological conditions. This is not yet so of after-potentials and oscillatory behaviour although evidence is mounting in support of these mechanisms⁴.

Temporal characteristics expected in the ECG from the two types of hypothesis are derived in the next chapter, and this forms a basis for examining data taken from ECGs. In Chapter IV cases are presented which show combinations of characteristics that are mutually incompatible on the basis of these hypotheses, and they also show characteristics not expected from either hypothesis. In Part II an hypothesis is formulated to explain the observed behaviour, and this is tested in Part III.

Fig.II,1: Diagrammatic ECG (not to scale) showing sinus beats, ventricular ectopic complexes (V.E.Cs), coupling intervals (CIs), preceding sinus periods (S_{R-R}), and inter-ectopic numbers (N's).

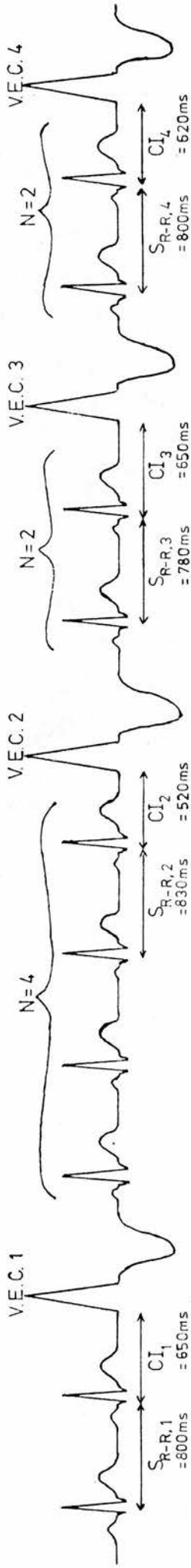


Fig.II,2: CI histogram for Fig.II,1:

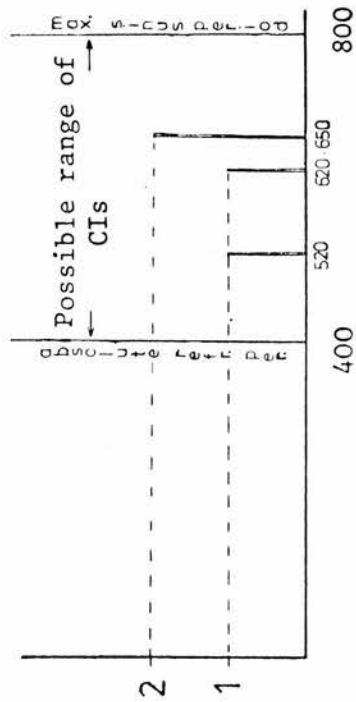


Fig.II,3: X-Y plot (S_{R-R} vs CI) for Fig.II,1.

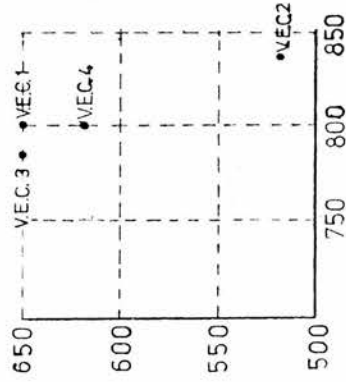
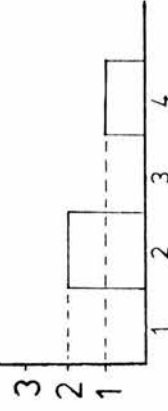


Fig.II,4: Inter-Ectopic Number histogram for Fig.II,1.



CHAPTER II Temporal Characteristics Expected
in the Electrocardiogram from the
Accepted Theories

Preliminary: Outline of the Characteristics Investigated
and of Their Anomalous Behaviour

Part of the aim of this work is to indicate the inadequacy of accepted accounts of the origin of single V.E.Cs in diseased hearts. To do this ECGs are inspected from three points of view - the resulting data are shown to be difficult to reconcile with most theories currently proposed to explain the type of ECG under consideration. The three measurements taken from each ECG and an indication of the results expected for the sinus-locked theories and pure parasystole are as follows:

i) Coupling Interval Histogram

This is obtained from the ECG (e.g. Fig.II,1) by measuring each CI as it arises and accumulating a record of the number of occurrences of each value of CI. Hence the CI histogram for Fig.II,1 is as shown in Fig.II,2.

The CI can not be less than the absolute (effective) refractory period of the ventricles since throughout this time the ventricles can not respond to ectopic excitation ^{77(p.12)}₂₃. Hence the minimum possible CI is dependent on various factors:

- a) The site of origin of the V.E.C. Different fibres of the ventricles have different recovery times depending on the duration of their action potentials ⁸³ ⁷⁹. A theoretical estimate of the minimum possible CI would require knowledge of the action potential durations in the vicinity of the ectopic site. Only then could it be decided if a given early ectopic impulse could propagate and excite the myocardium. The matter is further complicated by the effects of decremental conduction

through partially recovered fibres^{23 27} and of the supernormal phase of conduction^{22 18 77(p.28)}. Watanabe⁸⁴ investigated this situation experimentally by plotting the minimum CI against the QT interval for certain cases of parasystole. He found the minimum CI was consistently equal to the QT interval provided there was no 'U' wave present. Cases having a 'U' wave showed a similar remarkable relationship between the minimum CI and the 'QU' interval. Whether or not these findings are generally applicable it is fair to say that there exists some moment early in diastole after which the ventricles are fully responsive^{77(p.13)}. The minimum possible CI has a value somewhat less than this total refractory period, and it can be considerably less than the QT interval for 'R-on-T' ectopics^{74 7}.

- b) The heart rate also affects the ventricular refractory period^{77(p.13) 38} and thereby affects the minimum possible CI.

The CI can not be greater than the sinus period because if an ectopic impulse were to arrive after the onset of the QRS complex (so that the CI would be greater than the sinus period) it will find the ventricles refractory⁷⁷ and will not be seen. In fact the largest CIs correspond to fusion beats and arise when sinus and ectopic impulses invade separate parts of the myocardium simultaneously⁷⁷.

For the sinus-locked hypotheses the CI histogram has a peak at the value of fixation of the CI and is zero elsewhere. The opposite is true of pure parasystole where any value of CI between the ventricular refractory period and the sinus period is possible. These expected characteristics are elaborated later in this chapter.

- ii) Scattergram of Coupling Interval versus the Preceding Sinus Period (X-Y plot)

This is obtained by measuring each CI as it arises and also the immediately preceding sinus period (S_{R-R}). For each V.E.C. the CI (ordinate) is plotted against the sinus period (abscissa) as in Fig.II,3.

Highly patterned X-Y plots (like those in Chapter IV) are not expected from any arrhythmia containing non-consecutive V.E.Cs. The reasons for this, elaborated later in this chapter, depend on the assumption that there should be no "systematic" variation of the CI with the sinus period for either the sinus-locked or pure parasystolic theories.

iii) Histogram of Inter-Ectopic Numbers (N)

The term 'inter-ectopic number', N, is used to designate the number of sinus beats between successive V.E.Cs. Clearly N can take any integer value from 0, in which case there are no sinus beats between ectopics, upwards. Only N's lying between 1 and 40, i.e. $1 \leq N \leq 40$, are considered. The N histogram is obtained by accumulating a record of the number of occurrences of each N. Hence the N histogram for Fig.II,1 is as shown in Fig.II,4.

If there is a tendency for certain N's to arise in favour of other values of N, then these favoured values show up as peaks in the histogram. It shall be shown that generally speaking (but with exceptions) pure parasystole is characterized by high peaks separated by low troughs whereas the sinus-locked hypotheses should always be characterized by a "smooth" distribution in the N histogram.

These three measurements were chosen for the following reasons:

- a) They form a wide ranging description of an arrhythmia and hence between them they should constitute a correspondingly sensitive tool for detecting discrepancies between expected characteristics, based on theory, and real ECGs.
- b) They appeared to be amenable to statistical analysis. This would enhance their sensitivity as a detector of discrepancies between theoretical and real ECGs.
- c) They reveal interesting, unexpected behaviour that at least requires an explanation.

There is a fourth quantity, vis. inter-ectopic periods,

which was not investigated as it had already been thoroughly researched by C.W. Vellani⁸¹. It is included in the listing below for the sake of completeness. The following description of the expected characteristics of V.E.Cs (Table II,1) is subsequently justified on the basis of the two presently accepted theories relating to the origin of V.E.Cs. Variants of these two theories are considered later in this thesis.

Table II,1: An Outline Description of the Expected Characteristics of Arrhythmias Containing Single Ventricular Ectopic Complexes.

	Sinus-Locked Hypotheses	Pure Parasystole
a) CI Histogram:	Peak or peaks in histogram with zero surroundings.	No statistically significant peaks in the histogram.
b) CI versus S_{R-R} Scatter-gram:	No systematic variation of CI with sinus period - hence no statistically significant pattern in the X-Y plot other than a horizontal line or band representing fixation of the CI.	No systematic variation of CI with sinus period - no statistically significant pattern in the X-Y plot. (Similar to sinus-locked arrhythmias.)
c) Inter-Ectopic Number Histogram:	"Random" N's - i.e. if most frequent N is '5' then also expect reasonable numbers of '3's, '4's, '6's, '7's etc. (tailing off) resulting in a "smooth" unpatterned distribution.	Two possibilities: i) A marked propensity for certain N's to the possible exclusion of all others resulting in a highly "discontinuous", patterned distribution. ii) A "smooth", unpatterned distribution. (Same as for sinus-locked arrhythmias.)
d) Inter-Ectopic Period:	Inter-ectopic periods = multiples of the SINUS period.	Inter-ectopic periods = multiples of the ECTOPIC pacemaker period (different to the sinus period).

In Chapter XV ECGs are presented each having:

- a) peaks in the CI histogram indicative of a sinus-locked arrhythmia; b) patterns in the X-Y plot incompatible with

both sinus-locked arrhythmias and pure parasystole; c) multiple peaks in the N histogram indicative of parasystole. It will be argued that the simultaneous presence of these characteristics within each ECG is inconsistent with both sinus-locked and pure parasystolic mechanisms and that as a result there is need of a further hypothesis to explain these arrhythmias. The strength of this argument depends on the degree of incompatibility between observed characteristics and particular theoretical mechanisms. In order to assess this incompatibility the characteristics expected from the sinus-locked and pure parasystolic hypotheses are elucidated in some detail in the next section. In Chapter IV criteria are devised for comparing observed results to these theoretical characteristics.

Only relatively simple forms of sinus-locked mechanisms are considered here. The inadequacies of some of the variants proposed in the literature are discussed later in this thesis.

Derivation of the Expected Characteristics

Sinus-Locked Hypotheses

Focal enhancement, re-entry activity, and circus movement (macroscopic re-entry) can give rise to non-consecutive, sinus-locked V.E.Cs. In addition enhanced automaticity within specialized fibres of the ventricles (or alternatively ventricular escape) can also cause sinus-locked ectopic complexes. As discussed in Chapter I these are the only mechanisms postulated as capable of initiating non-consecutive sinus-locked V.E.Cs. Such complexes must be either actively initiated by (focal, re-entrant, or circus activity) or locked to (enhanced automaticity, or ventricular escape) the preceding sinus beat. The expected characteristics of sinus-locked V.E.Cs developed here apply equally to all these mechanisms.

i) Coupling Interval Histogram

For a sinus-locked arrhythmia each ectopic complex has nearly the same CI. As the histogram accumulates each

Fig.II,5: CI histogram for a case showing highly fixed coupling.
Accumulation 180 V.E.Cs.

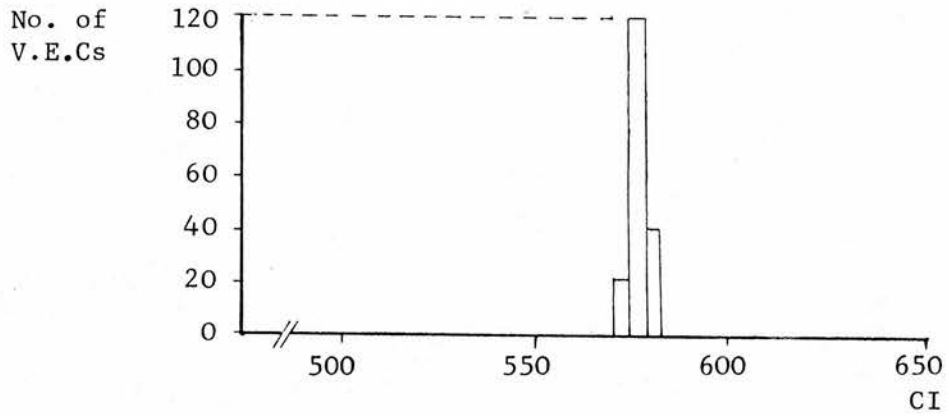
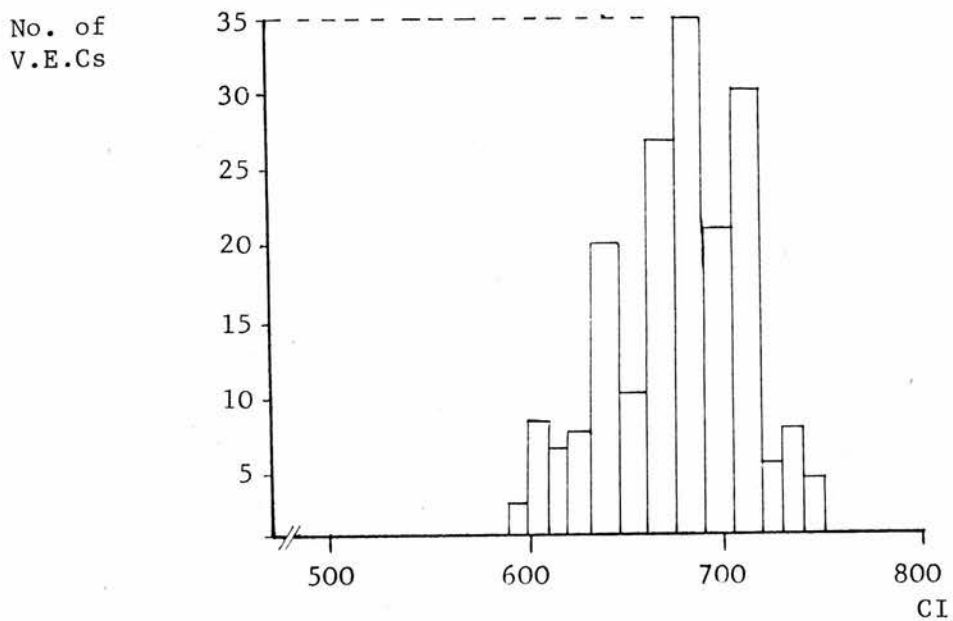


Fig.II,6: CI histogram for a loosely coupled case. Can this be regarded as sinus-locked? (see text)
Accumulation 180 V.E.Cs.



ectopic complex contributes one count within a restricted range of CIs. Two such histograms are presented in Figs. II,5 and II,6. Clearly Fig. II,5 must be regarded as truly fixed-coupled and indicative of a sinus locking mechanism, but what of Fig. II,6? How much variation in the CI is permissible before rejecting the hypothesis of sinus locking? Some workers obviously consider this an open and difficult question and so pass no opinion^{77 66}. Others range in their opinion from about 60ms⁹ or 80ms⁶¹ to 120ms⁷⁸ or even 180ms³⁴, although in Chapter V it shall be suggested that this last case is not sinus-locked. There does not appear to be any significant account of the subject published in the last twenty-five years. All that may be said of the expectations of CI histograms for the sinus-locked hypotheses is that they show fixation of the CI which may vary by as much as 200ms or perhaps even more. In other words there must be some tendency towards peaked histograms but it is impossible to say anything about the expected properties of these peaks. This statement also applies to cases having more than one source of sinus-locked ectopic complexes, for example two separate re-entry pathways. If these should happen to have similar conduction times then the two peaks merge and appear as one. No statistical test could resolve these peaks as their individual statistical behaviour is entirely unknown for the reasons stated above. Hence the expected properties of a doubly peaked histogram are even more obscure than the expectations of one with a single peak, and both of these are further obscured by the fact that they are mutually indistinguishable.

To sum up, sharply peaked CI histograms are indicative of a sinus-locking mechanism; however the diversity of modern opinion demands the acceptance of the possibility that wide peaks may arise in the CI histogram from such mechanisms.

Fig.II,7: X-Y plot for a truly "fixed-coupled" arrhythmia - the CI remains constant regardless of changes in the sinus period (S_{R-R}).

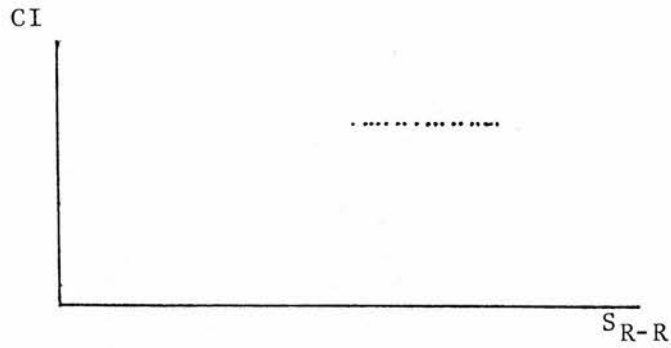
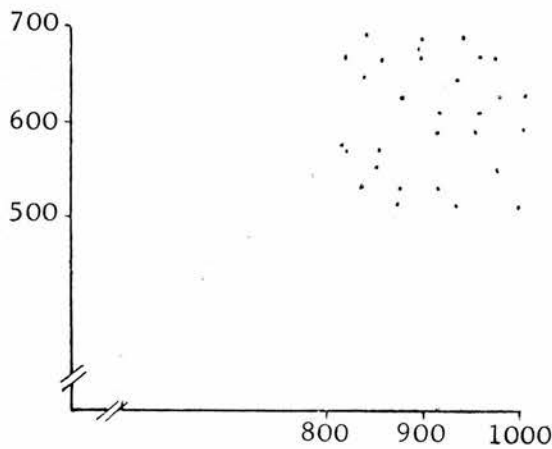
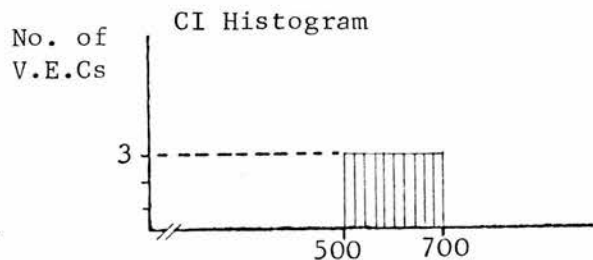
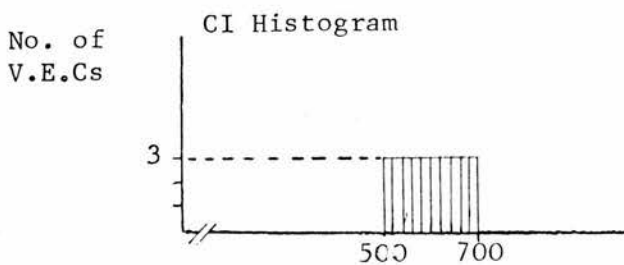
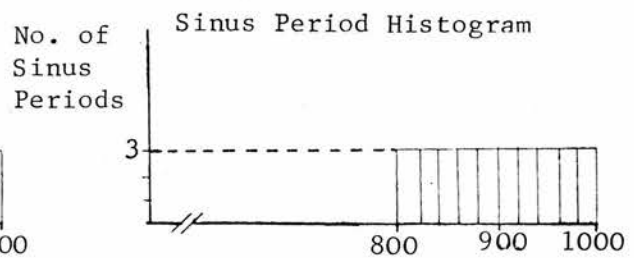
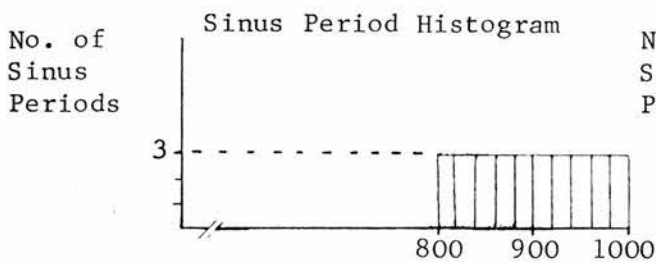
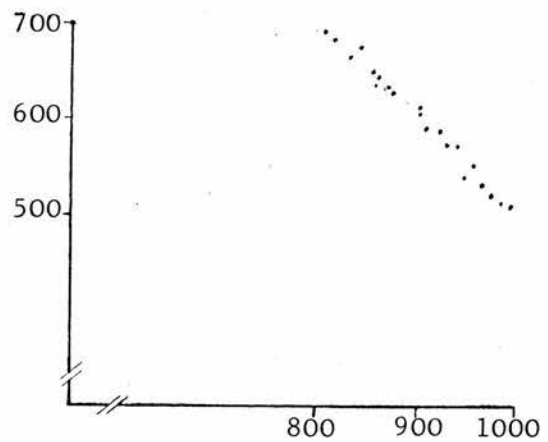


Fig.II,8: Hypothetical cases having the same CI and sinus period histograms but very different X-Y plots.

a.) X-Y plot shows no relationship between the sinus period (S_{R-R}) and the CI.



b.) X-Y plot shows a strong relationship between the sinus period (S_{R-R}) and the CI.



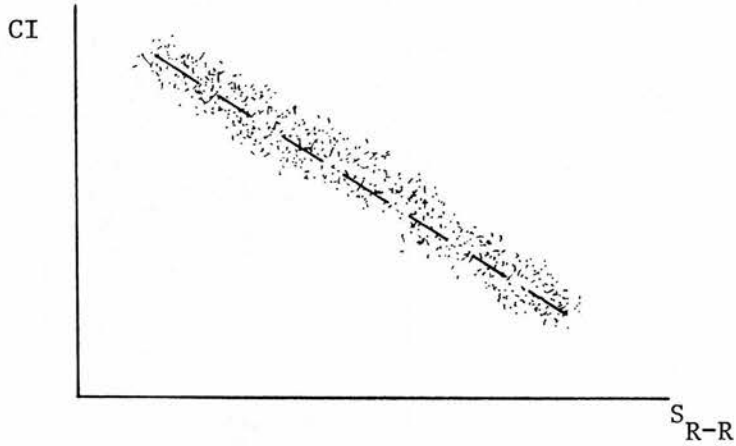
ii) Scattergram of CI versus Sinus Period

Like the CI histogram the type of X-Y plot expected from the sinus-locked hypotheses is partly dependent on the personal convictions of the observer. For a truly fixed-coupled arrhythmia the X-Y plot would appear as in Fig.II,7 where the CI remains absolutely constant. In practice the CI must be expected to vary somewhat. The question is how much this variation is related to changes in the sinus rhythm. Fig.II,8 shows two possible extremes both having the same variation in their CIs as shown by the accompanying histograms. (Note that the CI and sinus period histograms together contain less information than the X-Y plot alone. This is not a reason for discarding the CI histogram since certain aspects of the ECG are more suitably examined there than in the X-Y plot.) In Fig.II,8a the CI and sinus period are independent whereas in Fig.II,8b there is a strong relationship between them. Any of the sinus-locked mechanisms could accommodate a certain amount of patterning in the X-Y plot - it is a matter of deciding how much is reconcilable with these mechanisms. Consideration of the re-entry hypothesis will suffice to illustrate the difficulties involved in assessing this.

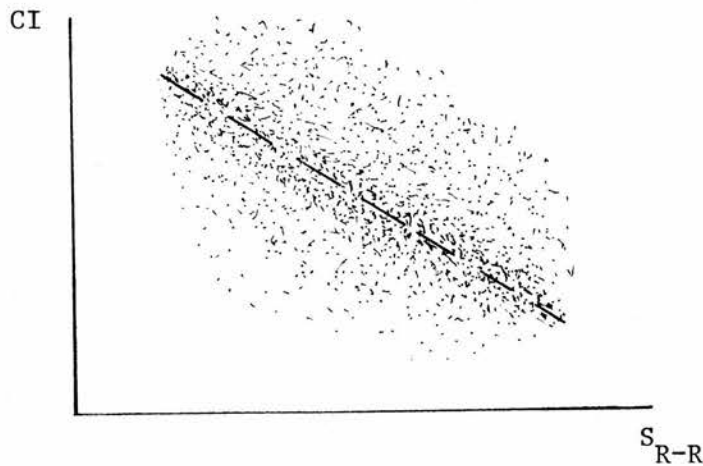
The CI of a re-entrant ectopic is the sum of three consecutive time intervals: the time taken for sinus excitation to reach the 'ectopic centre', the conduction time through the re-entry pathway, and the time taken for the resulting ectopic impulse to excite the surrounding myocardium. Variable conduction velocity through these pathways results in changes in the CI³⁴. Hence if the conduction velocity depends on the sinus rate the CI should show a corresponding dependency on the sinus rate⁶⁰. Singer, Lazarra and Hoffman⁷¹ have shown such rate dependent conduction velocity in Purkinje fibres. Indeed they point out that one might have expected such behaviour on the basis of Weidmann's earlier work on the relationship between the transmembrane potential and the sodium carrier system⁸⁶. Unfortunately the influence of the sinus rhythm on the CI in such a system depends on a host of unknowable factors, for example the extra-cellular sodium concentrations surrounding the various pathways and the auto-

Fig II,9: The degree of patterning depends on the strength of the systematic relationship as compared to the spontaneous random variations superimposed upon it.

- a. X-Y plot when the relationship between the CI and S_{R-R} (dotted line) dominates over the random variations in the CI and S_{R-R} .



- b. X-Y plot when the random variation in the CI and S_{R-R} dominate over an underlying relationship between them (dotted line).



maticity of these pathways. In addition the mechanisms responsible for sinus-locked ectopics has not been established^{84 9}. Hence the difficulty in estimating the expected dependence of CI on sinus rate is compounded by the fact that the genesis of the ectopic rhythm is unknown, and that even if it were, the parameters governing the CI would certainly be unknowable. The problem is akin to that of estimating the total expected variation of the CI only worse in that all the causes of this variation and their relative effects must be known. This may be appreciated by considering an example where only two factors influence the CI: say the first one acting alone would give rise to a direct relationship between the CI and sinus period, and that the second one would give rise to random unrelated changes in the CI. Fig.II,9a shows the expected X-Y plot if the first of these were dominant, whereas Fig. II,9b shows the expected pattern if the random process were dominant. In other words the relative effectiveness of these two influences must be known in order to predict the degree of patterning in the X-Y plot. The same argument applies if there are more than two influences present in that we require knowledge of the relative strengths of all the influences to predict the total degree of patterning.

To sum up, the X-Y plot of a simple sinus-locked mechanism is a horizontal line (Fig.II,7) or band (Fig.II,8a). Any other type of pattern indicates that the CI is not independent of the sinus period and hence such patterning would not arise from a simple sinus-locked mechanism. In practice a certain amount of such patterning may arise, although there must be some upper limit to this (other than horizontal bands). This upper limit can not be calculated because of the poor formulation of the sinus-locked hypotheses and our lack of knowledge of actual sinus-locked mechanisms. Hence the type of X-Y plot expected from the sinus-locked hypotheses is not well-defined. Nevertheless, untainted forms of these hypotheses can only give rise to horizontal lines and bands.

Fig.II,10: a. Manifest Bigeminy $N=1$
 b. Concealed Bigeminy $N=1+2n, n=,1,2,3,\dots$

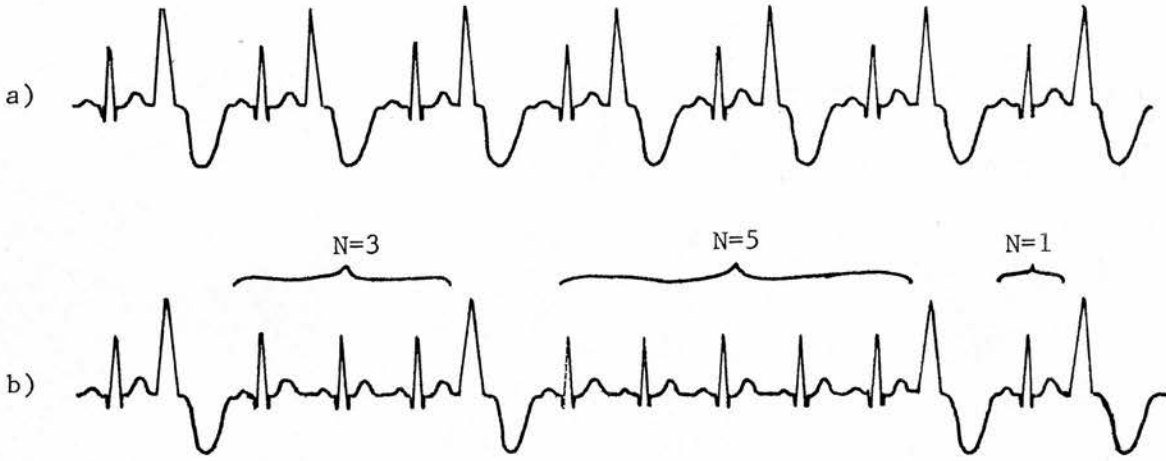


Fig.II,11: Typical Nhistograms for perfect concealed bigeminy and trigeminy.

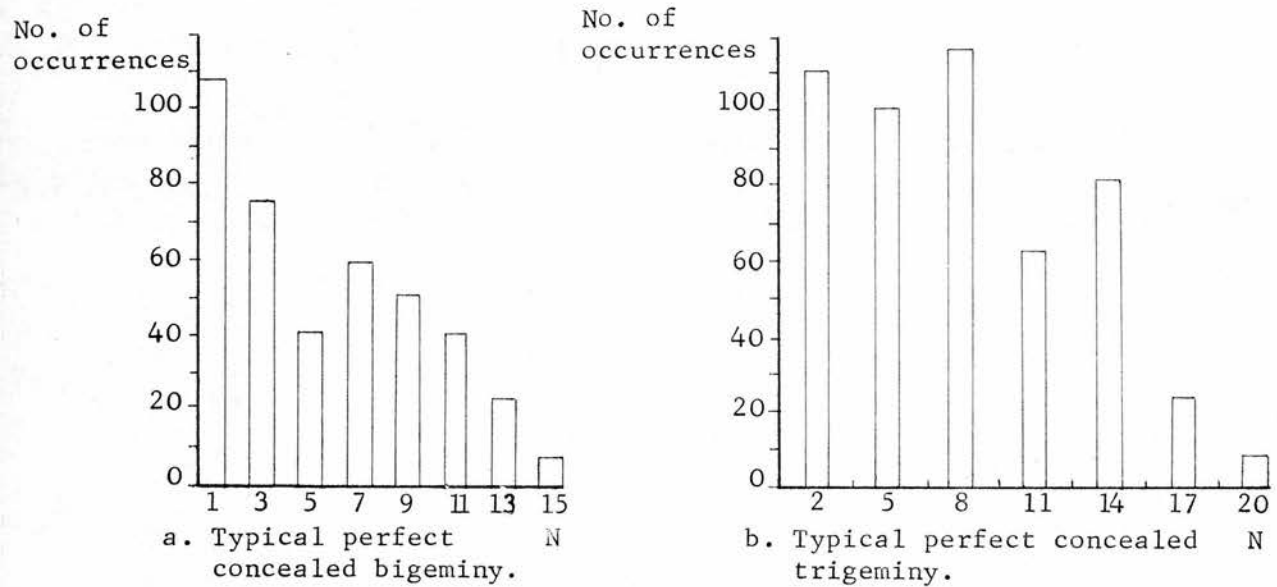
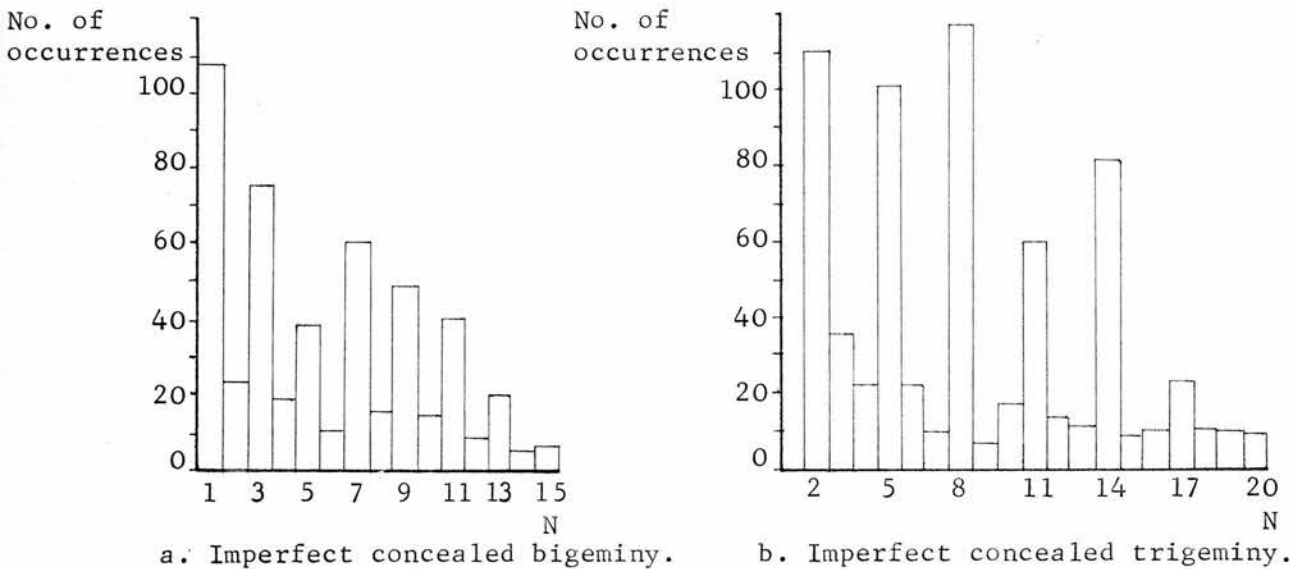


Fig.II,12: N histogram for cases similar to these in Fig.I,11 but where the concealed bigeminy and trigeminy are not perfect.



iii) Histogram of the Inter-Ectopic Numbers (N)

The expected characteristics of the inter-ectopic numbers (N) for the sinus-locked hypotheses has received little more attention than have the CI histogram and X-Y plot. However Schamroth and Marriott have pointed out two interesting N distributions⁵⁷⁻⁵⁹, namely 'concealed bigeminy' and 'concealed trigeminy'. Bigeminy refers to arrhythmias where sinus and ectopic complexes alternate so that the resulting sequence is sinus, ectopic, sinus, ectopic etcetera as in Fig.II,10a. Here N has a constant value of '1'. 'Concealed bigeminy'⁶¹ refers to arrhythmias where N is always odd (Fig.II,10b), i.e. $N = 1 + 2n$ where $n = 0, 1, 2 \dots$, hence bigeminy (or 'manifest bigeminy') is a special case of concealed bigeminy with $n = 0$ so that $N = 1$. 'Concealed trigeminy'⁶¹ refers to arrhythmias where N is always one of the numbers from the sequence $N = 2 + 3n$, $n = 0, 1, 2, 3 \dots$, i.e. $N = 2, 5, 8, 11 \dots$. 'Manifest trigeminy' is a special case where $n = 0$ so that N has a constant value of 2. Indeed it would be useful to talk of concealed quadrigeminy where $N = 3 + 4n$, $n = 0, 1, 2 \dots$, concealed quintageminy where $N = 4 + 5n$ and so on if these distributions were found to exist. The N histogram is most effective in emphasizing these distributions. Fig.II,11 shows hypothetical distributions for perfect concealed bigeminy and trigeminy. Fig. II,12a shows the hypothetical distribution for a case having a strong tendency towards concealed bigeminy but where N's not belonging to the sequence $N = 1 + 2n$ can also occur. Fig.II,12b shows an analogous case of imperfect concealed trigeminy. It was found that such cases having high peaks with intervening low but non-zero troughs are far more abundant than the type of perfect bigeminy and trigeminy illustrated in Fig.II,11 (cf. Chapter IV).

Although there has been a great deal of work on bigeminy since the phenomenon was first noticed (possibly as long ago as 1497⁶⁶), it seems that Schamroth and Marriott are the only ones to have considered the inter-ectopic numbers, and they have only been concerned with perfect concealed bigeminy and trigeminy. Certainly no-one has considered the

inter-ectopic numbers specifically arising from sinus-locked mechanisms. Hence the following argument contains a certain amount of conjecture but is based on those aspects of the literature that seem most pertinent. The inevitable limits of its applicability are discussed in Chapter IV.

The ectopic impulse responsible for sinus-locked V.E.Cs may be extinguished before it can excite the myocardium in which case no ectopic complex is seen and sinus rhythm proceeds unperturbed¹⁶. This phenomenon corresponds to the exit block which acts on ectopic impulses emerging from parasystolic foci. Thus 'exit block' seems a reasonable term to use for sinus-locked as well as parasystolic arrhythmias. For actively coupled ectopics, block may also occur before sinus excitation reaches the would-be ectopic focus and again no V.E.C. is seen. In addition there may be other factors prohibiting sinus excitation from initiating actively coupled V.E.Cs - if none of these factors are operative then each sinus complex is followed by a V.E.C. and simple bigeminy ensues.

Consider the effects of exit block. This can be written $x:y$, meaning that for every x ectopic impulses initiated within the ectopic focus only y penetrate the surroundings. For example 5:1 exit block means that only every 5th ectopic impulse will excite the myocardium, the other 4 being blocked by exit block. This is quite different to the block that occurs when an ectopic impulse is faced by refractoriness resulting from preceding sinus excitation. Now if at some moment the exit block is 5:1 it would seem reasonable to suppose that it could readily change to 4:1 or 6:1. That is, if at some moment every 5th sinus complex succeeds in initiating a V.E.C. so that $N = 5$ then it would be reasonable to suppose that N will not remain constant indefinitely but at some time it will change to either '4' or '6'. Having changed to '4' or '6', N may revert to its former value '5' or it may move further away to the values '3' or '7'. Of course it may suddenly change from '5' to '3' or from '5' to '7' leaving out '4' or '6'. The point of the argument is this: if N is '5' most of the time but also takes the values '3', '4', '6', and '7' then roughly speaking N ought to be '4' or '6' more often than '3' or '7'. This is equivalent to saying that if the most frequent exit block is 5:1 then 4:1 or 6:1 ought to occur more often

Fig.II,13: Hypothetical distributions of exit block compatible with sinus-locked mechanisms.

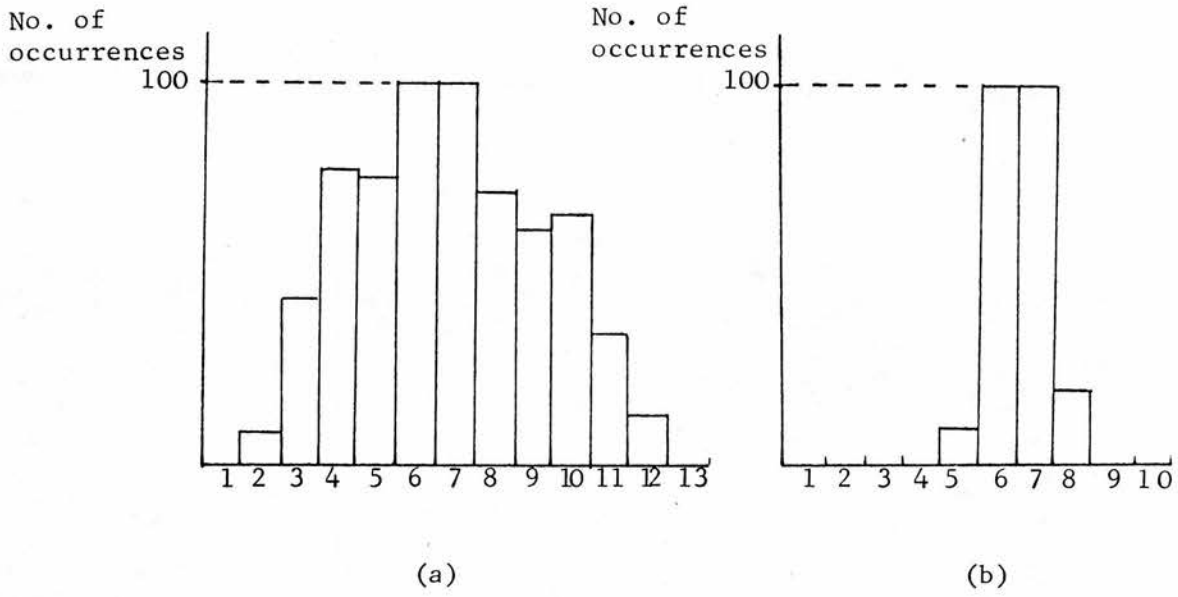
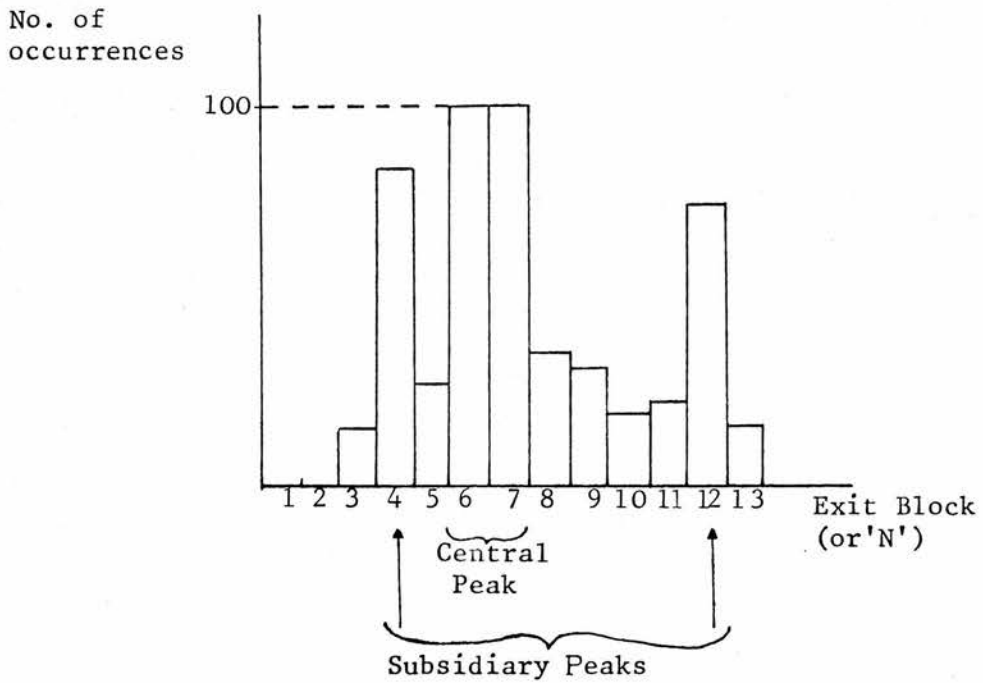


Fig.II,14: A hypothetical distribution of exit block unlikely to have arisen from a sinus-locked mechanism.



than 3:1 or 7:1. The reverse should certainly not happen, that is 3:1 and 7:1 should not predominate over 4:1 and 6:1 as in concealed bigeminy (Fig. II,12a). It would seem reasonable to assume that exit block should be a gradually varying function, not a grossly discontinuous function of the type depicted in Figs. II,11 and II,12. Nevertheless present knowledge is insufficient for estimating the expected "smoothness" of this exit block function.

The argument may be generalized as follows. For a given observation period some value or values of exit block must occur more often than all other values. In Fig. II,13 these maximum values are 6:1 and 7:1. The frequency of occurrence of exit blocks on either side of this maximum peak may tail off gradually (Fig. II,13a) or suddenly (Fig. II,13b). They should not tail off and then peak again at some value removed from the central maximum as in Fig. II,14. Multiple peaks separated by low troughs are even less likely for this would mean that these maxima were preferred to the intervening minima. Unfortunately there is no way of determining exactly how peaked the N histogram must be before rejecting the hypothesis of sinus-locking because the expected degree of 'peakiness' due to exit block is unknown.

One way multiple peaks might reasonably be obtained from a sinus-locked mechanism would be if the exit block were constant at some value for a period of time and then took up another value for a time. There would then be as many peaks as stationary values of exit block, but it seems highly unlikely that these would be equi-spaced as in concealed bigeminy and trigeminy. However, peaks which arise as N moves about rapidly between its favoured values requires a different type of explanation altogether. A mechanism involving two pathways which may be blocked independently of one another is considered in Chapter V.

The foregoing arguments also apply to all the other mechanisms that determine if a given sinus complex shall or shall not trigger a V.E.C. If each of these factors acting alone would elicit a "smooth" distribution of N then acting together they would also produce a "smooth" distribution

different from the individual distributions provided these are reasonably independent. The situation is akin to that of summing sources of random noise - if the sources are uncorrelated the result is also random noise but it bears little relationship to any of the individual sources.

To sum up: for the type of rapidly changing N seen in ECGs sinus-locked hypotheses should probably not give rise to N histograms with more than one peak. A multiplicity of peaks is certainly much less likely.

Pure Parasystole

The expected characteristics of pure parasystole are obtained by considering two (or more) independent, free running pacemakers (Chapter I). This thesis is concerned with cases having two pacemakers only, namely the sino-atrial node and a ventricular ectopic centre. The characteristics are the same when there are more than two pacemakers but such cases are not considered since multi-form ectopics are excluded from this study.

For two pacemakers to be considered independent certain conditions must be met regarding their periodicities. The period of each pacemaker varies from beat to beat as can be seen in the sinus period histograms in Chapter IV. One condition of independence requires that the variations in the sinus period be uncorrelated with variations in the ectopic period. Another condition requires that the average sinus and ectopic periods be independent, i.e. given the mean sinus period, the mean ectopic period is free to take any value within a certain range. These conditions are themselves related since the average period is partly dependent on the sum of the variations in the period. To be absolutely certain that these conditions are met, the sinus and ectopic periods would have to be monitored for an infinite time. Similarly to be certain of the opposite, namely that the sinus and ectopic periods are inter-dependent, also required infinite data. Fortunately finite measurements can be made which give probable estimates of the independence of two trains of pulses. In

order to make such estimates the expected characteristics of truly independent pacemakers must be known, and these are derived here. Some of the tests devised in Chapter IV use these results to show that real ECGs are highly unlikely to have arisen from independent pacemakers.

Fig.II,15: Hypothetical long term CI histogram arising from true parasystole having two independent pacemakers. The solid line shows the perfect histogram assuming the QT and S_{R-R} intervals remain constant throughout. The dotted line shows 'edge effects' due to changes in the QT and S_{R-R} intervals.

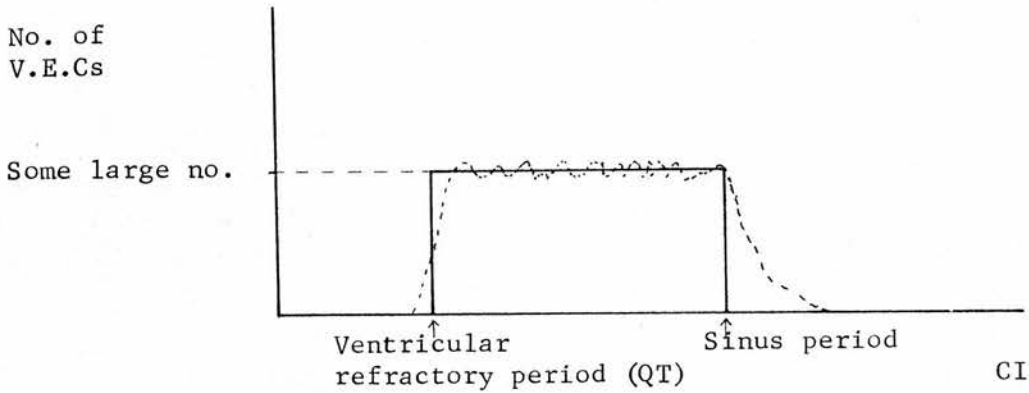


Fig.II,16: 2 independent pacemakers with periods S and E. Width of the shaded areas represent the size of the CIs. For simplicity $QT=0$.

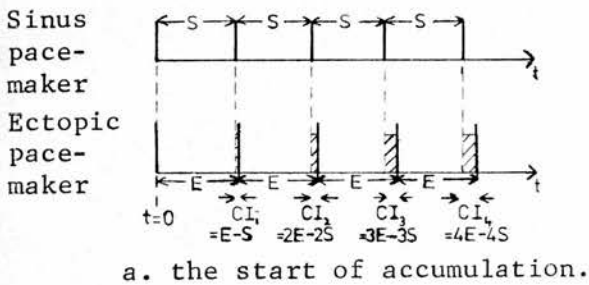
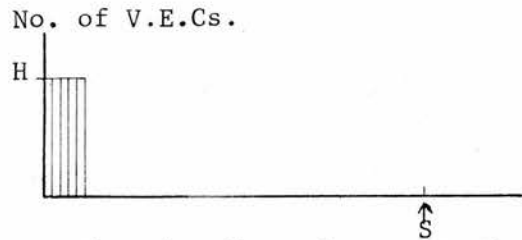
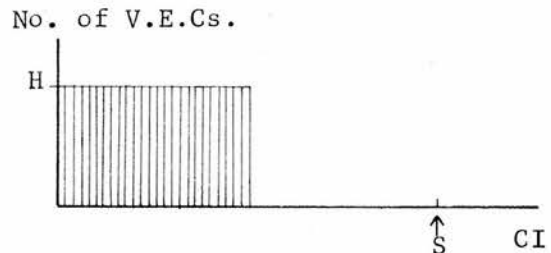
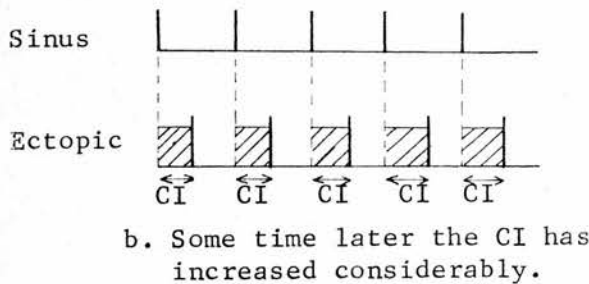


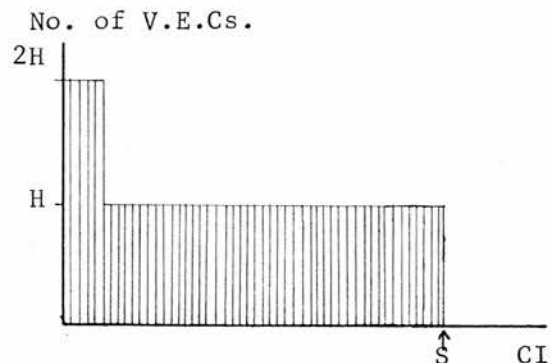
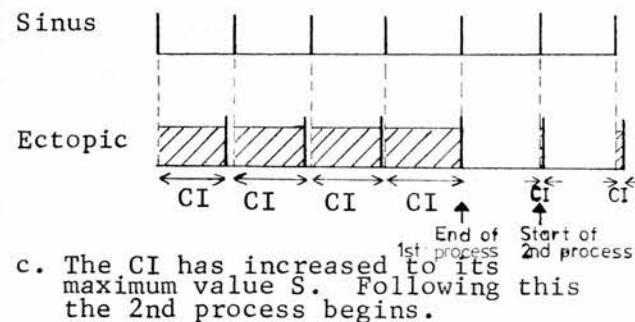
Fig.II,17: CI histograms at three stages of the 1st process. $QT=0$.



a. Shortly after the start of accumulation.



b. About half way through the 1st process.



c. On completion of the 1st process and the start of the 2nd.

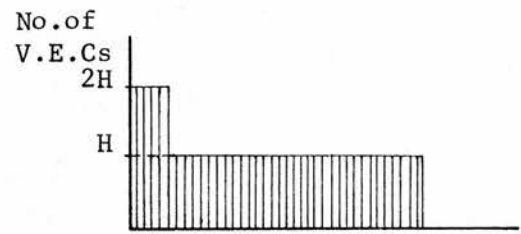
i) CI Histogram

Any case of pure parasystole having two independent pacemakers gives rise to all CIs equally often. If we wait long enough the CI histogram becomes rectangular as in Fig. II,15 showing that each CI occurs as often as any other. This statement is formally justified in Appendix I, but in order to give an intuitive insight into the processes involved two examples are given here.

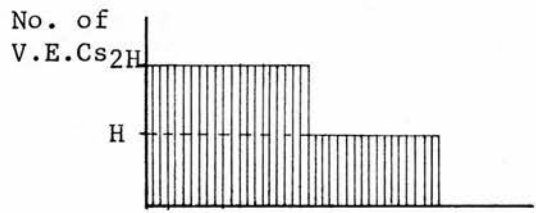
The CI histogram is made up of "bins" of width W , say, such that CIs lying between '0' and W are placed in the first bin, CIs between W and $2W$ are placed in the second bin and so on. Consider the CIs arising from two independent pacemakers having periods S and E (sinus and ectopic) represented in Fig. II,16a. E is slightly longer than S and both periods remain absolutely constant. If $S = E$ the pacemakers are not independent. They have been drawn starting together at time $t = 0$ but this is only a matter of convenience. The widths of the shaded areas represent the resulting CIs which are $(E - S)$, $(2E - 2S)$, $(3E - 3S)$ etc. For the sake of simplicity it has been assumed that there is no ventricular refractory period so that the minimum possible CI is infinitesimal. E and S are very nearly equal, hence successive CIs are also very nearly equal and only differ by an amount $(E - S)$. Since the bin width is W , the first $H (= \frac{W}{E-S})$ CIs are placed in the first bin. Similarly the next H CIs are placed in the second bin and so on. Fig. II,17a shows the situation after the first five bins have received H counts each. (To be accurate each bin receives $H \pm 1 = \frac{W}{E-S} \pm 1$ counts. This ± 1 has no effect on the final outcome.) This continues so that by the time the CI has increased by an appreciable amount (Fig. II,16b) the CI histogram is as in Fig. II,17b. Eventually the CI increases to its maximum value as in Fig. II,16c so that the histogram is as in Fig. II,17c. The progression from $CI = 0$ to $CI = S$ is called a "process". Figs. II,16 and II,17 depict the 1st process and the beginning of the 2nd. The 2nd process is similar to the 1st except accumulations in the histogram add onto those gathered during the 1st process.

Fig.II,18: CI histogram at three stages of the 2nd process.

a). Shortly after the start of the 2nd process



b). About half way through the 2nd process



c). On completion of the 2nd process

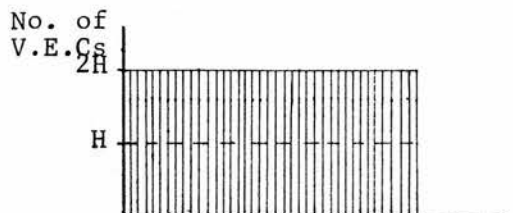
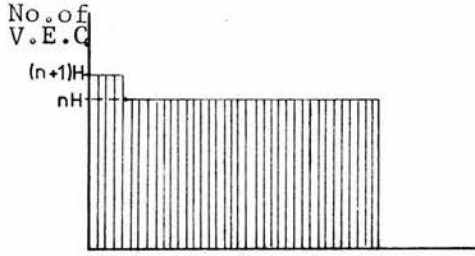
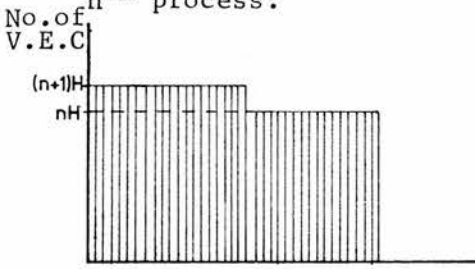


Fig.II,19: CI histogram at three stages of the nth process.

a). Shortly after the start of the nth process.



b). About half way through the nth process.



c). On completion of the nth process

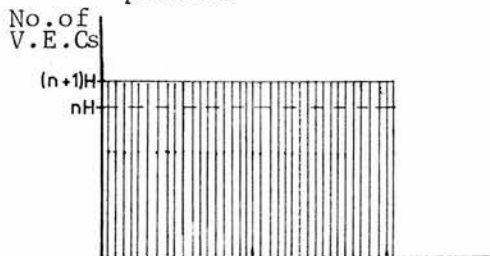


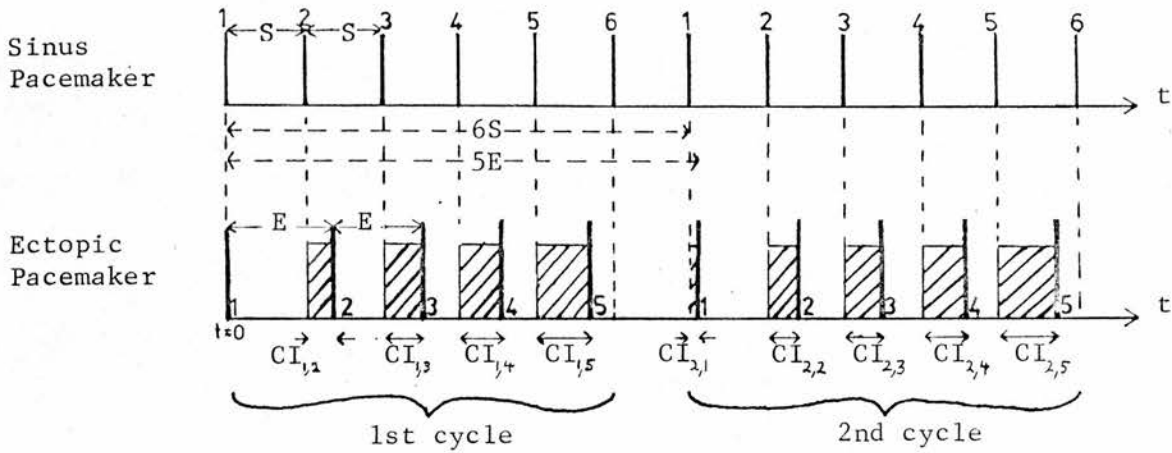
Fig. II,18 represents the histogram during the 2nd process at times equivalent to those shown in Fig. II,17. Before completion of the 2nd process some parts of the histogram are twice as high as other parts, but by the end of the process all parts have height 2H. During the 3rd process some parts of the histogram are 3H high while other parts are only 2H high, and during the nth process, Fig. II,19, the ratio of any one part compared to any other is never greater than $\frac{(n + 1)H}{nH} = 1 + \frac{1}{n}$. Clearly the flatness of the histogram is unlimited as more processes are accumulated (as $n \rightarrow \infty$, $1 + \frac{1}{n} \rightarrow 1$), and it is only a matter of time before any given degree of flatness is achieved.

The foregoing argument is based on the assumption that S and E remain constant. Exactly the same argument applies if S and E are replaced by \bar{S} and \bar{E} , the mean sinus and ectopic periods. Variations in S and E only spread the peaks arising in the histogram at any moment.

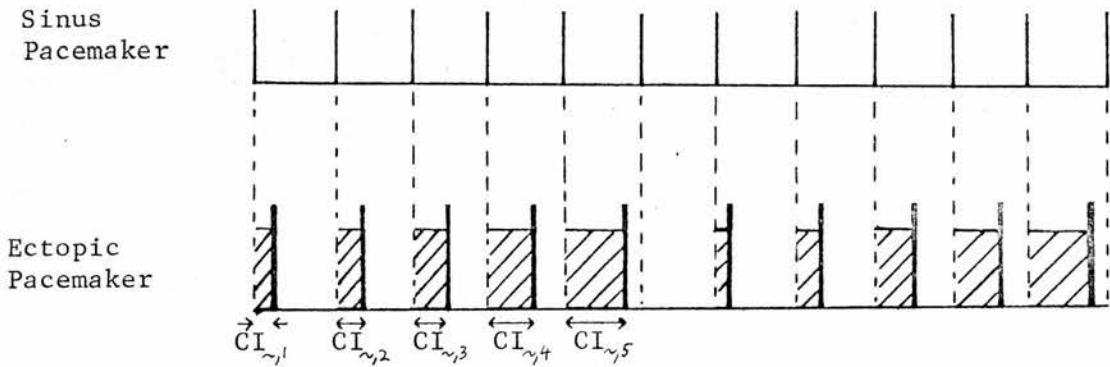
/

Fig.II,20: Two independent pacemakers where $5E$ is slightly longer than $6S$, i.e. $5E=6S+$. Widths of the shaded areas represent the size of CIs.

a). The 1st two cycles. Notation: $CI_{a,b}$ is the b^{th} CI of the a^{th} cycle
 cycle no. \swarrow CI no within
 \searrow the a^{th} cycle.



b). Two cycles taken some time later. N B $CI_{\sim,1} < CI_{1,2}$



c). CIs increased to their maximum values followed by the start of the 2nd process.



Similar reasoning applies when any multiple of the ectopic period is slightly greater than any multiple of the sinus period. (If some multiple of the ectopic period is exactly equal to some multiple of the sinus period the pacemakers must be considered as synchronized and not independent. See Appendix I.) For example when $5E$ is slightly greater than $6S$, so that $5E = 6S + \delta$, the situation is as shown in Fig. II,20a. The pacemakers have been drawn starting together at time $t = 0$ so that the first ectopic beat is coincident with the first sinus and no CI is seen. The first five ectopic beats, numbered '1', '2', '3', '4', '5', give rise to five separate CIs. The next five CIs nearly match the first five so that each set of five CIs is referred to as a 'cycle'. Every CI may then be designated by its cycle number and its position within the cycle, eg. $CI_{1,4}$ refers to the 4th ectopic of the 1st cycle. Hence the CIs of the 1st cycle are:

CIs of the First Cycle

Ectopic Complex No.	CI No.	Size of CI
1	$CI_{1,1}$	= 0
2	$CI_{1,2}$	= (E-S)
3	$CI_{1,3}$	= 2(E-S)
4	$CI_{1,4}$	= 3(E-S)
5	$CI_{1,5}$	= 4(E-S)

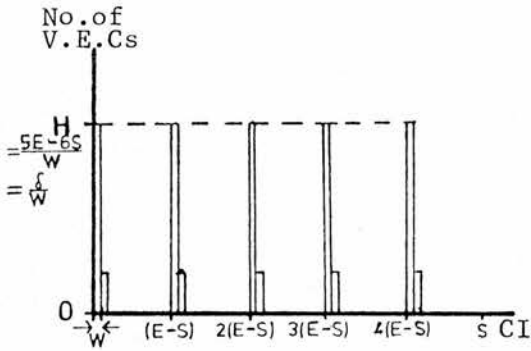
The 2nd cycle starts with a small phase difference between the sinus and ectopic pacemakers of $5E - 6S = \delta$. This is very small since the case is defined as 5 ectopic periods being slightly larger than 6 sinus periods. Hence the 1st CI of the 2nd cycle is equal to δ . Similarly the 2nd CI of the 2nd cycle, $CI_{2,2}$, is greater than the 2nd CI of the 1st cycle by an amount δ ,

$$\begin{aligned}
 \text{i.e. } CI_{2,2} &= 6E - 7S \\
 &= 5E - 6S + (E - S) \\
 &= \delta + CI_{1,2}
 \end{aligned}$$

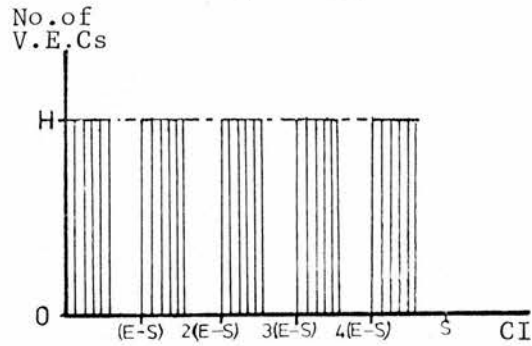
Similarly $CI_{2,3}$ is greater than $CI_{1,3}$ by an amount δ and so on.

Fig.II,21: CI histogram at various stages of the 1st and 2nd processes for $5E=6S+$

a). Shortly after the start of the 1st process



b). About half way through the 1st process.



c). Shortly after the start of the 2nd process.

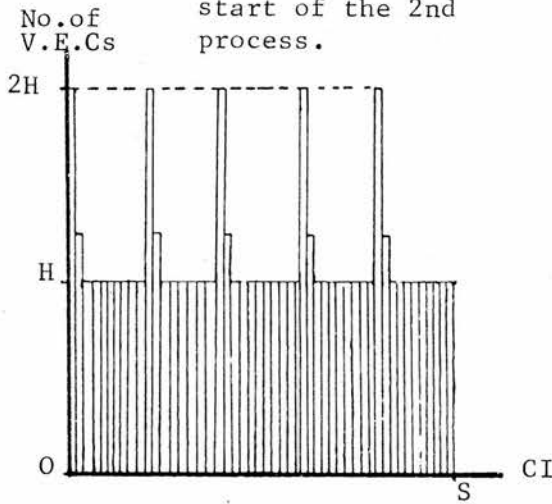
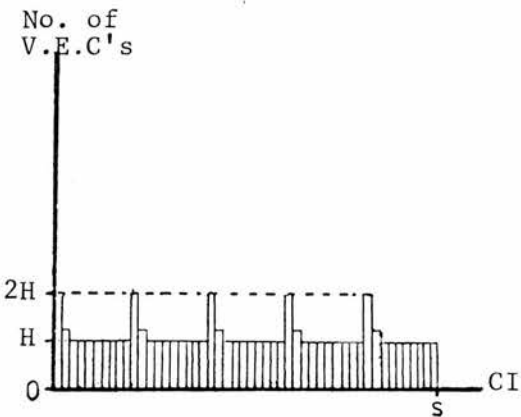
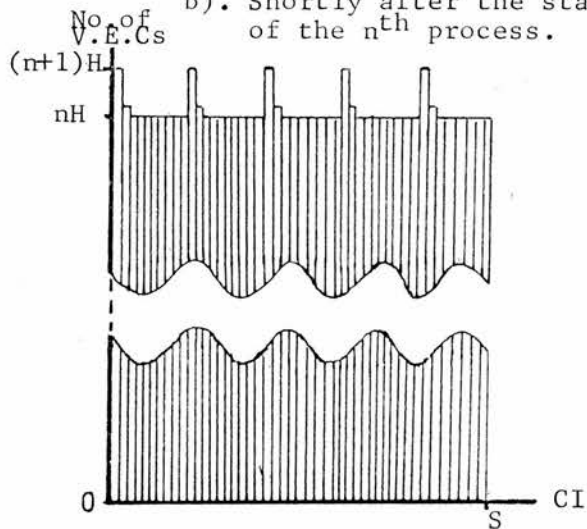


Fig.II,22: CI histograms at similar times in the 2nd and n^{th} processes for $5E=6S+$

a). Shortly after the start of the 2nd process.



b). Shortly after the start of the n^{th} process.



In other words, in each cycle each of the five CIs are incremented by an amount δ . If the bin width is W , say, then each of the five bins corresponding to these five CIs receive H ($= \frac{W}{\delta} = \frac{W}{5E - 6S}$) counts before adjacent bins receive any counts at all, Fig. II,21. This continues so that by the time the CIs have been incremented by an appreciable amount (Fig. II,20b) the histogram is as in Fig. II,21b. Eventually each CI attains the values shown in Fig. II,20c so that the histogram is as in Fig. II,21c. The progression depicted in Figs. II,20 and II,21 is analogous to that of Figs. II,16 and II,17 and again this is called the 1st process. Fig. II,22a shows the histogram some time during the 2nd process and Fig. II,22b is taken at a similar time in the n th process. As before, the flatness of the histogram is unlimited as more processes accumulate.

The argument that any case of pure parasystole would ultimately give rise to a flat CI histogram is based on the stipulation that the relationship between the mean sinus and ectopic periods (\bar{S} and \bar{E}) cannot be written in the form $j\bar{S} = k\bar{E}$, where 'j' and 'k' are positive integers. Such a relationship would imply that j sinus periods are synchronized to k ectopic periods, and this is incompatible with the concept of independent pacemakers (cf Appendix I). In other words, for pure parasystole, the ratio $\frac{\bar{S}}{\bar{E}}$ is irrational and may be written in the form $j\bar{S} = k\bar{E} + \delta$, where δ is a small time interval. k equi-spaced peaks arise in the CI histogram and then merge during each process, the length of each process depending on j , k , and δ . With the accumulation of these processes the k peaks become proportionately smaller compared to the body of the histogram already accumulated. Appendix I contains a formal proof that the irrationality of $\frac{\bar{S}}{\bar{E}}$ always leads to flat CI histograms.

Exit block surrounding the ectopic focus complicates all these arguments, however the following statement still holds under a constant or varying exit block (provided the changes in exit block are not specifically related to the CI): any case of pure parasystole must ultimately give rise to a flat distribution of CIs.

Fig II,23: X-Y plot for parasystole having constant sinus and ectopic periods. All points lie on the line AB.

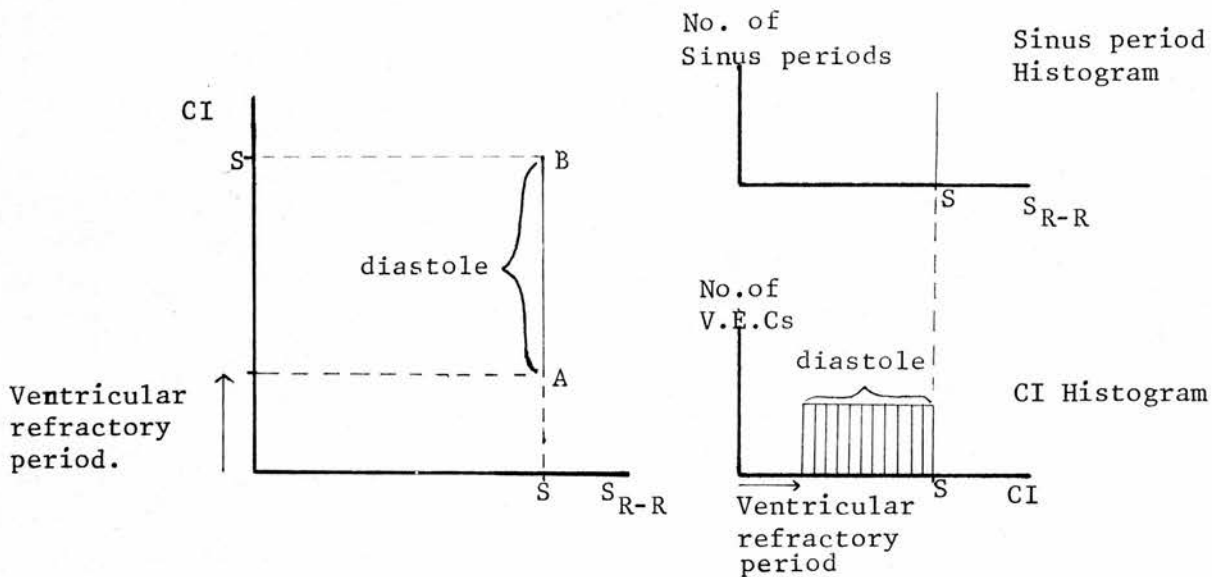
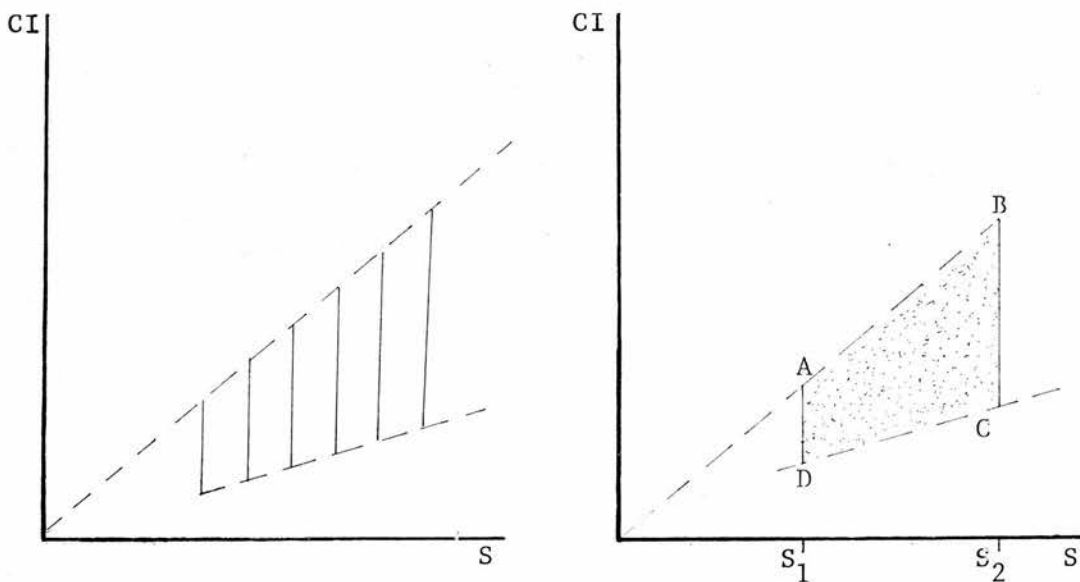


Fig II,24: X-Y plots for true parasystole. The lower dotted lines represent the lower bound for the CI and is determined by the ventricular refractory period. The upper dotted lines represent the upper bound and equals the sinus period.

- a.) Sinus pacemaker takes up six different values and remains constant at each one for some time. b.) Sinus and ectopic periods vary.



ii) Scattergram of CI versus Sinus Period

The events manifest in the X-Y plot are closely related to those of the CI histogram, and indeed the CI histogram represents part of the information contained in the X-Y plot. For cases of parasystole having constant sinus and ectopic periods the X-Y plot is made up of points lying on a vertical line as in Fig. II,23. The density of points is the same for all positions on the line since all CIs occur equally often as shown in the accompanying CI histogram. As before the minimum CI is determined by the ventricular refractory period, and the maximum CI is equal to the sinus period, the length of the line representing ventricular diastole. (Compare Figs. II,23 and II,7.) If the sinus period should take up and maintain a new value a second vertical line is produced, and for every subsequent change a further vertical line is produced, provided the sinus period remains constant at each value for a sufficient time.

A series of such lines is shown in Fig. II,24a. The minimum CI for each line is equal to the ventricular refractory period and this increases with increasing sinus period^{77 (p.13),38}. Since the maximum CI is equal to the sinus period, the maximum points lie on a line passing through the origin having slope +1. If the sinus period is not constant but changes continually, then the X-Y plot appears as in Fig. II,24b. This pattern must eventually become fairly evenly distributed as in the diagram subject to certain conditions. Points lying on any vertical line placed within ABCD (Fig. II, 24b) are equally distributed upon that line if accumulation continues for a sufficient time. However the density on one line may differ from that on another. For example if AD is half as long as BC then, provided there are as many sinus periods of size S_1 as there are of S_2 , AD is twice as dense as BC since each line contains the same number of points. In other words, if the distribution of sinus periods is rectangular so that the same number of points lie on any vertical line, then the intensity of points decreases as the range of diastole increases, i.e. as the sinus period increases. In addition the density of points on a vertical line depends on how often

that line (i.e. that sinus period) occurs. As a result the density of points will vary with sinus period according to the distribution of sinus periods - if this is rectangular there is no effect - if it contains a sudden large change then a corresponding sudden large change occurs in the density of points as we move from left to right. Thus the X-Y plot should always be examined in conjunction with the sinus period histogram so that this type of patterning is not falsely interpreted as indicative of inter-action between the CI and sinus period. This is equally true of the CI histogram. The test devised in Chapter IV (and in Appendix II) for inspecting the X-Y plot takes account of both histograms.

It is possible that certain patterns can arise under suitable circumstances if the accumulation time is not sufficiently long. Such patterning as may arise is reduced or destroyed by spontaneous variations in the ectopic period, however the following example shows the type of pattern that can arise if only temporarily. This is totally different from the type of density change induced by the sinus period and CI distributions.

/

Patterning occurs when changes in the sinus period repeatedly give rise to specific changes in the CI. Fig. II,25 shows such a situation where the last CI shown is shorter than the rest by an amount equal to the increase in the sinus period, S to S' . An increase in the sinus period has caused a specific decrease in the CI and a significant X-Y plot will arise if this can be repeated many times. Such a situation is depicted in Fig. II,26a with the corresponding X-Y plot in Fig. II,26b. The average sinus period is 1000ms and the ectopic period is constant at 1000ms. Thus the average CI over the 13 beat section shown is the same as the first CI, namely 500ms. In other words the average CI remains unchanged provided the average sinus period exactly equals the average ectopic period. This is also true if the average of some number of sinus periods exactly equals the average of some number of ectopic periods. However this would imply that the pacemakers are synchronized (Appendix I) and would ultimately give rise to peaks in the CI histogram. Under such circumstances particular sinus periods are accompanied by particular CIs and hence a lengthening of S can repeatedly induce an equal shortening of the CI. Hence the X-Y plot of Fig. II,26b is "centred" on a line of slope -1 passing through the point representing the average sinus period and CI. If such a pattern were to be repeated it would become statistically significant. (In fact it is significant at the 1% level, using the first test in Appendix II, on being repeated only four times.) The hypothesis that a peaked CI histogram was the result of pacemakers which happened to have nearly the same periods would be substantiated by a -1 slope in the X-Y plot. Such a situation is highly unlikely to arise from pure parasystole.

The matter is further complicated by changes in the ectopic period which are directly manifest as changes in the CI. (Imagine such a change taking place in either Fig. II,25 or II,26a.) If the ectopic period varies but maintains its average at 1000ms the pattern becomes diffused. Hence even in the unlikely event that the average sinus and ectopic periods are the same, and this would be manifest by a peaked CI histogram, their independent variations work against patterning in the X-Y plot. A sharply defined pattern would imply

that the sinus and ectopic pacemakers move together. Now if as must be the case for true parasystole, the average pacemaker periods (or multiples thereof) are not identical, then the "centre" lines of any temporary patterns will move about the X-Y plane and we are back at Fig. II,24b.

To sum up, generally there should be no significant pattern in the X-Y plot for any case of pure parasystole - this can be tested for statistically on the basis of the sinus period and CI histograms (Appendix II). In the unlikely event that the CI histogram shows the average sinus and ectopic pacemaker periods (or multiples thereof) to be nearly equal, a pattern "centred" around a line having slope -1 can arise. No other significant pattern can arise and even this pattern must eventually disappear. The existence of any other statistically significant X-Y pattern indicates that the sinus and ectopic periods are not independent and can not therefore be regarded as pure parasystole.

iii) Histogram of Inter-Ectopic Numbers (N)

The histogram of inter-ectopic numbers for pure parasystole can take on one of two forms: it can have either one peak which tails off resembling the N histogram of sinus-locked arrhythmia, or it can have a series of peaks typical of concealed bigeminy, trigeminy etc. As with the sinus-locked hypotheses, N is determined by exit block, but this is not the only governing factor for cases of parasystole. Two examples will suffice to show the type of pattern that can arise.

/

Fig II, 27: A case of parasystole capable of giving rise to a 'smooth' N distribution.

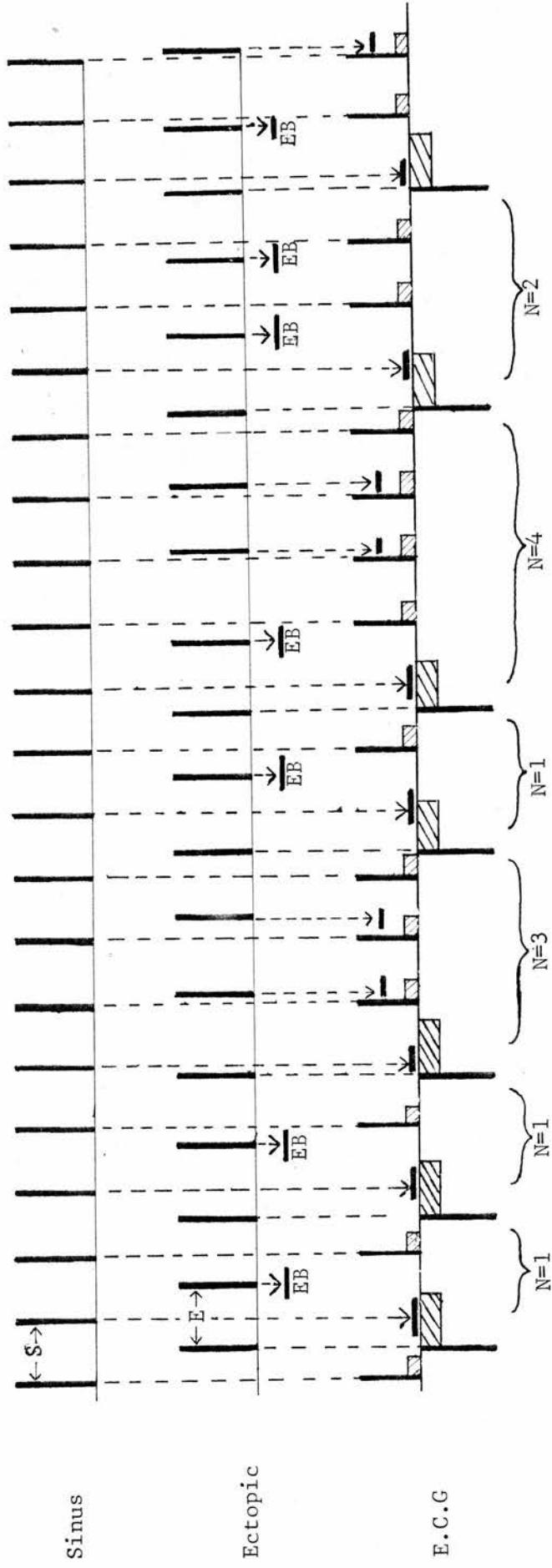
Top line: sinus pacemaker impulses

Middle line: ectopic pacemaker impulses

Bottom line: resultant E.C.G.

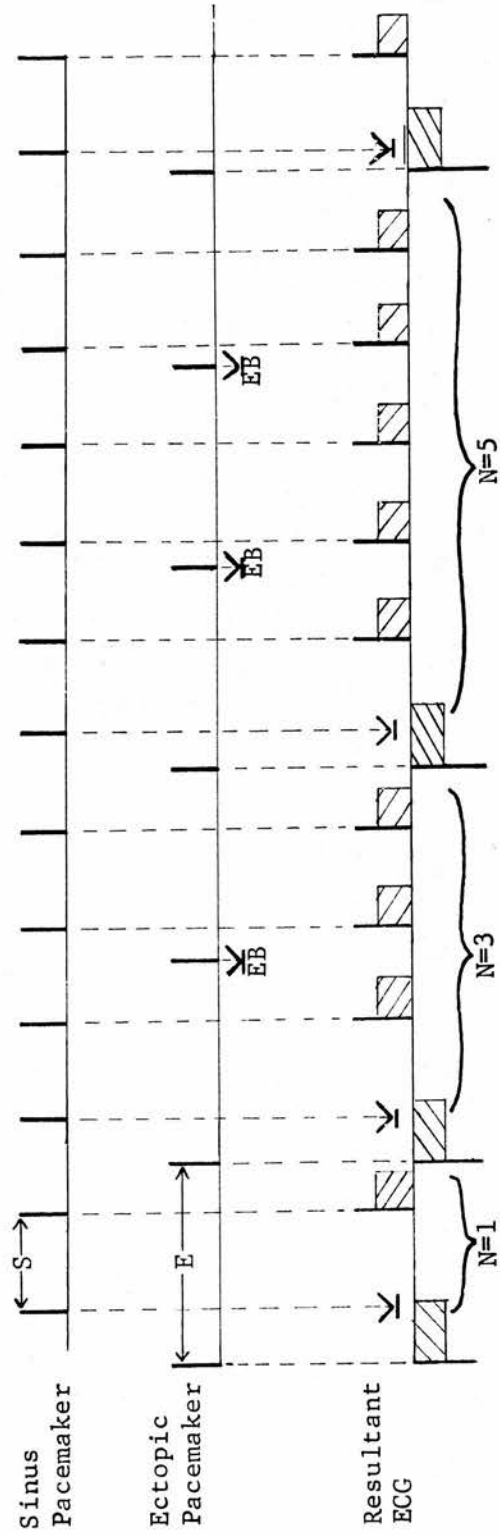
Shaded areas: ventricular refractory period

Horizontal bars: conduction block from refractoriness or exit block E: Exit block



A sinus-locked arrhythmia is capable of producing a V.E.C. after every sinus impulse reaching the ventricles. Consequently the N histogram has a single peak determined by the exit block. Similarly if a case of pure parasystole has the ability of producing a V.E.C. after every sinus impulse reaching the ventricles the N histogram will have a single peak. Fig. II,27 shows such a case where the ectopic period is slightly longer than the sinus period. Up to now the ventricular refractory period has been ignored since it has no effect on any of the foregoing arguments. This is not so here. The top line of Fig. II,27 represents sinus pacemaker impulses as they leave the atrio-ventricular node, and the ectopic pacemaker impulses are on the middle line. These impulses can initiate sinus (upstroke) and ectopic (downstroke) complexes in the resulting ECG shown in the bottom line. The ventricular refractory period following each complex is shown by the shaded areas, and if suitably timed these can prevent pacemaker impulses from propagating into the myocardium. When such block occurs a horizontal line is placed ahead of the dotted line coming from the pacemaker. Exit block acting on the ectopic focus is similarly represented but is labelled "E.B." in the diagram. Where necessary it is assumed that exit block prevents two successive ectopic impulses from initiating V.E.Cs, otherwise consecutive V.E.Cs appear in the ECG and such cases have been excluded from this investigation. As a result the first two inter-ectopic numbers are both '1'. The third and fifth numbers are large ($N = 3$ and $N = 4$) because each ectopic impulse is blocked by the preceding sinus excitation; it takes a few beats for the phase difference between the sinus and ectopic pacemakers to become large enough for this not to happen. The sixth inter-ectopic number is most relevant to the present argument. It is equal to '2' because the exit block at that point is 3:1. Had it been 4:1 the inter-ectopic number would have been '3', and for a large part of the time the following relationship holds: $N = E.B. - 1$. Hence if the exit block is distributed "smoothly" so also is N. This example may seem somewhat contrived but the point here is that a "smooth" distribution of N is possible for certain cases of parasystole. The next example shows that for some cases of

Fig II,28: Section of a case of parasystole where $E = 2S +$
 Key: same as for Fig II,27.
 $N = 1, 3, 5, 7, 9, \dots = 1 + 2n, n = 0, 1, 2, \dots$



pure parasystole a "smooth" distribution is impossible.

Fig. II,28 shows a section from a hypothetical case of pure parasystole where the ectopic period is slightly longer than twice the sinus period. The appearance of a V.E.C. (such as the first complex) prevents the next sinus impulse from propagating. After the first V.E.C. there is one sinus beat before the next ectopic impulse occurs capable of initiating a V.E.C. If this second ectopic impulse is successful in exciting the myocardium the V.E.C. appears and $N = 1$ as shown. Consider the next inter-ectopic number. Following the V.E.C. a sinus complex occurs after which another V.E.C. may arise but is blocked by exit block. Hence a further two sinus complexes occur before the next V.E.C. is due, therefore $N = 3$. The next inter-ectopic number is '5' because after the first sinus complex following the V.E.C. two ectopic pacemaker impulses are blocked, and for each of these two sinus complexes occur. Hence -

$$N = 1 + 2 + 2 = 5$$

↑
↑
↑

the first) [the second] (the fourth and
 sinus complex) and third (fifth arise from the second
 arise from (blocked ectopic impulse
 the first
 blocked ectopic
 impulse

For the section of ECG shown $N = 1 + 2(E.B.)$ and can be odd only. Other sections may occur where there is no such propensity for certain N s, but as the sinus and ectopic pacemakers move in and out of phase, certain stretches of ECG like that in the diagram will exhibit concealed bigeminy and give rise to an N histogram like that in Fig. II,11a. The effect of the intermittence of this bigeminy is to produce an N histogram like that of Fig. II,12a. By suitable choice of sinus and ectopic pacemaker periods a whole range of N distributions is possible.

To sum up, the distribution of inter-ectopic numbers for pure parasystole can take almost any form. The histogram may contain any number of peaks from 1 upwards and still be totally compatible with the hypothesis of two independent pacemakers. This is so even if the pacemakers are not independent.

Concluding Remarks

The characteristics expected from the sinus-locked and pure parasystolic hypotheses are summarized in Table II, 1(p.13). These are compared to the characteristics of real ECGs in Chapter IV, and for this purpose hundreds of hours of ECGs have been examined. This required long term tape recordings of ECGs, and automatic high-speed analysis of many records. The techniques used for this purpose are described in the next chapter.

CHAPTER III Methods of Measuring Temporal
Characteristics in the Electro-
cardiogram

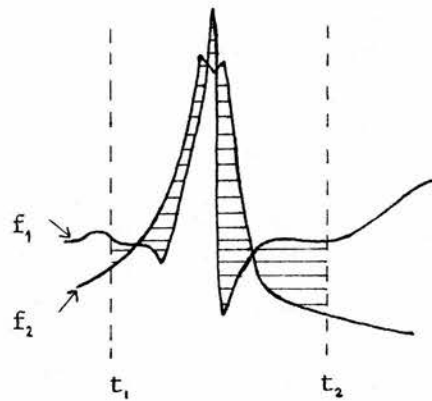
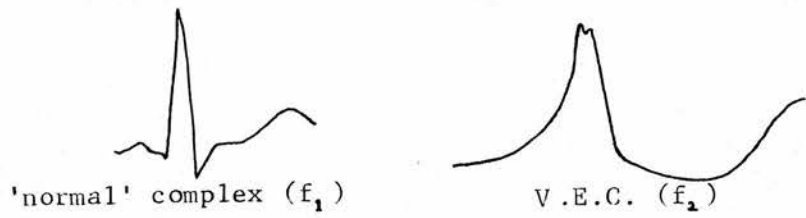
Measurement Procedure

ECGs were recorded on magnetic tape using machines designed by Neilson and built under his supervision in the Department of Medical Physics, Royal Infirmary, Edinburgh. The fidelity of the system is such that no visual differences can be discerned between original and recorded ECGs. The recording speed is 38 cm per min so that a 24 hour record is contained on a standard 1800 foot reel of tape. Playback can be at either 38 cm per min (i.e. X1) or at 38 cm per sec (i.e. X60), the latter allowing examination of a 24 hour record in as many minutes. All records were taken from the Coronary Care Unit, Royal Infirmary, Edinburgh using lead V5 or V6. These leads allow the maximum discrimination between complexes of ventricular and supra-ventricular origin⁷⁷.

High speed analysis of the recorded ECGs is facilitated by the "arrhythmia computer" designed and built by Neilson^{47 48}. A full account of this machine is to be published shortly so only a cursory description of its functioning is given here.

The ECG waveform passes through a complicated sequence of filters and rectifiers and, roughly speaking, this gives rise to a deflection in the output every time the ECG waveform changes direction sufficiently rapidly. For each change in direction, the height and width of the deflection in the output is largely determined by: i) the rate of change of direction of the original ECG waveform (i.e. its second derivative); ii) higher derivatives; iii) the magnitude of the

Fig.III,1: Computation of non-shared area (shaded) for two E C G complexes. (Adapted from Neilson⁴⁷)



$$\text{non-shared area (shaded)} = \int_{t_1}^{t_2} |f_1 - f_2| dt$$

deviation in the original ECG waveform caused by the rapid change of direction. The time constants of various parts of the system are set so that the deflections caused by a 'P', 'T' or other slowly changing waveform are small compared to the deflections caused by an ECG 'wave' associated with rapid ventricular depolarization. The output will be referred to as the 'derived waveform', and in effect it represents the sharpness and relative positions of 'corners' in the original ECG. As a result, a QRS complex and the ventricular depolarization of a V.E.C. cause characteristic derived waveforms, whereas atrial depolarization and ventricular repolarization are minimally represented in the derived waveform.

To analyse an ECG the arrhythmia computer is first 'taught' the shape of the 'normal' complex for the ECG under investigation. In other words, it 'remembers' the ECG waveform of the 'normal' complex. Every subsequent ECG waveform which has a derived waveform of sufficient size (see later) is compared to the 'normal' by electronically laying the 'normal' ECG waveform over the detected one and computing the magnitude of the area which they do not share (Fig.III,1). If this difference in area is greater than a certain threshold level (see later), the complex is automatically detected as abnormal which, for this study, would be a V.E.C. If, on the other hand, this area is less than a second threshold level (see later), the complex is detected as 'normal', and the memory of 'normal' is slightly updated to account for gradual small changes in the shape of the 'normal' complex.

It is most important that noise in the ECG in the frequency of interest (e.g. electromyographic deflections produced when the patient moves) is not detected as a waveform for comparison to the 'normal', otherwise false positives arise. This is achieved by a self-adaptive threshold which is automatically raised as the noise level increases - any deflection in the derived waveform larger than the ongoing threshold level causes the waveform to be analysed as described, otherwise the waveform (i.e. noise) is not detected and goes unexamined. A certain amount of external control over the behaviour of this self-adaptive threshold is provided, and

this permits very excellent discrimination between ECG complexes and spurious noise.

Once detected, a complex is compared to the 'normal' as described. As already indicated, this comparison uses two threshold levels in order to determine if the ECG waveform is: i) sufficiently different from the 'normal' to be regarded as a V.E.C.; ii) sufficiently close to the 'normal' to be regarded as 'normal'. Clearly there is a third possibility where the arrhythmia computer cannot decide whether a detected complex is 'normal' or abnormal. The two threshold levels are determined by the ongoing noise level and the total area under the curve of the 'normal' ECG waveform. In addition the experimenter also has a certain degree of control over the behaviour of these self-adaptive thresholds.

The three self-adaptive but partly externally controlled threshold levels make the arrhythmia computer most effective at detecting ECG complexes and then discriminating between 'normals' (i.e. of supra-ventricular origin) and V.E.Cs. A rudimentary quantitative assessment of the quality of this system is given in the next section under "errors".

For the purpose of measuring CIs and sinus periods, an ECG complex is timed from the temporal mean of a filtered version of its derived waveform as this is largely insensitive to noise in the ECG. Clearly this occurs some time after the start of the original waveform. Since the timing point is determined by the shape of the ECG complex, the timing of a given complex remains invariant. Errors accruing from the change in shape of both 'normals' and V.E.Cs are also considered in the next section.

Two timing outputs are taken from the arrhythmia computer. If a complex is determined as being 'normal', a pulse with height proportional to the time between it and the preceding 'normal' complex is output on channel A of the arrhythmia computer. The height of this pulse thus represents the sinus period provided the penultimate complex is not a V.E.C. When a complex is determined as being abnormal, a pulse with height proportional to the interval between it and the preceding beat

is output on channel B, hence the height of this pulse represents the CI as measured from the timing point on the preceding 'normal' complex to the timing point on the V.E.C. Both outputs are pulse height analysed on a Nuclear Chicago 512/1024 Multichannel Analyser to produce the sinus period and CI histograms.

The X-Y plot is accumulated by i) using the 'normal' pulses to generate a step function with height proportional to the sinus period and feeding this to the "X" input of a Telequipment OM53A storage oscilloscope; ii) simultaneously applying the CI pulses to the "Y" input of the storage oscilloscope. When no CI pulse is present, the point corresponding to $X = \text{last sinus period}$, $Y = 0$ is continuously accumulated and this is off the screen of the oscilloscope because of amplification. When a V.E.C. occurs, the point $X = \text{last sinus period}$, $Y = \text{CI}$ is accumulated for a time equal to the constant width of the CI pulse.

The measurement procedure is as follows: having accumulated and photographed the X-Y plot of interest, the sinus period and CI histograms are accumulated by making a re-run of the selected section of the ECG; the N histogram is then accumulated by making a further re-run and using the Nuclear Chicago Analyser to count the number of 'normal' output pulses between successive V.E.Cs. Because of the re-runs involved, a few beats at the beginning and end of the run are sometimes included in one measurement but not in the others. Examination of the data in the next chapter shows that a few (less than 5) extraneous points would make no difference to any of the arguments proposed there.

Assessment of Errors and Some Further Details

i) Detection of Sinus Complexes and V.E.Cs

The errors involved here fall into two groups: i) false detection of the presence of complexes (positive or negative); ii) incorrect evaluation of a complex as either a 'normal' or a V.E.C. For convenience these errors are regrouped into three: i) V.E.C. false negatives (i.e. missing

a V.E.C. when one is present); ii) 'normal' complex false negatives; iii) false positives (i.e. 'detection' of a complex when none is present). These errors were assessed by scrutinizing the ECG waveform simultaneously with the 'normal' pulse train on a wide, persistence screen 'Lan Scope'. The procedure was then repeated for the V.E.C. pulse train. It was easy to check that i) for every V.E.C. there arose one V.E.C. pulse, and vice versa that for every V.E.C. pulse there was a V.E.C. in the original ECG; ii) that for every sinus complex there was a corresponding 'normal' pulse output and vice versa.

For each case presented in the next chapter a randomly chosen section containing about 100 V.E.Cs was checked in this manner for V.E.C. false negative errors (i.e. missing a V.E.C. when one is present). No false negatives were present in any of the chosen sections. Assuming the false negatives to follow a Poisson distribution, the 95% confidence limits¹³ on the rate of false negatives are 0 and 3.7 per 100 V.E.Cs. (Of course for those cases containing 100 V.E.Cs or less these statistics are of no relevance since no false negatives arise.) For the 12 cases, the 95% confidence limits on the overall rate of false negatives are 0 and 3.7 per 1,200 V.E.Cs.

The same procedure was adopted to evaluate the rate of false negatives for 'normal' complexes. For each case, no errors arose in a randomly chosen 1000 beat section, and this gives the 95% confidence limits as¹³ 0 and 3.7 false negatives per 1000 'normal' complexes. For the overall rate of false negatives the 95% confidence limits are 0 and 3.7 per 12,000 'normal' complexes.

False positives for V.E.Cs and 'normal' complexes may be grouped together to give the number of false positives per 1000 sinus complexes, say. Alternatively, the false positives could be quoted in terms of the number per minute. Choosing the former, the rate of false positives is exactly the same as the rate of false negatives for 'normal' complexes - this is so because the observed rate for both these was 0 per 1000 sinus complexes in every case.

Clearly the effects of such errors on the N, CI, and sinus period histograms, and on the X-Y plot are negligible and so these are not considered when examining the data in the next chapter.

A systematic error arises in the X-Y plot when a sequence of bigeminy occurs which is two or more V.E.Cs long. Under these circumstances the measured sinus period prior to the CI is effectively twice the usual sinus period since one QRS complex is blocked. Because of amplification on the storage oscilloscope the sinus period is off screen and so no point is plotted. (Similarly, for every V.E.C. a double sinus interval is placed in the sinus period histogram, but again these are off scale.) A possible solution to this problem is to divide these long sinus intervals by 2, but there is no guarantee that the result would represent the true sinus period. Although the CIs accompanying such manifest (i.e. not concealed) bigeminy are accumulated in the CI histogram, there is no reason to believe that they would jeopardize any conclusions made concerning its peakiness. On the contrary, the only 'incorrect' result that could arise would be an underestimate of the peakiness associated with bigeminy since this could be masked by the less peaked behaviour of the non-bigeminal beats. This would serve to hide the real significance of the data presented in the next chapter, but would not lead to over-estimation of its significance which would invalidate the arguments presented there. In any case the occurrence there of manifest bigeminy is not frequent enough to be of central interest.

ii) Timing Errors

Timing errors arise in the tape recording system, the timing circuits of the arrhythmia computer, the Nuclear Chicago Multichannel Analyser, and the Telequipment storage oscilloscope. Within these units errors take various forms, namely calibration, non-linearity, noise and variation in the shape of ECG complexes. These errors are considered separately or together where appropriate.

When fed from a stabilized crystal controlled pulse generator at frequencies equivalent to 400ms, 800ms and 1000ms,

the arrhythmia computer gives a total variation in pulse height corresponding to less than 1ms. This variation in pulse height is measured on the storage oscilloscope using a high amplification in order to examine the tops of the pulses (base-line off screen by an order of magnitude). The sensitivity is made equivalent to 20ms/cm and this permits resolution between pulse heights differing by greater than 1ms.

The other error in the arrhythmia computer arises from variations in the shapes of 'normal' complexes and V.E.Cs (see p.36 of this chapter). This can be assessed roughly by using the output pulses to trigger the arrhythmia computer oscilloscope and then examining the variation in the position of ECG complexes at a high sweep speed ($50\mu\text{s}/\text{div}$ (X60) \equiv $3\text{ms}/\text{div}$ (X1)) with respect to these pulses. The maximum variation for both types of complex was less than 9ms for all cases and less than 6ms for 10 of them. These represent a 95%-ile spread of about 5ms and 3ms respectively.

The timing errors introduced by pulse height analysis of the arrhythmia computer pulses can arise from calibration, non-linearity in the range of interest, and noise (see above). The bin width used on the Nuclear Chicago Analyser corresponds to 5ms, hence errors less than 10ms cannot be assessed easily. Using the crystal oscillator as a reference source, the total error in the pulse height analysis part of the system was found to be less than 10ms. Accurate estimation of this particular error is not important since it is taken into account in the estimate of the overall system error which follows.

The main timing errors arise from wow and flutter in the tape recorder on record and playback. The total error accruing from the recording system, arrhythmia computer and pulse height analysis was estimated by recording the output from the crystal controlled pulse generator at 38cm/min and playing this back through the whole system at 38cm/s thus mimicking the procedure used for ECGs. The results are presented in Table III,1 in terms of the mean and the 95%-ile spread about the mean ($= 2 \times 1.96$ standard deviations) for

Table III,1: Timing errors accruing from the tape system, arrhythmia computer and pulse height analysis. The computations assume that the period, T, is distributed normally.

Period of crystal generator (ms)	No. of periods, n	Mean of measured output, \bar{T} (ms). $\bar{T} = \frac{1}{n} \sum_1^n T \quad \text{ms}$	95%-ile spread about the mean, D (ms). $D = 2 \times 1.96 \times \sqrt{\frac{1}{n-1} \sum_1^n (T - \bar{T})^2 - \frac{1}{12} h^2}$ where h = bin width = 5ms
800 ms	1653	797ms	26.5ms

the final output. The 95%-ile spread about the mean (D, column 4, Table III,1) uses the factor $(n - 1)$ to calculate the variance, s^2 , since this gives the most efficient unbiased estimate of the true variance, σ^2 , when \bar{T} is calculated from the data¹³. (Of course with $n = 1653$ the difference between using n and $(n - 1)$ is negligible.) The term $\frac{1}{12}h^2$ is Sheppard's correction¹³ for the estimate of a continuous variable grouped into class intervals of size h . The errors shown in Table III,1 have little effect on the interpretation of the data given in the next chapter. The effects are considered shortly.

The last source of error is drift in the Teleequipment storage oscilloscope and this only affects the X-Y plot. During a measurement the drift could be as much as 0.6 scale divisions. The drift is very low frequency so that the only possible effect is a small inconsistency (depending on the "sensitivity per division" setting) between the means of the CI and sinus period histograms, and these means as seen in the X-Y plot since these measurements are taken on separate runs of the ECG. In most cases this discrepancy is too small to be seen.

iii) Effect of Errors on the Interpretation
of the Data

The effect of drift in the storage oscilloscope is discussed at the end of the last section.

The effects of the false detection of complexes is so small as to be negligible (see earlier).

Some aspects of the timing errors (excluding those due to changes in the shapes of complexes) are given in Table III,1. The variations about the true value of the sinus periods and CIs are of interest whereas errors in their mean values are of secondary importance. As a result, only the variations in the timing errors are of interest, and to this end the 95%-ile spread is quoted in the last column of Table III,1. If these errors are random they can only reduce the peakiness of CI histograms and patterns in the X-Y plots,

whatever their size. If they are systematic then the problem is more complicated. A complete statement of the effect of timing errors (random and systematic) on the shapes of the CI histograms and X-Y plots would require a highly sophisticated statistical argument involving moments higher than the second (i.e. the standard deviation). However, the fact that a re-run of any ECG does not alter the observed patterns indicates that the errors introduced by wow and flutter, and noise in the system have no significant effect and so are ignored in the next chapter. The only remaining error is introduced by changes in the shapes of complexes, and since this is small compared to the errors just mentioned it is also ignored in the next chapter.

CHAPTER IV The Anomalous Nature of Frequent, Single
V.E.Cs Observed in Patients in a Coronary
Care Unit

In Chapter II it is argued that the sinus-locked hypotheses have characteristics quite distinct from those of pure parasystole. In general the CI and N histograms of these two hypotheses are diametrically opposed: the CI histogram is peaked in the sinus-locked case and flat for parasystole; the N histogram is "smooth" in the sinus-locked case and peaked for parasystole. In addition neither hypothesis should produce a highly patterned scattergram of CI versus sinus period. These results are used later in this chapter to show that neither sinus-locked nor pure parasystolic hypotheses are able to account for the characteristics of a large proportion of single V.E.Cs arising in diseased hearts. To this end ECGs are presented from the Coronary Care Unit, Edinburgh Royal Infirmary. It will be demonstrated that at least one third of these have characteristics which can not be explained by either pure parasystole or simple sinus-locking, and that as a result the universal applicability of these hypotheses is brought into doubt. In order to carry out this demonstration criteria are required for comparing observed to expected characteristics, and these are devised here.

Tests and Criteria for the Comparison of Expected to
Observed Characteristics

There is a fundamental difficulty in setting up quantitative tests and criteria for inspecting the CI histogram, X-Y plot and N histogram. These tests were designed to highlight discrepancies between expected theoretical characteristics and

observed results. As was shown in Chapter II, some of the theories under investigation have, up till now, been formulated only loosely and are therefore open to a considerable range of interpretation, i.e. their expected characteristics are not well-defined. This is particularly so of the sinus-locked hypotheses: the CI histogram may contain narrow or wide peaks; it is impossible to estimate the maximum degree of patterning that might arise in the X-Y plot; attempts at estimating the expected properties of the N histogram are highly restricted. As a result it is difficult to devise tests capable of detecting unequivocal discrepancies between the predictions of these theories and measured data. The antagonist of such a loosely formulated theory is obliged to demonstrate that all reasonable interpretations are unlikely to elicit the observed experimental results. This necessity to incorporate all reasonable interpretations into the tests has prevented some of them from being strictly quantitative. Hence the restricted effectiveness of these tests is a consequence of the poor predictive powers of the sinus-locked theories.

Each of the tests devised is aimed at making an estimate of the probability that a particular measured characteristic would have arisen from a particular theoretical mechanism: the first test estimates the probability of pure parasystole giving rise to the CI histograms observed (Table II,1, line a); the second test is concerned with the chances that observed X-Y plots could be produced by either a sinus-locked mechanism or pure parasystole (Table II,1, line b); the third test is concerned with the probability that observed N histograms would arise from a sinus-locked mechanism (Table II,1, line c).

i) Inspection of the Coupling Interval Histogram

The aim of this statistical test is to show that the investigated CI histograms are unlikely to have arisen from the mechanism of pure parasystole with two independent pacemakers. The null hypotheses, H_0 , is that the observed CI histogram does originate from a mechanism of pure parasystole, and the test rejects H_0 if the observed histogram is not sufficiently flat.

"Goodness of fit" to flatness is tested using the χ^2 distribution as follows: sinus diastole is divided into n equal segments (bins); if the observed number of CIs in the i^{th} bin is O_i then the total number of CIs is $\sum_{i=1}^n O_i$, and the expected number of counts in the i^{th} bin is $\frac{1}{n} \sum_{i=1}^n O_i = E_i = E$, say: the function $\sum_{i=1}^n \frac{(O_i - E)^2}{E}$ is then distributed as χ^2 with $(n - 2)$ degrees of freedom since one degree of freedom is lost through $\sum_{i=1}^n O_i$ being regarded as fixed by the experiment, and another is lost when E is estimated from the data¹³; statistical tables of χ^2 with $(n - 2)$ degrees of freedom give the level at which H_0 is rejected.

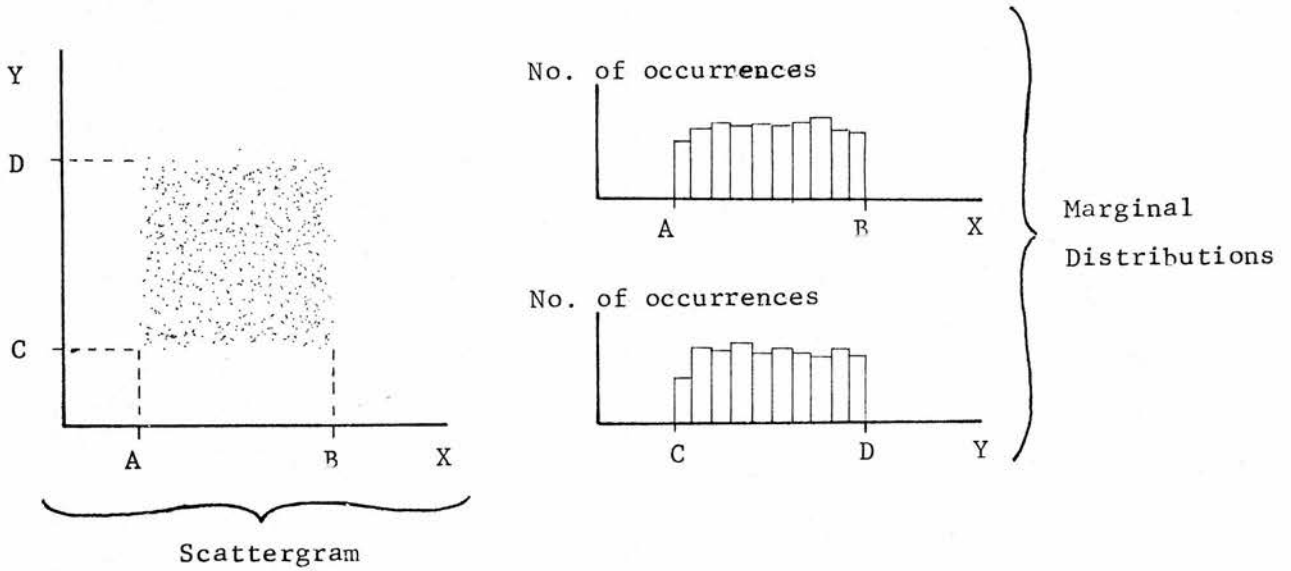
All the CI histograms presented in this chapter are rejected as coming from pure parasystole. The actual level of rejection is so great as to be beyond the range of statistical tables (i.e. 0.1%) and for this reason the calculated values of χ^2 are not quoted. Interpretation of this result is given after the presentation of the data.

ii) Inspection of the Scattergram of CI versus Sinus Period

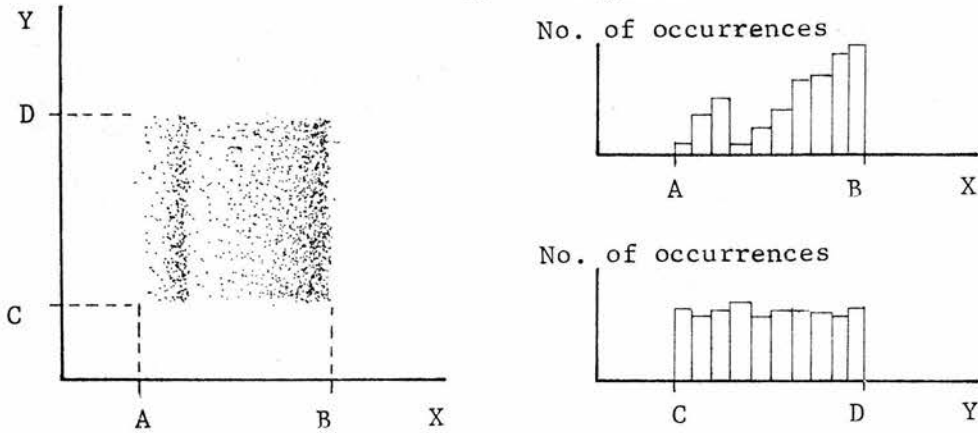
When dealing with the expected characteristics of the X-Y plot for sinus-locked and pure parasystolic hypotheses it was argued that neither mechanism acting in its purest form would produce significant patterns in the X-Y plot. It was pointed out that real sinus-locked mechanisms may be characterized by inter-dependent CIs and sinus periods but that the expected degree of interaction in the X-Y plot is not well defined. Pure parasystole could very occasionally induce a -1 slope but in general it should not produce any significant pattern when the CI and sinus period histograms are taken into account. Under these circumstances there seems little point in calculating the exact statistical significance of X-Y plots. The results could only be used to reject the hypothesis that there is no patterning and this would only advocate the rejec-

Fig. IV, 1: Three scattergrams having no systematic relationship between the X and Y variables. The difference in the patterns results from the different marginal distributions.

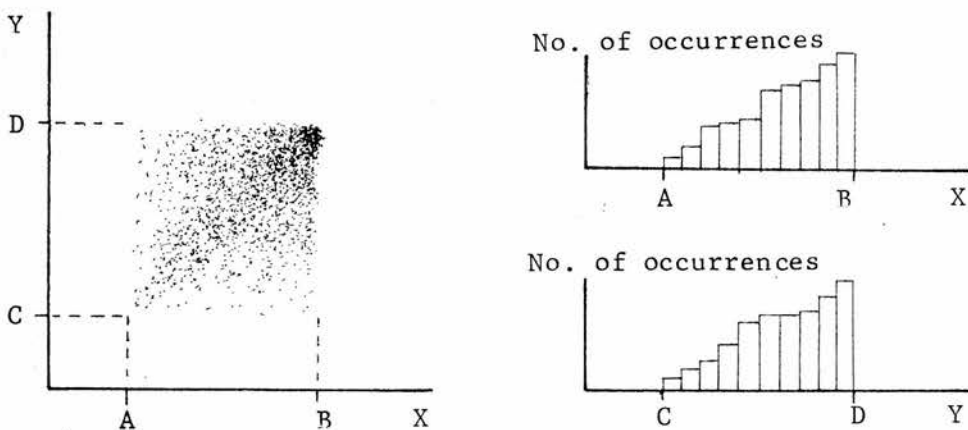
a) Marginal Distributions: both rectangular.



b) Marginal Distributions: X: "double ramp" Y: rectangular



c) Marginal Distributions: both "ramped".



tion of pure parasystole as the underlying mechanism. In addition it is not possible to set an exact significance level (1% say) that warrants the rejection of a sinus-locked hypothesis. Setting this level would be arbitrary, since it would be based on those aspects of the sinus-locked hypotheses which have not, up till now, been properly defined.

Interpretation by scrutiny of the original data is the only alternative. Appendix II contains two statistical techniques for examining the significance of X-Y plots. The first of these calculates the actual significance level and so is inappropriate for present purposes. The second is based on the principles of the first but relies on visual examination of the original X-Y plot and merely gives the observer a ready means for carrying out this examination. It is then up to the observer to accept or reject the sinus-locked and parasystolic hypotheses on the basis of his own concepts of these mechanisms. The X-Y plots presented later in this chapter are examined and interpreted in terms of this second test.

The rationale behind the second test is as follows: each X-Y plot has its own CI and sinus period distribution. These are the marginal distributions. For an observer to judge a particular X-Y plot as being patterned (i.e. to conclude that there is interaction between X and Y) he should have a clear visual notion of what a non-patterned plot having the same marginal distributions would look like. (This was pointed out in the discussion of the X-Y plots expected from parasystole.) Without this he may be led into believing there to be interaction where there is none. For example, the three plots in Fig. IV,1 all have no X versus Y interaction. The apparent correlation in Fig. IV,1c is a consequence of the ramp-like marginal distributions. In order to enable valid assessment of the measured X-Y plots, each one is presented along with a fictitious, randomly generated scattergram which is constructed in such a way as to have marginal distributions similar to the X-Y plot under investigation. Hence the randomly generated plot represents what the measured plot would look like had there been no X-Y interaction. Comparison of the two plots then provides a valid basis for making a visual judgement of

the degree and type of interaction between the CI and sinus period. On this basis each X-Y plot is discussed in relation to its randomly generated companion. The technique for generating the fictitious plots (Appendix II) takes into account the fact that CIs greater than the sinus period can not arise. As in the real data this gives an upper boundary line of slope +1 passing through the origin above which points do not occur.

The measured X-Y plot incorporates only those sinus periods which occur immediately prior to the appearance of a V.E.C. The random plot, on the other hand, uses all the sinus periods in the examined section of the ECG. Thus if V.E.Cs appear only when the sinus period takes on certain values this will be manifest in the measured plot but not in the fictitious one. This type of restriction on the behaviour of the CI is then revealed by comparing the plots.

It should be noted that the forms of the marginal distributions have no bearing on the validity of these tests, hence they may be used in situations where correlation or regression analysis would be invalid - if this were not so, the tests given in Appendix II would not be applicable to the data presented later in this chapter.

iii) Inspection of the Histogram of Inter-Ectopic Numbers

It will be argued that most of the N histograms presented are incompatible with simple sinus-locked hypotheses because they each contain more than one peak. This raises the problem of what is meant by a peak. The answer to this question can not be given in quantitative or statistical terms unless a great deal is known about the supposed underlying mechanism. In particular, the laws governing the expected spontaneous variations in the heights of adjacent bins in the histogram are unknown for sinus-locked mechanisms. As a result there is no way of estimating if the comparison of the number of counts in adjacent bins (or any two bins) is significantly different to that expected from a sinus-locked mechanism. There must be some precise a priori statement of the degree of peakiness expected, otherwise there is no basis for

interpreting the observed histograms. In other words, any statistical interpretation must begin by setting up a null hypothesis, H_0 , associated with the mechanism in question. H_0 could take one of many forms, e.g. Gaussian, rectangular, exponential etc. Only then can the observed distributions be said to contain peaks incompatible with H_0 at some specific level of significance. If the assumed form of the expected distribution is incorrect then the results of such a test would be invalid.

A way round this problem is to make H_0 so loose a description of the expected properties of the N histogram that there could be no reasonable objection to it. Unfortunately this may give a very conservative estimate of the significance of the data. Indeed, this was felt to be so for several tests which were used to evaluate some of the N histograms presented later in this chapter. It was concluded that these histograms could not be assessed quantitatively in terms of the sinus-locked hypothesis.

To sum up, there is a trade off between the power of a statistical test and our certainty of its validity. Since the validity of any strong quantitative test which attempts to reject a sinus-locked hypothesis is open to possible objection, such tests are not used. On the other hand, any all-embracing test is weakened by the fact that it does not use all the information available in the data. Thus it was decided to present the N histograms without quantifying their obvious inconsistency with the sinus-locked theories.

The Anomalous Nature of Arrhythmias
Containing Single V.E.Cs

Selection and Presentation of Cases.

The tests devised in the previous section will be used to demonstrate the inadequacy of both simple sinus-locked and pure parasystolic hypotheses as explanations of the origin of all single V.E.Cs arising in diseased hearts. The material examined for this purpose came from the Coronary Care Unit, Edinburgh Royal Infirmary, and was collected by C.W. Vellani,

Department of Medicine, over a period of four months. In the first instance cases were selected on the sole criterion that they contained single V.E.Cs. A continuous recording of 24, 48 or 72 hours was taken from each of 100 such cases. Of these, 39 had runs of frequent V.E.Cs, i.e. more than 10 per minute. These 39 records were further examined in the X-Y plot and it was found that at least 12 showed patterning. These 12 cases are presented in this chapter. It is felt that nearly one in three (i.e. 12 in 39) cases having strong X-Y patterns is highly significant since patterning of the type observed is not expected. In addition, for a pattern to build up, the physiological parameters determining it must remain constant, otherwise various patterns are superimposed all obscuring one another's features - the overall effect may be totally indistinct, and for this reason some strong interactions between CIs and sinus periods may have gone unobserved. Indeed it was often felt that one was watching a sequence of short-lived patterns develop into an inconsequential picture. (For reasons of expediency it was decided not to illustrate this impression.) Therefore it is almost certain that more than 12 of the 39 cases studied had strong interaction between the CI and sinus period.

One X-Y plot was taken for each of the 12 cases. The CI and sinus period histograms were accumulated on a re-run of the relevant section of magnetic tape, and the N histogram was accumulated on a further re-run. The means and variances of the CI and sinus period histograms are not presented since they are of no direct use and, if quoted, could give the impression that the processes underlying these histograms are assumed to be statistically stationary. No such assumption has been made although a strong X-Y pattern is probably indicative of statistical stationariness.

Using the first test devised in the last section it is found that each of the CI histograms may be rejected as coming from pure parasystole at something more significant than the 0.1% level. In accordance with the second test a fictitious randomly generated X-Y plot is formed from the CI and sinus

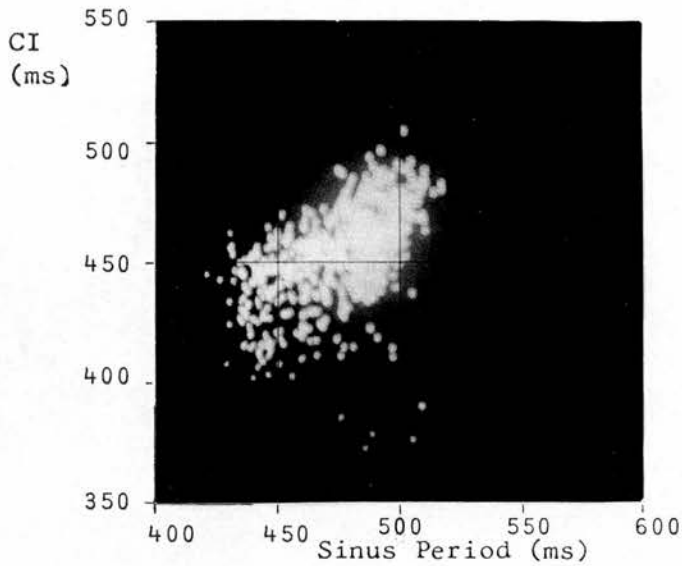
period histograms. This is presented along with the measured X-Y plot in order to examine the degree and type of interaction between the CI and sinus period. Finally, interpretation of the N histogram is entirely descriptive as it would seem to be obvious when a histogram shows multiple peaks incompatible with a sinus-locked mechanism. Each case is discussed separately.

To sum up, 39 ECGs with frequent V.E.Cs were selected on a random basis from the Coronary Care Unit in the Edinburgh Royal Infirmary. Of these, 12 were found to have an interaction between the CI and sinus period. A section of ECG was chosen from each of these cases on the basis of the X-Y plot alone. Only then were the CI, sinus period and N histograms accumulated and examined. Each of these cases is examined for the following anomaly: CI histogram incompatible with pure parasystole; X-Y plot incompatible with pure parasystole and simple sinus-locking; N histogram incompatible with simple sinus-locking.

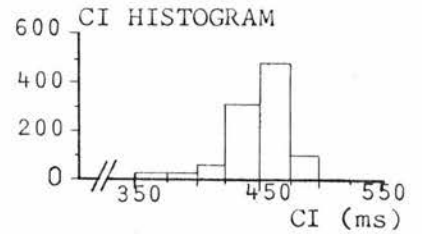
All interpretation of the data is based on the theories of pure parasystole and the simple sinus-locked mechanisms considered hitherto. More complex mechanisms are considered in Parts II and III of this thesis.

CASE 1

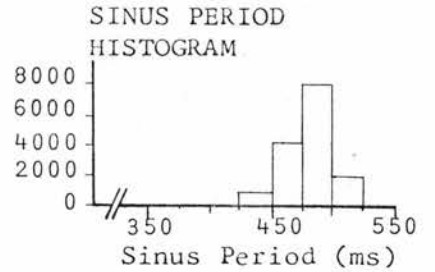
MEASURED X-Y PLOT AND HISTOGRAMS



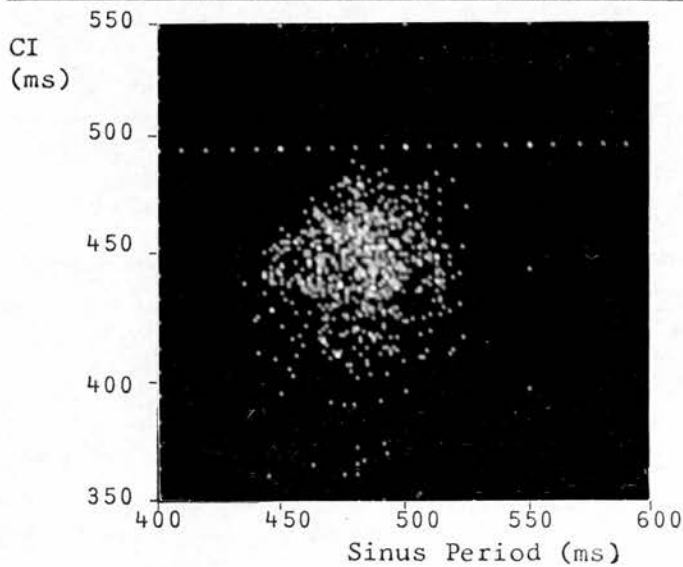
No. of
VEC



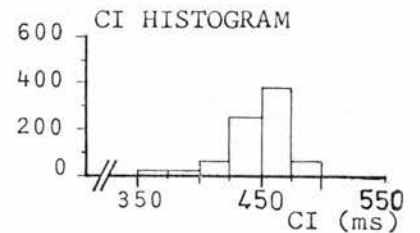
No. of
Sinus
Periods



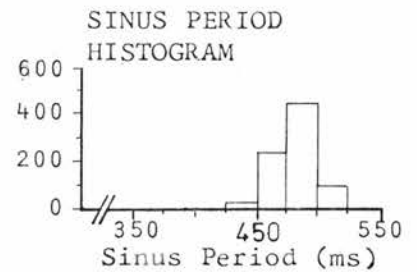
RANDOMLY GENERATED X-Y PLOT AND HISTOGRAMS



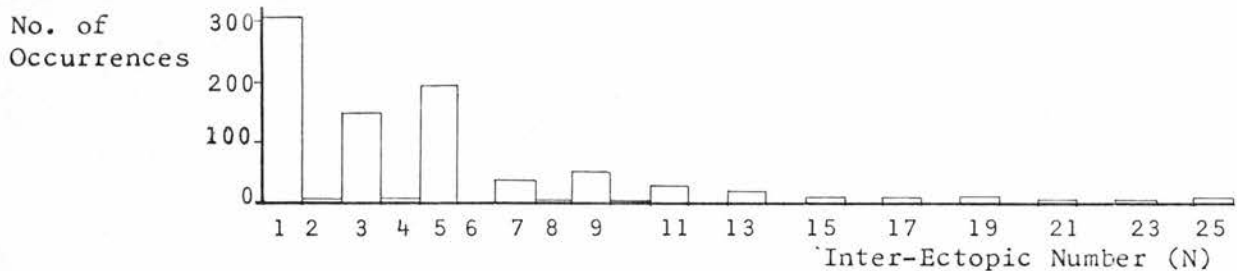
No. of
VEC



No. of
Sinus
Periods

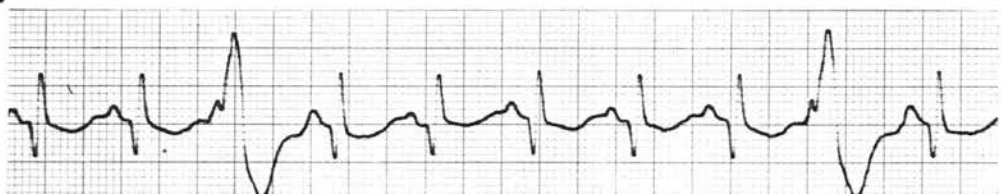


MEASURED HISTOGRAM OF INTER-ECTOPIC NUMBERS



SAMPLE OF E.C.G.

(25 mm/s)



CASE 1

CI Histogram: Incompatible with pure parasystole.

X-Y Plot: Number of points in measured plot = 988
Number of points in random plot = 800

In addition to the upper boundary line resulting from the restriction on the maximum size of the CI (see Appendix II), the measured plot has a highly defined shape which is not present in the random plot. It is felt that such strong interaction between the CI and sinus period is incompatible with both pure parasystole and simple sinus-locked mechanisms.

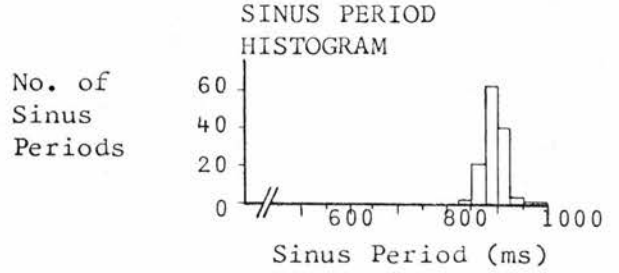
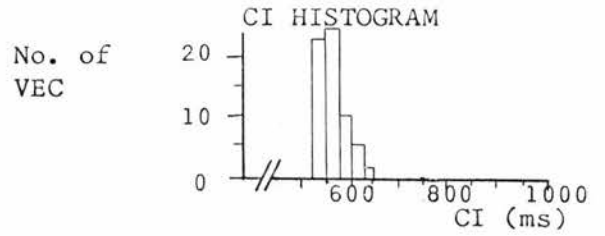
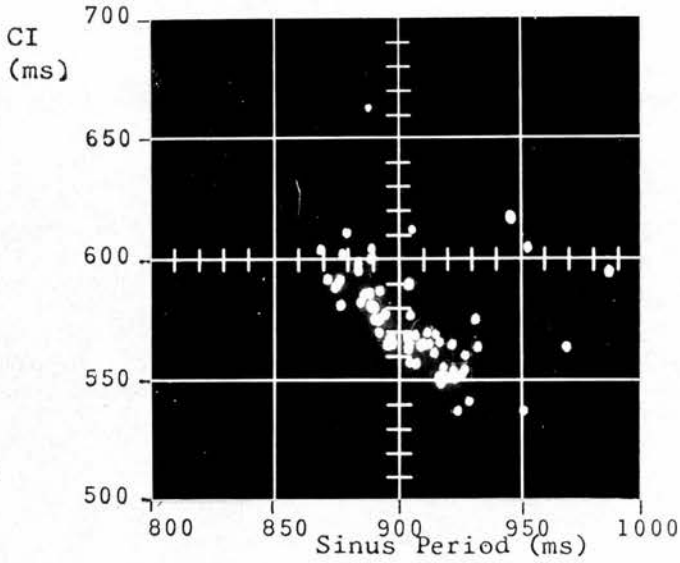
N Histogram: Very strong multiple peaks (imperfect concealed bigeminy) incompatible with a simple sinus-locked mechanism.

Conclusions:

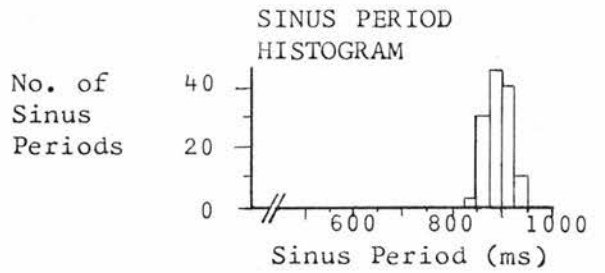
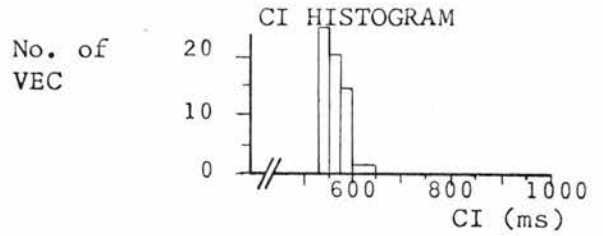
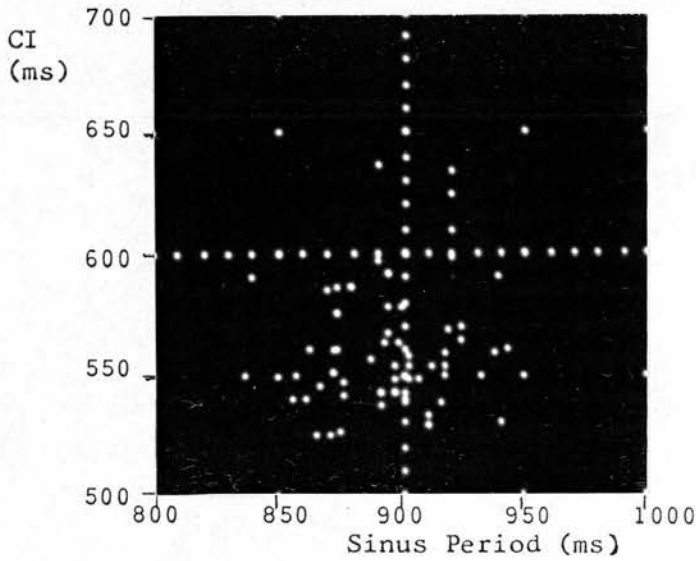
- i) Taken together, the CI and N histograms cannot be interpreted consistently in terms of either pure parasystole or simple sinus-locking.
- ii) The X-Y plot cannot readily be interpreted in terms of either pure parasystole or simple sinus-locking.

CASE 2

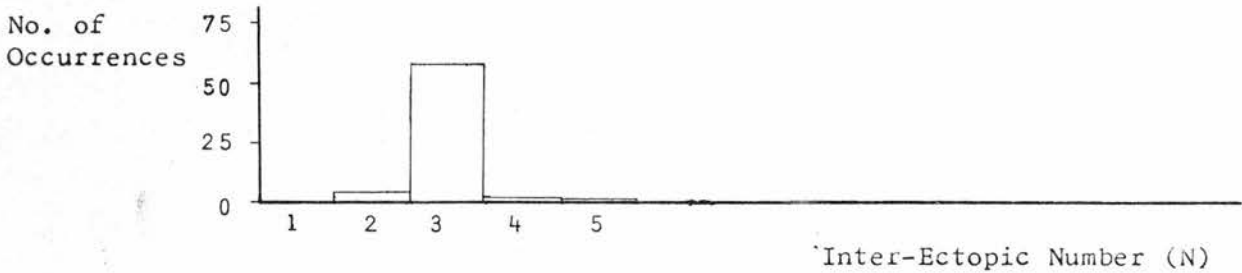
MEASURED X-Y PLOT AND HISTOGRAMS



RANDOMLY GENERATED X-Y PLOT AND HISTOGRAMS

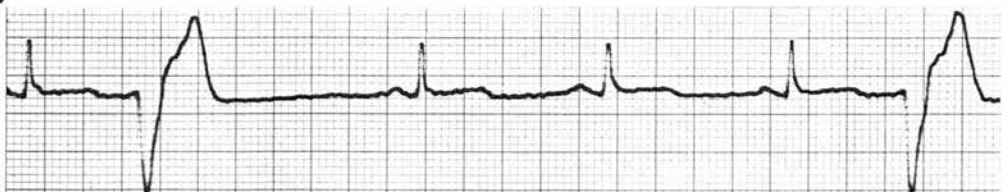


MEASURED HISTOGRAM OF INTER-ECTOPIC NUMBERS



SAMPLE OF E.C.G.

(25 mm/s)



CASE 2

CI Histogram: Incompatible with pure parasystole.

X-Y Plot: Number of points in measured plot = 66
Number of points in random plot = 66

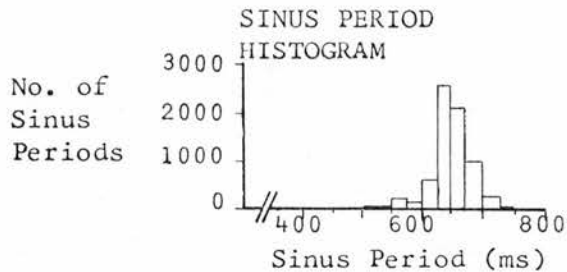
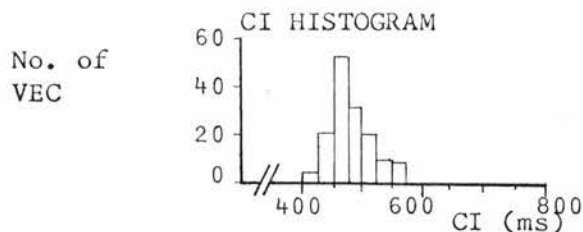
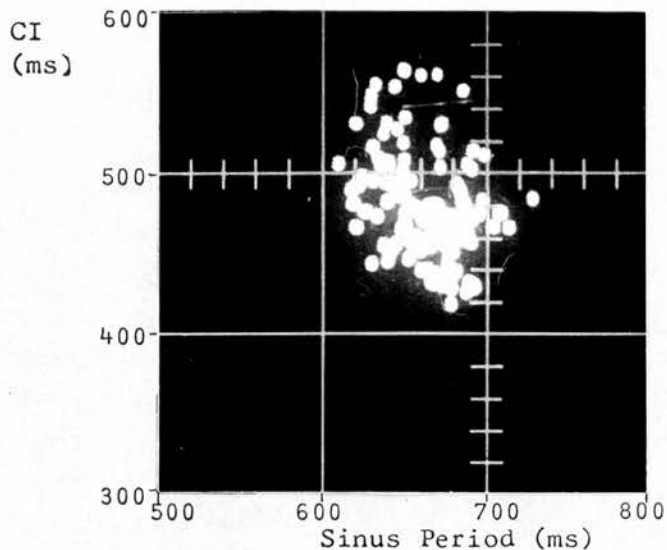
A strong pattern in the measured plot, no hint of which appears in the random plot - incompatible with both pure parasystole and simple sinus-locked mechanisms.

N Histogram: One central peak compatible with the sinus-locked hypotheses and parasystole.

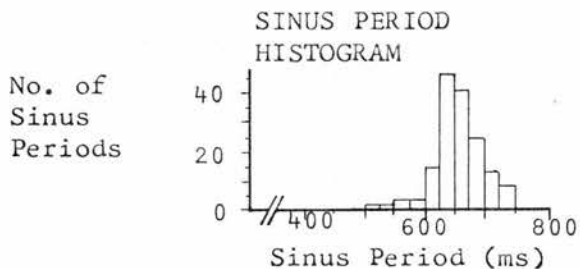
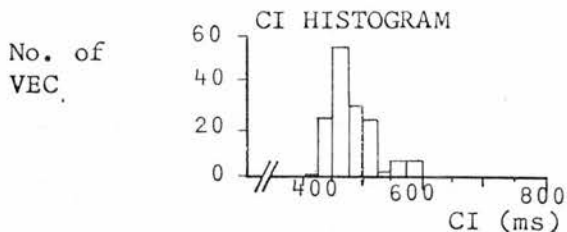
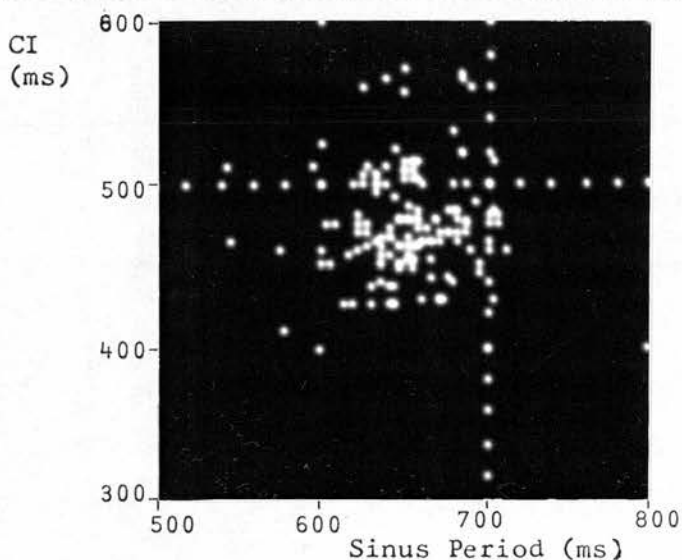
Conclusions: X-Y plot cannot readily be explained.

CASE 3

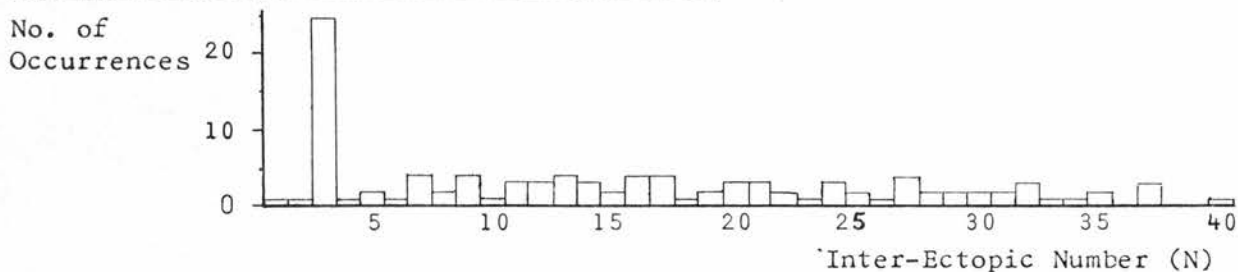
MEASURED X-Y PLOT AND HISTOGRAMS



RANDOMLY GENERATED X-Y PLOT AND HISTOGRAMS

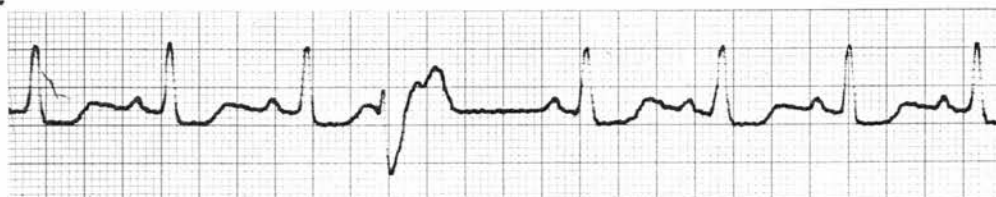


MEASURED HISTOGRAM OF INTER-ECTOPIC NUMBERS



SAMPLE OF E.C.G.

(25 mm/s)



CASE 3

CI Histogram: Incompatible with pure parasystole.

X-Y Plot: Number of points in measured plot = 142
Number of points in random plot = 142

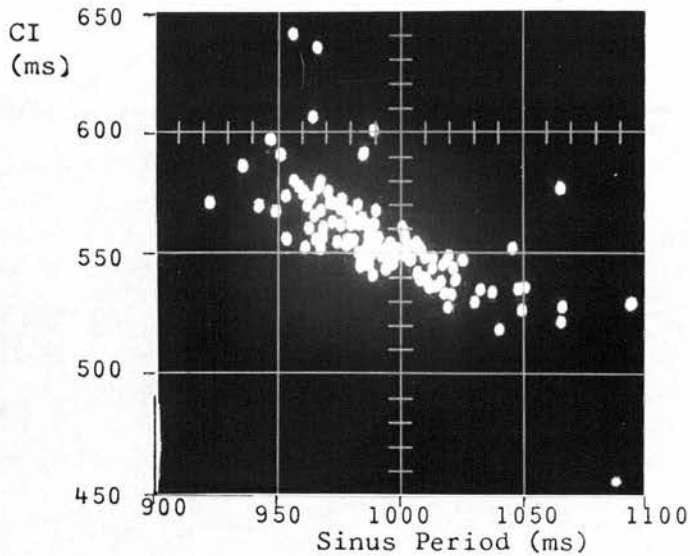
The random plot does not have a lower boundary line whereas the measured plot does (slope ≈ -1). The measured plot is more confined than the random one.

N Histogram: One central peak compatible with the sinus-locked hypotheses and parasystole.

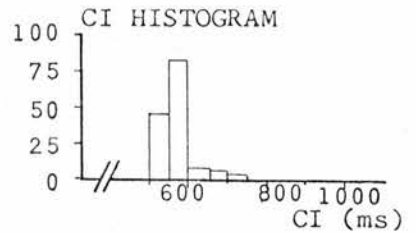
Conclusions: X-Y plot cannot readily be explained.

CASE 4

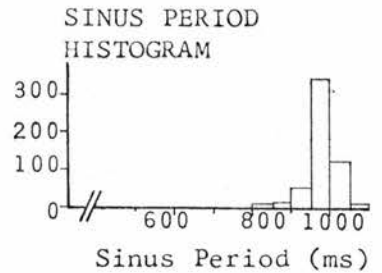
MEASURED X-Y PLOT AND HISTOGRAMS



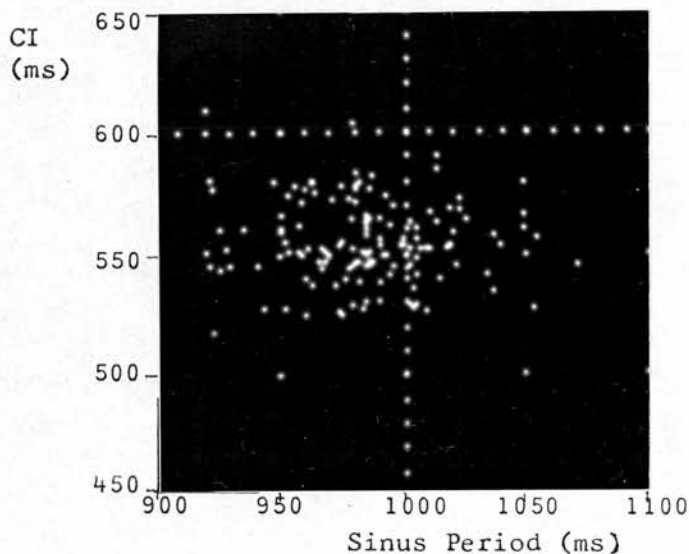
No. of
VEC



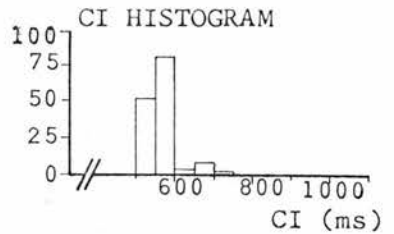
No. of
Sinus
Periods



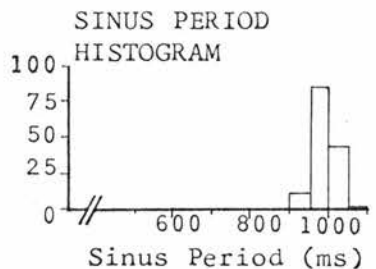
RANDOMLY GENERATED X-Y PLOT AND HISTOGRAMS



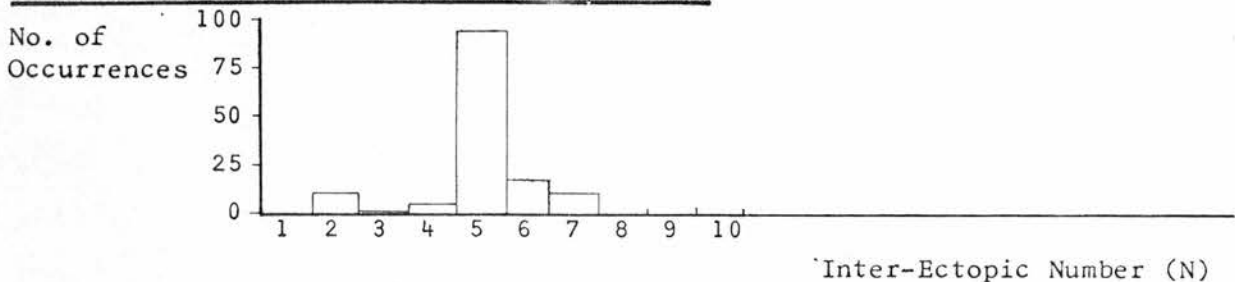
No. of
VEC



No. of
Sinus
Periods

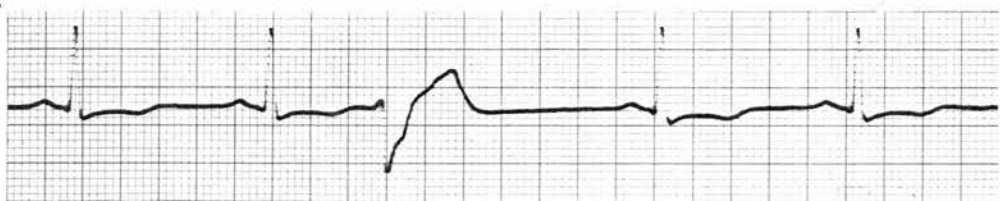


MEASURED HISTOGRAM OF INTER-ECTOPIC NUMBERS



SAMPLE OF E.C.G.

(25 mm/s)



CASE 4

CI Histogram: Incompatible with pure parasystole.

X-Y plot: Number of points in measured plot = 144
Number of points in random plot = 144
Very strong patterning present.

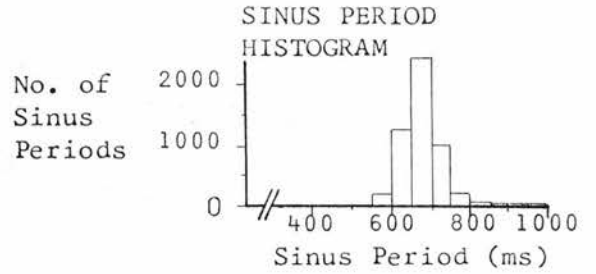
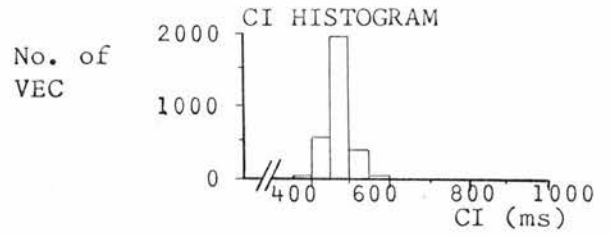
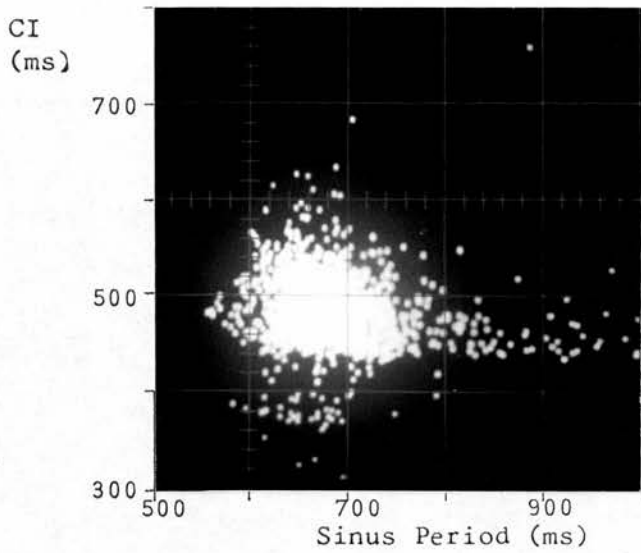
N Histogram: A double peak incompatible with simple sinus-locking.

Conclusions:

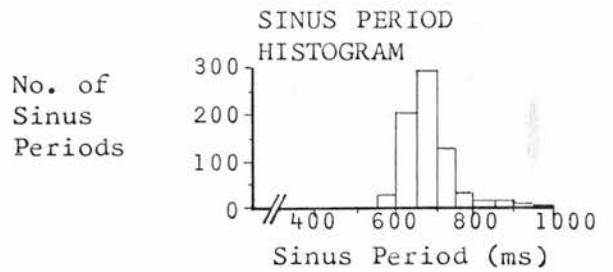
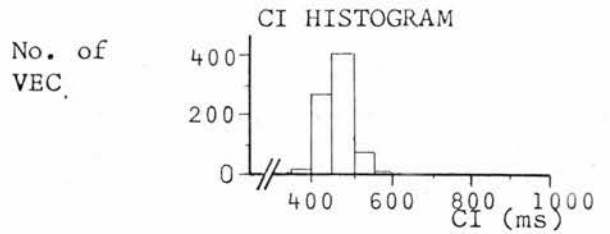
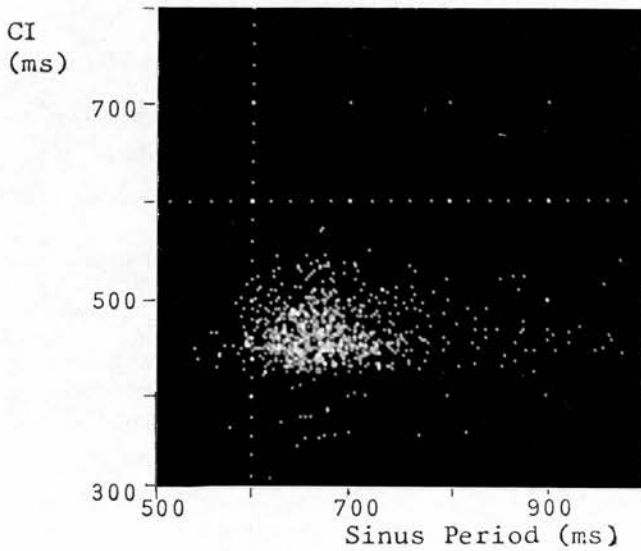
- i) CI and N histograms inconsistent.
- ii) X-Y plot cannot readily be explained.

CASE 5

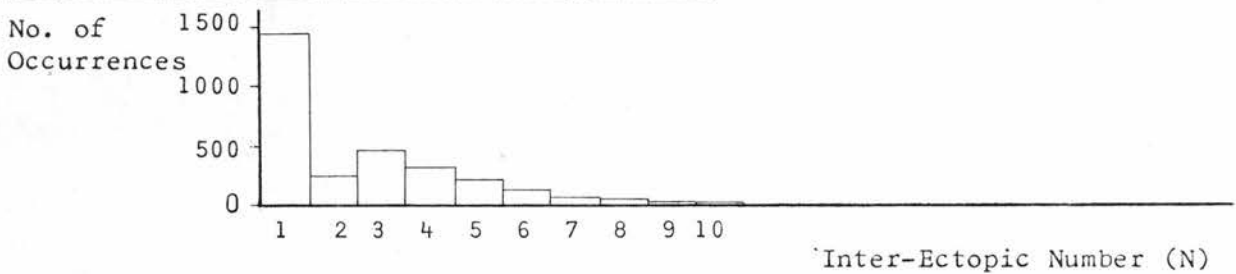
MEASURED X-Y PLOT AND HISTOGRAMS



RANDOMLY GENERATED X-Y PLOT AND HISTOGRAMS

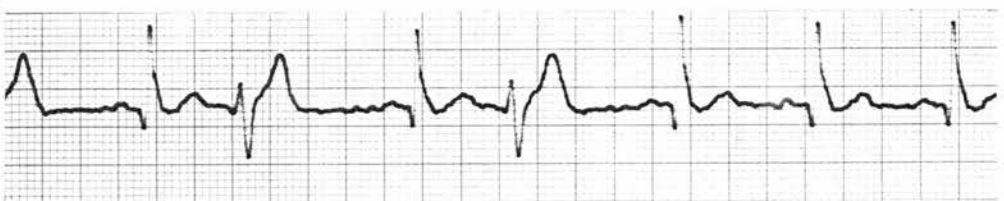


MEASURED HISTOGRAM OF INTER-ECTOPIC NUMBERS



SAMPLE OF E.C.G.

(25 mm/s)



CASE 5

CI Histogram: Incompatible with pure parasystole.

X-Y Plot: Number of points in measured plot = 3044
Number of points in random plot = 833

Although there is a tendency towards confinement in the random plot it is not as severe as in the measured plot. (If the density of points in the random plot is everywhere multiplied by 4 so that the total number of points is the same for both plots, then the right hand tail of the random plot would contain more points than the tail of the measured plot.)

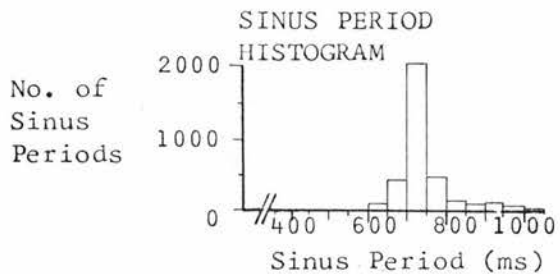
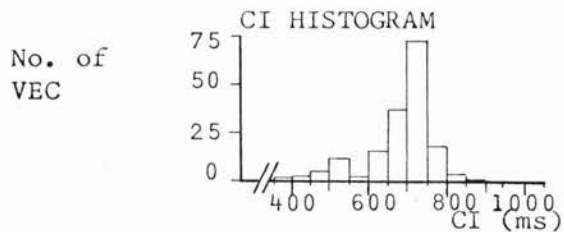
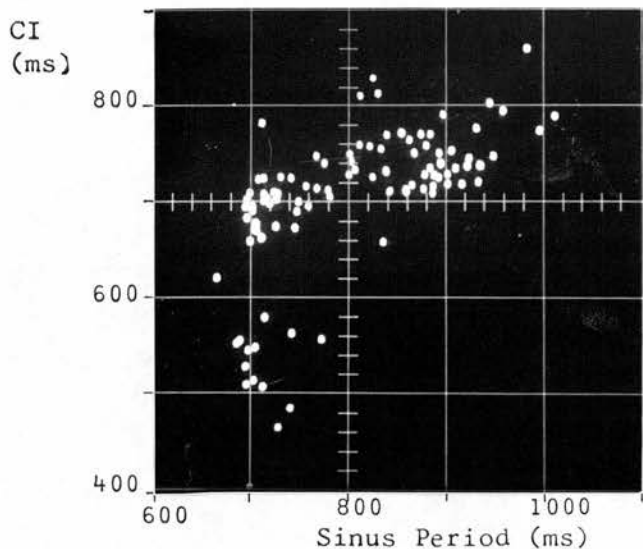
This is an excellent illustration of the use of the random plot: without it one might conclude that the lower horizontal boundary is significant - this is not so as is shown by a similar boundary in the random plot.

N Histogram: One central peak compatible with the sinus-locked hypotheses and parasystole.

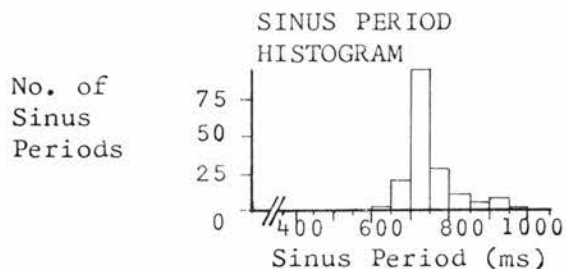
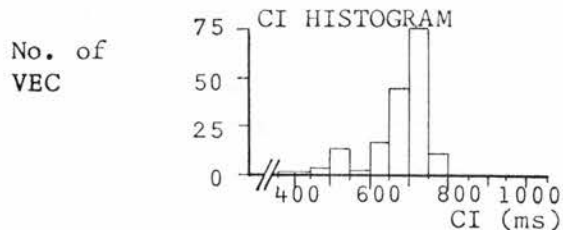
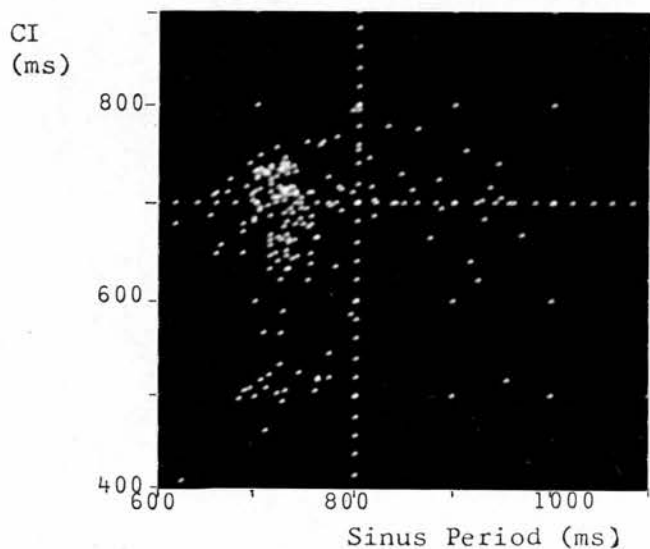
Conclusions: X-Y plot cannot readily be explained.

CASE 6

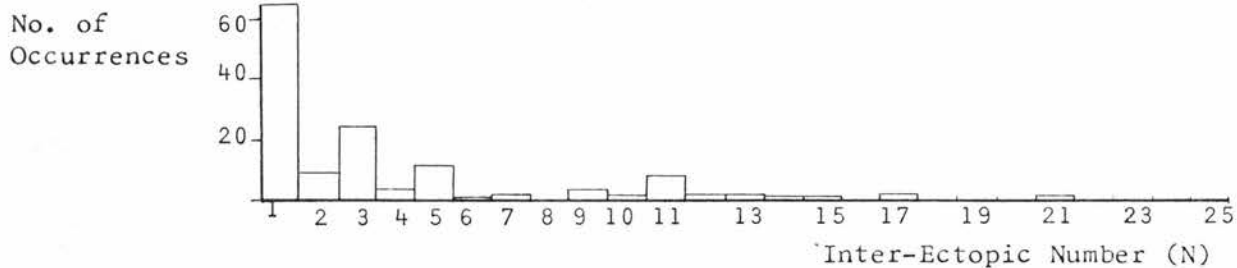
MEASURED X-Y PLOT AND HISTOGRAMS



RANDOMLY GENERATED X-Y PLOT AND HISTOGRAMS



MEASURED HISTOGRAM OF INTER-ECTOPIC NUMBERS



SAMPLE OF E.C.G.

(25 mm/s)



CASE 6

CI Histogram: Incompatible with pure parasystole.

X-Y Plot: Number of points in measured plot = 172
Number of points in random plot = 172

The measured plot shows less scatter (i.e. more patterning) than the random plot.

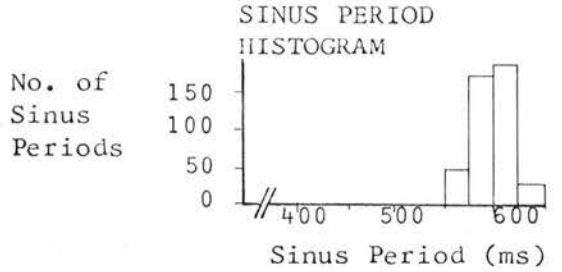
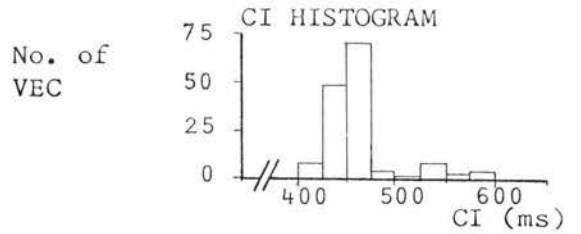
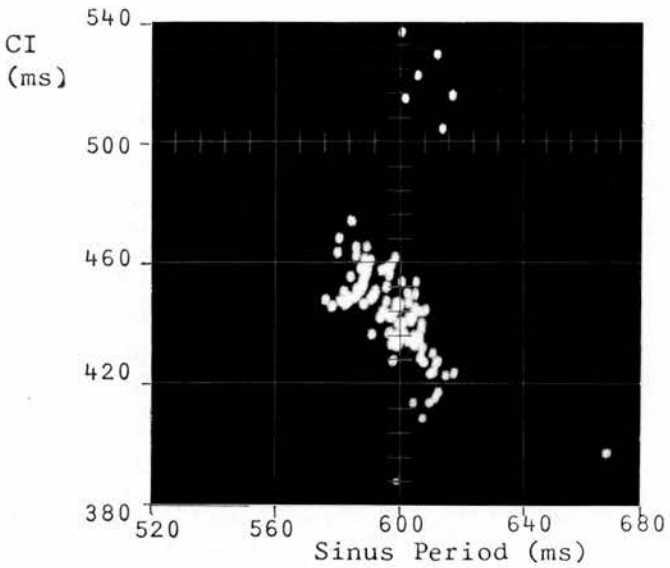
N Histogram: Strong multiple peaks (imperfect concealed bigeminy) incompatible with simple sinus-locked mechanisms.

Conclusions:

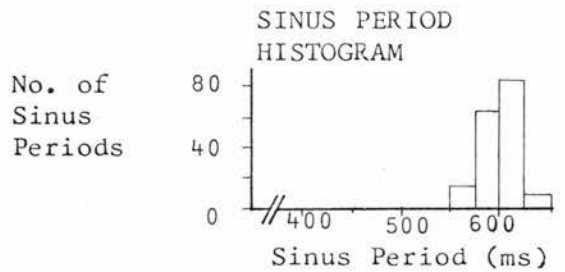
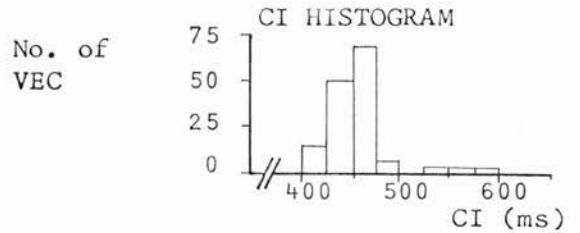
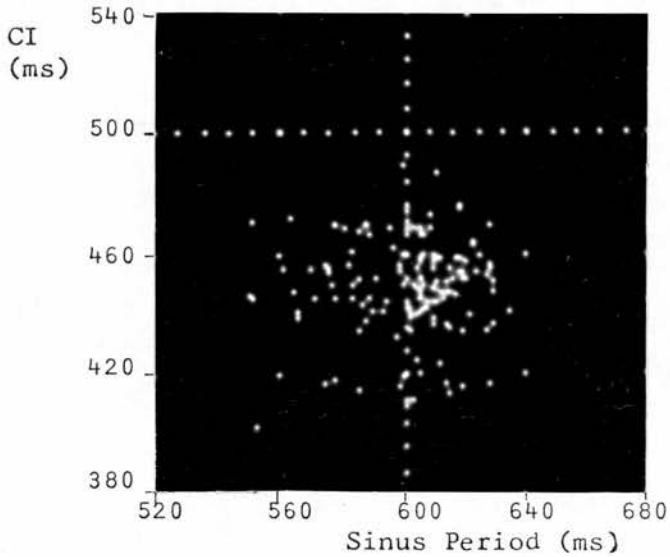
- i) CI and N histograms inconsistent.
- ii) X-Y plot cannot readily be explained.

CASE 7

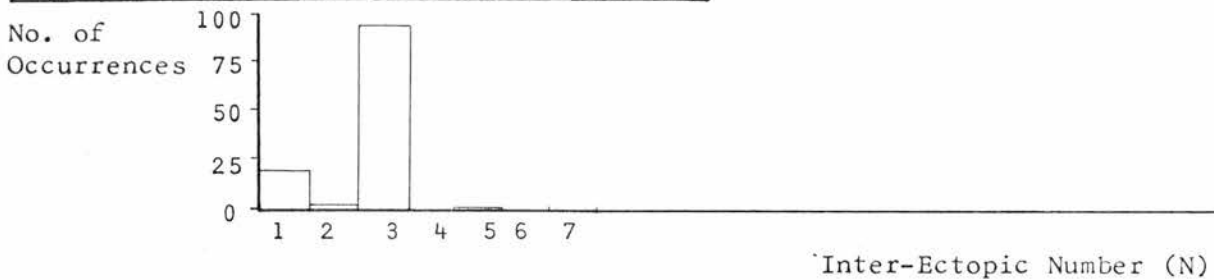
MEASURED X-Y PLOT AND HISTOGRAMS



RANDOMLY GENERATED X-Y PLOT AND HISTOGRAMS

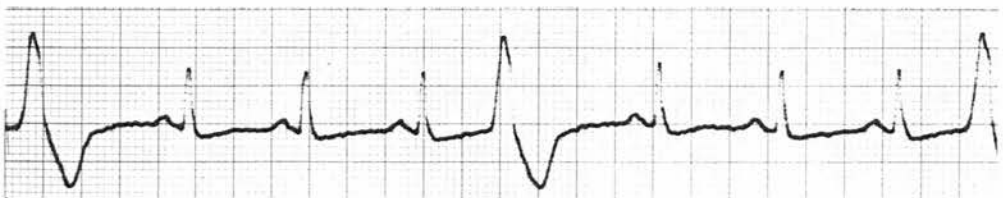


MEASURED HISTOGRAM OF INTER-ECTOPIC NUMBERS



SAMPLE OF E.C.G.

(25 mm/s)



CASE 7

CI Histogram: Incompatible with pure parasystole.

X-Y Plot: Number of points in measured plot = 147
Number of points in random plot = 147

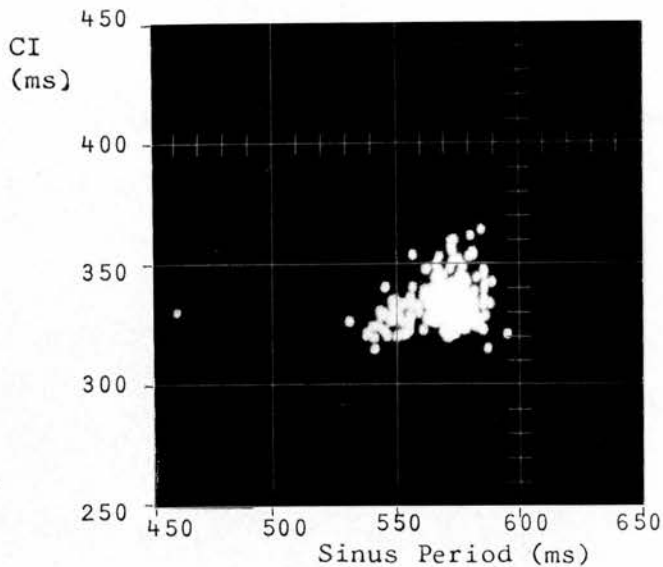
Very strong interaction between the CI and sinus period.

N Histogram: A strong double peak (nearly perfect concealed bigeminy) incompatible with simple sinus-locking.

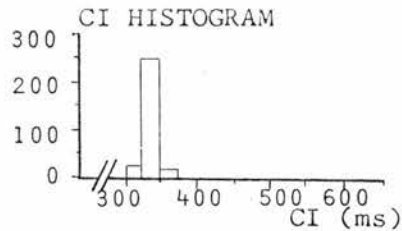
Conclusions: i) CI and N histograms inconsistent.
ii) X-Y plot cannot readily be explained.

CASE 8

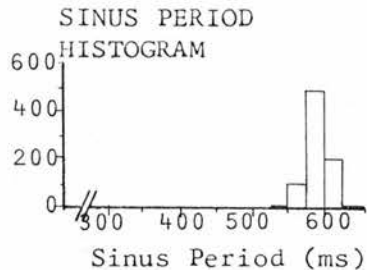
MEASURED X-Y PLOT AND HISTOGRAMS



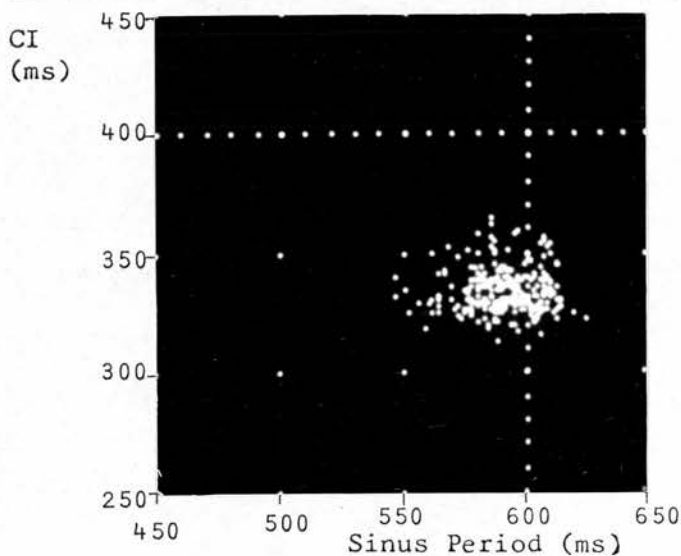
No. of VEC



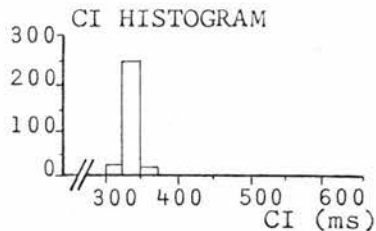
No. of Sinus Periods



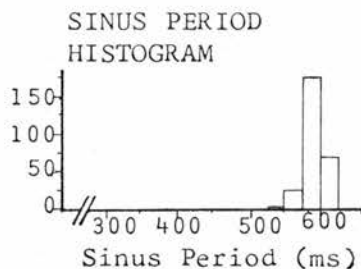
RANDOMLY GENERATED X-Y PLOT AND HISTOGRAMS



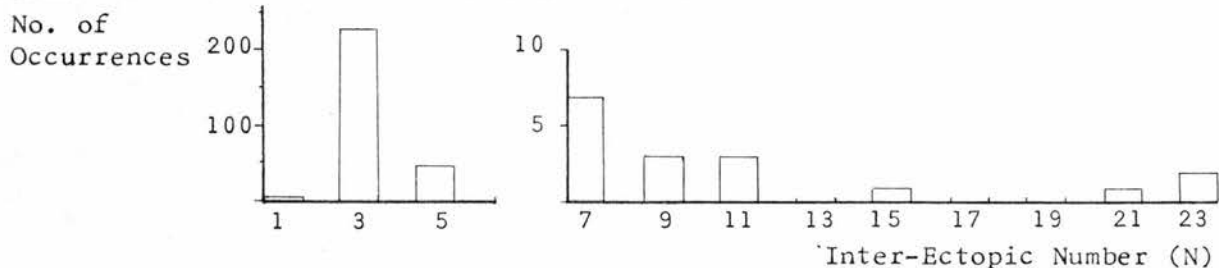
No. of VEC



No. of Sinus Periods

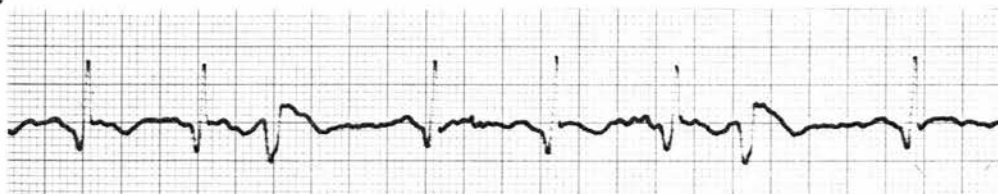


MEASURED HISTOGRAM OF INTER-ECTOPIC NUMBERS



SAMPLE OF E.C.G.

(25 mm/s)



CASE 8

CI Histogram: Incompatible with pure parasystole.

X-Y Plot: Number of points in measured plot = 263
Number of points in random plot = 263

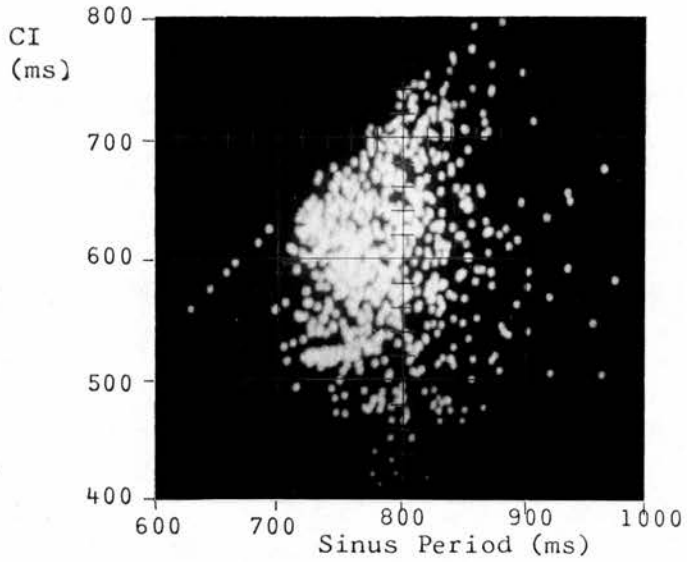
Strong patterning in the measured plot
some aspects of which are not shown in the
random plot.

N Histogram: Perfect concealed bigeminy incompatible with
simple sinus-locked mechanisms.

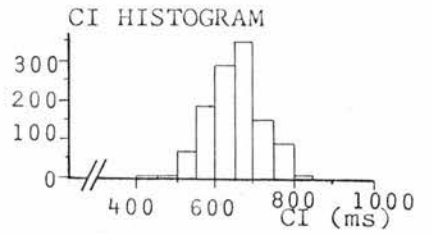
Conclusions: i) CI and N histograms inconsistent.
ii) X-Y plot cannot readily be explained.

CASE 9

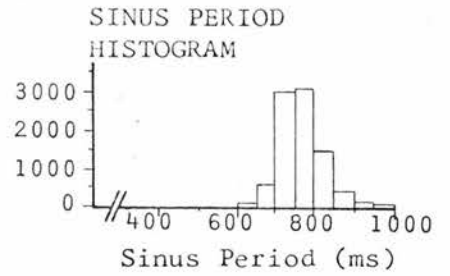
MEASURED X-Y PLOT AND HISTOGRAMS



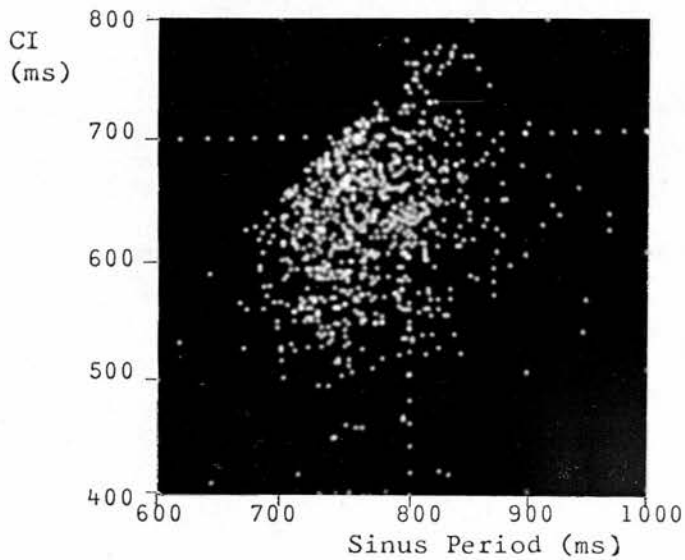
No. of VEC



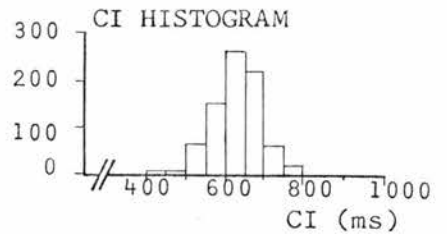
No. of Sinus Periods



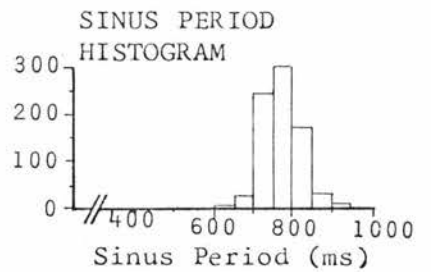
RANDOMLY GENERATED X-Y PLOT AND HISTOGRAMS



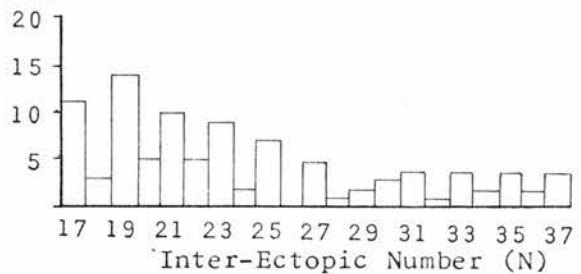
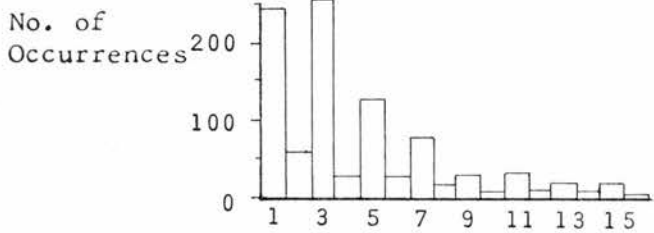
No. of VEC



No. of Sinus Periods

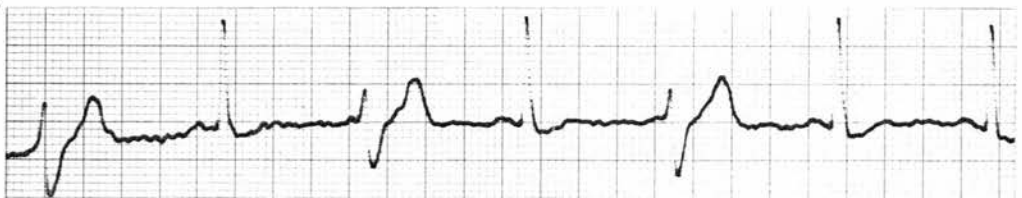


MEASURED HISTOGRAM OF INTER-ECTOPIC NUMBERS



SAMPLE OF E.C.G.

(25 mm/s)



CASE 9

CI Histogram: Incompatible with pure parasystole.

X-Y Plot: Number of points in measured plot = 1158
Number of points in random plot = 800

The strong patterning at the left side of the measured plot is not present in the random plot. (Note the usual upper boundary in both plots.)

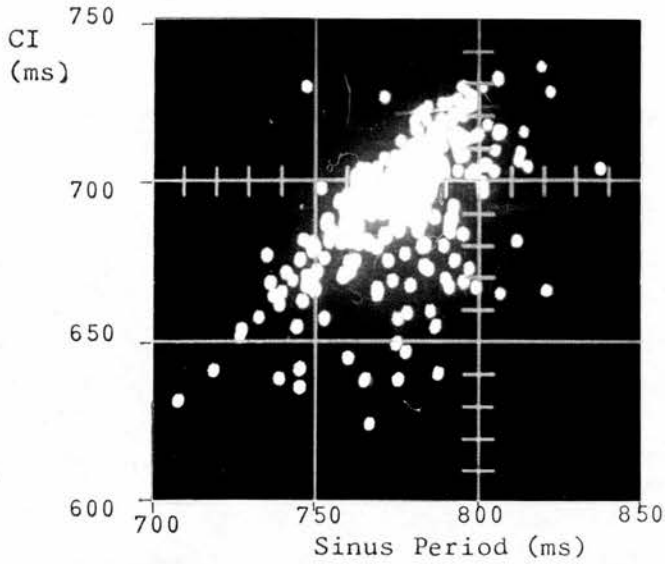
N Histogram: Multiple peaks incompatible with simple sinus-locked mechanisms.

Conclusions:

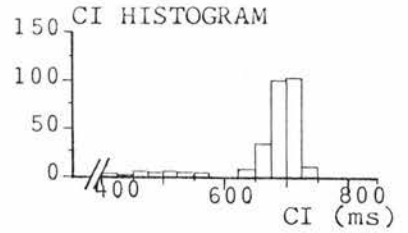
- i) CI and N histograms inconsistent.
- ii) X-Y plot shows some patterning probably incompatible with single sinus-locking and pure parasystole.

CASE 10

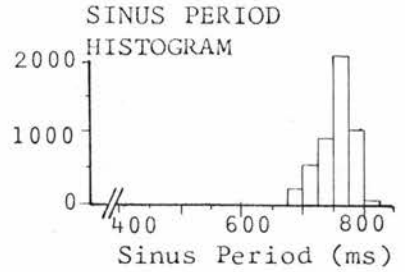
MEASURED X-Y PLOT AND HISTOGRAMS



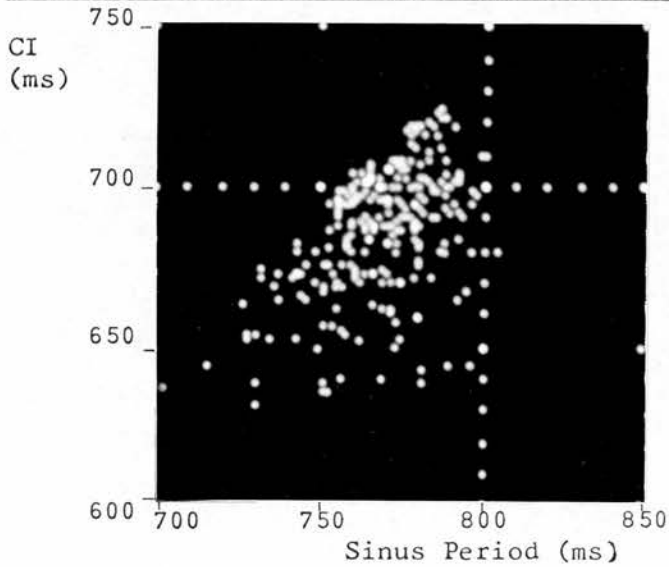
No. of
VEC



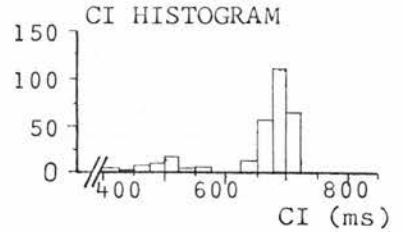
No. of
Sinus
Periods



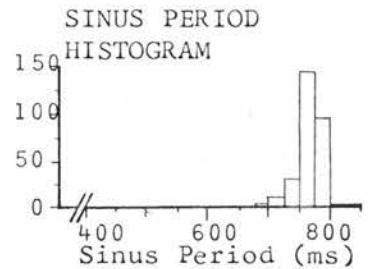
RANDOMLY GENERATED X-Y PLOT AND HISTOGRAMS



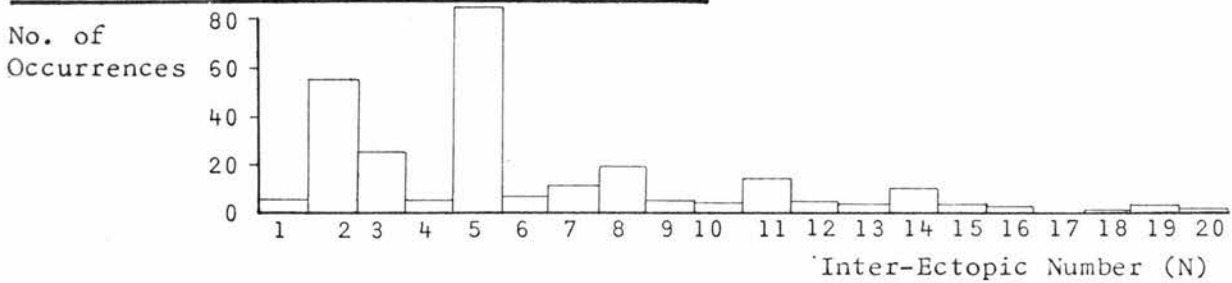
No. of
VEC



No. of
Sinus
Periods

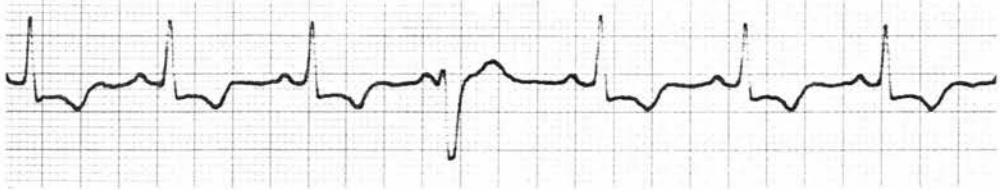


MEASURED HISTOGRAM OF INTER-ECTOPIC NUMBERS



SAMPLE OF E.C.G.

(25 mm/s)



CASE 10

CI Histogram: Incompatible with pure parasystole.

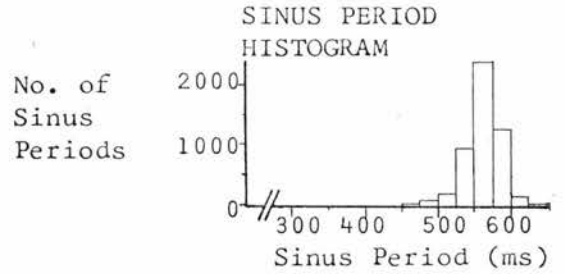
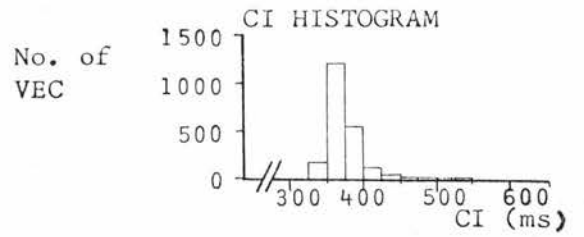
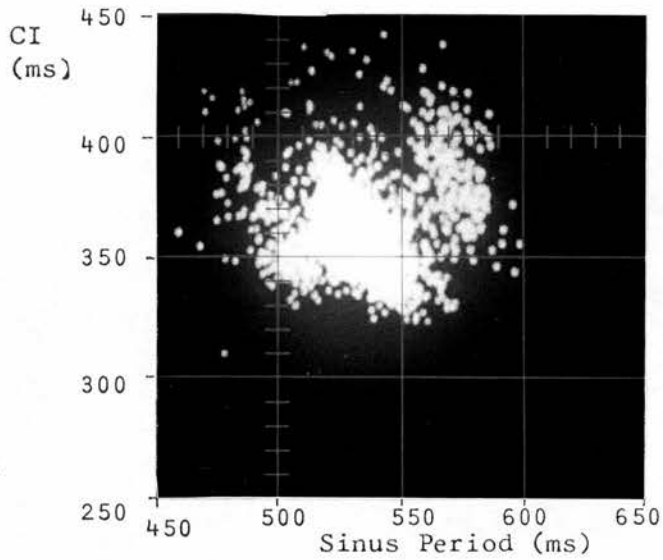
X-Y Plot: Number of points in measured plot = 299
Number of points in random plot = 299
Measured plot shows more restriction
than random plot.

N Histogram: Multiple peaks incompatible with simple
sinus-locking.

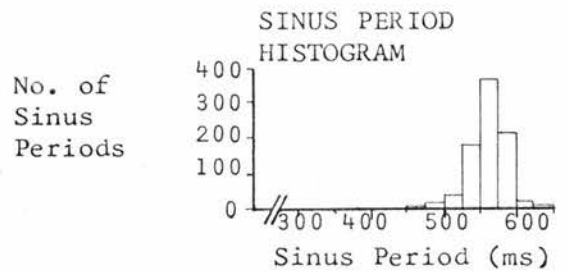
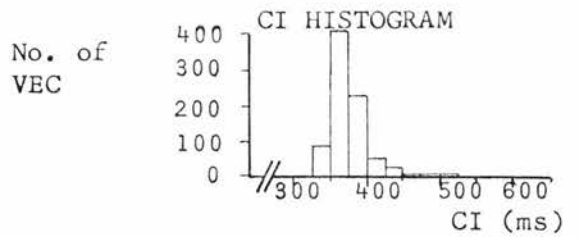
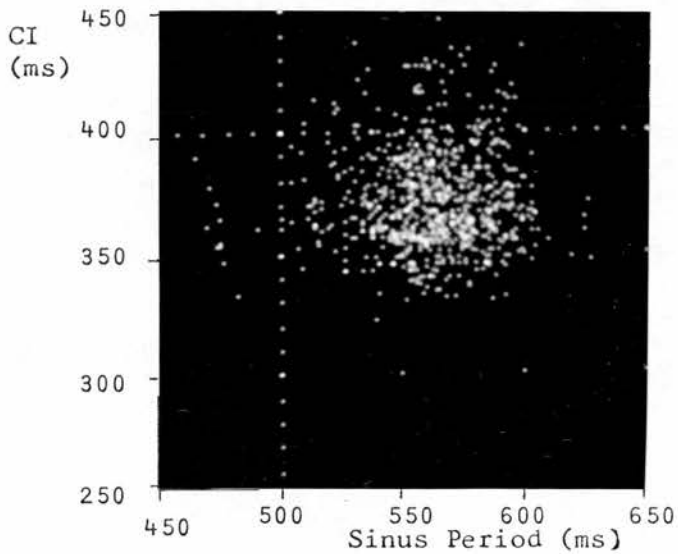
Conclusions: i) CI and N histograms inconsistent.
ii) X-Y plot shows some patterning probably
incompatible with simple sinus-locking
and pure parasystole.

CASE 11

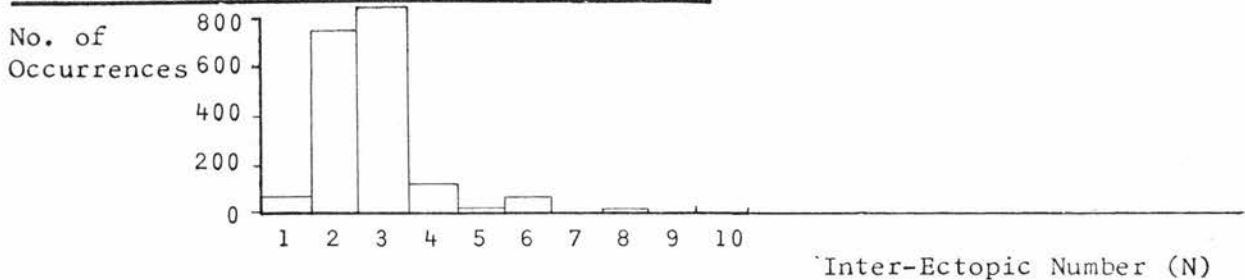
MEASURED X-Y PLOT AND HISTOGRAMS



RANDOMLY GENERATED X-Y PLOT AND HISTOGRAMS



MEASURED HISTOGRAM OF INTER-ECTOPIC NUMBERS



SAMPLE OF E.C.G.

(25 mm/s)



CASE 11

CI Histogram: Incompatible with pure parasystole.

X-Y Plot: Number of points in measured plot = 1941
Number of points in random plot = 800

Many of the sharp boundaries in the measured plot cannot be accounted for on the basis of chance since they are not reflected in the random plot. In particular there is absolutely no sign of an area of rarefaction in the random plot. The phenomenon of a "forbidden gap" is discussed further in the next section.

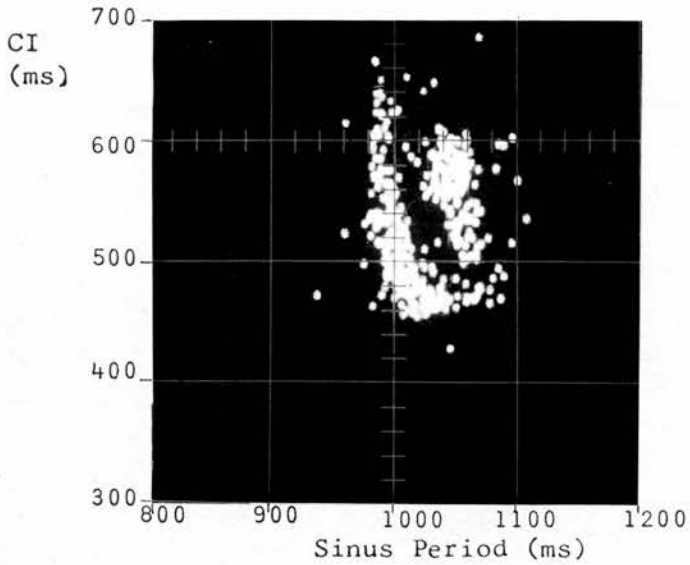
N Histogram: A tendency towards a double peak.

Conclusions:

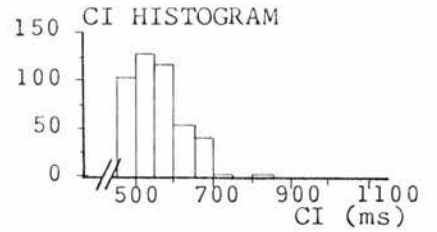
- i) Slight inconsistency between the CI and N histograms.
- ii) X-Y plot cannot readily be explained.

CASE 12

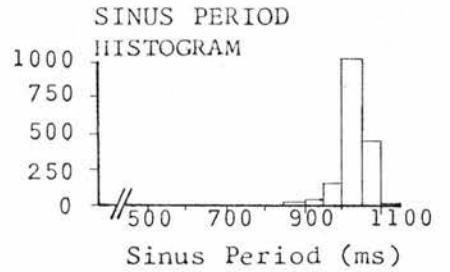
MEASURED X-Y PLOT AND HISTOGRAMS



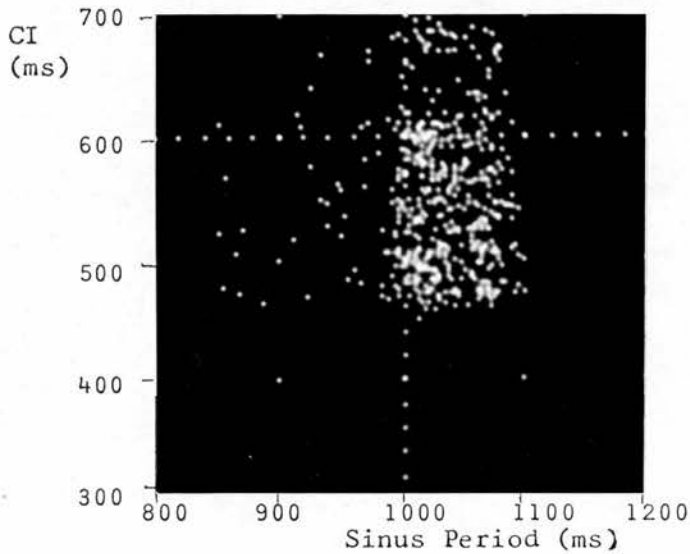
No. of VEC



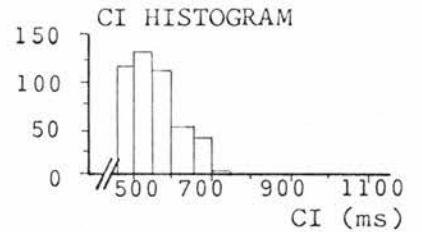
No. of Sinus Periods



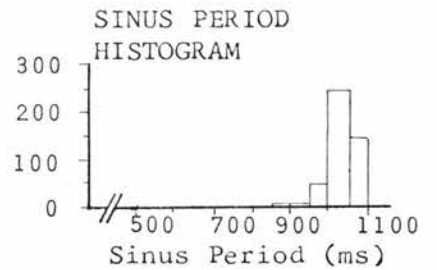
RANDOMLY GENERATED X-Y PLOT AND HISTOGRAMS



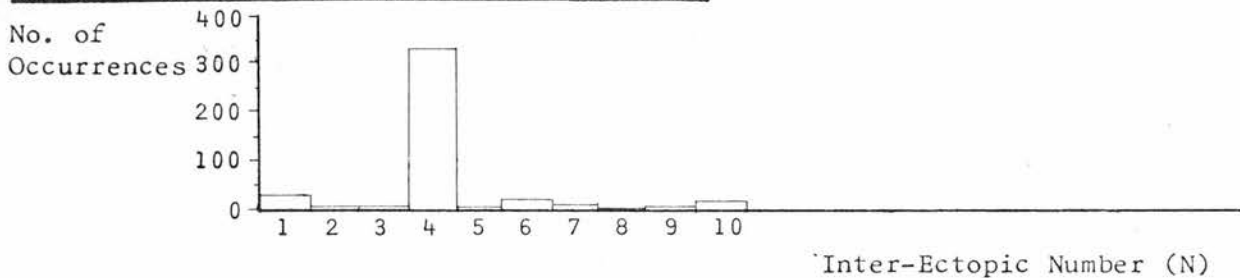
No. of VEC



No. of Sinus Periods

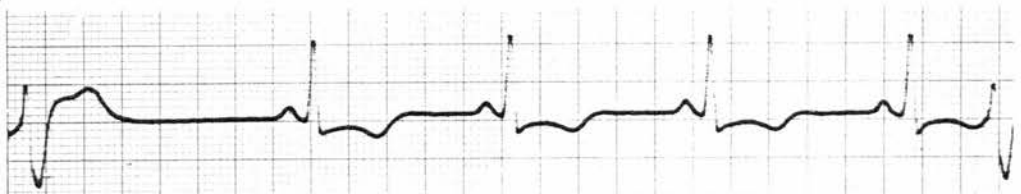


MEASURED HISTOGRAM OF INTER-ECTOPIC NUMBERS



SAMPLE OF E.C.G.

(25 mm/s)



CASE 12

CI Histogram: Incompatible with pure parasystole.

X-Y Plot: Number of points in measured plot = 466
Number of points in random plot = 466

A most prominent "forbidden gap" from which points are excluded. There is no hint of this in the random plot.

N Histogram: Strong multiple peaks (at $N = 1 + 3n$, $n = 0, 1, 2, \dots$) incompatible with simple sinus-locking.

Conclusions:

- i) CI and N histograms inconsistent.
- ii) X-Y plot cannot readily be explained.

Concluding Remarks

As already indicated, cases 11 and 12 show a most remarkable phenomenon in their X-Y plots. Not only are points restricted to two distinct regions, but these regions were plotted concurrently - i.e. at the time of taking each plot, the order of the appearance of points showed rapid fluctuations back and forth from one allowed region to the other with points never landing in the "forbidden gap" between the allowed regions. This clearly indicates that the underlying process must be capable of giving rise to two sets of points simultaneously and that the "forbidden gap" is inherent in the functioning of the whole system.

Such behaviour was occasionally noticed in other cases. However case 12 is the best example of the phenomenon, most instances of which were found to be impossible to illustrate without excessive numbers of photographs (~40 for each case). The reason for this is directly attributable to the properties of the clusters between which a "forbidden gap" may be formed. It often seemed that a pair of clusters would move about the X-Y plane in such a way as to overlay any blank area that might arise between them. By the time there were enough points capable of showing a clear area of rarefaction the would-be "forbidden gap" had been obliterated by the movement of the separate clusters over this area. This effect could be avoided by terminating the accumulation early in the process, but then it was found that there were not enough points to demarcate two distinct clusters - the gaps between points in each cluster were then as great as the gap between the cluster themselves. Briefly, a small accumulation could not be separated into two groups because of the large gaps between all points, whereas a larger accumulation gave time for the two groups to merge thus obliterating their separate identities. Nevertheless, watching the accumulation of several cases gave a strong impression of the simultaneous presence of two clusters. (Thus it is claimed that the underlying processes were not statistically stationary and so a pattern could never be established.) If in such a case the V.E.Cs all come from a single source, and since each V.E.C. had the same shape it is reason-

able to assume that they do, then there must be some aspect of the functioning of that source which induces a "forbidden gap" in the X-Y plot. The existence of a "forbidden gap" implies that for a given sinus period the CI is compelled to lie within one of two regions but may not lie between or outside of these regions.

The anomalous nature of the ECGs investigated may be summarized briefly. Of the 39 cases with frequent, single V.E.Cs, 12 show some interaction between the CI and sinus period, and 10 of these show a very strong interaction. This is not expected from either sinus-locked or parasystolic mechanisms. The simultaneous occurrence of two close but distinct clusters with an intervening "forbidden gap" is even more perplexing. In addition, while the fixation in the CI in all 12 cases appears to indicate a sinus-locked mechanism, the distribution of inter-ectopic numbers frequently (10 cases) is highly patterned indicating a parasystolic mechanism. Any single hypothesis of the origin of these V.E.Cs must be capable of accounting for the simultaneous presence of all these phenomena.

In conclusion it is felt that the material presented in this chapter reveals deficiencies in currently accepted accounts of the origin of V.E.Cs in diseased hearts. Some solutions to the problem of the origin of these beats are proposed and investigated in the remainder of this thesis.

PART II

A General Hypothesis -
"Pulling of Ventricular
Ectopic Pacemakers"

CHAPTER V The Essential Attributes of a Mechanism
Capable of Explaining these Arrhythmias -
"Pulled" Parasystole versus Re-Entry with
Wenkebach Conduction

In this part of the thesis a general arrhythmic mechanism is postulated to account for all the ECGs examined in Part I. Particular forms of the mechanism are considered in Part III. The reign of the proposed mechanism is not restricted to the type of ECG presented in Part I: for example it can account for arrhythmias not having X-Y patterns but which show peaked CI histograms along with highly patterned distributions of inter-ectopic numbers. In other words a single hypothesis will be proposed to explain most of the 39 cases investigated and not just those 12 which were presented because they happen to have stable X-Y patterns. However, the most severe test of the hypothesis will be to see if it can cope with the 'double anomaly' which results when using the sinus-locked and pure parasystolic hypotheses to explain these arrhythmias - i.e. can the new hypothesis explain rhythms which simultaneously produce X-Y patterns, peaked CI histograms and highly patterned distributions of inter-ectopic numbers? If it can, not only will it pose as a possible solution to the origin of single V.E.Cs, but it will also serve as a unifying concept replacing the separate sinus-locked and pure parasystolic hypotheses by a single mechanism.

Such a general mechanism must have the following attributes:

- a) In order to account for some of the measured distributions of inter-ectopic numbers the factors controlling the appearance of V.E.Cs must have periodicity greater than the sinus period. For example, in concealed bigeminy the 'rule' says that the number of sinus beats between ectopics is always odd (Chapter II, p.18), i.e. after the appearance of a V.E.C. followed by a compensa-

tory pause and a sinus beat, the next V.E.C. may appear only after a further 2, or 4, or 6, or $2n$ sinus beats - the governing factors have a periodicity of two sinus beats, for if a V.E.C. does not appear when it could have done then we must wait two more sinus beats before another may appear.

- b) In order to account for the X-Y plots, the exact time of arrival of the V.E.C. in the sinus cycle must be partially or totally dependent on the duration of the previous sinus period.
- c) Whatever the cause of this dependency it must tend to keep the CI fixed to part of sinus diastole, thus producing peaked CI histograms.
- d) Some of this allowed section of sinus diastole must be inaccessible to V.E.Cs in order to produce a "forbidden gap" in the X-Y plot. The "forbidden gap" itself may be somewhat dependent on the sinus period.

It seems that there may be two general types of hypothesis capable of satisfying these criteria, the first based on parasystole, the second on re-entry.

A General Hypothesis Based on Parasystole

The first general hypothesis is designated "pulled parasystole" and is the general mechanism advocated in this thesis. In Part III it is shown to have all the attributes just mentioned in that it can account for the observations presented in the last chapter. The only difference between pulled and pure parasystole is that in the former, the pacemakers are no longer independent whereas for pure parasystole the pacemakers are truly independent.

In 1946 Segers demonstrated interaction between autonomous pacemakers in the frog's heart⁶⁸. This work is considered in the next chapter, but for present purposes it suffices to note the following phenomena demonstrated by Segers: synchronization between two separate pacemakers at a specific phase difference; the ability for two pacemakers to attain

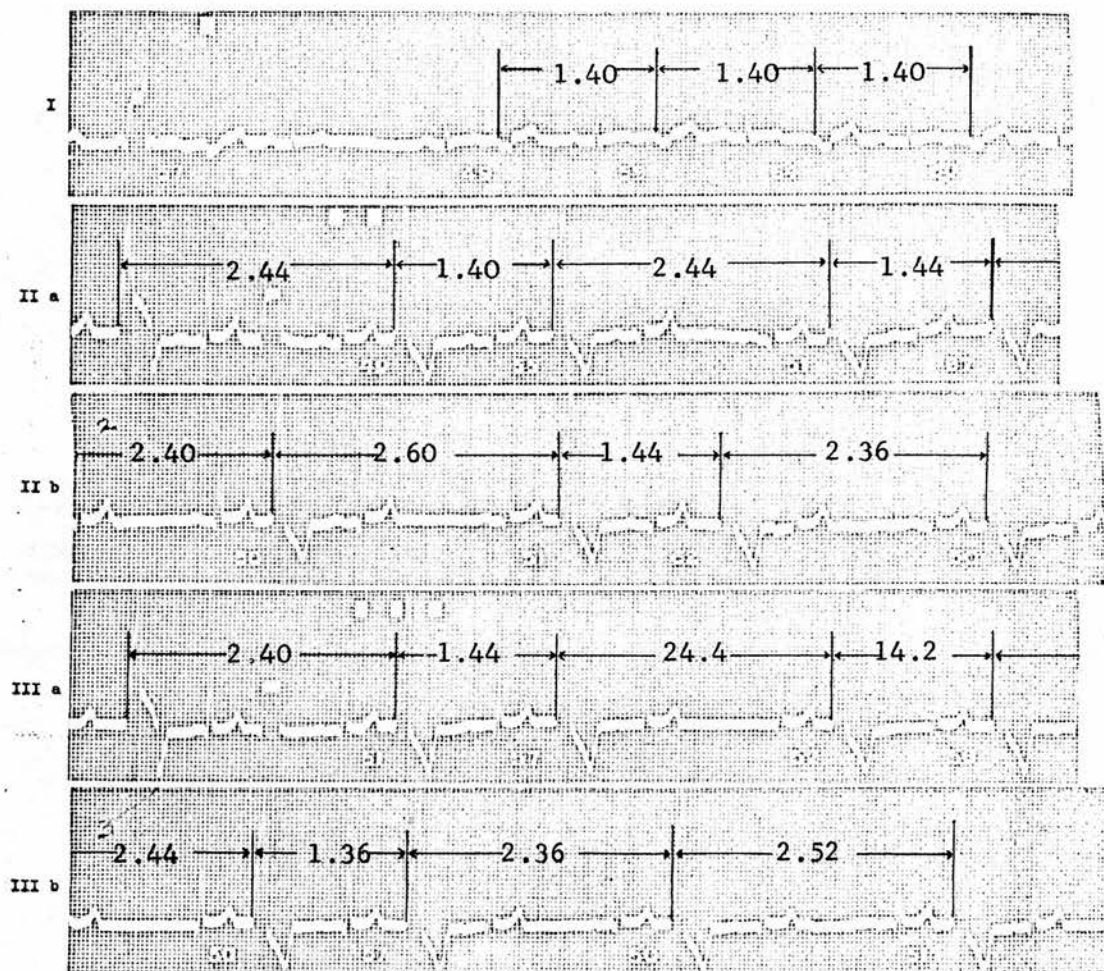
and hold synchrony for some time, followed by a loss of synchrony, a marching of one pacemaker past the other, and the re-establishment of synchrony - the maintenance of synchrony he called "accrochage" (hooking, or tuning in) between the pacemakers. The general hypothesis proposed here depends on such interaction or "pulling" between the sinus rhythm and the ventricular parasystolic pacemaker. It will be argued that the characteristics presented in the last chapter are manifestations of such accrochage. In particular, multiple peaked N histograms result naturally from an ectopic rhythm which is synchronized to some multiple of the sinus period.

Although Segers demonstrated mechanical and electrical interactions, it is felt that the primary influence is probably electrical and comes about when sinus initiated ventricular excitation reaches the ectopic pacemaker. Indeed, it would be surprising if an ectopic pacemaker were totally insensitive to ventricular excitation.

In Part III, four mechanisms of electrical pulling are formulated on the basis of well-established cardiac electrophysiology. For all of these, the magnitude of the effect of sinus excitation on the ectopic period critically depends on the time of arrival of the QRS complex in the ectopic cycle. This variability can cause the ectopic pacemaker to become synchronized to a fluctuating sinus rhythm. Under such circumstances changes in the sinus period cause small changes in the apparently constant CI, and this gives rise to a characteristic X-Y plot.

These four hypotheses are tested with the aid of purpose built electronic simulators of the mechanisms involved. The performance of each model is compared to the characteristics seen in the last chapter, and it will be shown that the simultaneous presence of peaked CI histograms, multiple peaked N histograms, strong X-Y patterning and a "forbidden gap" is readily achieved with some of these mechanisms.

Fig.V,I: Case 1 of Mack and Langendorf³⁴ (1950) with acknowledgement. Markings above the E C G traces have been added to the original

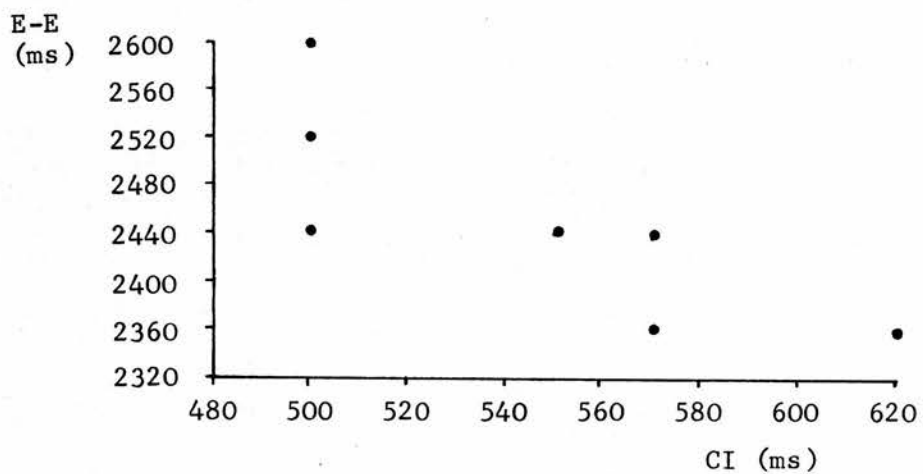


Hypotheses Based on Re-Entry - Difficulties

The second general type of hypothesis that might be capable of satisfying all the criteria mentioned earlier consists of a re-entry mechanism in conjunction with the Wenkebach phenomenon. The Wenkebach phenomenon consists of a particular type of variable conduction velocity along a specific pathway - successive impulses take progressively longer to traverse the pathway and eventually an impulse is dropped. The next impulse to arrive is conducted quickly and the process begins again^{61 77}. This phenomenon could function in conjunction with any sinus-locked mechanism and could facilitate interaction between the CI and sinus period. For example, the CI of a re-entrant V.E.C. depends on the conduction velocity within the re-entrant path and this in turn may depend on the frequency of stimulation (see Chapter II, p.16) i.e. the sinus rate. Hence the sinus rate may partly determine the CI. In addition the CI would have a strong tendency to remain in a specific part (or parts) of sinus diastole simply because of the re-entrant origin of the V.E.C. - Wenkebach conduction may superimpose a number of specific changes in the CI, and this would lead to a number of specific CIs. Hence V.E.Cs could still appear to have a strong preference for specific parts of diastole. At first sight this mechanism seems worthy of investigation.

A mechanism involving Wenkebach type conduction in the re-entry path has been proposed by Mack and Langendorf to account for V.E.Cs with variable coupling³⁴. Their cases show "progressive lengthening of the coupling eventually leading to the omission of a ventricular premature systole." (Fig.V,1). However their first case may be interpreted equally well, if not better, as pulled parasystole. For instance, if the lengthening of the CI in the top trace of Fig.V,1 is due to progressive conduction block affecting sinus re-entry, why are the inter-ectopic intervals constant at 1.40sec? Surely this is pure parasystole. With only two exceptions, all of the 19 inter-ectopic intervals in this first case are either 1.40 ± 0.04 sec. or 2.40 ± 0.04 sec., and this suggests the V.E.Cs originate from an ectopic pacemaker with period approximately 0.35 ± 0.02 sec.: if the ectopic pacemaker is subject to exit

Fig.V,2: Plot of the long inter-ectopic intervals (ordinate) versus preceding CI (abscissa) for the ECG in Fig.V,1.



block of 4:1 and 7:1 the resulting inter-ectopic intervals are $4 \times (0.35 \pm 0.02) = 1.40 \pm 0.08$ sec., and $7 \times (0.35 \pm 0.02) = 2.45 \pm 0.14$ sec., and these agree well with the measured intervals. Now consider the hypothesis of pulled parasystole which postulates an ectopic period influenced by sinus excitation. The influence varies according to the time of arrival of the sinus excitation in the ectopic cycle. Hence if the pulling hypothesis is correct, changes in the phase difference between the sinus and ectopic pacemakers will induce corresponding changes in the ectopic periods (i.e. the inter-ectopic intervals). The first case presented by Mack and Langendorf shows such a relationship between the longer inter-ectopic intervals (associated with 7:1 exit block) and the phase difference (CI) between the sinus and ectopic complexes. In Fig.V,2 the long inter-ectopic intervals are plotted against the preceding CI, and the result argues for an inter-ectopic interval influenced by sinus excitation: the influence depends on the time of arrival of sinus excitation in the ectopic cycle - the larger the phase difference (CI) the smaller is the inter-ectopic interval. Indeed this seems to account remarkably well for the two inter-ectopic intervals (2.60s and 2.52s) that might cast doubt on the existence of a separate ectopic pacemaker. Finally, the fact that each of the 10 long inter-ectopic intervals is terminated by the same size CI (0.50 ± 0.01 s) can also be explained by pulled parasystole: the two intervening sinus complexes work so as to bring the ectopic pacemaker into synchrony, whereas when there is only one sinus complex the ectopic pacemaker has a greater chance of proceeding unperturbed. This phenomenon can also be explained by the re-entry cum Wenkebach mechanism proposed by Mack and Langendorf. However, the ability to explain this phenomenon alone does not overcome the deficiencies in the re-entry cum Wenkebach hypothesis already indicated.

The most severe shortcoming of the re-entry cum Wenkebach hypothesis in the form proposed by Mack and Langendorf is its apparent inability to produce distributions of inter-ectopic numbers with more than one peak. The arguments are exactly the same as those in Chapter II which are concerned with the effects

of conduction block on sinus-locked mechanisms: N is determined by conduction block before, within or after the ectopic site; since conduction block tends to hover around some fixed value so does N. Now one of the most prominent features of Wenkebach type conduction failure is its tendency to hover around some fixed value. Therefore it would seem incapable of inducing an N histogram with multiple peaks when working in conjunction with a re-entry mechanism, at least in the manner envisaged by Mack and Langendorf.

Anderson and Bailey¹ have proposed a re-entry cum Wenkebach mechanism which could account for multiple peaks in the N histogram, although this was not their specific intention. The success of their theory in explaining a phenomenon for which it was not directly intended is, in itself, considerable support for it. They envisage Wenkebach conduction in a distal, small Purkinje bundle such that when conduction fails the shape of the 'normal' ventricular complex remains unaltered. If the Wenkebach block were 5:4, say, then this bundle would conduct during 4 consecutive sinus beats but fail on every 5th. This would permit retrograde activation of the bundle by the sinus excitation which had just failed to excite it in the normal (orthograde) direction. Such "periodic reentry" would give rise to "coupled premature beats" with an inter-ectopic number of '5'. Of course if the retrograde activation were to fail also, then another 5 (or perhaps 6) sinus beats would pass before re-entry could occur again, and this would result in an inter-ectopic number of '10' (or perhaps '11'). No inter-ectopic number between '5' and '10' could possibly arise while the 5:4 Wenkebach conduction persisted, and the allowed sequence of N's would be '5', '10', '15' '5n', where n = 1, 2, 3 The allowed sequence of inter-ectopic numbers can take many forms depending on the nature of the Wenkebach cycle, hence this mechanism may well be capable of producing the type of N histogram presented in the last chapter. However, the shapes of the V.E.Cs examined indicated that in most cases they originated in the left or right bundle branches, not the distal Purkinje system. This hypothesis is discussed further in Chapter IX.

Concluding Remarks

The two general types of hypothesis considered here would seem to encompass the most reasonable adaptations of existing theory. Indeed, V.E.Cs must arise from some form of sinus-locked or parasystolic mechanism as there is no other logical possibility to their origin - either the V.E.C. is set by the preceding sinus beat (sinus-locked) or it is autonomous and exists in its own right (parasystole). On examination of the data it seemed that a modified form of pure parasystole was more promising than a modified form of sinus-locking. For this reason various pulling mechanisms were formulated and investigated, no more attention being paid to the sinus-locked hypotheses. This choice is supported further by diverse experimental and clinical findings which may be regarded as indicative of pulled parasystole. These findings are reviewed in the next chapter.

CHAPTER VI Divers Reported Evidence Supporting the
Hypothesis of a Pulling Mechanism

A considerable body of evidence indicative of pulling in mammalian hearts has accumulated over the last 30 years. For convenience the evidence cited here is divided into four parts: i) direct experimental work on mammalian hearts or heart fibres; ii) reported arrhythmias; iii) the successes of models and ideas in areas of cardiac arrhythmology not concerned with V.E.Cs but which are in some way germane to the pulling hypothesis; iv) recent work carried out in this laboratory by C.W. Vellani and J.M.M. Neilson. It should be noted that some of the results cited will not be interpreted in the manner intended by their originators.

Experimental Evidence of Pulling in Mammalian Heart Fibres

In his classic paper, *Les Phénomènes de Synchronisation au Niveau du Coeur*, Segers studied the interactions between separated segments of frog's hearts⁶⁸. Two segments having different automaticities were brought together so that any interaction between them could not have been due to normal conduction. It was found that pairs of segments tended to synchronize at a phase difference specific to each pair, and that for some pairs the synchrony did not always persist but was intermittent as described in the last chapter. That is, spells of temporary synchrony ("accrochage") alternated with spells of relative independence with the two segments proceeding at different rates. During synchrony the ratios between adjusted cycle lengths could be any of 1/1, 2/1, 3/1, 4/1, 3/2. By electrically isolating the segments mechanical

interaction was demonstrated, and vice versa, by mechanical isolation electrical influence was shown. The influence should either accelerate or decelerate a segment's activity. Segers concludes by casting doubt on the independence of atria and ventricles during A-V dissociation and suggests that they might synchronize in the absence of normal A-V conduction thus producing "dissociation isorhythmic".

The work of Segers strongly indicates that ventricular excitation, initiated by the S-A node, could act on an ectopic pacemaker to produce permanent or intermittent synchrony between ectopic and sinus rhythms. The two separate rhythms could synchronize in a variety of ratios and phase differences. Doubtless these would depend on the inherent periodicities of the separate rhythms and the extent to which the ectopic pacemaker is protected by entrance block. Indeed, electrical interaction can be thought of as resulting from 'incomplete' entrance block which transmits electrotonic potentials capable of altering the periodicity of the ectopic pacemaker without triggering it.

Subthreshold electrotonic potentials might reach an ectopic pacemaker in one of two ways. Either the fibres leading into the ectopic focus exhibit decremental conduction^{26 66 77} so that an action potential becomes subthreshold by the time it reaches the ectopic focus, or electrotonic currents flow between the ectopic focus and the surrounding myocardium when this is excited. In either case the fibres accessing the ectopic focus must evince uni-directional block so that impulses initiated within the ectopic pacemaker may be conducted away, while incoming impulses are prevented from directly triggering the ectopic focus. Such uni-directional block is well established under a variety of experimental conditions that could prevail within diseased hearts^{11 27 71}.

It is interesting to note that most, if not all, types of conduction block depend on some sort of decremental conduction whereby the stimulus becomes progressively smaller as it is propagated^{11 20 24 27 79 88}. Eventually it becomes subthreshold with respect to the depressed fibre and can not

initiate the regenerative action necessary for an 'active' response. All that is left is a 'passive' electrotonic potential which exponentially dies away to nothing within the depressed section. However if the electrotonic potential is still sufficiently large when it reaches a normal section it instigates a full action potential^{11 24 71 79}. With hindsight it is easy to see that all these phenomena result naturally from the work of Hodgkin²⁰ (1937) and others² (1964) who established the nature of propagation in nerve and cardiac fibres. Such propagation is totally dependent on the electrotonic ("extrinsic") potential. Thus it is not surprising to find that blocked impulses give rise to subthreshold, electrotonic stimuli. The pulling hypotheses devised in Part III employ the effects of subthreshold stimuli on automatic heart fibres.

Clearly the electrical influence shown by Segers does not result from decremental conduction along anatomical pathways. Rather it must be due to electrotonic currents of one segment passing through the membranes of fibres in the other. Such action has been demonstrated by direct recording of transmembrane potentials of adjacent fibres in the cat ilium⁷⁶. If two adjacent fibres can interact then it seems reasonable to suppose that an ectopic pacemaker would be affected by rapid depolarization of the myocardium surrounding it. This could give rise to 'non physiological' stimuli in that electrotonic excitations of the ectopic focus do not traverse anatomical pathways in order to reach that focus. Both conventional, and 'non anatomical' types of electrotonic spread are used in devising pulling hypotheses in Part III.

Finally, two further experimental results are considered pertinent to pulled parasystole. By the application of a suitable periodic stimulus, the dog ventricle in vivo can achieve frequencies above or below its inherent frequency⁴², and this clearly indicates that a response different from the usual "all or none" is possible. Secondly, experimentally induced parasystole in dogs can show constant or varying CIs, just the type of behaviour expected from pulled parasystole⁶⁵.

A variety of arrhythmias occurring in human hearts also lend strong support to the tenet of pulling, and some of these are reviewed in the next section.

Arrhythmias Indicative of Pulling in the Human Heart

This section is concerned with certain aspects of the following three human arrhythmias: those which show fixed and variable coupling of single V.E.Cs; parasystole; certain A-V arrhythmias. It is argued that all the arrhythmias cited are consistent with, if not indicative of, pulling in the human heart.

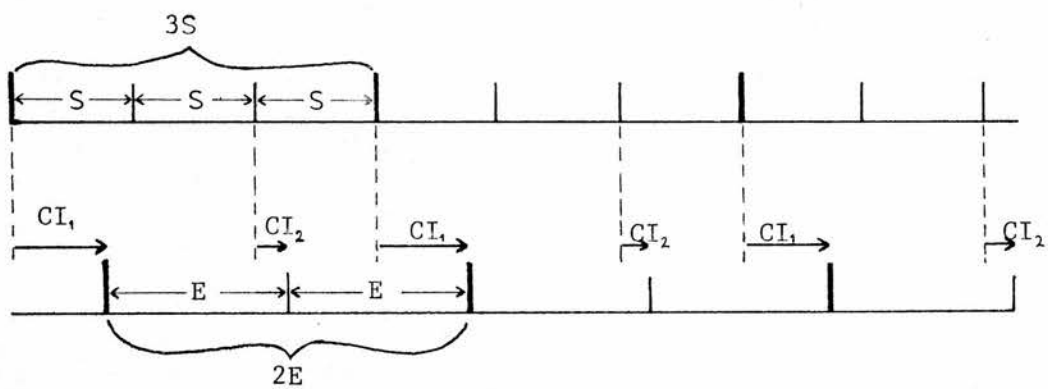
i) Some Aspects of Arrhythmias Showing Fixed and Variable Coupling of Single V.E.Cs

Surawicz and MacDonald⁷⁸ (1964) examined a series of 88 cases having "unifocal ventricular ectopic beats", and the following is a selection of their findings in individual cases: intermittent parasystole, all episodes of which begin with the same CI; grossly irregular inter-ectopic intervals not related to the sinus rhythm; a relationship between the CI and the preceding sinus period; clustering of V.E.Cs in early and late diastole. All these may be regarded as indicative of pulling.

The first phenomenon can be interpreted in terms of a pulling mechanism which is effective only when no V.E.Cs are propagated, and this could function as follows. A propagated V.E.C. prevents the sinus impulse from exciting the ventricular myocardium and so the pulling influence is temporarily lost and the ectopic pacemaker proceeds with its own periodicity. Pulling becomes active again when the two pacemakers attain a suitable phase difference. This phase relation is maintained until another V.E.C. is propagated which a) reveals this specific phase via the CI, and b) causes a further loss of synchrony.

Secondly, grossly irregular inter-ectopic intervals can arise from a pulling mechanism which is not strong enough to establish a stable synchrony so that "accrochage" is never properly achieved.

Fig.VI,1: Two ectopic periods synchronized to three sinus periods produce two distinct CIs, CI_1 and CI_2 .



Thirdly, the relation between CIs and sinus periods results from the phase dependence of the pulling mechanism. Such phase dependence is absolutely necessary if synchrony is to be maintained: if the sinus period changes, however slightly, then so must the ectopic rhythm - if by taking up a new phase with respect to the sinus pacemaker the ectopic rhythm is influenced appropriately, then synchrony is maintained. In other words, the pulling mechanism must induce changes in the ectopic rhythm corresponding to changes in the sinus rhythm, and in order to achieve this there must be some ready means of realizing an appropriate variability in the sinus' influence on the ectopic pacemaker. Such variability can only come about through an altered phase relation: if the sinus and ectopic rhythms keep a constant phase they must surely have a constant effect on one another. Hence any appropriate pulling influence must be phase dependent, and if the dependence is of a suitable kind then an ectopic rhythm will follow changes in the sinus rhythm with a phase relationship (i.e. CI) appropriate to the sinus period, and this would be manifest in the X-Y plot. Only some pulling mechanisms could act in such a manner so as to maintain synchrony. Those that do will keep the CI fairly constant and will show some sort of inter-dependence between the CI and sinus period, possibly of the type found by Surawicz and MacDonald. Unfortunately they calculate the "correlation coefficient" for various cases without first establishing that the conditions necessary for its intelligible use are satisfied. In fact the marginal distributions (i.e. the CI and sinus period histograms) of their illustrated scattergram do not appear Gaussian and hence their subsequent use of the size of the "correlation coefficient" is totally unjustified.

Finally, the clustering of uniform V.E.Cs in two regions of diastole is a further indication of synchrony. For example, if two ectopic periods are synchronized to three sinus periods then two distinct CIs arise as in Fig. VI,1.

It may be concluded that all four primary phenomena noted by Surawicz and MacDonald are interpretable in terms of pulled parasystole.

ii) Some Aspects of Clinical Parasystole

Various phenomena indicative of pulling have been noted in clinical studies of parasystole. These studies are interpreted here in a manner which does not necessarily reflect the opinions of the original authors.

As already discussed, episodes of parasystole, all of which start with the same CI, may be interpreted as pulled parasystole - this phenomenon is not unknown^{44 62 78}. In fact, any case that shows both "extrasystoles" (i.e. "fixed coupling") and parasystoles of the same shape is direct evidence of intermittent synchrony or "accrochage". Chung⁹ cites ten separate studies of this phenomenon. In addition, varying CIs in conjunction with consistent shortening (or lengthening) of those inter-ectopic intervals which contain a sinus beat^{44 62} indicates that the ectopic rhythm is separate from, but not independent of, the sinus rhythm.

Various authors give examples of arrhythmias which they believe show synchronization at a phase difference between two pacemakers^{7 43 70}. The phase difference is sometimes rate dependent and, as already discussed, this may be interpreted as a sure indication of pulling.

iii) Some Aspects of A-V Arrhythmias

Pulling and synchrony between atria and ventricles during A-V dissociation has often been reported^{35 36 54 67}. It has also been shown during complete heart block⁶⁹ and electrical pacing¹⁴. Indeed, the mechanism of synchrony may be very complex and involve a host of feedback paths acting together. One such path has been suggested by Levy et al³⁰ whereby the P-R interval is kept relatively constant during A-V dissociation: the P-R interval determines the stroke volume; the stroke volume determines the arterial pressure which, via the baro-receptor reflex, affects the frequency of the S-A node which in turn affects the P-R interval. He goes so far as to suggest a similar feedback mechanism that might be responsible for fixed coupling in parasystole³¹.

Since pulling and synchrony between atria and ventricles is possible during A-V dissociation and even during complete heart block, it seems eminently reasonable to suppose that a protected ventricular pacemaker would be pulled by the activity of the myocardium surrounding it.

The Successes of Models and Ideas Related to the Pulling Hypothesis

Ever since the elegant work of Van Der Pol and Van Der Mark⁸⁰ in 1929 it has been realized that the heart beat can be visualized as a relaxation oscillation. That is, an oscillation consisting of two or more distinct phases which follow on from one another by virtue of the fact that the completion of one phase automatically starts the next.

Roberge, Bhéreur and Nadeau^{3 53} have reconsidered this work in the light of modern knowledge. Using a unijunction transistor, they have constructed a minimum parameter model which mimics well the physiological relaxation oscillations of pacemaking fibres. Two of these were connected in such a way as to represent atrial and A-V nodal activity, i.e. the automatic cells mainly responsible for governing the P and R waves of the ECG. By primarily altering the inherent rates of and the degree of coupling between the two automatic centres the following "arrhythmias" were readily reproduced: i) sinus rhythm and A-V nodal rhythm; ii) incomplete heart block and Wenkebach cycles; iii) complete dissociation, isorhythmic dissociation and dissociation with capture. On the basis of this model it is tempting to think of much heart activity in terms of variously coupled relaxation oscillators. Pulling of an ectopic pacemaker would then constitute a typical example of such activity.

The Work of Vellani and Neilson on Ventricular Ectopic Rhythms

The present study arose from the extensive work of Vellani and Neilson in this laboratory on ventricular ectopic

rhythms⁴⁸. It has been argued that the intervals between V.E.Cs initiated by a sinus-locked mechanism would manifest only the sinus rhythm, or multiples and sub-multiples thereof. By using power spectrum analysis on the inter-ectopic intervals⁸¹, it was clearly demonstrated that relatively fixed-coupled V.E.Cs had a periodic component not related to the sinus rhythm. The most obvious conclusion is that the V.E.Cs have their own periodic source which is pulled into a relatively constant phase relation with the sinus rhythm.

Finally, several cases with apparent fixation of the CI showed a most remarkable phenomenon⁸¹: short inter-ectopic intervals had a periodicity distinctly different from that of longer inter-ectopic intervals, and neither of these reflected the sinus rhythm. It is difficult to see how such a phenomenon could arise from any type of modified sinus-locked mechanism. On the other hand, a modified form of parasystole might well show such behaviour.

Concluding Remarks

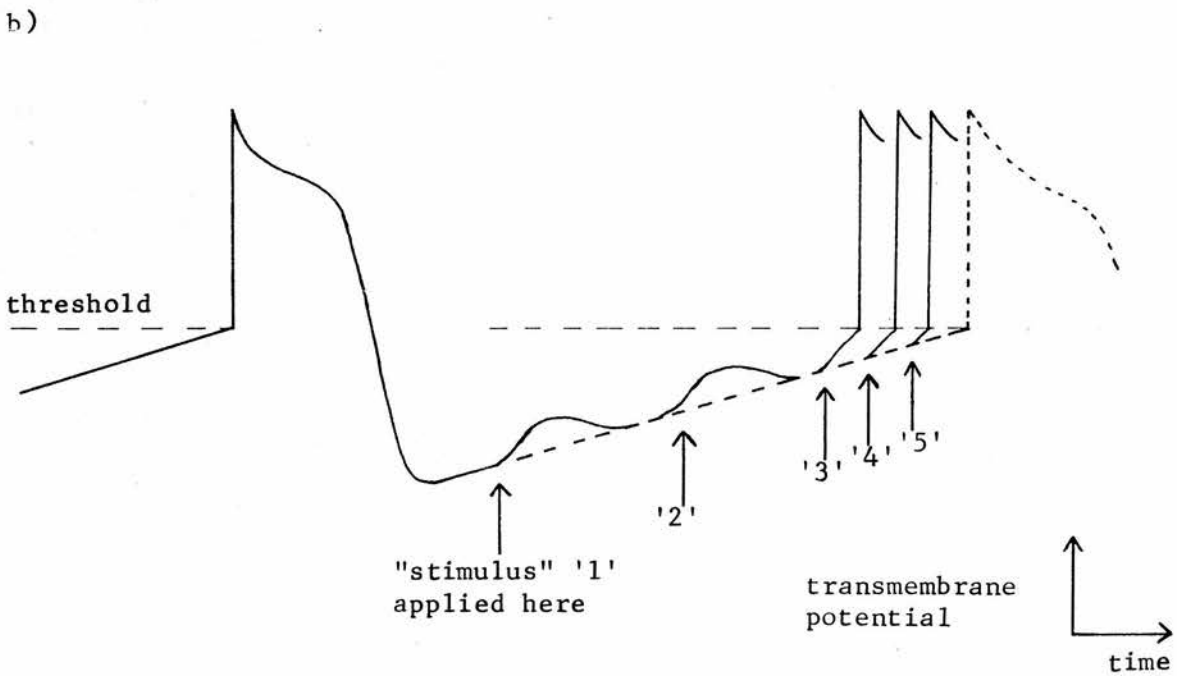
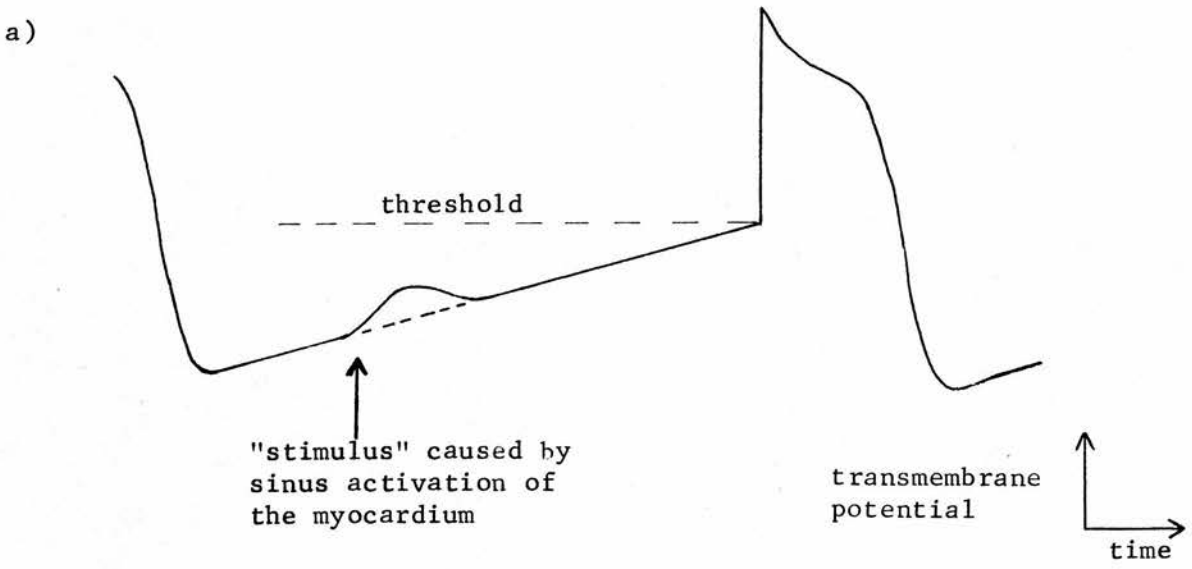
There seems to be considerable evidence to indicate the existence of pulling in various guises: the experimental work of Segers on separated segments of frogs' hearts; diverse A-V and parasystolic arrhythmias; the successes of models, based on pulling, in explaining some of these; the periodicity analysis carried out by Vellani in this laboratory.

The results in Chapter IV can also be interpreted as indicative of pulling. The next part of this thesis is devoted towards accounting for those results by postulating various electrophysiological pulling mechanisms. These are then tested by comparing the characteristics expected from such mechanisms with the measured characteristics presented in Chapter IV.

PART III

Investigation of Some Possible
Electrophysiological Pulling Mechanisms

Fig.VII,1: Mechanism of the preliminary pulling hypothesis.
Sinus activation of the myocardium may shorten the ectopic pacemaker cycle.



CHAPTER VII A Preliminary Hypothesis of Electrotonic Pulling of Ventricular Pacemakers During Parasystole - Some Theoretical Behaviour of a Simplified Model - Investigation with an Electronic Analogue

The Preliminary Pulling Hypothesis: An Hypothesis Proposed by C.W. Vellani

This chapter is devoted to an examination of a pulling mechanism proposed by C.W. Vellani⁸¹. He postulates that the ectopic pacemaker in ventricular parasystole is not totally impervious to the electrical activity of its surroundings: in particular, sinus activation of the myocardium affects the transmembrane potentials within the ectopic site in the manner depicted in Fig. VII,1a. Sinus activated "stimuli", associated with the QRS complex, may shorten the ectopic cycle if they bring the transmembrane potential up to threshold (Fig. VII,1b). Hence "stimulus" '3' has the largest effect on ectopic periodicity, whereas '1' and '2' have no effect, and '4' and '5' have smaller effects. Clearly there is a discontinuity in the way the power of these "stimuli" (to shorten the ectopic period) varies with their time of arrival at the ectopic site: '4' is more powerful than '5', and '3' more powerful than '4', but "stimuli" of this magnitude arriving before '3' have no effect since they do not cause the ectopic fibre to attain threshold. Thus as the "stimuli" arrive more and more early in the ectopic cycle their pulling effect progressively increases to a critical value, beyond which there is no pulling effect whatsoever.

Such a mechanism is consistent with a phenomenon demonstrated by Weidmann⁸⁷. Under certain circumstances it would seem that the size of the stimulus required to initiate an

action potential in an automatic fibre is reduced as the fibre proceeds in its phase 4 depolarization. Hence "stimuli" '3', '4', and '5' are successful in initiating an action potential, whereas '1' and '2' are not.

The mechanism proposed by C.W. Vellani will be referred to as the preliminary pulling hypothesis, and is similar to a mechanism proposed by Schamroth⁵⁹ involving Wedensky Facilitation. Both mechanisms may be viewed in terms of the spread of electrotonic potential through the entrance block which protects the ectopic pacemaker. However, the rectangular 'enhancing trough' of Schamroth would not produce the stable type of synchrony necessary for concealed bigeminy and trigeminy as he suggests: there is no ability for the ectopic cycle to adjust to fluctuations in the sinus rhythm. Later in this chapter it is shown that even an angled 'trough', to which the preliminary hypothesis is equivalent, can not produce stable synchrony of the type necessary for concealed bigeminy and trigeminy. The reason for this would seem to be that for such a mechanism to produce these arrhythmias, the sinus excitation must perform two incompatible functions simultaneously: it must precipitate the ectopic focus into firing but must not prevent the resulting ectopic impulse from propagating (cf Schamroth⁴).

The present chapter is concerned with the analysis of the ramifications in the ECG of the preliminary pulling hypothesis. The aim is to make quantitative predictions from the hypothesis and compare these to the data presented in Chapter IV. To do this a simplified mathematical model of the mechanism is constructed. This is made so as to conform to an electronic analogue built by J.M. Neilson, hence the performance of these two models should recapitulate one another and may be used as mutual checks.

Perhaps the most useful aspect of this dual approach arises from the need first to establish the modes of behaviour possible with the pulling mechanism, and second, the need to gain insight into the functioning of each mode. Strictly speaking the electronic analogue suffices for both these

purposes since, in effect, it performs the analysis and displays the results. However a mathematical analysis provides further understanding of particular modes of action and the transistions between them, although in many situations this approach is too cumbersome to be of use. Both approaches have their advantages and disadvantages as will become apparent.

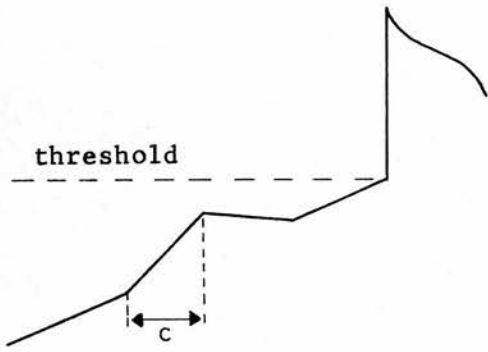
Mathematical Analysis of Some Consequences of the Preliminary Pulling Hypothesis

This section is devoted to a mathematical analysis of the X-Y plot in some synchronized modes possible with the preliminary pulling hypothesis. Two simplifications are made to the preliminary hypothesis: the first is to approximate the effect of sinus activated myocardium on ectopic phase 4 depolarization by straight line segments as in Fig. VII,2a; the second is to assume that after the "stimulus", phase 4 depolarization does not return to its original path but retains a constant displacement from it as in Fig. VII,2b. The latter simplification has no effect during synchrony, and in fact has no significant effect outside it (see later).

/

Fig.VII,2: Straight line approximations to the preliminary pulling hypothesis

a) First approximation



b) Second approximation

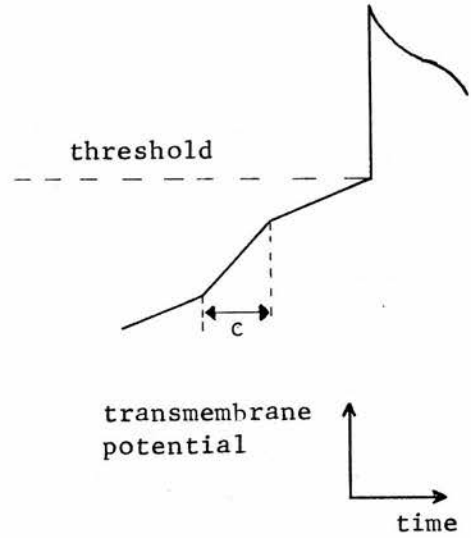
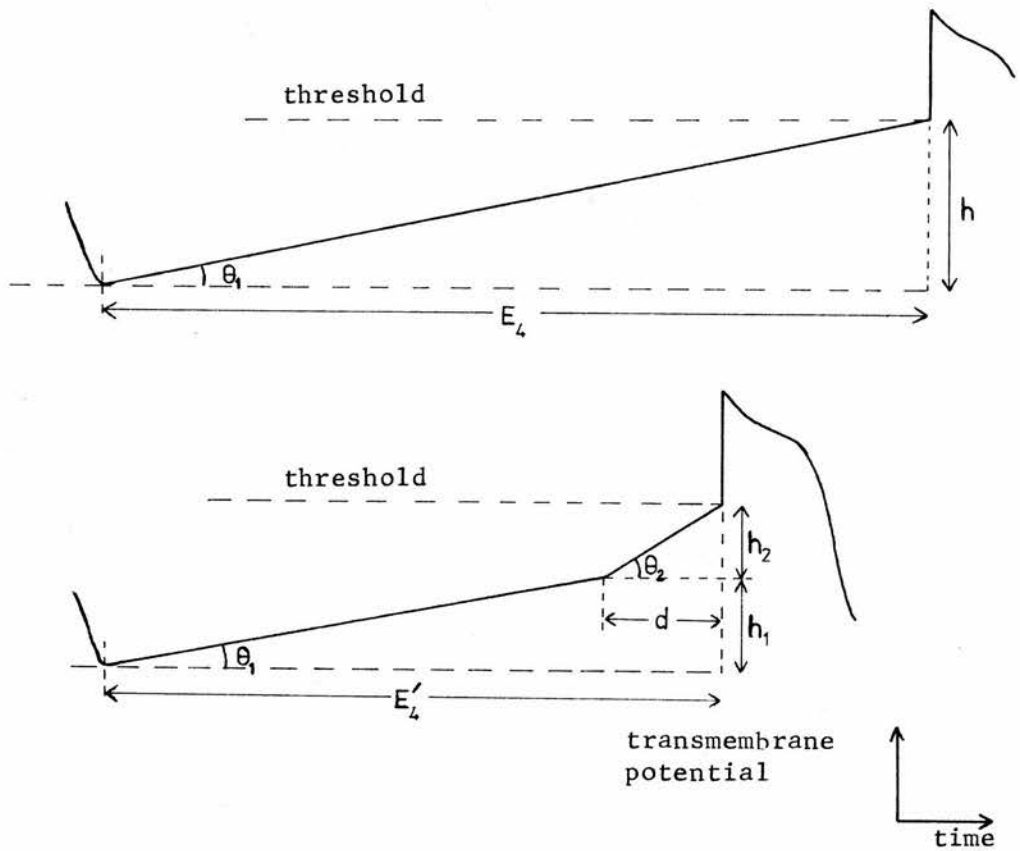


Fig.VII,3: Relation between the pulling strength, P , and the change in the rate of phase 4 depolarization.



Synchronization occurs when the QRS complex associated with sinus activation of the myocardium arrives late in ectopic diastole as in Fig. VII,3. The magnitude of the change induced in the ectopic cycle is then critically dependent on the exact time of arrival of the QRS complex in the ectopic cycle (Fig. VII,1b), and it will be shown that this variation may, under certain circumstances, cause the ectopic pacemaker to become synchronized to a fluctuating sinus rhythm. The "pulling strength" is a constant of the system and may be defined as (Fig. VII,3):

$$P = \frac{\text{reduction in the ectopic cycle}}{\text{time-interval for which the pulling acts}}$$

This is related to the change in slope of the ectopic fibre's phase 4 depolarization caused by the QRS complex:

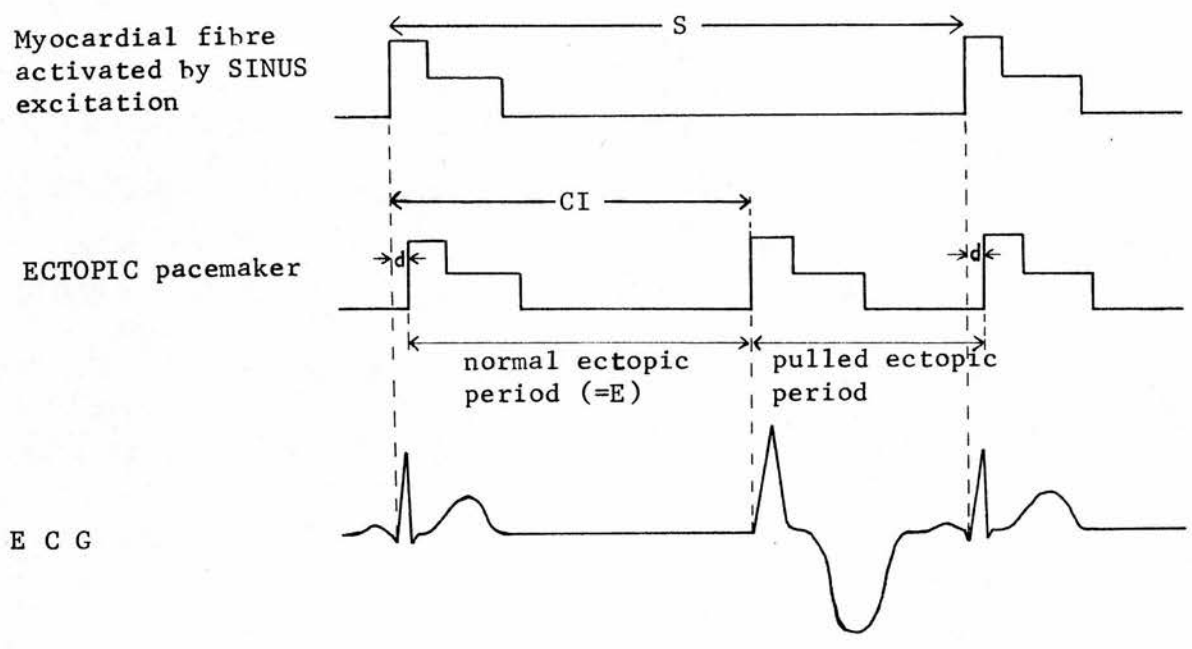
	let d = time-interval for which the pulling acts.	
Reduction in ectopic cycle	= $E_4 - E'_4$	where E_4 = duration of ectopic phase 4 depolarization
$\therefore P$	= $\frac{E_4 - E'_4}{d}$	and E'_4 = reduced duration of ectopic phase 4 depolarization
Now E_4	= $\frac{h}{\tan \theta_1}$	
and E'_4	= $\frac{h_1}{\tan \theta_1} + c$	
$\therefore E - E'_4$	= $\frac{h - h_1}{\tan \theta_1} - c$	
But h	= $h_1 + h_2$	
and h_2	= $d \tan \theta_1$	
$\therefore E_4 - E'_4$	= $\frac{d \tan \theta_1}{\tan \theta_1} - d$	
i.e.	$\frac{E_4 - E'_4}{d} = \frac{\tan \theta_2}{\tan \theta_1} - 1$	
	= P	

i) Synchrony Under a Slowly Changing Sinus Rhythm - the Static Theory

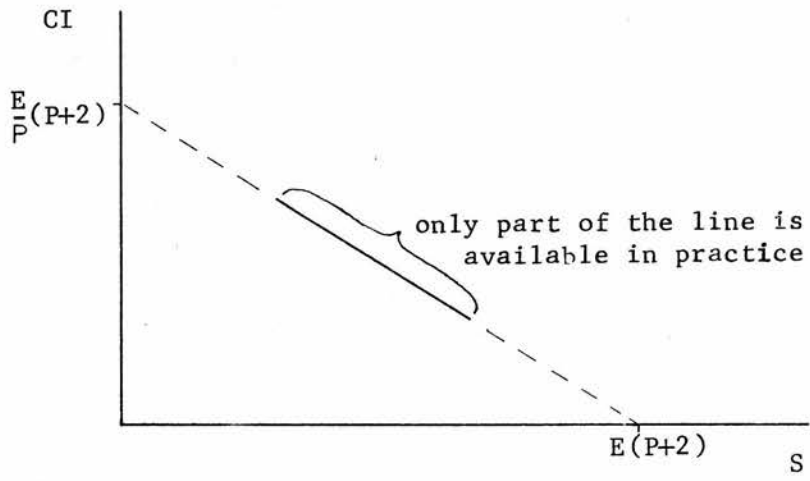
Various modes of synchrony are possible with the preliminary pulling hypothesis, one of the simplest arising when the sum of two unpulled ectopic periods is slightly longer than one sinus period. This situation is referred to as

Fig.VII,4: A synchronized mode for the preliminary pulling hypothesis where $2E=S+$

a) Diagrammatic action potentials and ECG



b) X-Y plot for E and P constant: slope = $-\frac{1}{P}$



$2E = S+$. The top line in Fig. VII,4a represents the repetitive discharge of a typical myocardial fibre which is only activated by sinus excitation, hence this line represents sinus periodicity. (The waveforms correspond to those produced by the electronic analogue discussed later.) The middle line represents an ectopic pacemaker fibre, and the bottom line the resultant ECG. It is assumed that the ectopic complex is interpolated and does not prevent the QRS complex from appearing. This restraint is lifted when using the electronic analogue to investigate the preliminary pulling hypothesis.

The synchrony in Fig. VII,4a is inherently stable, for if the sinus period should shorten then d is increased and this causes a shortening in the ectopic period - i.e. reduction of the sinus period induces a corresponding reduction in the ectopic period. For a given sinus period (S), ectopic period (E), and pulling strength (P), the CI and X-Y plot is determined as follows (Fig. VII,4a):

For synchrony to arise, the sum of one normal plus one pulled ectopic period must equal one sinus period.

i.e. $E + (E - Pd) = S$, since the shortening due to pulling is Pd .

$$\begin{aligned} \therefore d &= \frac{2E - S}{P} \\ \therefore CI &= d + E \\ &= \frac{2E - S}{P} + E \\ &= \frac{E(P + 2)}{P} - \frac{S}{P} \end{aligned} \quad (1)$$

Hence for constant E and P the X-Y plot appears as in Fig. VII,4b. Variations in either E (considered shortly) or P cause departures from the straight line: increasing P reduces the slope, and increasing E raises the line. As a result, such a mechanism would produce scatter about a straight line if P or E vary during accumulation of the X-Y plot.

In order to illustrate the behaviour in other synchronized modes, the following two cases are derived here:

$$3E = S+$$

$$qE = S+ \text{ where } q \text{ is some integer greater than } 1$$

Some of the results for the following two general cases are also quoted:

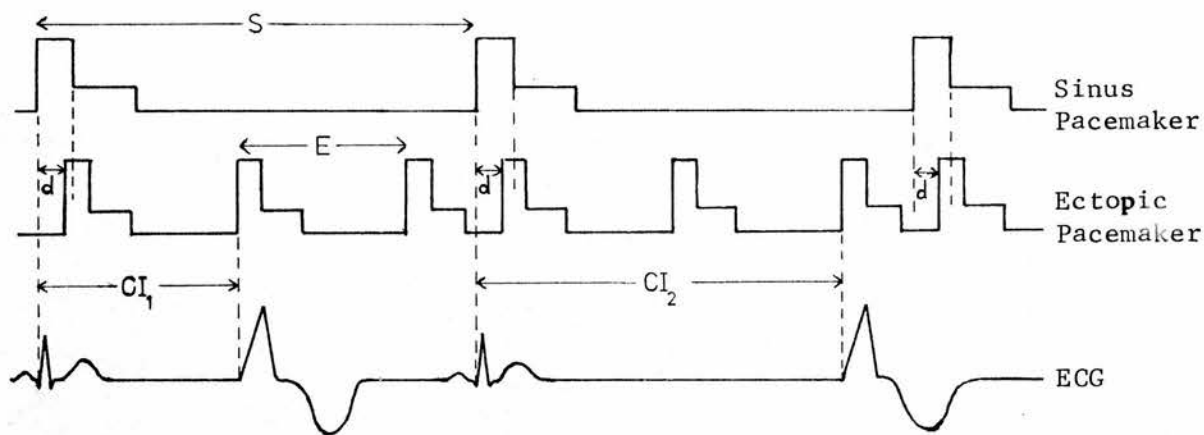
$$qE = (q - 1)S +$$

$qE = rS +$ This is the most general case but will be restricted to $q > r$, i.e. $E < S$.

For simplicity it is assumed that there is no exit block affecting the impulses emerging from the ectopic focus and that the ectopic complex never prevents the QRS complex from appearing. More realistic conditions are considered in the next chapter.

/

Fig.VII,5: Synchronized mode where $3E=S+$



b) X-Y plot
for E and P
constant

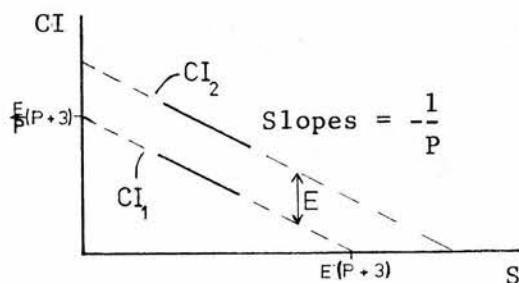
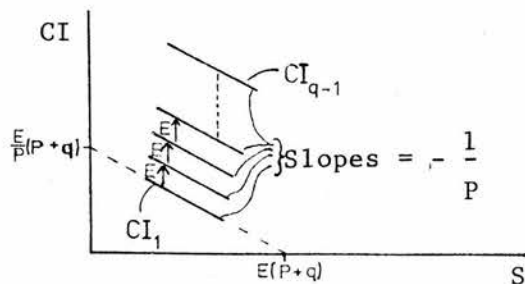
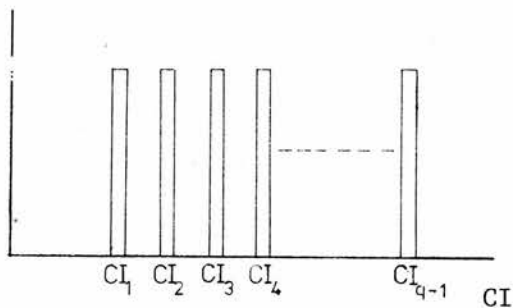


Fig.VII,6: Synchronized mode where $qE=S+$

a) X-Y plot
for E and P
constant



b) CI Histogram
No. of
occurrences



$$3E = S+ \text{ for } P \text{ and } E \text{ constant}$$

Fig.VII,5 shows the situation when three ectopic periods become synchronized to one sinus period. Two distinct CIs occur. As before, for synchrony

$$E + E + (E - Pd) = S$$

$$\therefore d = \frac{3E - S}{P}$$

Now

$$CI_1 = E + d$$

$$= E + \frac{3E - S}{P}$$

$$= \frac{E}{P}(P + 3) - \frac{S}{P}$$

(2)

and

$$CI_2 = CI_1 + E$$

$$= \frac{E}{P}(2P + 3) - \frac{S}{P}$$

$$qE = S+ \text{ for } P \text{ and } E \text{ constant}$$

This is a generalization of the type of case just considered, and the analysis takes the same form. By inspection of equations (1) ($2E = S+$) and (2) ($3E = S+$) it is clear that

$$CI_1 = \frac{E}{P}(P + q) - \frac{S}{P}$$

$$CI_2 = CI_1 + E$$

$$CI_3 = CI_2 + E = CI_1 + 2E$$

$$\vdots$$

$$CI_{q-1} = CI_1 + (q - 1)E$$

$$= \frac{E}{P}(P + q) - \frac{S}{P} + (q - 1)E$$

Thus there are $(q - 1)$ parallel lines in the X-Y plot (Fig.VII,6a) and $(q - 1)$ peaks in the CI histogram (Fig. VII,6b).

Fig.VII,7: X-Y plot for $qE=(1q-1)S+$ with Pand E constant

$$i^{\text{th}} \text{ slope} = -\left[\frac{q-1}{p} - (q-1-i)\right]$$

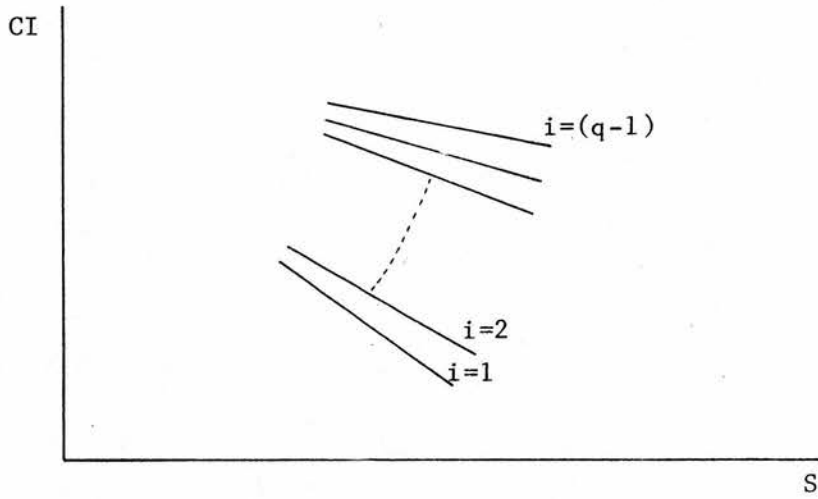
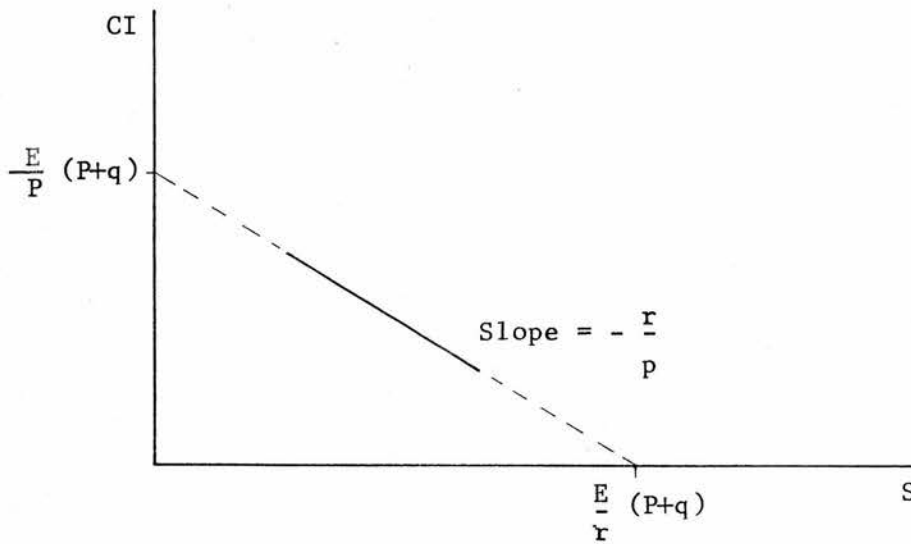


Fig.VII,8: X-Y plot for $qE=rSt$ with Pand E constant (only showing the line corresponding to CI).



For the case $qE = (q - 1) S +$ there are again $(q - 1)$ lines but all of different slope as shown in Fig. VII,7.

Fig. VII,8 shows the line corresponding to CI_1 for the case $qE = rS +$ where again there are $(q - 1)$ distinct CIs and lines.

As S varies there comes a critical point where S and E are too disparate for the pulling to maintain synchrony. Such points are called 'end points' in the X - Y plot. For a given E there are two end points, one where S is too large and the other where S is too small for synchrony to be maintained.

End points for $2E = S +$

For a constant E the end points are obtained as follows:

$$\begin{aligned} Pd &= 2E - S && \text{(as before)} \\ \text{i.e. } S &= 2E - Pd \\ \text{i.e. } E &= \frac{S + Pd}{2} \end{aligned} \tag{3}$$

At one end point $d = c$ since synchrony is about to be lost through S being too small.

$$\text{Now } CI = E + d$$

$$\therefore \text{ at the end point } CI = E + c \tag{4}$$

At this point S is determined, so put

$$S = S'$$

What is S' ? Substituting in (3):

$$S' = 2E - Pc \tag{5}$$

For the same E the other end point is attained when $d = 0$ since synchrony is about to be lost through S being too large.

$$\text{Again } CI = E + d$$

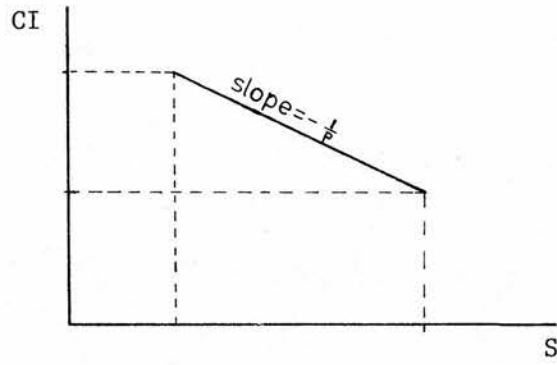
$$\therefore \text{ at the end point } CI = E$$

Putting $S = S''$ and substituting in (3)

$$S'' = 2E$$

Fig.VII,9: End points for the case $2E=S+$

a) E fixed



b) E varying

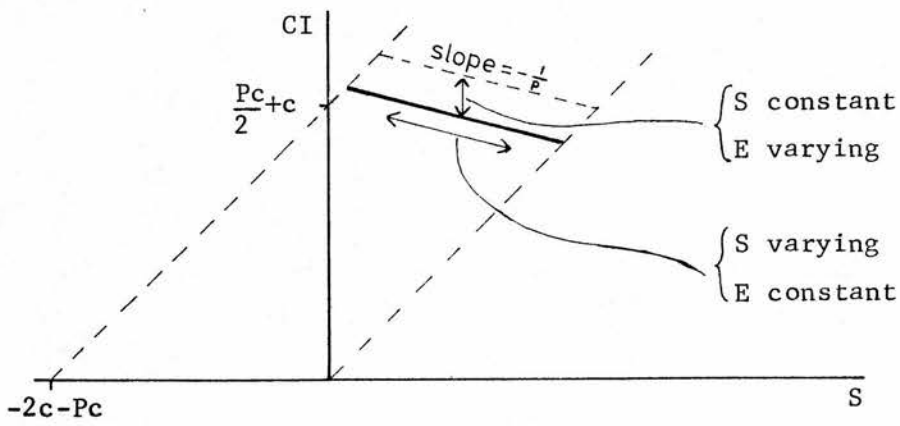
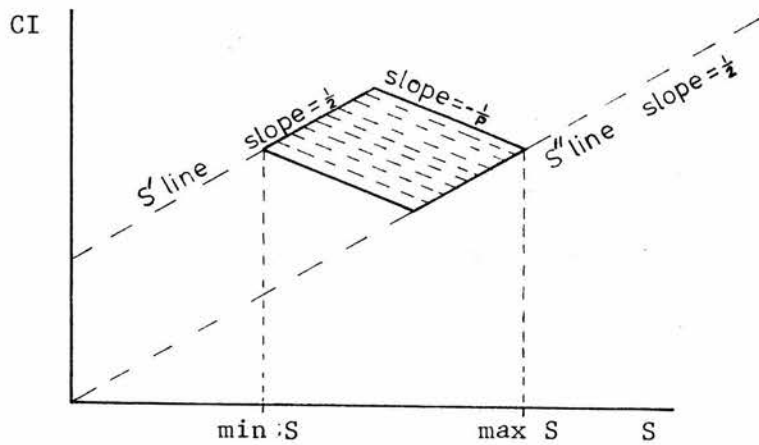


Fig.VII,10: X-Y plot with S and E varying for $2E=S+$



These end points are shown in Fig.VII,9a. The end points move as E varies.

The relationship between the position of the end points and E is obtained as follows:

$$\text{Consider } S': S' = 2E - Pc \quad (\text{from (5)})$$

$$\text{i.e. } E = \frac{S' + Pc}{2}$$

$$\text{but } CI = E + c \quad (\text{from (4)})$$

$$\begin{aligned} \text{eliminating } E: CI &= \frac{S' + Pc}{2} + c \\ &= \frac{S'}{2} + \frac{Pc}{2} + c \end{aligned}$$

$$\text{Consider } S'': S'' = 2E \quad (\text{from (6)})$$

$$CI = E \quad \text{when at } S''$$

$$\text{eliminating } E: CI = \frac{S''}{2}$$

As S varies with E constant, points lie on the solid line (Fig.VII,9b). If S moves outside the region between S' and S'' synchrony is lost. If E takes up a new value points lie on another line (dotted) parallel to the first with shifted end points as shown. With both S and E varying, but maintaining synchrony, points lie within the shaded area shown in Fig.VII,10.

$$\text{End points for } 3E = S +$$

The behaviour of the end points for the case $3E = S +$ is obtained in a similar manner.

For a Constant E:

$$Pd = 3E - S$$

$$\text{i.e. } E = \frac{S + Pd}{3} \quad (7)$$

Achieve S' when $d = c$:

$$\therefore E = \frac{S' + Pc}{3}$$

Fig.VII,11: X-Y plot with S and E varying for $3E=S+$. For E constant (Fig.VII,5) there are two lines and these become parallelograms when E varies.

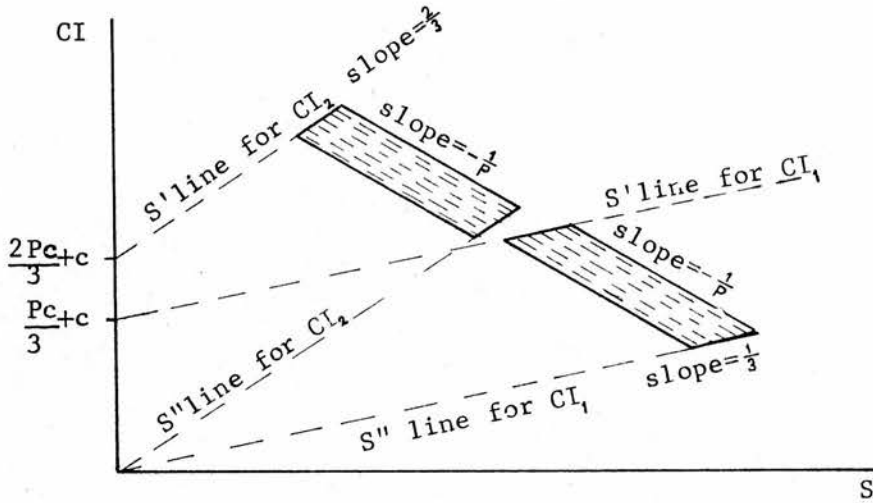
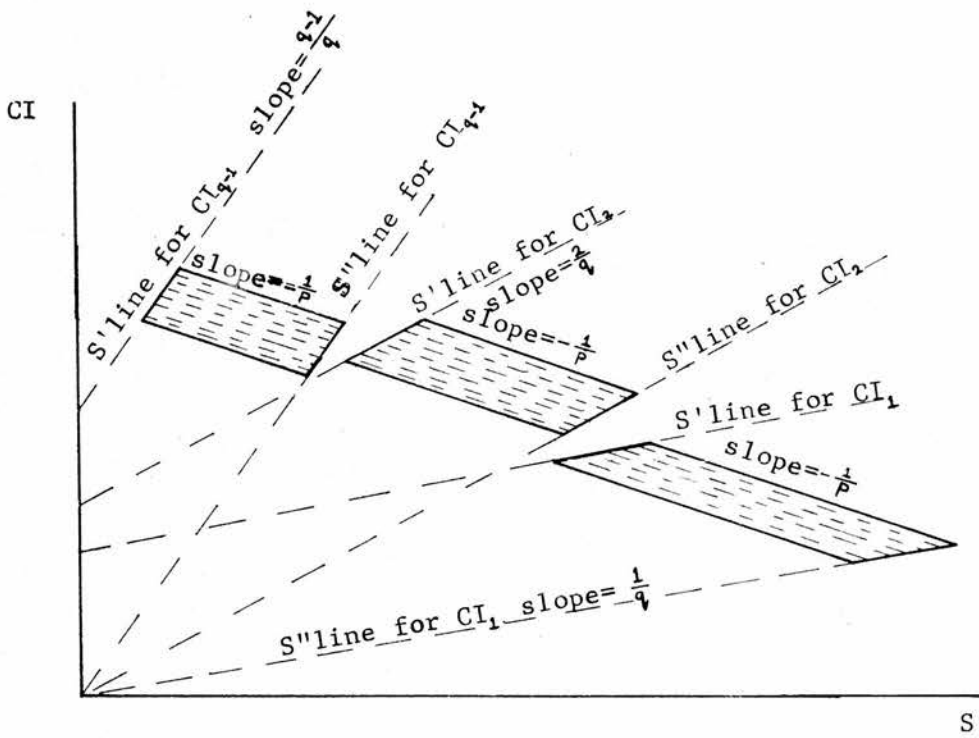


Fig.VII 12: X-Y plot with S and E varying for $qE=S+$.



$$\begin{aligned} \text{and } CI_1 &= E + d \\ &= E + c \end{aligned}$$

$$\begin{aligned} \text{eliminating } E: CI &= \frac{S' + Pc}{3} + c \\ &= \frac{S'}{3} + \frac{Pc}{3} + c \end{aligned}$$

$$\begin{aligned} \text{Also, } CI_2 &= CI_1 + E \\ &= \frac{2S'}{3} + \frac{2Pc}{3} + c + \frac{S' + Pc}{3} \\ &= \frac{2S'}{3} + \frac{2Pc}{3} + c \end{aligned}$$

Achieve S'' when $d = 0$:

$$\therefore E = \frac{S''}{3} \quad ((7) \text{ with } d = 0)$$

$$\text{and } CI_1 = E + d = E$$

$$\text{eliminating } E: CI_1 = \frac{S''}{3}$$

$$\begin{aligned} \text{Also, } CI_2 &= CI_1 + E \\ &= \frac{S''}{3} + \frac{S''}{3} \quad ((7) \text{ with } d = 0) \\ &= \frac{2S''}{3} \end{aligned}$$

These results are depicted in Fig.VII,11.

End points for $qE = S+$

The end points for $qE = S+$ are obtained by induction from the last two cases and the diagram is as shown in Fig. VII,12. As in Fig.VII,6 there are $(q - 1)$ separate CIs. What was a line when E is constant (Fig.VII,6) becomes a parallelogram when E varies (Fig.VII,12).

End points for $qE = (q - 1)S+$, and $qE = rS+$

Selected parallelograms for varying S and E are shown for the cases $qE = (q - 1)S+$ (Fig.VII,13), and $qE = rS+$ (Fig.VII,14).

Fig.VII,13: X-Y plot of CI_1 and CI_{q-1} with S and E varying for $qE=(q-1)S+$

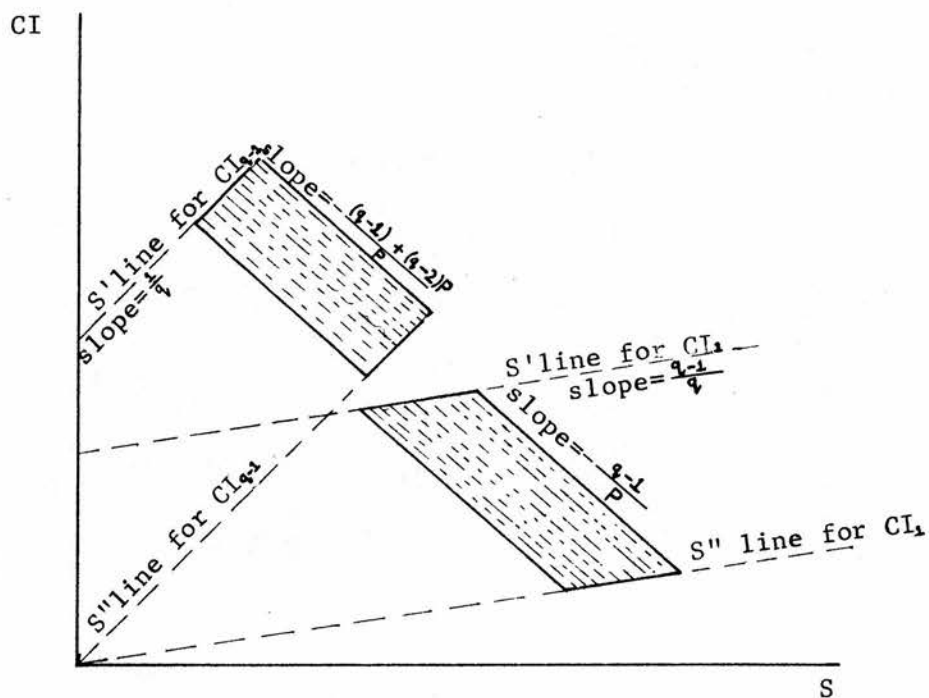
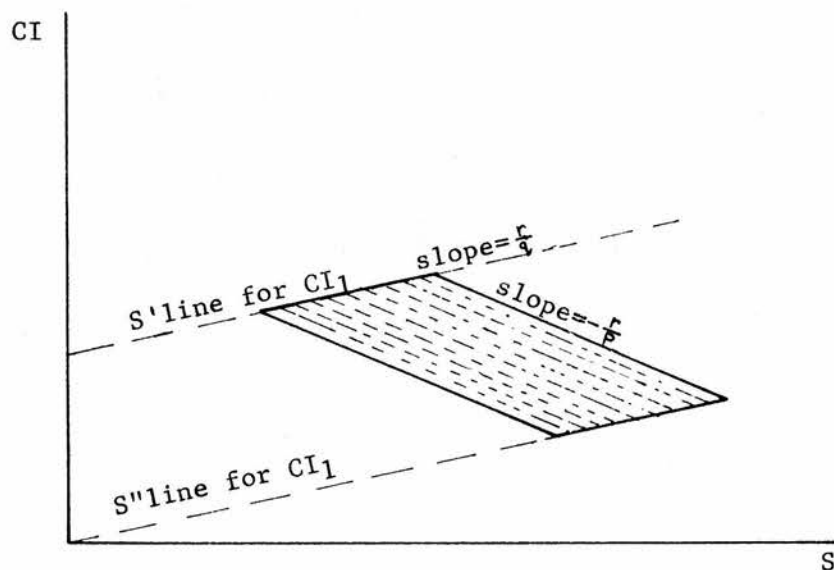


Fig.VII,14: X-Y plot showing CI_1 for the case $qE=rS+$ with S and E varying.

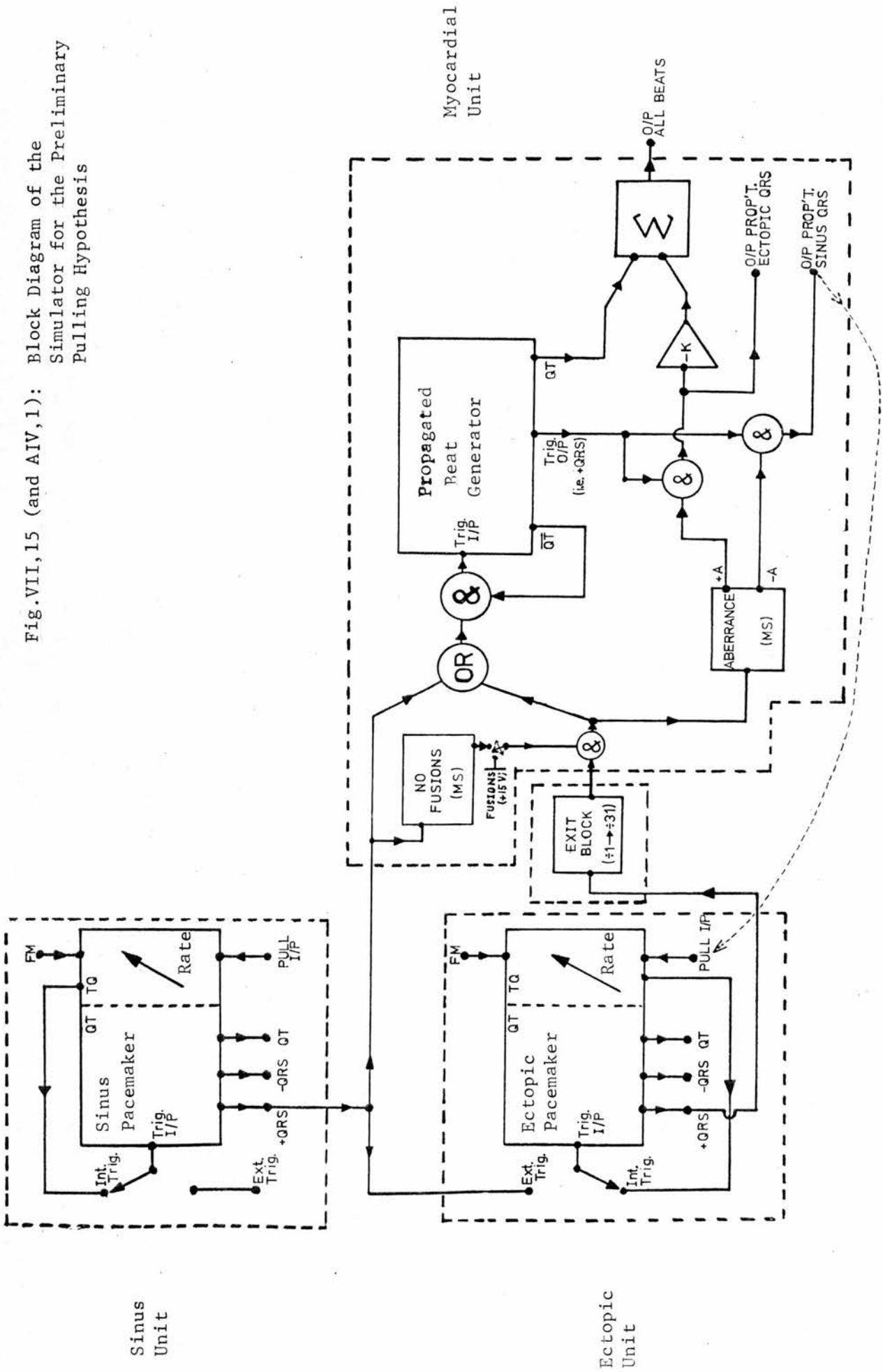


ii) Synchrony Under a Rapidly Changing
Sinus Rhythm - the Dynamic Theory

The static theory given so far describes how the following four parameters determine the X-Y plot in certain synchronized modes: the sinus period S, the ectopic period E, the electrotonic pulling strength P, and the maximum width of pulling c. For constant P and c, the boundaries of synchronized regions in the X-Y plot form parallelograms. Whether or not these boundaries are seen depends on S and E taking up suitable values. The dual question of the transition between synchronized modes and the time spent in and out of synchrony is most complicated and involves expressions in S, E, P, and c so complex as to make it very difficult to obtain a meaningful concept of the arrhythmic capabilities and properties of the preliminary pulling hypothesis. The purpose of an analysis is to provide just such a picture where S, E, P, and possibly c all vary in a physiologically plausible manner. Hence at this level a purely mathematical approach is self defeating.

The difficulties are greatly exacerbated by the complexities of the dynamic theory presented in Appendix III. This describes the behaviour in the X-Y plot when E, P and c are constant, and S varies rapidly in a manner similar to real sinus rhythm - a sudden change in S instantaneously leaves the CI somewhere between the steady-state value it takes before and after the change in S. In other words, a point occurs in the X-Y plot that does not lie on the appropriate steady-state line derived earlier (Figs.VII,4-9). Having been perturbed by a sudden change in S, the system approaches its new steady-state asymptotically at a rate primarily dependent on P. A complete algebraic description of the arrhythmic behaviour of the preliminary pulling hypothesis would be considerably more complicated than the analysis in Appendix III since the effects of changing E and P, and the conditions determining the mode of synchrony in all sections of the X-Y plane must be taken into account. The effects of exit block, and blockage of sinus impulses by V.E.Cs complicate the analysis still further. Hence there

Fig.VII, 15 (and AIV,1): Block Diagram of the Simulator for the Preliminary Pulling Hypothesis



is an over-riding need for a more appropriate form of analysis, and this is provided by the electronic simulator.

Testing of the Preliminary Hypothesis with an Electronic Analogue

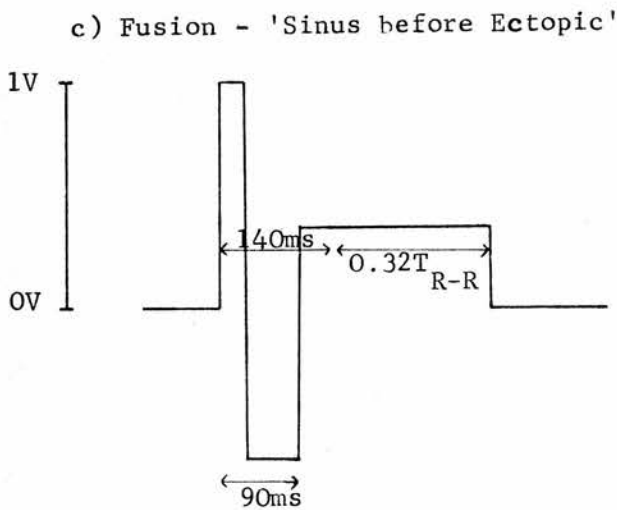
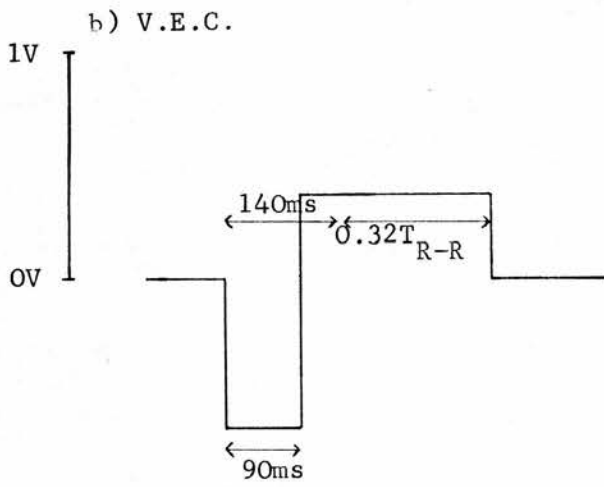
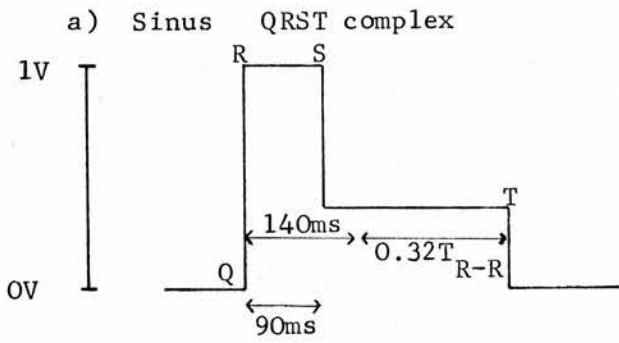
i) Description of the Simulator

Analysis of the arrhythmic properties of the preliminary hypothesis is readily performed on an electronic simulator, the basis of which was provided by J.M. Neilson. Only temporal aspects are modelled accurately since the present investigation is not concerned with the detailed shapes of either action potentials or ECG complexes. The model operates at 60 times real speed so that, for example, a rate of 70 beats per minute is represented by a rate of 70 beats per second.

The model consists of three interacting units (Fig. VII,15): a sinus unit representing sinus excitation as it reaches the ventricular conduction system; an ectopic unit consisting of a protected pacemaker fibre and an exit block function which acts on pulses emerging from the ectopic pacemaker; a myocardial unit which, when not refractory, produces QRS complexes when stimulated by the sinus unit, and V.E.Cs when stimulated by the ectopic unit.

All three units have similar central circuits which produce the 'systole' (QT) and 'diastole' corresponding to the unit's function. The phases of each unit are represented by appropriately shaped pulses. The pacemaker circuits each have a section causing diastole to be terminated after a specific interval of time, whereas diastole on the 'propagated beat' circuit is terminated by the arrival of an external stimulus from one of the other units. As a result, the pacemaker circuits exhibit 'automaticity' whereas the myocardial unit does not. Depending on the unit, the QT interval represents the refractory period of the sinus pacemaker, the ectopic pacemaker, or the ventricles. On each unit the absolute (or effective²³) refractory period only is simulated, and equals $140\text{ms} + 0.32T_{R-R}$ where T_{R-R} is the

Fig.VII,16: Complexes produced by the myocardial unit.



average cycle time for the unit in question. The relative refractory period of the ectopic pacemaker is most important to some of the pulling mechanisms examined in the next chapter, hence this is incorporated in the model where necessary. For the preliminary hypothesis relative refractoriness has little or no effect on the timing of events and so is not simulated. The rate of each pacemaker is controlled by external potentiometers which determine the appropriate diastolic intervals.

Exit block acts on the ectopic pacemaker pulses and can be set at any value between 1:1 (no block) and 1:31.

The myocardial unit produces two shapes of beat according to which unit stimulates it (Fig.VII,16). This is achieved by the aberrance monostable which may also produce fusion beats of the type 'sinus before ectopic' (Fig.VII, 16). The facility to produce fusion beats may be turned off. Details of the logic and circuitry of the simulator are given in Appendix IV.

Pulling is achieved by applying the sinus QRS complex produced by the myocardial unit to the diastolic timing section of the ectopic pacemaker. The result is exactly as shown in Fig.VII,2b. Details are given in Appendix IV.

To sum up, the model simulates the following functions of the preliminary pulling hypothesis. Spontaneous automaticity of the sinus and ectopic pacemakers is simulated by a QT interval which, when completed, initiates a ramp voltage function similar to phase 4 depolarization in automatic fibres - upon reaching a set threshold the ramp initiates another QT interval which on completion initiates a further ramp. The myocardial unit does not exhibit automaticity but may respond characteristically to sinus or ectopic pulses from the pacemaker units. The myocardial unit responds to these pulses only if they are not blocked by myocardial refractoriness or, in the case of ectopic pulses, by exit block. The refractory period of the myocardial unit is given by:

$$\text{myocardial QT} = 140\text{ms} + 0.32T_{R-R_m}, \quad T_{R-R_m} = \begin{matrix} \text{average} \\ \text{myocardial} \\ \text{period} \end{matrix}$$

or may be switched to:

$$\text{myocardial QT} = 140\text{ms} \quad (\text{constant}).$$

The QT intervals of the sinus and ectopic units are as follows:

$$\text{sinus QT} = 140\text{ms} + 0.32T_{R-R_s}, \quad T_{R-R_s} = \begin{array}{l} \text{average sinus} \\ \text{pacemaker period} \end{array}$$

ectopic QT = a selectable constant lying between 100ms and 600ms.

QRS complexes produced by sinus activated myocardium may pull the ectopic pacemaker by transiently altering the rate of the ramp function determining ectopic diastole.

ii) Mathematical Check of the Simulator's Performance

X-Y plots produced by the electronic model are examined in order to show that its static behaviour is in accordance with that predicted by the static theory. The method of obtaining the X-Y plot is essentially as described in Chapter III for real data. The only difference is that the arrhythmia computer is not used since the necessary timing of the intervals between sinus and ectopic 'events' can take place within the model. Accumulation of the X-Y plot is then identical to the method used for the real data.

The model is tested by measuring the slopes and positions of straight lines produced by it in the X-Y plot for the case $2E = S+$, and this is done for various values of P and E. As a further check the case $3E = 2S+$ is also examined, but only superficially.

For $2E = S+$ the relevant equations are:

$$CI = \frac{E}{P}(P + 2) - \frac{S}{P} \quad \text{where } P = \frac{\tan\theta_2}{\tan\theta_1} - 1$$

$$\therefore \text{for constant P and E, slope} = -\frac{1}{P}.$$

$\tan\theta_1$ and $\tan\theta_2$ are measured directly from the slopes of 'depolarization' (i.e. recovery of monostable M_4 , Fig.A IV,2), and P is deduced from this. The results of four experiments

Table VII, 1: Performance of the Electronic Model of the Preliminary Pulling Hypothesis in Four Cases of $2E = S +$ with Different Values of P. (All numbers are rounded to 2 figures except S and CI measured from the X-Y plot)

MEASURED VALUES										PREDICTED VALUES			DIFFERENCE BETWEEN MEASURED AND PREDICTED VALUES (%)	
from Model (errors $\approx \pm 5\%$)		from X-Y Plot				in X-Y Plot				CI	Slope			
E(ms)	$\tan \theta_1$	$\tan \theta_2$	P	S(ms) (not rounded)	CI(ms) (not rounded)	Slope	CI(ms)	Slope	$= -\frac{1}{P}$					
500	0.7	$\frac{3.3}{2}$	1.4	900	540	-0.73	570	-0.74	-0.74	+5½%	-1½%			
500	0.7	1.4	1.0	1000	490	-0.95	500	-1.0	-1.0	- 2%	-5½%			
500	0.7	1.2	0.7	1000	475	-1.3	500	-1.4	-1.4	- 5%	-7½%			
500	0.7	1.0	0.43	1000	460	-2.1	500	-2.3	-2.3	-8½%	-9½%			

CI
(ms)

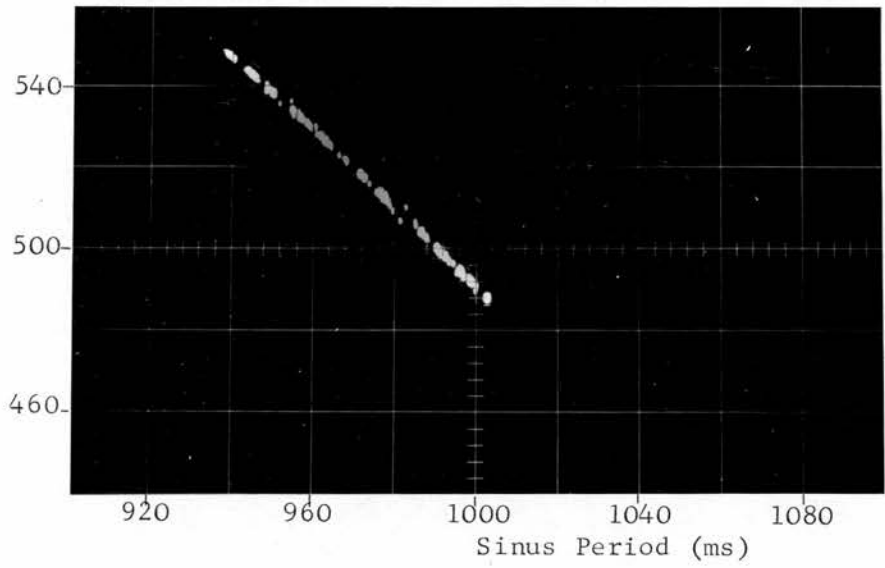


Fig.VII,17:
X-Y plot produced
by the electronic
model of the
preliminary pulling
hypothesis for the
case $2E=S+$.
 $P=1$, $E=500\text{ms}$.

Table VII,2: Performance of the Electronic Model for the Case 3E= 2S+. Experimental details same as for Table VII,1.

		MEASURED VALUES					PREDICTED VALUES					DIFFERENCE BETWEEN MEASURED AND PREDICTED VALUES (%)			
from Model		from X-Y Plot					in X-Y Plot								
E (ms)	P	S (ms)	CI ₁ (ms)	SI ₁	CI ₂ (ms)	SI ₂	CI ₁ (ms)	SI ₁	CI ₂ (ms)	SI ₂	CI ₁ (ms)	SI ₁	CI ₂ (ms)	SI ₂	
800	2.5	1060	200	-1.7	680	-0.80	180	-1.8	690	-0.80	+10%	-6%	-1½%	<1%	

CI
(ms)

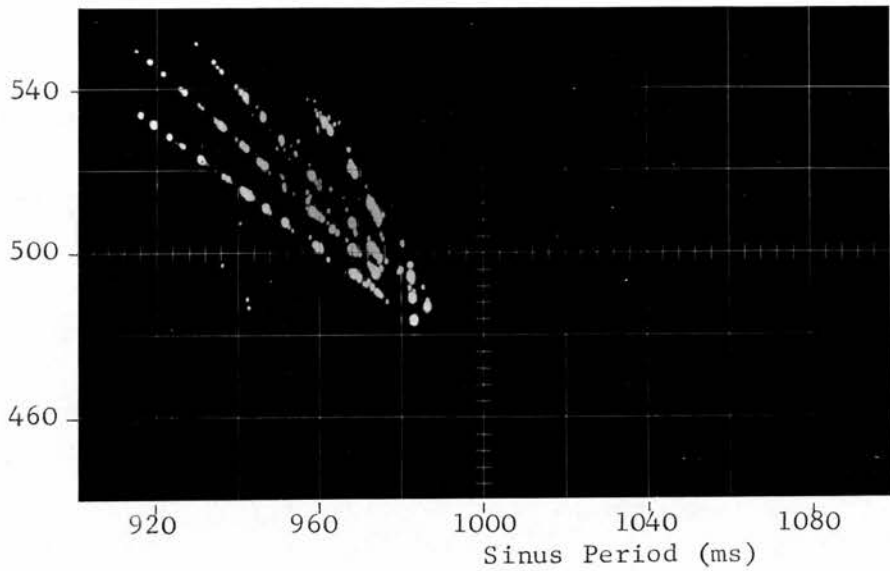


Fig.VII,18:
X-Y plot produced
by the electronic
model of the
preliminary pulling
hypothesis for
the case $2E=S+$.
0.4 P 1.5,
E=500ms.

CI
(ms)

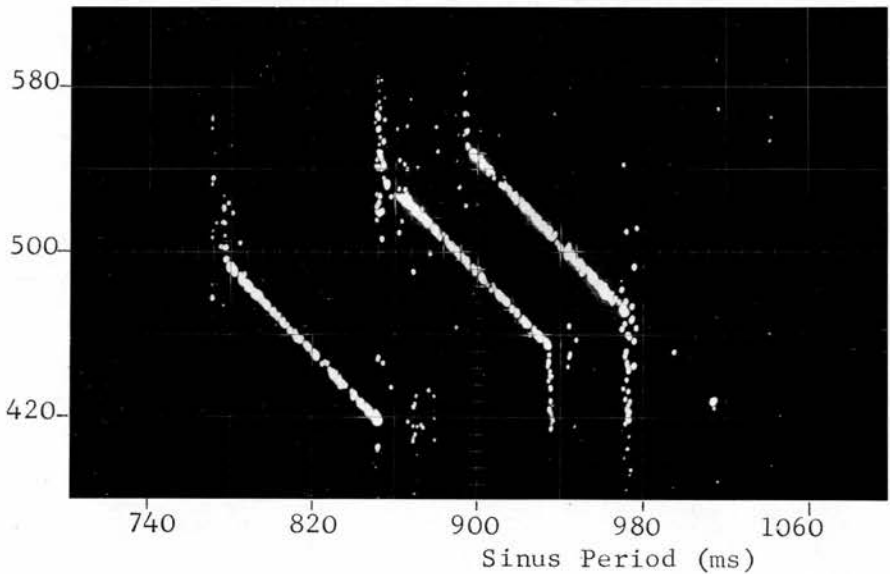


Fig.VII,19:
X-Y plot produced
by the electronic
model of the
preliminary pulling
hypothesis for
the case $2E=S+$.
P=1.0, E=420,
450, 480ms.

CI
(ms)

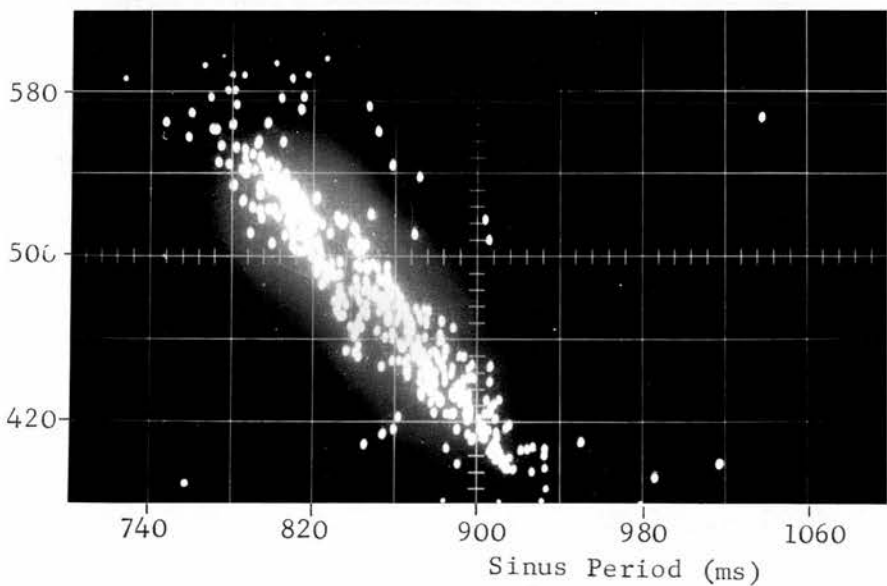


Fig.VII,20:
X-Y plot produced
by the electronic
model of the
preliminary pulling
hypothesis for the
case $2E=S+$ with a
rapidly varying
sinus period.
P=0.86, E=450ms.

are presented in Table VII,1, and the actual X-Y plot of the second of these is presented in Fig.VII,17. As can be seen in the photograph, the departure from linearity is negligible and is lost in the size of the dots making up the plot. E and P (via $\tan\theta_1$ and $\tan\theta_2$) were measured on a Hewlett Packard 140A oscilloscope, the errors being approximately $\pm 5\%$ and are due to the rise times of pulses and the width of the oscilloscope beam. Then for a given value of S, the CI and slope are calculated to give the "Predicted Values". In Table VII,1 these are compared to the "Measured Values" taken directly from the X-Y plots. All the measured values are within -10% of the predicted values and most are better than this. This is in total accord with the errors expected to accrue from the 5% errors in E, $\tan\theta_1$, $\tan\theta_2$ and the manipulation of these used to obtain the "Predicted Values".

A further check is to superimpose lines of different P in order to see whether they converge at the point $S = 2E$ as predicted by the static theory. In this case $E = 500\text{ms}$, and the predicted point of convergence is therefore $S = 1000\text{ms}$, $CI = 500\text{ms}$. Fig.VII,18 shows a strong tendency for the lines to converge at a point lying between $S = 995$ and 1005ms , $CI = 465$ and 475ms , and this agrees with the predicted value.

The effect of varying E while keeping P constant is shown in Fig.VII,19. Theory predicts that the slope of the lines bounding the region of synchrony have slope $+\frac{1}{2}$ (cf. Figs.VII,9b and VII,10). The loss of synchrony takes place at the junctions between the lines of negative slope and the vertical lines. The boundary lines through these junction points have slope 0.45 (lower) and 0.49 (upper), and this agrees well with theory.

The results of a test on the case $3E = 2S +$ are presented in Table VII,2. The method used was exactly the same as for Table VII,1. There are two separate CIs (CI_1 , CI_2) with separate slopes ($S1_1$, $S1_2$). The agreement between measured and predicted values is satisfactory.

Finally, the effect of a rapidly varying sinus period

Fig.VII,21:
 X-Y plot produced
 by the electronic
 model of the
 preliminary
 pulling hypothesis
 with a slowly
 increasing sinus
 period. $E_A=200\text{ms}$,
 $E_4=300\text{ms}$, $P=1$,
 exit block =3:1.

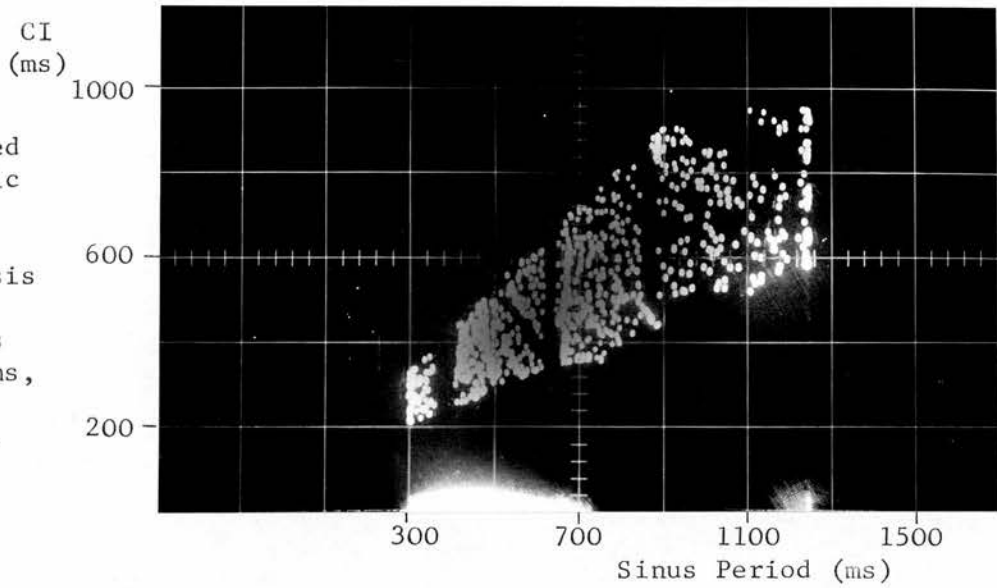
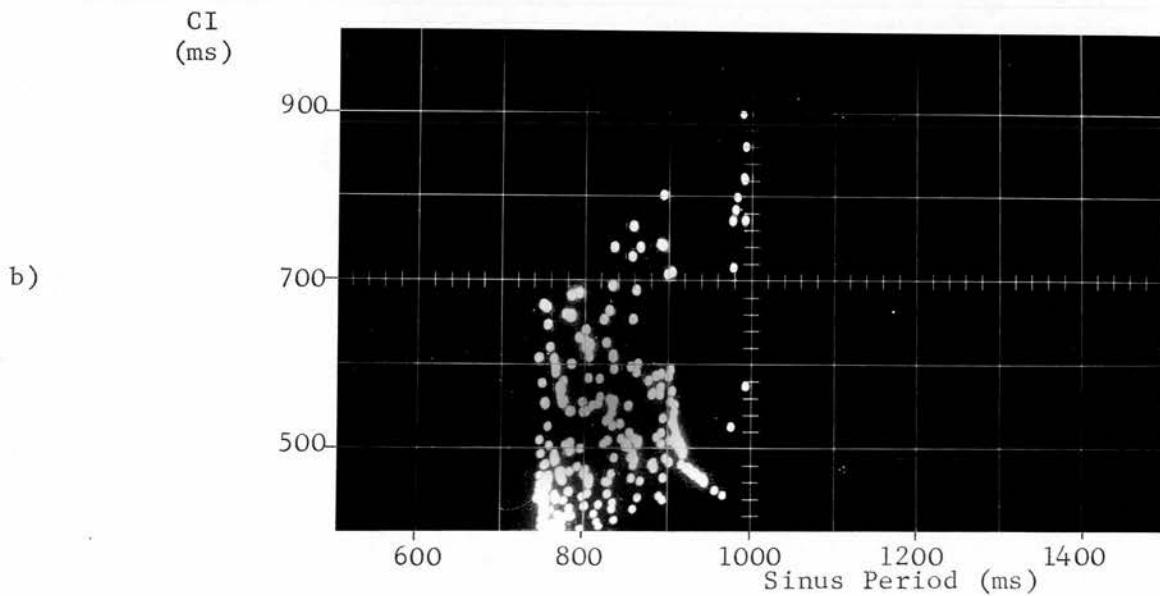
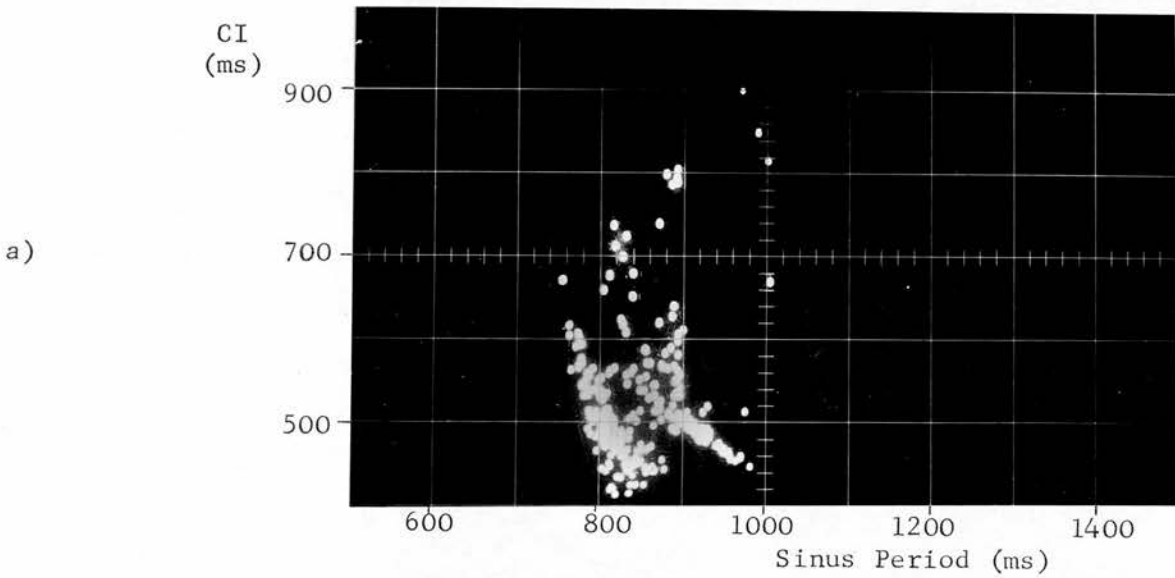


Fig.VII,22: Breakdown of patterns on changing the exit block (see text).



is shown in Fig.VII,20. P and E are constant at 0.86 and 450ms respectively.

Since the electronic model behaves as expected in several selected synchronized, static situations, it is concluded that the model may be used to investigate more complex circumstances. In particular, de-synchronized and dynamic situations which are mathematically unwieldy may be investigated.

iii) Comparison of the Simulator's Performance with the Data Measured from ECGs.

This part of the investigation was carried out by examining the X-Y plot and inter-ectopic numbers simultaneously under many circumstances. The model was given an initial set of parameters, namely $E = E_A$ (ectopic action potential duration, i.e. ectopic QT) + E_4 (duration of ectopic phase 4 depolarization), P, and exit block; S was increased slowly throughout its range (400ms to 1400ms) and the X-Y plot photographed, for example Fig.VII,21; each section of the X-Y plot was enlarged on the oscilloscope screen and investigated with various combinations of exit block under both slowly and rapidly changing S - patterns of inter-ectopic numbers were noted throughout; the whole procedure was then repeated for a succession of values of E_A and E_4 ranging from $E_A = 100\text{ms}$, $E_4 = 300\text{ms}$, to $E_A = 550\text{ms}$, $E_4 = 4000\text{ms}$.

This investigation produced many X-Y plots and more than 25 photographs. At first sight a few of these seemed to compare favourably to some of the data presented in Chapter IV. On further examination it was frequently found difficult to make a reasonable claim for the model's behaviour. A typical example is shown in Fig.VII,22. Fig.VII, 22a was taken under the following conditions: $E_A = 200\text{ms}$, $E_4 = 300\text{ms}$, $P = 1.2$, exit block = 5:1, S changing rapidly. The inter-ectopic number (N) was consistently equal to 2 for the right-hand line, and equal to 4 for the lower portion of the left-hand band, but for CIs greater than 500ms many Ns occurred and the distribution of N was "smooth" (see

Chapter II for a discussion of this term). At first sight this behaviour seems somewhat reminiscent of Case 12 (Chapter IV), but on altering the exit block the X-Y and N patterns break down as shown in Fig.VII,22b. This phenomenon of unstable pattern formation is highly characteristic of the preliminary pulling hypothesis and was one of the main factors indicating the need for further pulling hypotheses.

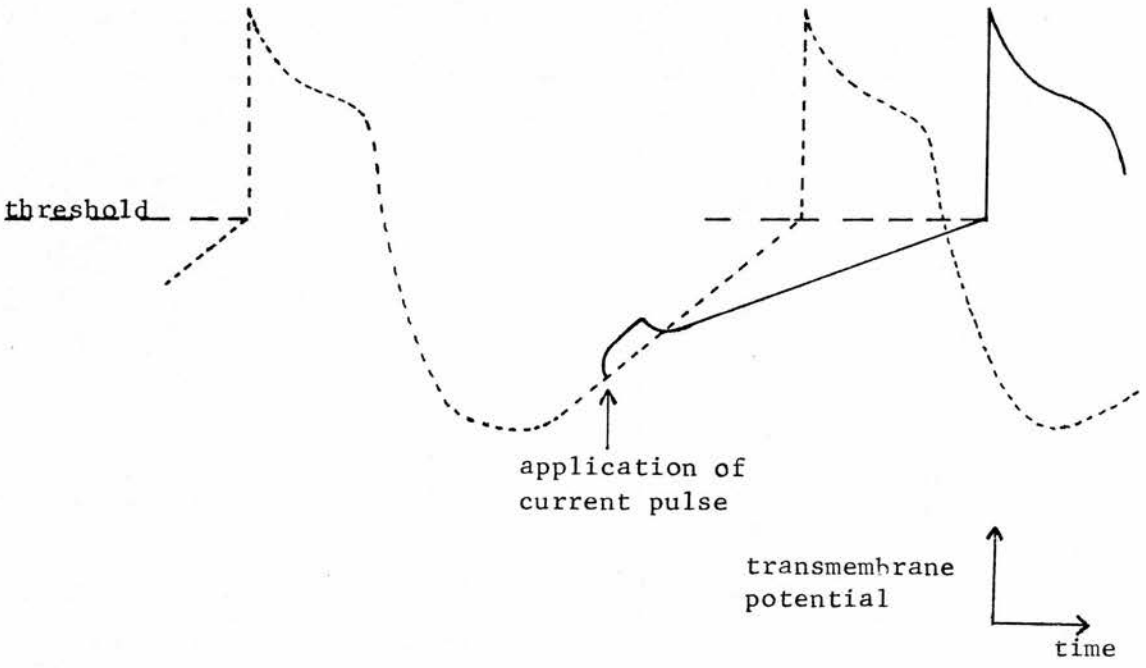
The other main shortcoming of the preliminary pulling hypothesis is that it seems incapable of producing well defined triangles of the type exhibited by Cases 5, 8 and 11 (Chapter IV). In addition, it was found impossible to obtain concealed bigeminy under any circumstances.

It may be argued that the pulling strength used was insufficient to represent the preliminary pulling hypothesis realistically. With E_4 equal to 4000ms the maximum shortening was arranged to be 1600ms, and this proportion was typical of all the settings used. It is felt that pulling which affects shortening in E_4 greater than 40% of its inherent value is unlikely to come about through the mechanism of the preliminary pulling hypothesis.

Changing the pulling mechanism to the type shown in Fig.VII,2b had little effect on the behaviour.

In order to determine whether the general hypothesis of pulling is tenable it is clearly necessary to formulate and investigate further pulling hypotheses.

Fig.VIII,1: (After Weidmann,1951) Post cathodal depression delaying the onset of the action potential after the application of a sub-threshold, cathodal current pulse.



CHAPTER VIII Testing of Further Pulling Hypotheses
with the Simulator

The Three Hypotheses and an Outline of Their Electronic
Simulation

The inadequacies of the preliminary pulling hypothesis has led to a consideration of other possible pulling mechanisms. This has resulted in three further hypotheses which will be referred to as i) phase 4 cathodal extension ii) phase 4 anodal shortening, and iii) action potential extension. The following discussion includes an outline description of the way in which these hypothetical pulling mechanisms are simulated by the appropriate electronic analogues.

i) Phase 4 Cathodal Extension

This hypothesis is based on the effect of cathodal current on the transmembrane potential of pacemaker fibres undergoing spontaneous phase 4 depolarization. Weidmann⁸⁵ has shown that the time taken for such a fibre to attain its threshold potential may be increased by the application of a subthreshold pulse of cathodal current, and the onset of the following action potential is thereby delayed. Fig. VIII,1 (after Weidmann) illustrates the mechanism responsible for this delay. The dotted line represents the normal course of events with no external stimuli. The solid line shows the fibre's response to a subthreshold pulse of cathodal current. On completion of the pulse the membrane not only returns to the potential it would have attained of its own volition, but proceeds to depolarize at a lower rate than before.

Fig.VIII,2: (After Weidmann, 1951) Dotted line represents the normal sequence of events. Solid lines 1,2,3 represents the effect of altering the strength of sub-threshold stimuli.

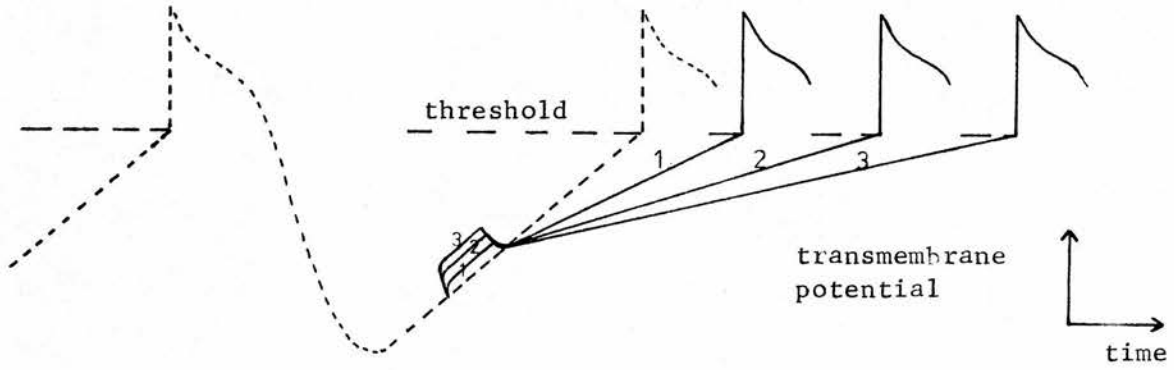
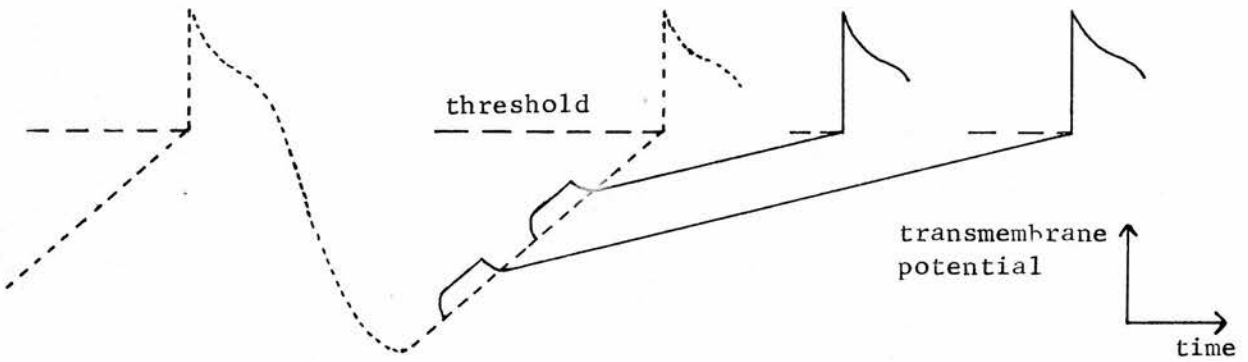


Fig.VIII,3: Extension of the ectopic cycle depends on the time of arrival of the sub-threshold stimulus.



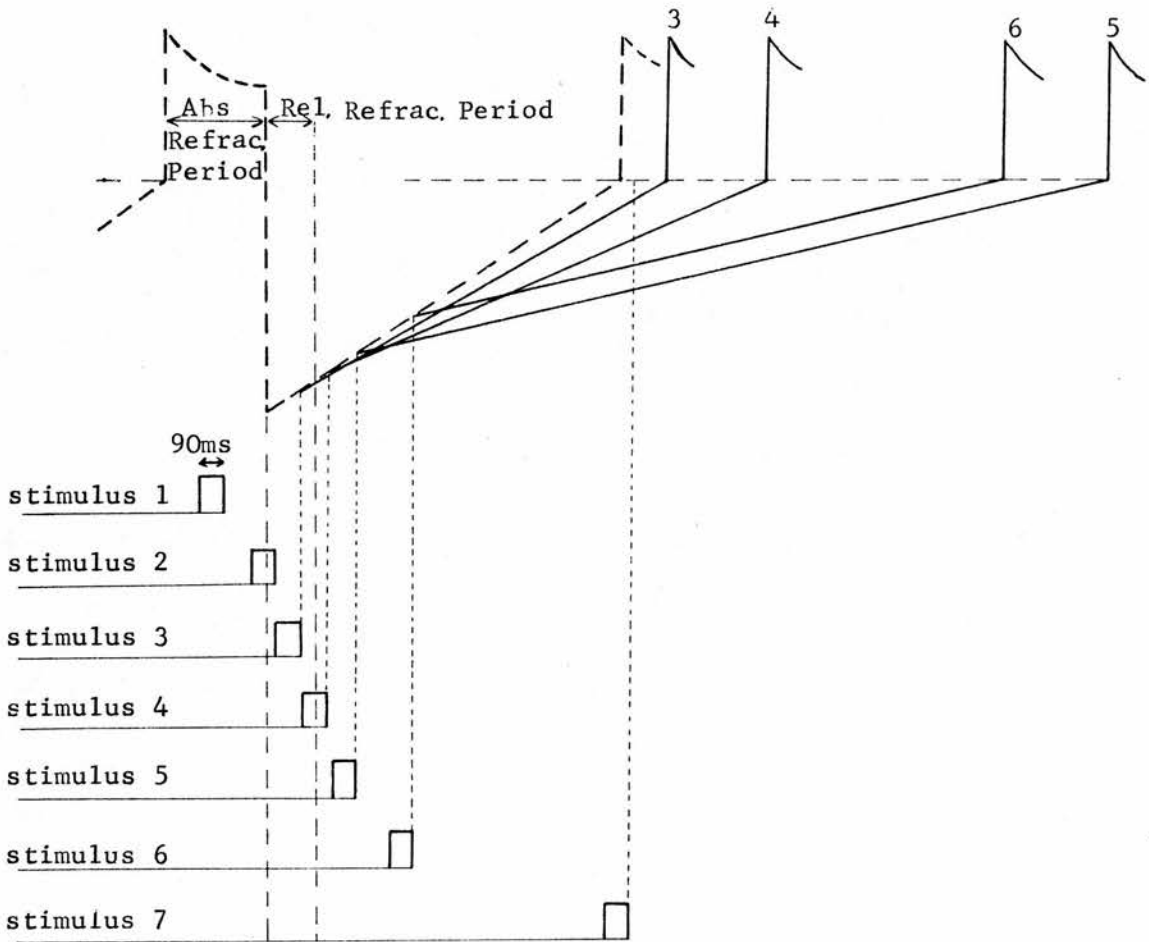
For the present hypothesis it is proposed that sinus excitation may induce a subthreshold pulse of cathodal current within the ectopic site: as sinus initiated depolarization passes over the ectopic area, the density and direction of electrotonic current flow changes rapidly within and around that area. As a result the ectopic pacemaker may receive a pulsed stimulus coincident with sinus excitation, and this induces post cathodal depression. The following discussion indicates how, under such circumstances, the lengthening of the ectopic cycle is determined by the time of arrival of the sinus stimulus within the ectopic cycle.

Fig. VIII,2 (after Weidmann⁸⁵) illustrates how the magnitude of the response to the subthreshold stimulus determines the severity of post cathodal depression. Even if the response is constant the extension of the ectopic cycle is dependent on the time of arrival of the sinus stimulus (Fig. VIII,3). The degrees of post cathodal depression following stimuli '1' and '2' are the same in that both stimuli give rise to the same change in the slope of phase 4 depolarization. However, this altered slope acts for a longer time following stimulus '1' than it does following stimulus '2', hence the variability of the impact of these stimuli on the ectopic cycle length.

This variability is simulated on the electronic model by altering the slope of phase 4 depolarization of the 'ectopic pacemaker' by a fixed amount following each sinus activation of the myocardial unit. In addition two things are clear: firstly, the ectopic pacemaker cannot respond while absolutely refractory, and secondly, the transition from no response to full response (subthreshold) is not discontinuous but takes place gradually^{23 27}, the magnitude of the response being determined by the relative refractoriness of the ectopic pacemaker.

/

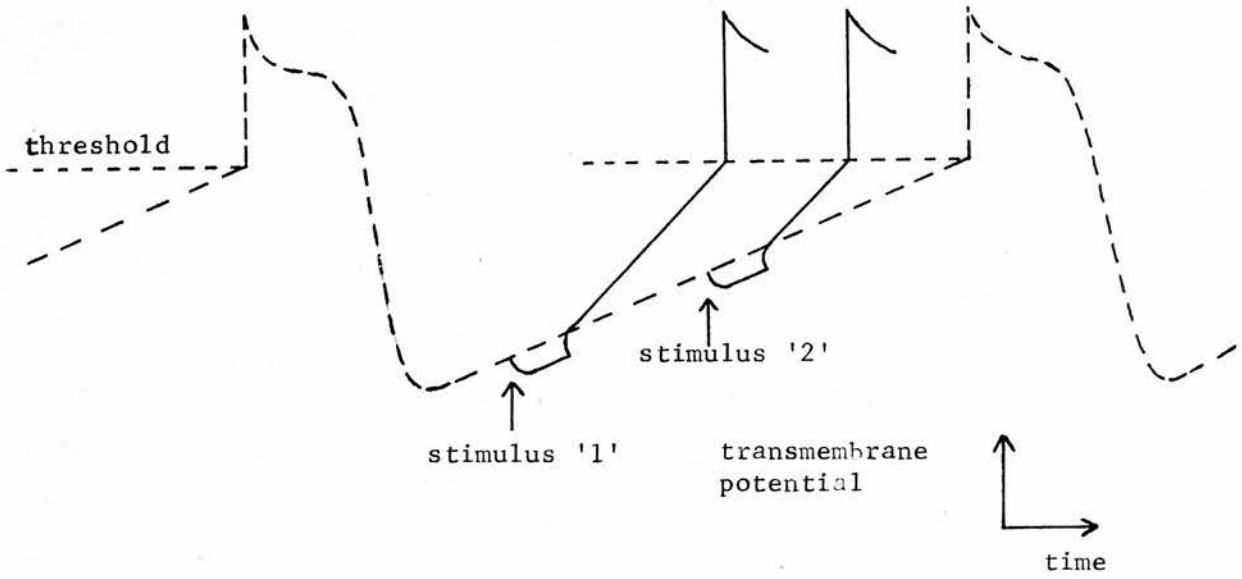
Fig.VIII,4: Detailed functioning of the model of Phase 4 Cathodal Extension. The dotted line represents normal ectopic pacemaker activity. Note that post cathodal depression (change in slope of phase 4 depolarization) is greater following stimulus '4' than that following '3'. Stimuli '5' and '6' induce the same degree of post cathodal depression but '5' has the greater effect on the ectopic period.



Furthermore, the assumption is made that the size of the response determines the degree of post cathodal depression as in Fig. VIII,2. Taking all these factors into consideration the electronic model of "phase 4 cathodal extension" was designed to function as follows (Fig. VIII,4). Stimuli '1' through '7' result from sinus activation of the myocardium and have a duration of 90ms (X1). Post cathodal depression acts from the moment of completion of the stimulus, and its degree is determined by the moment of onset of the stimulus (Fig. VIII,4). Stimuli '1' and '2' have no effect since the ectopic pacemaker is in its absolute refractory period which is set externally at any constant value lying between 100ms and 600ms (X1). Stimulus '3' has a minimal effect as it arrives early in the relative refractory period, whereas stimulus '4' has a greater effect since the ectopic fibre is nearer full recovery. Stimuli '5' and '6' induce the maximum change in the rate of ectopic phase 4 depolarization, but '5' has the greater effect on the ectopic period because its post cathodal depression acts for a longer time. The ectopic fibre discharges before stimulus '7' can have any effect.

Details of the electronic simulation are given in Appendix V. The basic simulator is identical to that of the preliminary pulling hypothesis. Various additional timing circuits are employed in order to manufacture a voltage waveform which, when applied to the ectopic "pull input", results in a simulation of post cathodal depression as depicted in Fig. VIII,4. In addition to all the parameters concerned with the basic simulator, the model of phase 4 cathodal extension has two further parameters with values which can be chosen as follows: i) point in the ectopic cycle after which the response is maximum (selectable between 70ms and 140ms after the completion of ectopic QT, i.e. E_A); ii) degree of post cathodal depression resulting from this maximum response (the % increase in the duration of ectopic phase 4 (E_4) in response to an optimally timed stimulus is selectable between 0% and 100% (at least)).

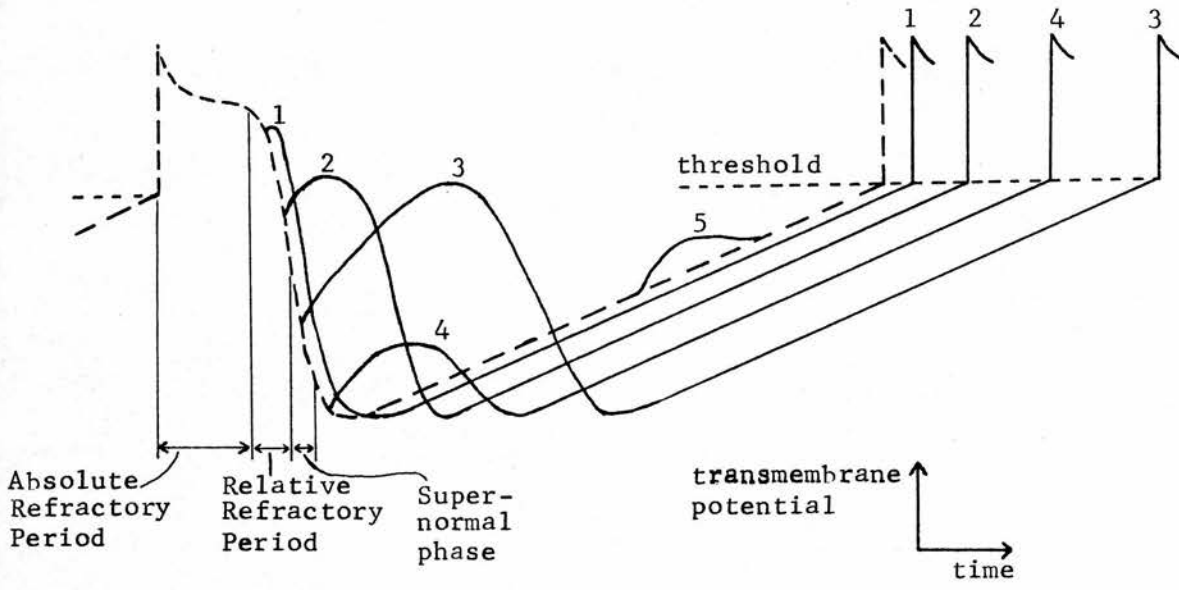
Fig.VIII,5: Post Anodal Enhancement. The reduction in duration of phase 4 depolarization depends on the timing of the anodal current pulse.



ii) Phase 4 Anodal Shortening

In phase 4 anodal shortening the sinus excitation applies a negative going anodal current pulse to the ectopic pacemaker, and this results in post anodal enhancement⁸⁵ and shortens the duration of ectopic phase 4 depolarization. The effect is illustrated in Fig. VIII,5 and is the exact opposite to post cathodal depression. Electronic simulation of phase 4 anodal shortening is achieved by inverting the waveform applied to the "pull input" for phase 4 cathodal extension (see Appendix V). The % shortening in ectopic phase 4 (E_4) in response to an optimally timed anodal stimulus is selectable between 0% and 50% (at least).

Fig.VIII,6: Lengthening of the action potential of an ectopic pacemaker by the application of sinus initiated, sub-threshold stimuli. Dotted line represents the usual course of action.



iii) Action Potential Extension

This hypothesis makes use of an electrophysiological phenomenon demonstrated by Kao and Hoffman²⁷ and involves an effective lengthening of the action potentials of Purkinje fibres. This is achieved by the application of a stimulus during the relative refractory period and the super-normal phase of excitability.

Fig. VIII,6 illustrates the envisaged effects on the ectopic pacemaker fibre of five subthreshold stimuli. The dotted line represents the usual course of the ectopic fibres' transmembrane potential with no external stimulus. The five stimuli arise from sinus activation of the myocardium and are subthreshold since the ectopic pacemaker is surrounded by entrance block. As a result, the response to stimulus '5' has no effect on ectopic periodicity. This is in accord with the results of Singer et al⁷¹ where a reduction in responsiveness is shown to accompany phase 4 depolarization in depressed fibres. Stimulus '1' causes a small lengthening in the ectopic's action potential and thereby increases that particular ectopic cycle time. Stimuli '2' and '3' cause greater increases in the ectopic cycle time. It is assumed that stimulus '4' would induce a smaller lengthening than does stimulus '3' since the transition from the maximum effect of stimulus '3' to the minimum effect (probably nil) of stimulus '5' must be gradual. In any case this assumption is made, and hence the mechanism is conceived of as follows: i) as before, the absolute refractory period of the ectopic pacemaker is set at a constant value (selectable on the simulator), but now this is followed by a period of relative refractoriness; ii) if the ventricular myocardium is activated by sinus excitation during the ectopic's relative refractory period, then the width of the ectopic's action potential is increased; iii) the extent of this increase is determined by the exact time of arrival of the sinus excitation at the ectopic site - it is a maximum somewhere in the ectopic's super-normal phase (if it has one), and gradually decreases to zero as the sinus arrives earlier or later in the ectopic cycle.

If response '3' should be a full sized action potential the mechanism may still be regarded as pulled parasystole provided the response is graded with respect to the time of arrival of the stimulus. The ectopic pacemaker is still autonomous although subservient to sinus rhythm, and the resulting arrhythmias are best visualized in terms of the interaction of two separate rhythms. Even if response '3' is a full action potential it can never give rise to a V.E.C. since the myocardium is refractory from the sinus excitation which gives rise to it - the only result is a large lengthening of the ectopic cycle. However, if response '5' were to be a full action potential the case would not be considered as parasystolic since the ectopic site would not be capable of acting as a separate pacemaker.

The electronic analogue of this hypothesis uses the basic simulator but re-sets the ectopic pacemaker according to the timing of sinus activation of the myocardial unit. Values of certain parameters are selectable as follows: maximum subthreshold response (between 35ms and 400ms); time in ectopic phase 4 at which the maximum response takes place (between 20ms and 200ms after the end of ectopic 'QT' (i.e. E_A); time in ectopic phase 4 after which there is no response (between 20ms and 200ms after the time of maximum response). Details of the electronic simulation are given in Appendix VI.

A Quantitative Check on the Static Performance of the Three Simulators

To do this certain measurements are taken from the X-Y plots produced by the simulators in static (slowly changing S) bigeminy. These are compared to the predictions of a mathematical analysis of the situation. The analysis and results are presented in Appendix VII.

The purpose of this check is to enable the models to be used with confidence to investigate more complex situations. Two checks are undertaken, the first on phase 4 cathodal extension, the second on action potential extension.

CI
(ms)

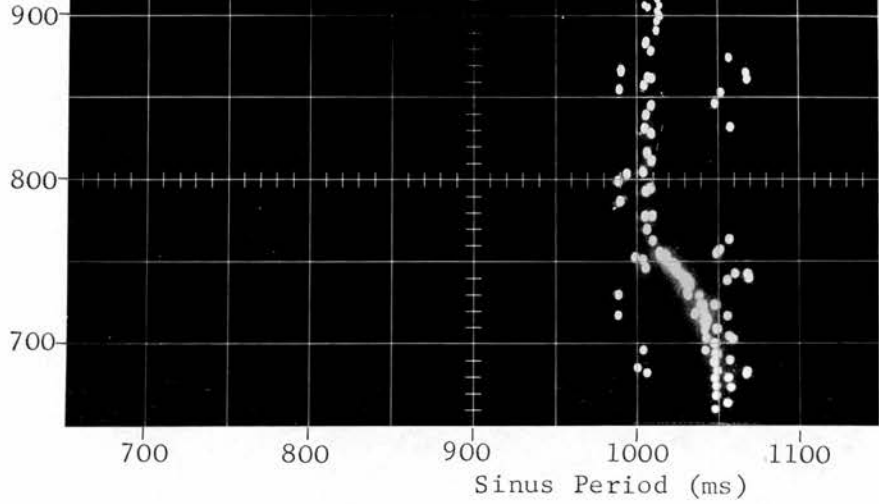


Fig.VIII,7:
Phase 4 Cathodal
Extension. A
stable X-Y pattern.
 $E_A=200\text{ms}$, $E_4=300\text{ms}$,
max. extension of
 $E_4=100\text{ms}$.

CI
(ms)

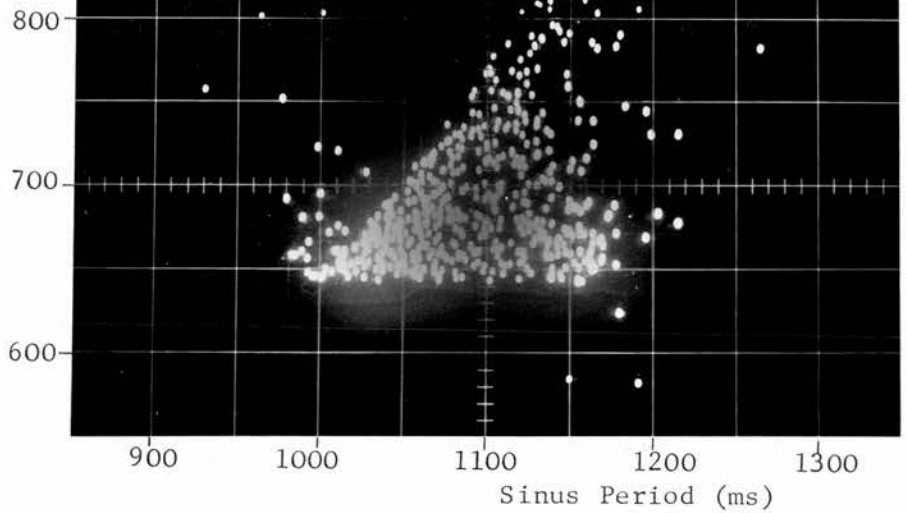


Fig.VIII,8:
Phase 4 Cathodal
Extension. A
stable triangle
between $S=1000$
and 1175ms .
 S varies rapidly.
 $E_A=300\text{ms}$, $E_4=700\text{ms}$,
max. extension of
 $E_4=360\text{ms}$.

Fig.VIII,9: Phase 4 Cathodal Extension. X-Y plot for a case of concealed trigeminy, i.e. $N=2+3$ (E.B.) $E_A=600\text{ms}$, $E_4=900\text{ms}$, max. extension of $E_4=300\text{ms}$.

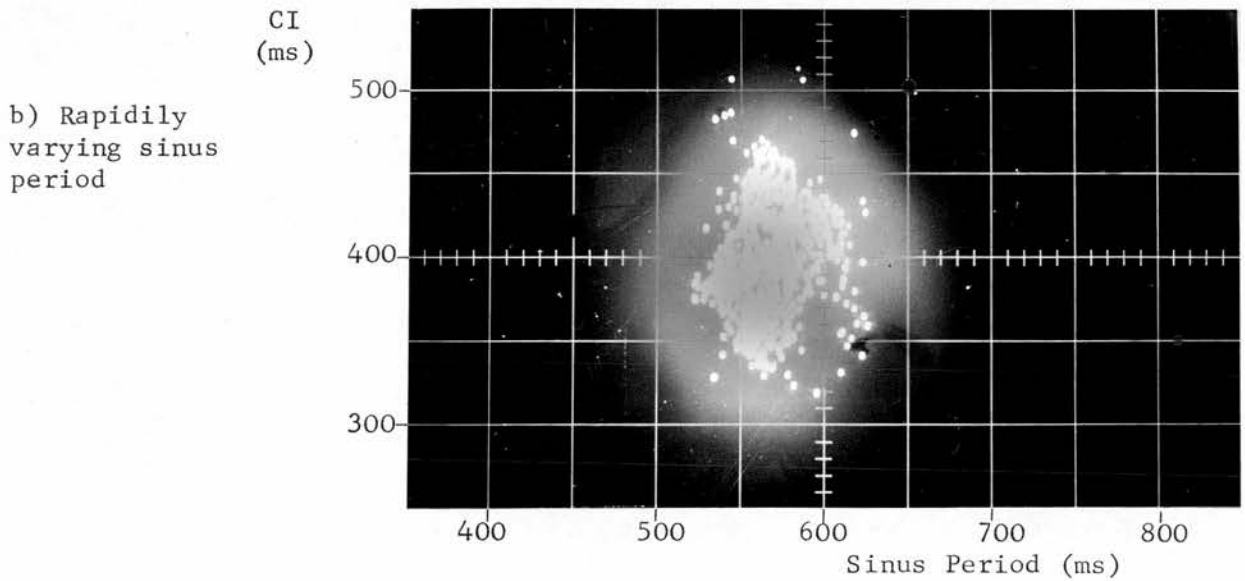
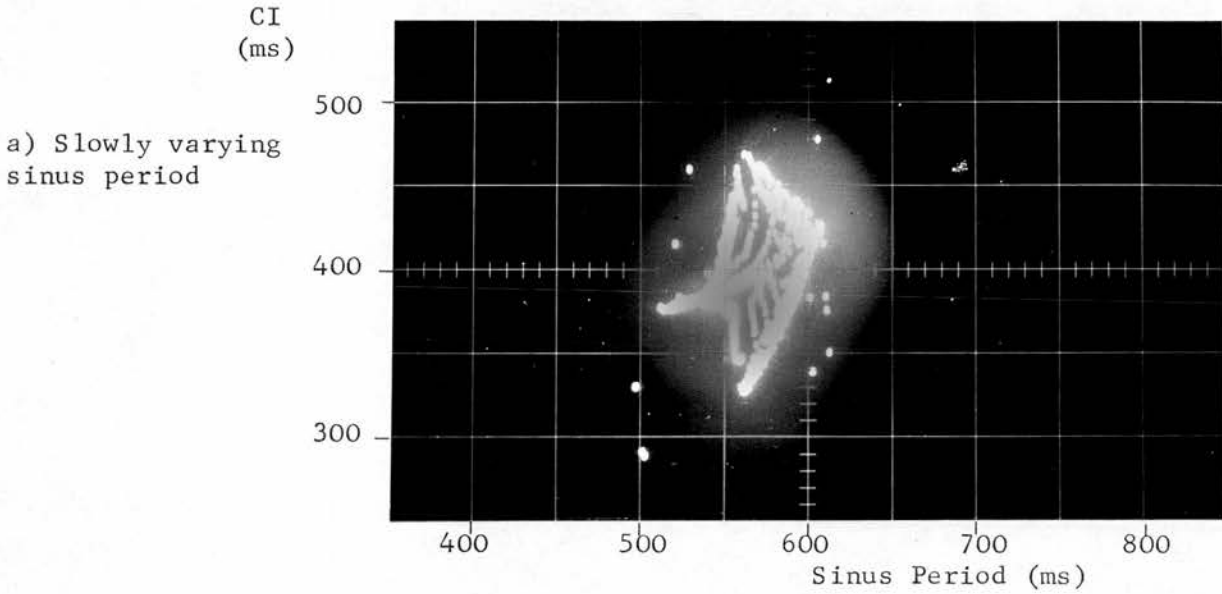
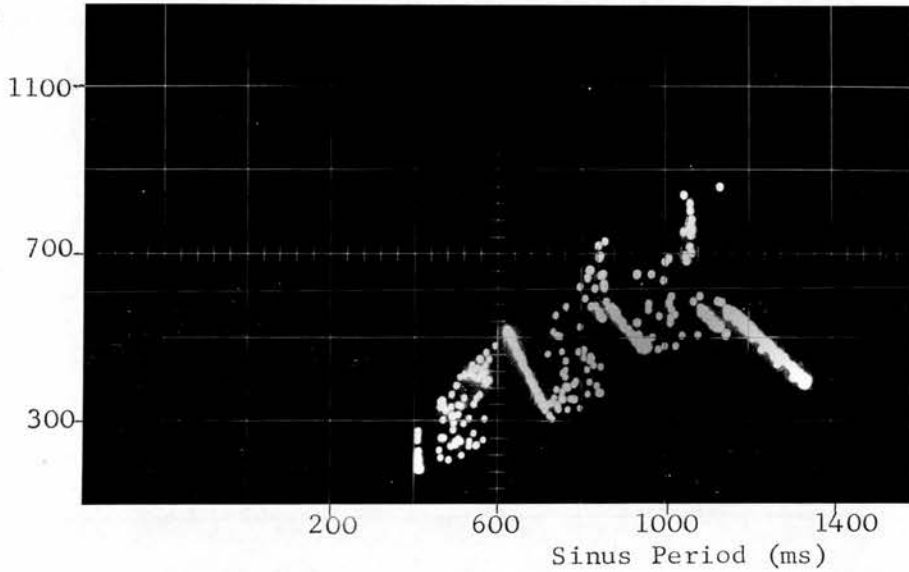


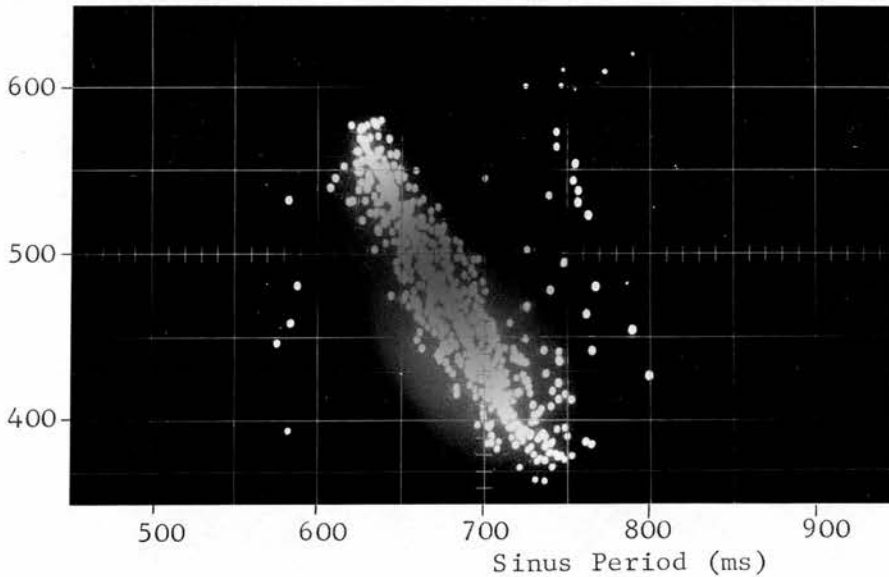
Fig.VIII,10: Phase 4 Anodal Shortening. $E_A=350\text{ms}$, $E_4=1400\text{ms}$,
 max. shortening of $E_4=625\text{ms}$.

CI
(ms)



a) Sinus period varies slowly. For the two middle lines the N's represent concealed bigeminy (left middle) and concealed trigeminy (right middle).

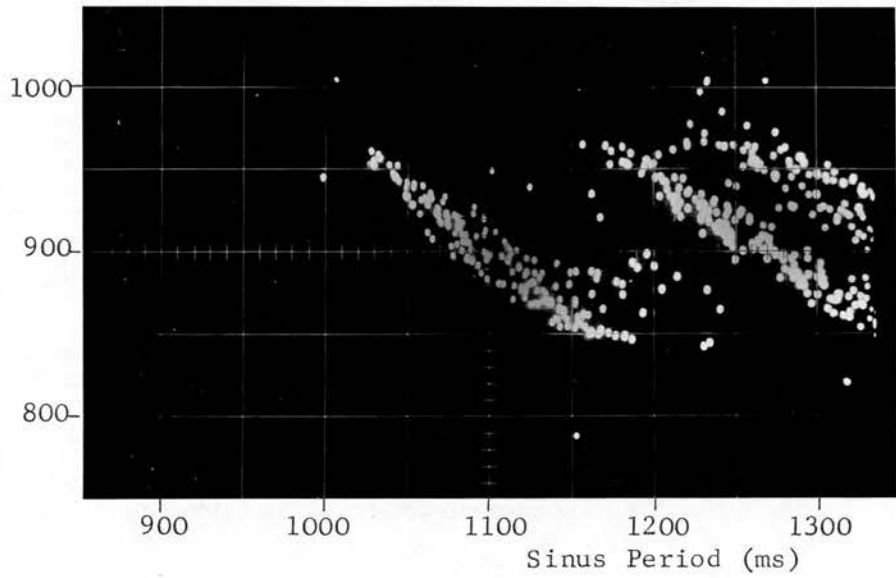
CI
(ms)



b) An expansion of the area corresponding to concealed bigeminy.

CI
(ms)

Fig.VIII,11:
Phase 4 Anodal
Shortening
showing 'forbidden
gaps' in the
X-Y Plot.
 $E_A=350\text{ms}$, $E_4=1650\text{ms}$,
max. shortening
of $E_4=800\text{ms}$.



CI
(ms)

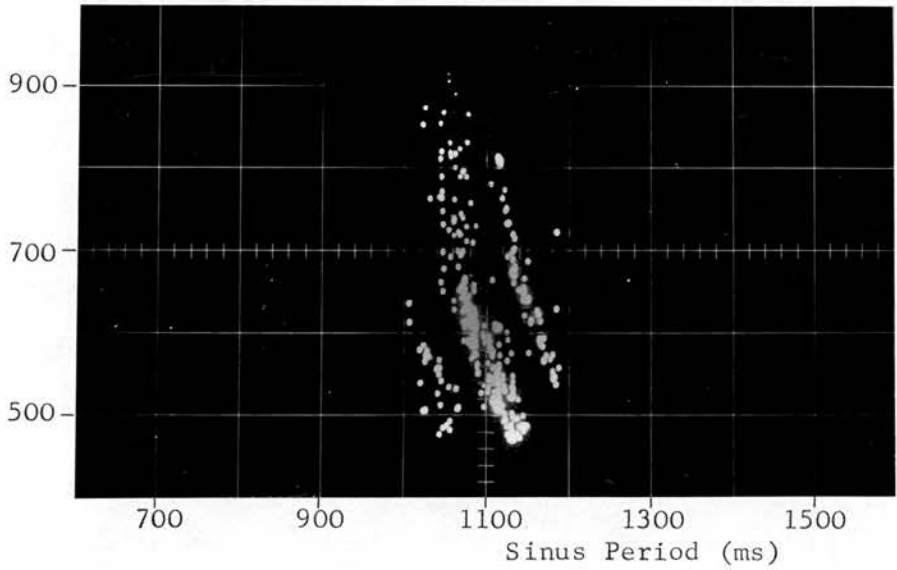


Fig.VIII, 12:
Phase 4 Anodal
Shortening.
 $E_A=350\text{ms}$,
 $E_4=1150\text{ms}$, max.
shortening of
 $E_4=250\text{ms}$. In the
middle band N is
always one of the
following nos.
depending on the
exit block:
 $N=2,4,5,6,10$.
Note the presence
of 'forbidden
gaps'.

The shortcomings of this pulling hypothesis lie in its inability to produce stable patterns: in order to achieve realistic patterns, E_A has to be inordinately large (eg. 600ms), and even then only a few select patterns are produced. The maximum lengthening used caused a 100% increase in the value of E_4 . As before, it is felt that for a hypothesis to be tenable it must be capable of inducing the type of pattern seen in Chapter IV under general, not highly selected, conditions. For this reason the hypothesis of phase 4 cathodal extension is rejected as being the sole mechanism responsible for the observations presented in Chapter IV.

ii) Phase 4 Anodal Shortening

This hypothesis is most promising in that it has a strong tendency to produce patterns under the most general conditions. Figs. VIII,10 through 12 give an indication of the possibilities. The values of parameters accompany the figures.

iii) Action Potential Extension

In order to run the model of this hypothesis three new parameters must be specified, namely i) the time interval following the ectopic action potential during which excitability recovers to some maximum value; ii) the subsequent time interval during which excitability is lost; iii) the duration of the maximal response to optimally timed sinus stimuli (i.e. at the peak of ectopic excitability). These are designated i) recovery of excitability (R.O.E.), ii) loss of excitability (L.O.E.), and iii) response (R) respectively. All are measured in milliseconds.

/

Fig.VIII,13:
Action Potential
Extension.
 $E_A=300\text{ms}$,
 $E_4=700\text{ms}$,
R.O.E.=25ms,
L.O.E.=250ms,
R=35ms.

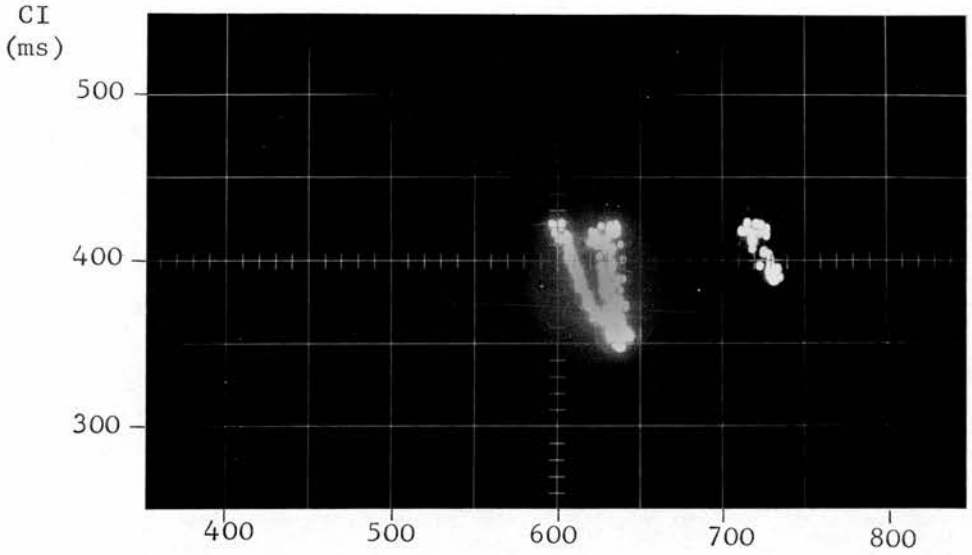


Fig.VIII,14:
Action Potential
Extension.
 $E_A=300\text{ms}$,
 $E_4=700\text{ms}$,
R.O.E.=190ms,
L.O.E.=25ms,
R=35ms.

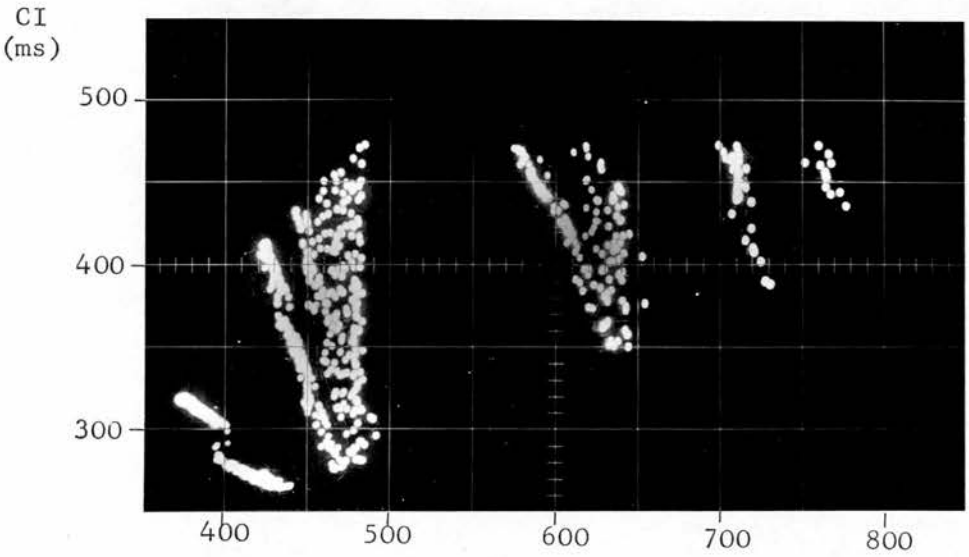
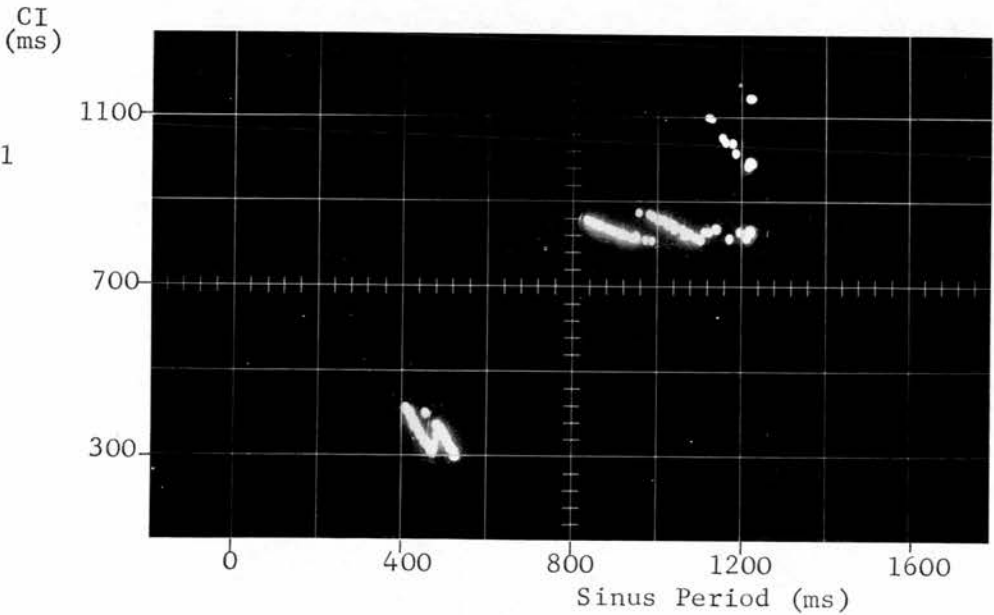


Fig.VIII,15:
Action Potential
Extension.
 $E_A=600\text{ms}$,
 $E_4=900\text{ms}$,
R.O.E.=25ms,
L.O.E.=600ms,
R=100ms.



This hypothesis is most promising. It often produces stable X-Y patterns over a large range of S in the presence of changing exit block. Some of the most dramatic behaviour is illustrated in Figs. VIII,13 through 15. The value of parameters accompany the figures. For Fig. VIII, 13 the inter-ectopic numbers are determined by the exit block as follows, and no other N's occur:

For the left hand line:

exit block (E.B.):	1	2	3	4	5n
inter-ectopic number (N):	4	9	no	19	245n(?)
			V.E.Cs			

For the middle band the 'rule' is:

exit block (E.B.):	1	2	3	4	5
inter-ectopic number (N):	2 or 7	2 or	8	5	7 or
		some no.			some no.
		>30			>30

For the right hand line the Ns constitute concealed trigeminy (N = 2 + 3(E.B.)).

Each line and band in Fig. VIII,14 has its own law relating N to E.B., and for most of these certain Ns do not occur. Figs. VIII,13 and 14 both show a restriction on the occurrence of V.E.Cs: they can only arise when the sinus period lies within specific ranges - outside these ranges no V.E.Cs arise.

Fig. VIII,15 shows the considerable ability of this mechanism to produce "forbidden gaps" (cf Chapter IV). Again each line has its own sequence of N's.

Action potential extension can be made to produce most of the types of behaviour observed in Chapter IV except for the triangles shown by Cases 5, 8, and 11. On the other hand, such patterns are readily produced by the model of phase 4 cathodal extension. Acceptance of the general pulling hypothesis does not imply that any one mechanism is responsible for all cases of pulled parasystole, and indeed more than one mechanism may act in a given case.

Concluding Remarks

For each mechanism attempts were made at matching the simulator's behaviour to the beat for beat behaviour seen in

selected ECGs. This was done by: i) using real sinus rhythm to drive the sinus pacemaker on the simulator; ii) only allowing V.E.Cs to appear in the simulator during a 600ms time band surrounding the appearance of each V.E.C. in the real case being copied - if the simulator and real case were functioning in a similar manner then this procedure would ensure that the exit block on the model was matched exactly to that of the real case. Thus the inter-ectopic numbers on the model would conform to those of the real case.

To start an experiment the ectopic pacemaker was triggered so that the first CI equalled some pre-selected CI of the real data. From that moment on, the CIs produced by the model were monitored in the X-Y plot, and this was compared to the plot produced by the real ECG.

These experiments were never particularly successful in that there were large discrepancies between the manufactured and the real X-Y plots. It may be that in real cases some of the parameters varied even over the short period of time for which these experiments were run. As a result, any fixed set of parameters would not represent the real situation sufficiently accurately to reproduce the beat for beat behaviour. Of course it may be that the hypotheses considered do not represent pulling mechanisms. Alternatively, it may be that a combination of mechanisms is required, for example the preliminary hypothesis in conjunction with action potential extension. It is felt that the complexities of such a combined system would be so great as to undermine any claim of uniqueness that would be made - i.e., perhaps a few systems of such complexity could match a given ECG beat for beat. This being so, the conclusions drawn from such an experiment would be highly dubious. Hence this approach was pursued no further.

Although the evidence in this chapter shows that certain pulling mechanisms could account for the type of behaviour observed earlier in Chapter IV, it remains for further investigations to substantiate or refute the general hypothesis of pulled ventricular parasystole. A suggestion

for the form of such an investigation is made in the next part of this thesis. As further supporting evidence it also includes a small selection of reported ECGs which may be accounted for on the basis of the general hypothesis of pulled ventricular payasystole.

PART IV

Applicability of the General Hypothesis

CHAPTER IX Conclusions and Further Suggestions

Particular Pulling Mechanisms

In Chapter IV it is suggested that the mechanism of the preliminary pulling hypothesis is generally incapable of producing stable patterns in the X-Y plot and N histogram. Under highly specific circumstances it is possible to produce a semblance of stability on the electronic model of this mechanism. However it is felt that the difficulty of finding combinations of parameters that will achieve this is indicative of the inadequacies of the preliminary pulling hypothesis in accounting for the type of ECG investigated in Chapter IV. In particular its inability to produce either concealed bigeminy or isolated triangles in the X-Y plot are examples of its shortcomings.

Similarly the main shortcoming of the hypothesis of phase 4 cathodal extension lies in its inherent instability.

Of phase 4 anodal shortening, and action potential extension, the latter seems to be the more promising, its only apparent deficiency being an inability to produce isolated triangles in the X-Y plot. This is precisely the asset of phase 4 cathodal extension, hence it may be that these two (i.e. action potential extension and phase 4 cathodal extension) acting together can mimic accurately the arrhythmic patterns seen in the ECGs in Chapter IV. Combinations of hypotheses are not examined since experiments based on simulation of such complex systems are open to criticism, particularly when all the necessary parameters are assessed from the data being simulated and not by some other means. If combined pulling mechanisms do in fact operate in ventricular parasystole then

different types of experiment are needed to substantiate this - modelling could be viewed as little more than circumstantial evidence. Nevertheless it is interesting to note that certain of the hypothetical pulling mechanisms may be combined in pairs whereas others may not: of the 6 possible pairs (number of ways of choosing 2 items from 4) 2 consist of physiologically incompatible mechanisms which may not be combined. These are: i) phase 4 cathodal extension with phase 4 anodal shortening (since one requires a positive stimulus and the other a negative one); ii) the preliminary hypothesis with action potential extension (since the latter assumes that sinus stimuli become less effective with advancing phase 4 depolarization of the ectopic focus, whereas the former assumes that they become more effective). Because each hypothetical mechanism may not be combined with one of the other three, there is clearly no permissible combination involving three or more of these mechanisms.

Of the four permissible pairs perhaps action potential extension in conjunction with phase 4 cathodal extension is the most promising. On purely physiological grounds action potential extension is highly plausible: a reduction in the maximum diastolic potential of the ectopic focus is all that is necessary to bring about entrance and exit block and this may well occur in the diseased heart⁷¹; under such conditions the ectopic focus shows reduced responsiveness as it proceeds in its phase 4 depolarization and this is exactly what is required for action potential extension. In other words, the factors that bring about a parasystolic pacemaker may be exactly the same factors that facilitate action potential extension. Action potential extension could act in conjunction with phase 4 cathodal shortening whereby those sinus stimuli arriving in ectopic phase 3 extend the action potential duration, and those arriving later only cause a local response which gives rise to post cathodal depression. The writer believes that this combination represents the most likely pulling mechanism - its two components are totally compatible and may even be thought of as being deducible from the physiological conditions responsible for entrance block.

A further possible pulling mechanism may be envisaged as resulting from increased latency of response which accompanies phase 4 depolarization of a pacemaker fibre⁷¹. Such a mechanism has a strong resemblance to the preliminary pulling hypothesis where sinus excitation induces the ectopic focus to fire early: for both mechanisms the pulled ectopic period increases as sinus excitation arrives later in ectopic diastole. The means whereby this happens are quite different for the two mechanisms: as sinus stimuli arrive later and later the amount of shortening decreases for the preliminary hypothesis whereas for this last mechanism the amount of lengthening increases. It remains to establish the arrhythmic properties of this last mechanism. In addition it is conceivable that it would act in conjunction with either or both action potential extension and phase 4 cathodal extension. A full account of the detailed functioning of such a combination of mechanisms where any of the parameters may vary, would be well nigh impossible. The important principle to establish is that of a separate ectopic rhythm which is pulled and may thereby become synchronized to the dominant rhythm and thus appear similar to a sinus-locked mechanism.

In the remainder of this chapter a suggestion is made for a further test of the general hypothesis of pulled ventricular parasystole. Some reported arrhythmias are also evaluated in terms of this general hypothesis.

Suggestion for a Further Test of the General Hypothesis of Pulled Ventricular Parasystole

A breakdown of entrance block surrounding the pulled ectopic pacemaker would cause it to become temporarily locked to the sinus rhythm. On regaining entrance block the two pacemakers would take up their previous phase relationship which would depend on the pulling mechanism. During such an episode the N histogram and X-Y plot should both show points lying outside the patterns that arise during pulled synchrony. In other words, breakdown of the pattern in one aspect of the

ECG should systematically correspond to breakdown in the other. As an example consider a case of imperfect concealed bigeminy (see Chapter II). Those inter-ectopic numbers not belonging to the sequence $N = 1 + 2n$, $n = 0, 1, 2, \dots$ represent out-of-sync beats and these, if the general hypothesis is correct, would be manifest in the X-Y plot as points extraneous to the pattern produced under pulled synchronism. In other words, N's belonging to a strict sequence are accompanied by points lying within a specific pattern in the X-Y plot, whereas for N's not in the sequence the points in the X-Y plot should probably lie outside the specific pattern. It should be noted that there is no guarantee that all out-of-sync points would lie outside the synchronized area in the X-Y plot. This would depend on the pulling mechanism and the values of all its associated parameters.

A sequence of N's may also be interrupted when pulled synchrony is lost through insufficient pulling. This should also cause a break in the X-Y plot. Whatever the cause of the disturbance of the N pattern it is felt that a close beat by beat examination of the N histogram and X-Y plot may provide a sensitive test of the validity of the general hypothesis of pulled ventricular parasystole.

Some Reported Arrhythmias that may be Explained by the General Hypothesis of Pulled Ventricular Parasystole

Schamroth and Dolara have reported a case of paroxysmal ventricular tachycardia where the first CI of each paroxysm is related to the immediately preceding R-R interval⁶⁰. As before (Chapter VI, p.78) this arrhythmia may be interpreted in terms of synchronized sinus and ectopic rhythms which become desynchronized as a result of the occurrence of an ectopic beat. Up to that time the phase difference between the rhythms depends, amongst other factors, upon the sinus rate. This phase difference is revealed in the first CI of each paroxysm so that each first CI is dependent on the on-going sinus period. In fact the scattergram of Schamroth and Dolara is akin to the X-Y plots presented in this thesis: they select the first CI in each run of consecutive V.E.Cs

whereas for the ECGs considered in Chapter IV the V.E.Cs are all isolated from one another so that no selection of CIs is necessary. Both types of scattergram support the general hypothesis advocated in this thesis.

The arrhythmias cited in Chapter VI under the sub-heading "Some Aspects of Clinical Parasystole" may all be interpreted as pulled ventricular parasystole. In addition the cases of Langendorf and Pick²⁸ may be viewed as indicative of pulled ventricular parasystole: they give examples of individual cases which show both fixed and variable coupling which they interpret as "intermittent parasystole" since the inter-ectopic intervals are sometimes, but not always, related to the sinus rhythm. However, it may be that this last observation does not necessarily represent intermittent parasystole, rather it may be interpreted at least as credibly as a manifestation of intermittent synchrony in pulled parasystole.

Concluding Remarks

It is believed that the evidence presented in this thesis shows the inadequacy of existing theories of the origin of single V.E.Cs and that the hypothesis of pulled ventricular parasystole may be capable of accounting for the origin of all single V.E.Cs. Nevertheless the hypothesis of Anderson and Bailey where Wenkebach cycles occur in a distal Purkinje bundle (see Chapter V) cannot be dismissed without further investigation. Pulled parasystole differs from re-entry with Wenkebach in that the CIs in the former can, if synchrony is lost, take up any value whereas in the latter they are restricted to certain parts of diastole determined by the minimum and maximum conduction velocities in the re-entry pathway. This distinction may be of clinical significance in that any desynchronized case of parasystole could initiate 'R-on-T' ectopics whereas a case of re-entry with Wenkebach conduction will not in general be capable of any major change in the CI (eg. from late to early diastole).

The emphasis throughout the second and third parts of

this thesis has been on the interactions between separate pacemakers. This may be viewed in terms of relaxation oscillators with incomplete coupling. Roberge et al make use of similar concepts in their account of A-V conduction and of A-V arrhythmias (see Chapter VI, p.79). In particular, they show that Wenkebach cycles result naturally from a model of two relaxation oscillators (master and slave) with appropriate coupling. The stimulus-response relationship shows cyclic interruption such that for every n stimuli of the master pacemaker the slave responds with $(n - 1)$ pulses each having a slightly different phase relation to the master pulses. Indeed, certain solutions of Van der Pol's equation for relaxation oscillations⁴⁵ show this phenomenon. Because of the coupling between the oscillators the $n:(n - 1)$ stimulus-response ratio is maintained over a range of driving frequencies - each frequency has its set of phase differences between master and slave pacemakers. Rosenbleuth⁵ has also suggested that such action (appearing in the A-V node) is the result of the "modulation of two frequencies".

In effect, all these workers use the fact that automaticity in individual heart fibres represents a fine example of relaxation oscillations: the electrical activity of each specialized fibre is highly non-linear and if left to itself falls into a natural cycle consisting of several distinct quasi-stable states, the termination of one leading on into the next. It is therefore hardly surprising to find that both normal and abnormal conduction in these fibres can be described in terms of the inherent rhythms and coupling between such oscillators. It is no less surprising to find that the explanation of the origin of V.E.Cs also seems to involve such concepts.

APPENDIX I An Outline Proof that for Independent Pacemakers the CIs are, in the Long Term, Uniformly Distributed

In Chapter II it is indicated that for two pacemakers to be considered independent, the ratio of their mean periods (\bar{S} and \bar{E}) must be an irrational number. This may be justified as follows: if one of the mean periods is regarded as fixed, then independence implies that the other is a priori free to take up any value within some continuous range (greater than measure zero); under such circumstances the ratio of the mean periods is irrational with probability 1, and rational with probability 0. In other words, if two numbers (\bar{S} and \bar{E}) are chosen independently, then the probability of their having a rational ratio is vanishingly small, hence the ratio is irrational with probability 1.

Consider the situation where the sinus and ectopic periods remain absolutely constant at values \bar{S} and \bar{E} . Let $\{x\}$ denote the fractional part of x , e.g. $\{3\frac{1}{2}\} = \frac{1}{2}$. If the pacemakers start at the same moment, the CIs are $\{n\frac{\bar{S}}{\bar{E}}\}$, $n = 1, 2, 3, \dots$ (The initial CI clearly is not going to affect the argument.) The problem is to show that this function is uniformly distributed in $[0, 1)$. It has been shown that a necessary and sufficient condition for $\{f(1)\}$, $\{f(2)\}$, $\{f(3)\} \dots$ to be uniformly distributed in $[0, 1)$ is that

$$\lim_{n \rightarrow \infty} \frac{\sum_{v=1}^n e^{2\pi j h f(v)}}{n} = 0 \text{ for every integer } h^{89}.$$

In this case, $f(v) = \frac{\bar{E}}{\bar{S}} v$ where $\frac{\bar{E}}{\bar{S}}$ is an irrational number lying between 0 and 1. Hence the condition is satisfied and the CIs are uniformly distributed.

If the pacemaker periods vary about their mean values, then provided the variations are not correlated

$$\left(\text{i.e. } \lim_{t \rightarrow \infty} \frac{\sum(S - \bar{S})(E - \bar{E})}{\sum(S - \bar{S})^2 \cdot \sum(E - \bar{E})^2} = 0 \right), \text{ the long-term distrib-}$$

ution remains uniform. The concept of independence clearly implies that this is so in that the variations in one period are not related (i.e. uncorrelated) to variations in the other.

										Marginal Totals
	X_1	X_2	X_3	...	X_i	...	X_{c-2}	X_{c-1}	X_c	
Y_r										$\sum_{i=1}^c O_{i,r}$
Y_{r-1}										$\sum_{i=1}^c O_{i,r-1}$
Y_{r-2}										$\sum_{i=1}^c O_{i,r-2}$
Y_j										
Y_3										$\sum_{i=1}^c O_{i,3}$
Y_2										$\sum_{i=1}^c O_{i,2}$
Y_1										$\sum_{i=1}^c O_{i,1}$
Marginal Totals	$\sum_{r=1}^r O_{i,r}$	$\sum_{r=1}^r O_{i,r}$	$\sum_{r=1}^r O_{i,r}$				$\sum_{r=1}^r O_{i,r}$	$\sum_{r=1}^r O_{i,r}$	$\sum_{r=1}^r O_{i,r}$	$\sum_{r=1}^r \sum_{i=1}^c O_{i,j}$ = N

Fig. AII, 1: An X-Y plot may be regarded as a contingency table (see text).

APPENDIX II Examination of the X-Y Plots

i) A Statistical Test Based on χ^2

An X-Y plot may be formally tested for interaction between the X and Y variables by considering the plot as a contingency table with r rows and c columns (Fig.AII,1). The cell corresponding to the i^{th} row and j^{th} column is written (X_i, Y_j) and there are rc cells altogether. Let the observed number of counts in (X_i, Y_j) be $O_{i,j}$. Then the total number of counts in the 1^{st} column is $\sum_{j=1}^c O_{1,j}$, and in the I^{th} column is $\sum_{j=1}^c O_{I,j}$. Similarly the total number of counts in the J^{th} row is $\sum_{i=1}^r O_{i,J}$. These marginal totals are presented in the right hand column and bottom row of Fig. AII,1. The sum of the marginal totals over all rows or all columns equals the total number of points in the plot.

The rationale of this statistical test is as follows: given the observed marginal totals, the expected number of counts is calculated (see below) for each cell assuming the null hypothesis, H_0 , of no interaction between the X and Y variables. Let the expected number of counts in (X_i, Y_j) be $E_{i,j}$. A test of the "goodness of fit" between the observed and the expected (under H_0) plots is then carried out in the usual manner using the χ^2 distribution: the function

$$\sum_{j=1}^c \sum_{i=1}^r \frac{(O_{i,j} - E_{i,j})^2}{E_{i,j}}$$

is distributed as χ^2 with $(r-1)(c-1)$

degrees of freedom since the marginal totals are regarded as fixed by the experiment.⁹⁰ Statistical tables give the values of χ^2 above which H_0 is to be rejected at some chosen significance level.

$E_{i,j}$ is obtained as follows. The probability of a point lying anywhere in the J^{th} row is

$$\frac{\text{number of points in } J^{\text{th}} \text{ row}}{\text{the total number of points, } N} = \frac{\sum_{i=1}^c O_{i,j}}{N}$$

Similarly, the probability of a point lying anywhere in the I^{th} column is $\frac{\sum_{j=1}^r O_{I,j}}{N}$. Therefore the probability of a point lying in cell $(X_{I,J})$ is

$$\frac{\sum_{i=1}^c O_{i,J} \sum_{j=1}^r O_{I,j}}{N^2}$$

The expected number of points in (X_I, Y_J) is the probability of a point lying in that cell multiplied by the total number of points observed (N), that is,

$$E_{I,J} = \frac{\sum_{i=1}^c O_{i,J} \sum_{j=1}^r O_{I,j}}{N}$$

For this test to be valid the size of the cells must be made so that no $E_{i,j}$ is less than about 5^{90} . There are no other restrictions on its use.

This test gives a significance level at which the patterns observed in X-Y plots may be rejected as arising by chance alone. Unfortunately this is not very informative as regards the inadequacies of sinus-locked and pure parasytolic hypotheses. The following test was used in Chapter IV because it attempts to elucidate the form of these inadequacies on the basis of a visual comparison between the observed X-Y plot and a randomly generated X-Y plot having similar marginal distributions but no X-Y interaction. The randomly generated plot provides a basis for deciding whether the measured plot contains features that would not arise by chance alone. In other words, both the extent and type of interaction between the X and Y variables may be assessed.

ii) A Test Based on Visual Examination of the Data.

The rationale of this test is to produce an X-Y plot

having marginal distributions similar to those of the measured plot but created in such a way that the X-Y interaction is totally random. A method described by Tocher⁹¹ is employed whereby a sequence of random numbers is used to generate a near copy of a given distribution - the order of events that go to make up the copy is determined by the random numbers, but the copy is generated in such a way as to ensure that the total number of events in each class interval is nearly the same as in the measured plot.

The method used to generate the fictitious X-Y plot is an extension of the procedure used for a single fictitious distribution. Two sequences of random numbers are used to generate the X and Y events separately and these make up the marginal distributions of the fictitious plot. The 1st point in this plot consists of the 1st X and 1st Y events, the 2nd point consists of the 2nd X and 2nd Y events, and the nth point consists of the nth X and nth Y events. The process is terminated when the number of points in the fictitious plot equals the number in the measured plot.

For some of the points thus generated the Y value may be greater than the X value (i.e. the CI greater than the sinus period). Since this cannot occur in the measured plot it must also be prevented from happening in the fictitious one hence both will have an upper boundary line of slope +1 passing through the origin: this particular X-Y interaction is inherent in the definitions of the terms used and is of no significance in the context of this thesis. Any other type of interaction will be present in the measured plot but not in the fictitious one. (The upper line in the fictitious plot is placed so as to correspond with the measured one - this is always of slope +1, but because of the way in which the beats are timed (see Chapter III) this does not necessarily pass through the origin.)

All points in the fictitious plot lie on a grid of unit size 5ms because the measured marginal distributions are grouped into class intervals of this size. This produces a regular speckled appearance in the fictitious plot not

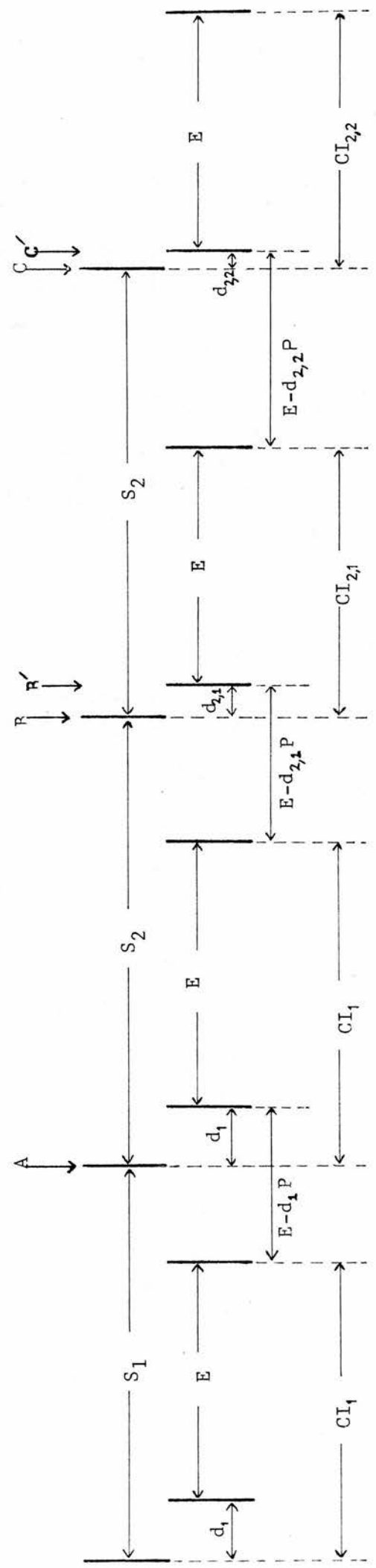
present in the original. This artefact is faded out by adding different random numbers lying between 0 and 5ms to the X and Y coordinates formed from the measured marginal distributions.

A program for carrying out this routine was written in Focal-12, executed on a PDP-12 computer and the results displayed on the computer oscilloscope. Here the dots were much finer than on the Telequipment storage oscilloscope (OM53A) used to display the measured X-Y plots, so that in order to facilitate a good comparison between these plots the photographs of the computer plot were slightly blurred when being developed.

Limited storage space on the PDP-12 only permits 833 points and a grid of 166 points to be displayed at one time. Four of the original plots contain more than 833 points, hence the fictitious plots of these cases are terminated early. However, 833 points is sufficient to indicate any "pattern" inherent in the marginal distributions so that a comparison between the plots is still valid.

Fig. AIII, 1: $2E=S+$.

A change in S from S_1 to S_2 occurs at B leading to the following CIs: $CI_{2,1}$: $CI_{2,2}$: $CI_{2,3}$ etc. $CI_{2,\infty} = CI_2 =$ steady-state (i.e. static) value of CI for $S=S_2$. $S_2 > S_1$, $\therefore d_2 < d_1$.



For the case $2E = S_+$ the first few beats of the dynamic situation are shown schematically in Fig. AIII,1: up to the time marked B the ectopic is statically synchronized to the sinus which has period S_1 and the coupling interval, CI_1 , has magnitude $(E + d_1)$. At B the sinus period changes to S_2 which will, after a long time, lead to a steady-state CI (CI_2) of $(E + d_2)$. In the interim, successive CI's have values $(E + d_{2,1})$, $(E + d_{2,2})$, $(E + d_{2,3})$ etc. Hence $CI_2 = (E + d_2) = (E + d_{2,\infty}) =$ steady-state value of CI. Thus the n^{th} CI after the change in S is written $CI_{2,n}$. If there is another change in S to S_3 then the n^{th} CI after this further change is written $CI_{3,n}$ and this is also investigated.

We wish to find the difference between the CI after the change in S, and the eventual steady-state CI.

For the initial steady-state

$$\begin{aligned} Pd_1 &= 2E - S_1 \\ CI_1 &= d_1 + E \end{aligned}$$

and for the final steady-state

$$\begin{aligned} Pd_2 &= 2E - S_2 \\ CI_2 &= d_2 + E \end{aligned} \tag{1}$$

$$\text{Now } CI_{2,1} = d_{2,1} + E$$

$$\begin{aligned} \therefore CI_{2,1} - CI_2 &= (d_{2,1} + E) - (d_2 + E) \\ &= d_{2,1} - d_2 \end{aligned}$$

To calculate $d_{2,1}$ consider the interval A to B' in Fig. AIII,1. This may be written in two ways which are equated:

$$AB' = S_2 + d_{2,1} = d_1 + E + (E - d_{2,1} P)$$

$$\therefore d_{2,1} (1 + P) = d_1 + 2E - S_2$$

$$\therefore d_{2,1} = \frac{1}{(1+P)} \left(\frac{2E - S_1}{P} + 2E - S_2 \right) \quad (2)$$

and $d_2 = \frac{1}{P} (2E - S_2)$ - from (1)

$$= \frac{1}{(1+P)} \left(\frac{1+P}{P} (2E - S_2) \right)$$

$$= \frac{1}{(1+P)} \left(\frac{2E - S_2}{P} + 2E - S_2 \right) \quad (3)$$

$$\therefore d_{2,1} - d_2 = \frac{S_2 - S_1}{P(1+P)} \quad (\text{i.e. (2) - (3)}) \quad (4)$$

$$= CI_{2,1} - CI_2 \quad \left. \vphantom{\frac{S_2 - S_1}{P(1+P)}} \right\} \begin{array}{l} \text{N.B.: } (S_2 - S_1) \\ \text{may be} \\ \text{positive or} \\ \text{negative} \end{array}$$

$CI_{2,2} - CI_2$ may now be calculated:

as before,

$$CI_{2,2} - CI_2 = d_{2,2} - d_2,$$

and considering the interval B to C':

$$S_2 + d_{2,2} = d_{2,1} + E + (E - d_{2,2} P)$$

i.e. $d_{2,2} (1+P) = d_{2,1} + 2E - S_2$

But $d_{2,1}$ is known,

$$\therefore \text{substituting } d_{2,2} = \frac{1}{(1+P)} \left\{ \underbrace{\frac{1}{(1+P)} \left[\frac{2E - S_1}{P} + 2E - S_2 \right]}_{\text{from (2)}} + 2E - S_2 \right\}$$

\therefore employing

equation (3):

$$d_{2,2} - d_2 = \frac{S_2 - S_1}{P(1+P)^2} \quad (5)$$

$$= CI_{2,2} - CI_2 \quad \left. \vphantom{\frac{S_2 - S_1}{P(1+P)^2}} \right\} \begin{array}{l} \text{N.B.: } (S_2 - S_1) \text{ may} \\ \text{be positive} \\ \text{or negative} \end{array}$$

Comparing equations (4) and (5) it would seem that

$CI_{2,n} - CI_2 = d_{2,n} - d_2 = \frac{S_2 - S_1}{P(1+P)^n}$. This is in fact so, as can be proved by induction.

To prove $d_{2,n} - d_2 = \frac{S_2 - S_1}{P(1+P)^n} \quad (6)$

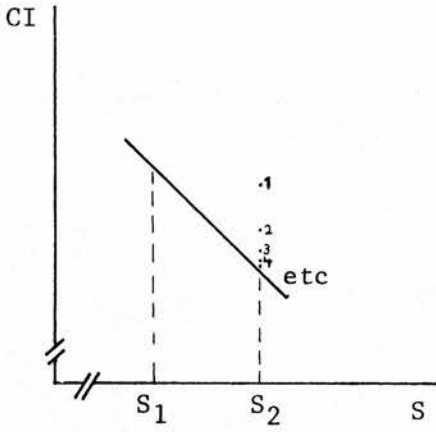


Fig.AIII,2: Quick change from S_1 to S_2 taking less than one cycle to complete. Nos. 1,2,3,4 etc represent successive CIs immediately after the change in S . See text.

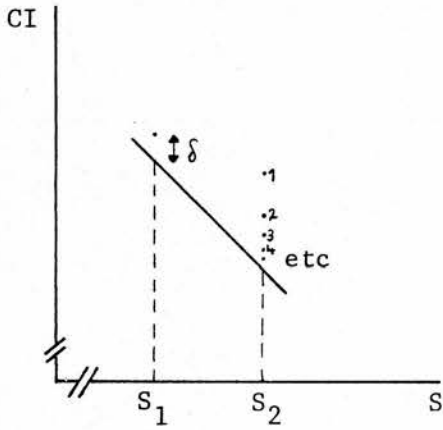


Fig.AIII,3: Initial conditions are: $S=S_1$: 'phase shift' from steady-state = δ . δ can be positive or negative. See text.

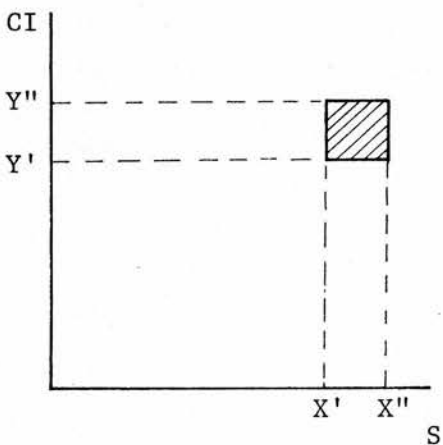


Fig.AIII,4: Shaded area represents the region of interest and corresponds to a synchronized zone. See text.

Considering the $(n + 1)^{\text{th}}$ interval of which A to B' is the first and B to C' the second, the following statement can be made:

$$\begin{aligned}
 S_2 + d_{2,(n+1)} &= d_{2,n} + E + (E - d_{2,(n+1)}P) \\
 \text{i.e. } d_{2,(n+1)}(1 + P) &= d_{2,n} + 2E - S_2 \\
 &= d_{2,n} + Pd_2 \quad (\text{from equation (1)}) \quad (7)
 \end{aligned}$$

Assume equation (6) is true for n . Then for $(n + 1)$ we write

$$\begin{aligned}
 S_2 - S_1 &= P(1 + P)^{(n+1)}(d_{2,(n+1)} - d_2) \\
 \text{and for } n: S_2 - S_1 &= P(1 + P)^n(d_{2,n} - d_2).
 \end{aligned}$$

Dividing by $P(1 + P)^n$:

$$\begin{aligned}
 (1+P)(d_{2,(n+1)} - d_2) &= d_{2,n} - d_2 \\
 \text{i.e.} \\
 (1 + P)d_{2,(n+1)} - d_2 - d_2P &= d_{2,n} - d_2 \\
 \text{i.e. } d_{2,(n+1)}(1 + P) &= d_{2,n} + Pd_2.
 \end{aligned}$$

But this is identical to equation (7) which is true. Hence if equation (6) is true for n it is also true for $(n + 1)$. Equation (6) is true for $n = 1$, hence it is true for all positive integers n .

Equation (6) is sufficient when the initial conditions are those of steady-state for $S = S_1$ giving an X-Y plot as in Fig. AIII,2. However, equation (6) is inadequate if there is an initial starting phase, δ , as in Fig. AIII,3. This phase shift is the residue of the previous change from some S to S_1 - the change from S_1 to S_2 occurs before the system has had time to settle to its steady-state at $S = S_1$. Thus if the theory can cope with the δ 's it can then describe the total dynamic action from when points first appear in the region of interest (i.e. X' to X'' , Y' to Y'' , Fig. AIII,4) to when they leave it. Thus the first δ results from the initial jump into the region of interest, and this jump will often be from a non-synchronized state to a synchronized one. The remaining action is essentially synchronized till S takes a value outside the range X' to X'' . 'Essentially synchronized'

implies that every sinus beat arriving just prior to an ectopic pulls that ectopic linearly in the sense that the equation "Pd = shortening in ectopic diastole" still holds - i.e. d is shorter than c. X', X'', Y', Y'' are chosen so that for the mode of synchrony (determined by q and r: $qE = rS+$ in general) only essentially synchronized points lie within the region of interest. Having attained the first δ by a jump into the region of interest, all subsequent δ 's arise from the difference between actual and steady-state values of the CI.

By inductive reasoning similar to that used to obtain $d_{2,n} - d_2$ produced by a change in S, it may be shown that the response to an initial phase shift, δ , plus a change in S (i.e. ΔS) is:

$$d_{2,n} - d_2 = \frac{\Delta S}{P(1+P)^n} + \frac{\delta}{(1+P)^n}$$

hence $CI(n) = \underbrace{\frac{E}{P}(2+P) + \frac{S_2}{P}}_{\text{steady-state response to an input } S = S_2} + \underbrace{\frac{\Delta S}{P(1+P)^n} + \frac{\delta}{(1+P)^n}}_{\text{transient response to a change } \Delta S \text{ in } S \text{ and a starting phase, } \delta}.$

The following analysis uses the fact that no terms involving products of ΔS and δ occur. The problem is: given an initial δ and subsequent changes in S at the N_2^{th} , N_3^{th} , etc. sinus beats, what is the n^{th} CI, $CI(n)$? For the first δ and first S

$$CI(n) = \frac{E}{P}(2+P) - \frac{S_1}{P} + \frac{\delta}{(1+P)^{n-1}}$$

This holds until there is a change in S (from S_1 to S_2) at the N_2^{th} beat, say, so that if $H(n-a)$ is defined as

$$H(n-a) = \begin{cases} 1 & n \geq a \\ 0 & n < a \end{cases}$$

$$CI(n) = \left[\frac{E}{P}(2+P) - \frac{S_1}{P} + \frac{\delta_1}{(1+P)^{n-1}} \right] \left[H(n-1) - H(n-N_2) \right]$$

At $n = N_2$ S changes to S_2 and the new extra starting phase is

$$\delta_2 = \frac{\delta_1}{(1+P)(N_2-1)} = \frac{\delta_1}{(1+P)(N_2-N_1)}$$

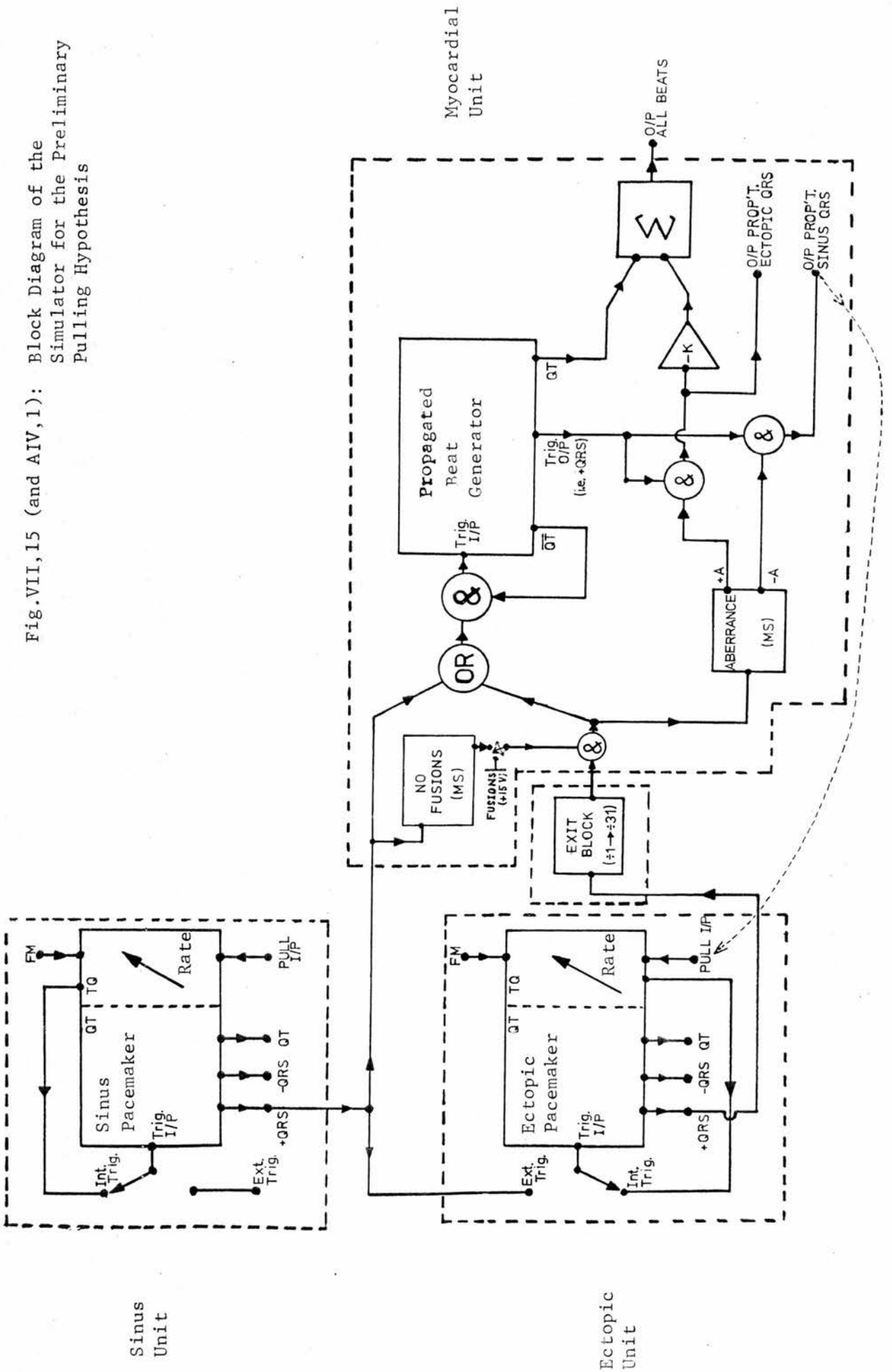
= what the transient would have been if there had been no change in S.

Extending this to the i^{th} change in S , ΔS_i , it may be shown that

$$CI(n) = \left[\frac{E(2+P)}{P} - \frac{S_i}{P} + \frac{1}{(1+P)^{(n-N_i)}} \left\{ \frac{S_i}{P(1+P)} + \sum_{j=2}^{j=i-1} \frac{S_j}{P(1+P)^{(N_i-N_j+1)}} + \frac{\delta_1}{(1+P)^{(N_i-1)}} \right\} \right] \times [H(n-N_i) - H(n-N_{i+1})]$$

Similar expressions may be obtained in the general case, $qE = rS+$, where there are $(q - 1)$ separate CIs to be considered...

Fig.VII,15 (and AIV,1): Block Diagram of the Simulator for the Preliminary Pulling Hypothesis



APPENDIX IV The Electronic Analogue of the
Mechanism of the Preliminary
Pulling Hypothesis

General Description

The block diagram in Fig. AIV,1 shows the basic concept of the simulator. The rates of the two pacemaker units may be varied independently of each other via rate control knobs which determine 'diastole' of each pacemaker. There is also a facility to trigger the sinus pacemaker unit from an external source.

Both pacemakers have a rate-pull input enabling outputs from various parts of the simulator to exert a pulling influence over either pacemaker. These pulling effects can be varied by means of external control knobs.

The '+QRS' output from the ectopic unit is fed directly into the exit block counter. This counter then produces one pulse for every 'n' ectopic cycles so that exit block = 1:n. 'n' takes a value between 1 and 31 according to the positions of five external switches.

The differentiated output from the exit block counter normally passes through the "No Fusions" AND gate - this pulse is gated in an OR gate with the differentiated '+QRS' output from the sinus unit and the result is fed into an AND inhibit gate. The output from the AND inhibit gate is then fed into the trigger input of the propagated beat generator. The function of the AND inhibit gate is to prevent re-triggering of the propagated beat generator during its QT interval. The AND gate in question is arranged to be closed during the QT interval and thereby simulates the absolute refractory period of the myocardium.

The differentiated output of the exit block counter is also fed into the aberrance monostable which produces a 100ms pulse (X1). This pulse determines the region in which an ectopic beat can occur. Because of the AND gate fed from

the +A output, the ectopic beat can only occur in a time band 100ms from the leading edge of the propagated beat 'QRS' pulse, whether caused by the sinus or ectopic unit. The inverted output from this gate is then added with the QT signal from the propagated beat generator to produce the "all beats output". Hence fusion beats arise if the ectopic pulse arrives within 100ms of the start of the sinus pulse. By switching to "No Fusions" the aberrance monostable can only be activated when the propagated beat card is triggered by the ectopic unit.

The 'ectopic QRS' output comes from the gate mentioned above.

Similarly the sinus QRS output comes via an AND gate which is open for 100ms (X1) from the leading edge of the propagated '+QRS' initiated by the sinus unit.

Although the times quoted for various parts of the simulator have been in real time, the simulator functions at 60 times real speed (i.e. 'X60').

Sinus and Ectopic Pacemaker Units

The function of the sinus card is to produce a QT_s complex that varies according to the law

$$QT_s = 0.14 + 0.32T_{R-Rs} \quad \text{where } T_{R-Rs} = \begin{array}{l} \text{average cycle} \\ \text{time of the sinus} \\ \text{pacemaker} \end{array}$$

Figure AIV,2 shows the circuit diagram in question. Monostable M_1 produces the 0.14 sec pulse for the constant part of the law. Monostable M_2 produces the QRS complex which has a duration of 90ms (X1).

The output from the monostable M_1 is fed via an inverter to a fourth order operational amplifier filter whose cut off frequency is 0.25 Hz at real time. The output from this filter is then fed to a current controlling transistor in monostable M_3 . The function of this part of the circuit is to produce the $0.32 T_{R-Rs}$ component in the QT law. For example as the rate increases so does the d.c. level from the

monostable M_1 and hence the output from the filter increases also. This in turn increases the current in the current controlling transistor in monostable M_3 . Thus, as a result of the increased discharge current the "on" time (i.e. the QT interval) of monostable M_3 is shortened.

Monostable M_4 determines the 'diastolic interval' when switched to internal-trigger.

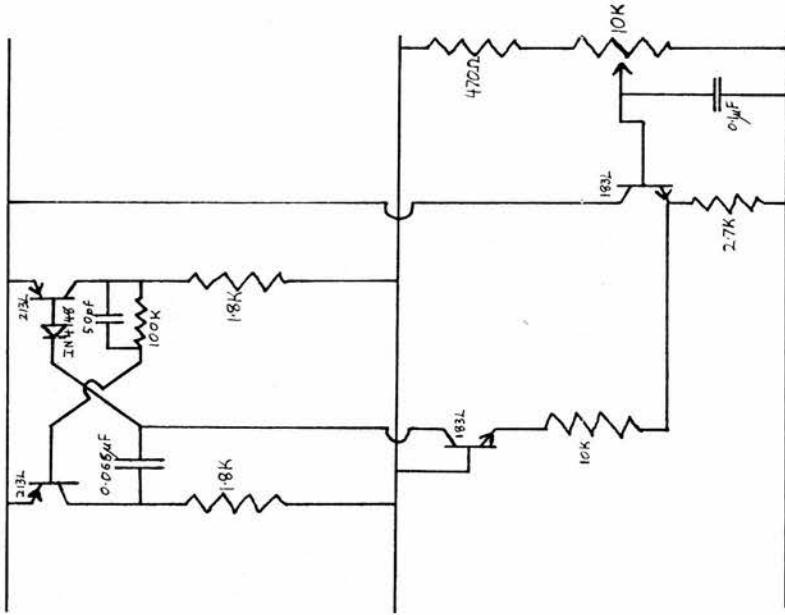
The sequence of operation of the four monostables M_1 , M_2 , M_3 , and M_4 is as follows. A trigger pulse arrives at the input either from an external source or from the internal trigger monostable M_4 . This trigger pulse triggers M_1 and M_2 simultaneously where M_2 produces the 90ms (X1) QRS complex and M_1 produces a pulse of 140ms (X1). When M_1 resets, it in turn triggers M_3 and as was mentioned above the duration of M_3 depends upon the output QRS rate. The output from monostables M_1 , M_2 , and M_3 are added together to produce the QT output. The use of various diodes and capacitors (10 pf at the junction of the IN4148 and the 330K) is necessary to ensure a clean QT waveform when its components are added together.

The rate-determining monostable, M_4 , has its period (i.e. 'diastole') controlled by both the external rate-control potentiometer and the voltage at the pull input. The rate control potentiometer alters the current in the 18 K resistor and thus alters the period. Similarly the pull input also alters the current in the 18 K resistor, and thus also alters the period.

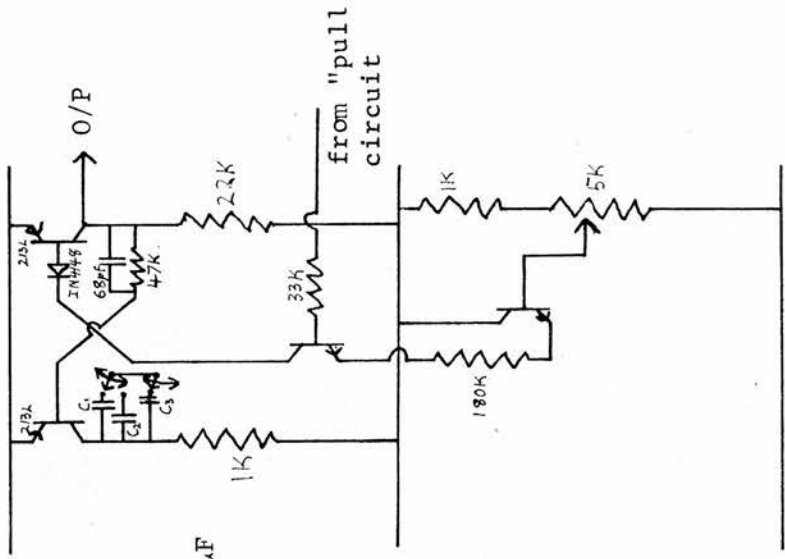
There are two ranges of QRS rates obtainable by selecting the appropriate switch position. The switch in turn alters the size of the capacitor in monostable M_4 .

The ectopic pacemaker circuit is similar to the sinus circuit except in that the QT_E interval (i.e. E_A) is set by the 10K potentiometer (inset, Fig. AIV,2) and is independent of the ectopic rate; in addition, the TQ_E interval (E_4) can be extended up to 5000ms (X1).

Ectopic QT Interval

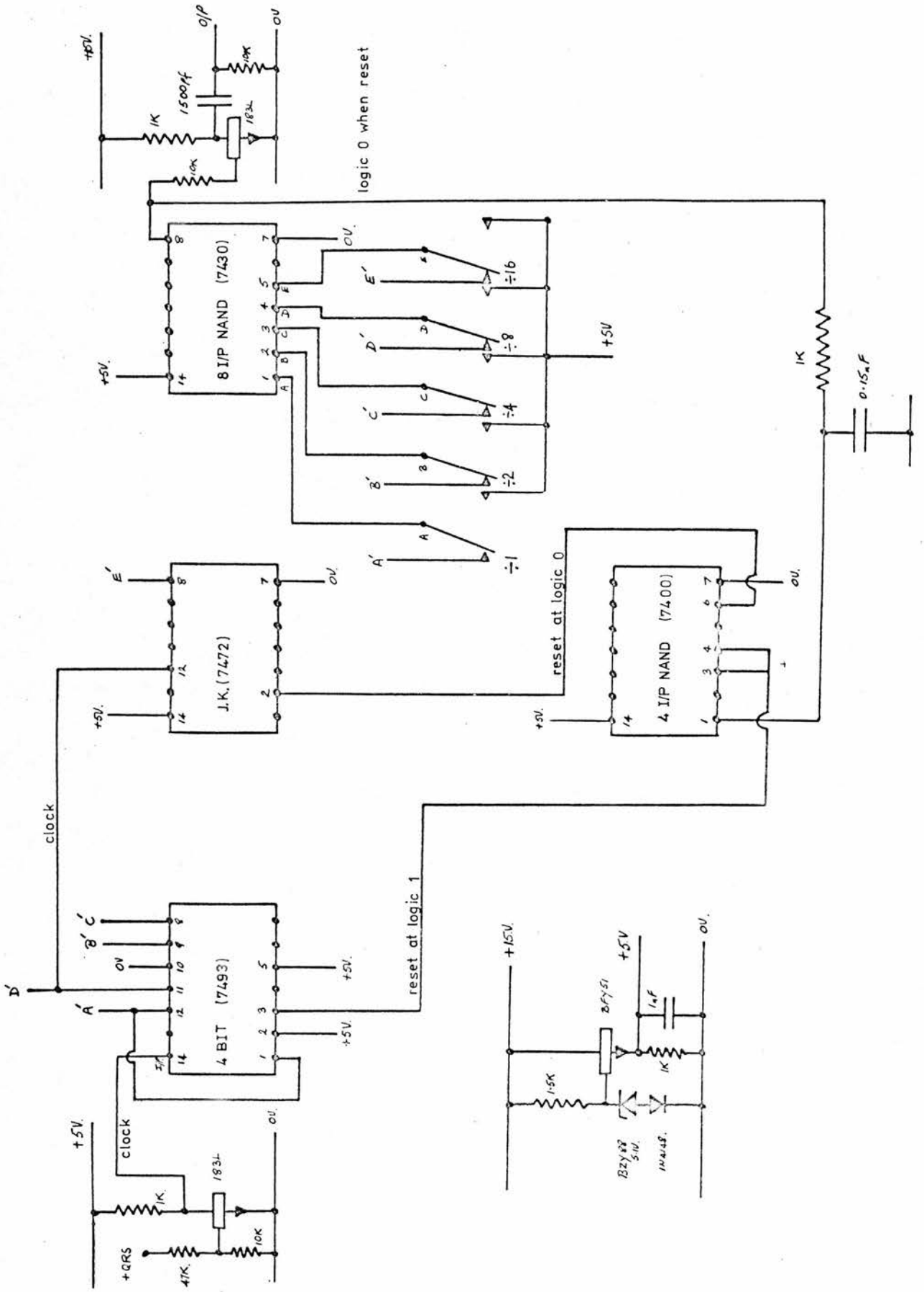


Ectopic diastolic timer



$C_1 = 1.500 + 680\text{pF}$
 $C_2 = 0.01\mu\text{F}$
 $C_3 = 0.047 + 0.015\mu\text{F}$

Fig.AIV,3: Exit Block Counter: $\div 1 \rightarrow \div 31$



Exit Block Counter (Fig. AIV,3)

The QRS pulse from the ectopic pacemaker is fed into a transistor stage which reduces its amplitude to the required logic level, i.e. 5V Pk. The pulse then passes to a 4 bit counter (7493) the final D' output going to the JK (7472). These two I.Cs perform the basic divide by 32 function.

The output from each stage of the binary counter is fed into an 8 I/P NAND (7430) gate so that only when there is a logic 1 at all inputs will there be a logic 0 at the output. The output from the (7430) is then fed into a transistor amplifier stage where the signal is both amplified back up to the 15 volt level and also re-shaped. The signal from this stage represents the final output from the counter.

As well as going to the above mentioned amplifier stage the signal from the (7430) also goes to a series RC network. This network has the effect of slugging the reset pulse before it goes into the (7400) NAND gate, the (7400) being used as two inverter stages. It is necessary to slug the reset pulse, otherwise the output pulse is far too fast to trigger succeeding stages. The 4 bit (7493) requires a logic 1 to reset and the JK (7472) requires a logic 0 to reset.

Thus the overall operation is as follows. Suppose the number '6' is chosen. This requires selection of the following switch positions: $\div 2$ switch, plus $\div 4 = \div 6$. Thus only when both the B' and C' outputs are at logic 1 will there be a logic 0 at the output of the (7430). This pulse, returning to logic 0 level, is passed through the series RC network into the inverting stage. The inverted pulse is then applied to the reset input of the 4 bit (7493). Similarly a further inversion takes place before the reset pulse is applied to the JK (7472).

Myocardial Unit (Fig. AIV,4)

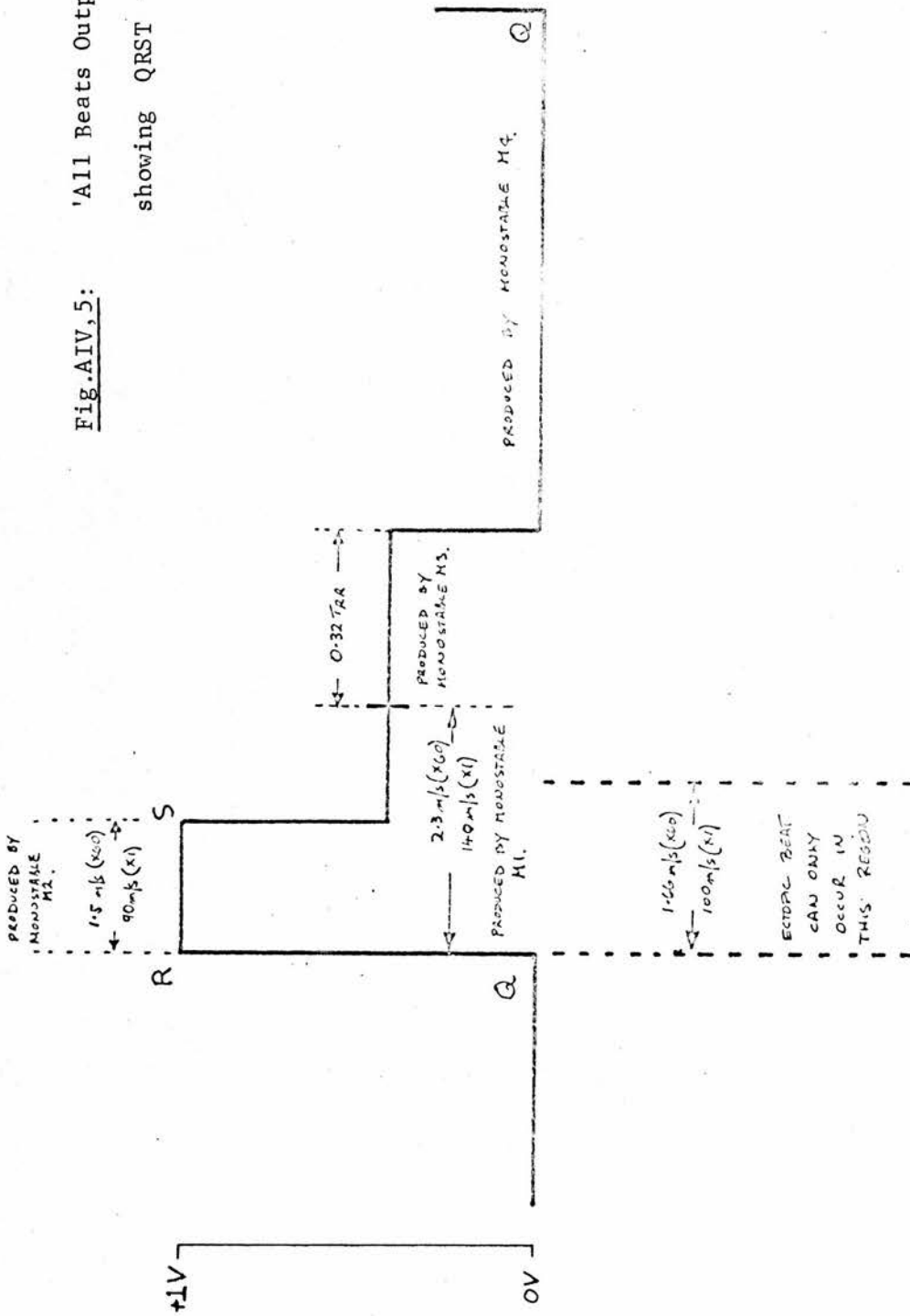
The propagated beat generator is similar but not identical to the sinus and ectopic pacemaker circuitry. The propagated beat generator does not have the facility for internal triggering. It is always triggered from either the sinus unit or the exit block counter. In addition, the propagated beat QT interval can be chosen to follow either of two laws:

i) $QT = 0.14 + 0.32T_{R-R}$ sec ; ii) $QT = 140\text{ms}$ (constant).

Switching between these two never had a profound effect on the simulator's behaviour.

A description of the aberrance monostable with its associated gates, invertors, and adder is given in the 'general description' of the simulator.

Fig. AIV.5: 'All Beats Output' showing QRST waveform.



Specification

Sinus Unit

Outputs:

+QRS O/P: +15V pk pulse 1.5ms wide (X60) = 90ms (X1)
-QRS O/P: -15V pk pulse 1.5ms wide (X60) = 90ms (X1)
QT O/P: + 1V pk Width dependent on QT law: = $0.14 + 0.32T_{R-R}$

Inputs:

External Trigger
Pull input

T_{R-R} Ranges:

Range 1: 250ms (X1) - 480ms (X1)
Range 2: 370ms (X1) - 1200ms (X1)

Ectopic Unit

Same specification as sinus pacemaker except that the QT_E interval (E_A) is constant at a value set by an external potentiometer: $240ms < QT_E < 600ms$.

E_4 has three ranges:

Range 1: 30ms (X1) - 100ms (X1)
Range 2: 140ms (X1) - 900ms (X1)
Range 3: 900ms (X1) - 5000ms (X1)

Exit Block Counter

The exit block counter provides a division in steps of unity from 1 to 31 by means of 5 two-position switches. The total division is obtained by adding the switched total together.

Propagated beat generator and associated circuitry

Outputs:

"All beats O/P". This output is essentially a QT formed from the sinus and ectopic pacemakers as described on pages 126/7.

Amplitude of the "all beats O/P": 1V pk/pk.

O/P ectopic QRS pulse corresponding to the ectopic beat:
15V pk.; 1.5ms (X60) = 90ms (X1) wide.

O/P sinus QRS pulse corresponding to the sinus beat:
15V pk.; 1.5ms (X60) = 90ms (X1) wide.

APPENDIX V The Electronic Analogues of Post
Cathodal Extension and Post
Anodal Shortening

The electronic simulation of post cathodal extension consists of the basic simulator (Appendix IV) and some additional circuitry. The additional circuitry produces a voltage waveform which, when applied to the "pull input" of the ectopic unit, results in 'post cathodal extension' of that unit.

The block diagram of, and voltage waveforms at various points in the additional circuitry is shown in Fig. AV,1. The circuit functions so as to produce an output level between 0V and -10V. The level is determined by the time interval between the ectopic pacemaker's QT and the start of a propagated sinus pulse responsible for post cathodal extension (i.e. the start of sinus initiated myocardial QT). The output level (negative) is made directly proportional to this time interval and is switched on at the moment of completion of the propagated sinus QRS pulse. When the output is applied to the pull input of the ectopic pacemaker the rate of recovery of monostable M_4 (Fig. AIV,2) is then altered in proportion to the time interval just mentioned, and this is in effect post cathodal extension.

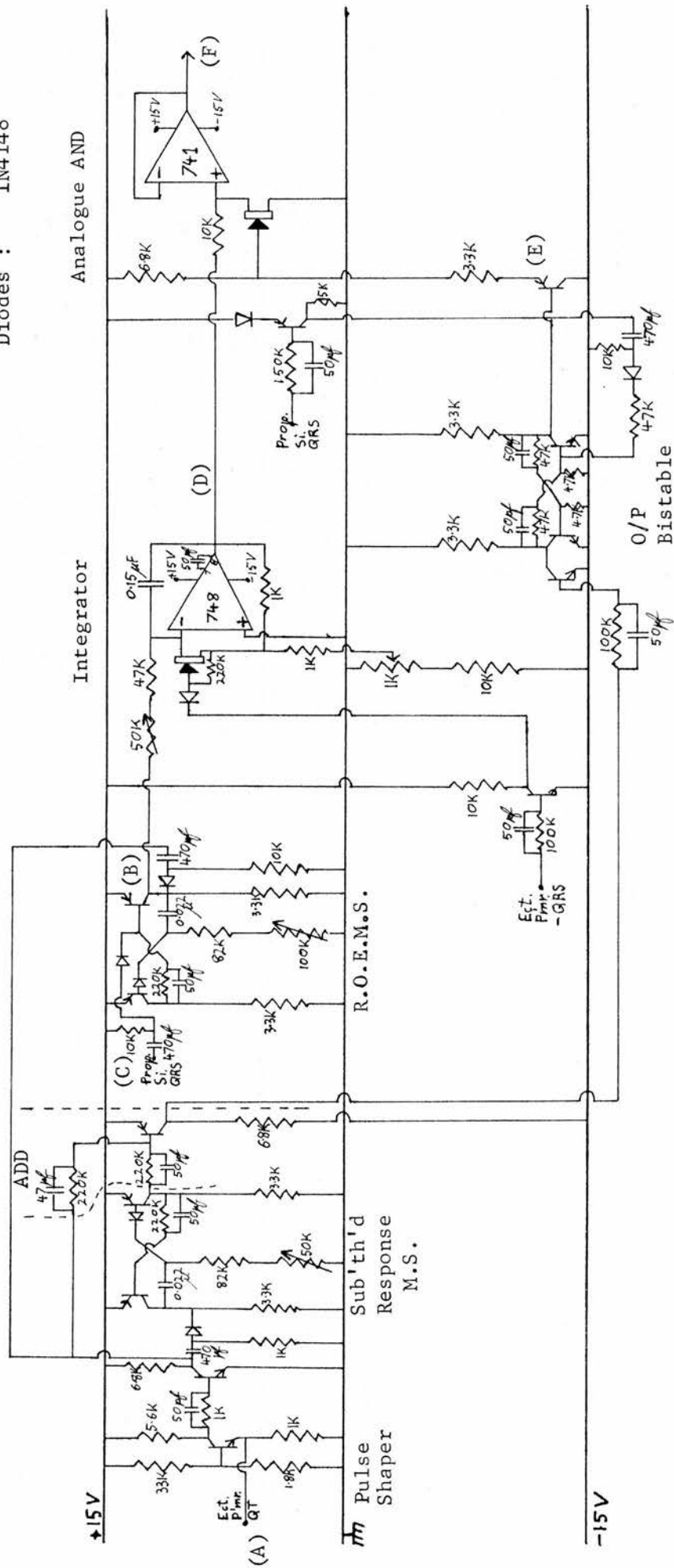
The sequence of events is as follows (Fig. AV,1). The integrator output is set to zero by the leading edge of ectopic pacemaker QT. Following this, the final falling edge of ectopic pacemaker QT triggers the 'recovery of excitability monostable' (R.O.E.M.S.), the output of which is applied to the integrator to produce a negative going ramp. The level attained by the ramp on completion of the R.O.E.M.S. pulse is held at the integrator output. However, the leading edge of the propagated sinus QRS pulse terminates the R.O.E.M.S. pulse (if not already completed) so that the level held at the integrator output is then proportional to the time interval 'end of ectopic pacemaker QT - start of propagated sinus QRS'. The "output bistable" determines when the integrator output is transmitted to the final output

Fig. AV.2:

Additional circuitry used to simulate Post Cathodal Extension.
 Post Anodal Shortening has a further inversion at the output.

Transistors: PNP BC213L
 NPN BC183L

Diodes : IN4148



of the analogue AND - via the bistable, pulse shaper and subthreshold monostable the AND is turned off at the start of ectopic QT, and held off until the trailing edge of the propagated sinus QRS pulse switches it on (via the bistable).

The full circuit diagram is shown in Fig. AV,2.

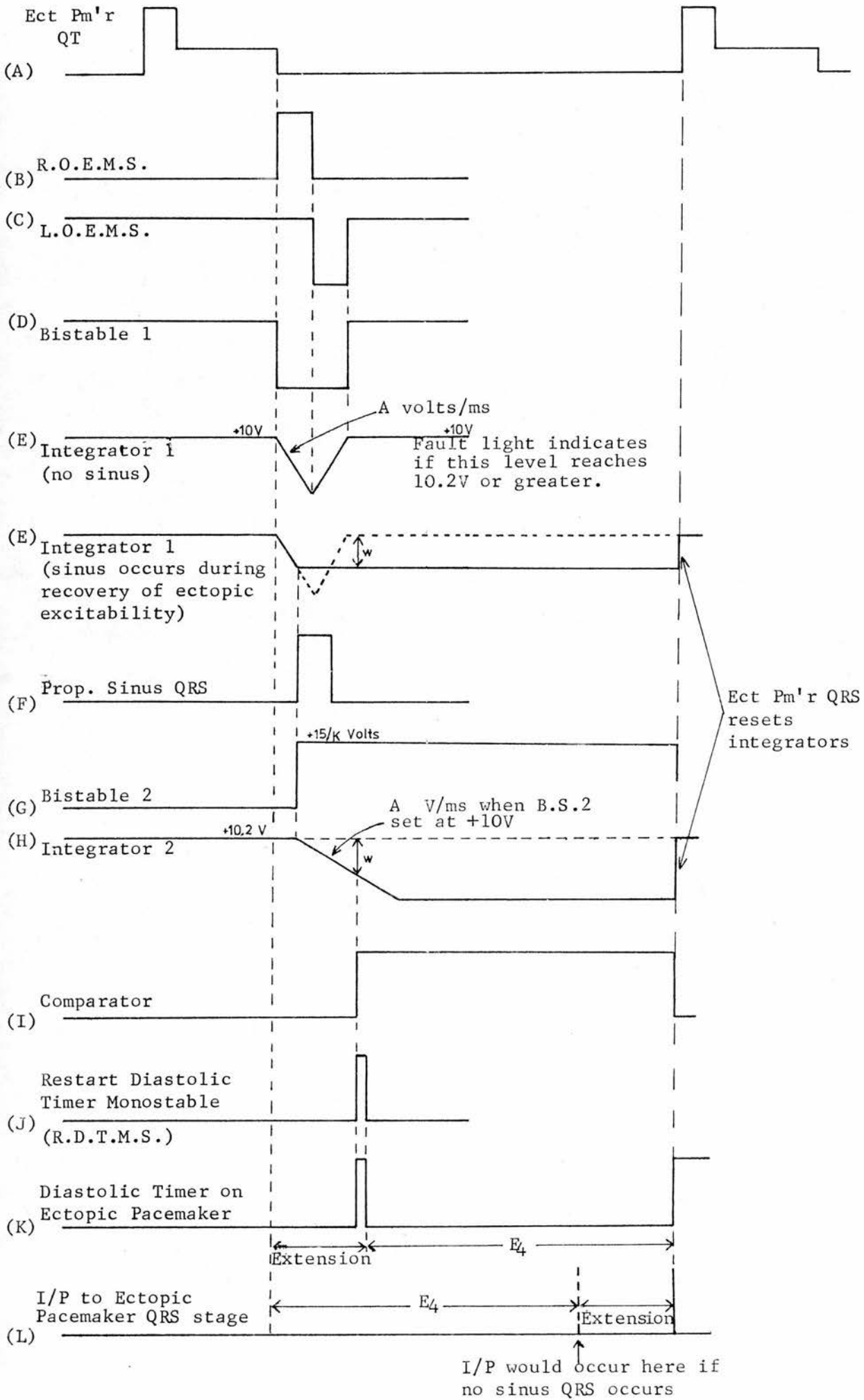
The strength of pulling is determined by the setting of the pull input potentiometer on the basic simulator (25K by M_4 in Fig. AIV,2).

Post anodal shortening uses the same circuitry with an additional analogue inversion.

All necessary specifications are given on the voltage waveforms of Fig. AV,1.

Fig.AVI,1:

Voltage waveforms for simulation of Action Potential Extension.



APPENDIX VI The Electronic Analogue of Action
Potential Extension

The simulation of action potential extension involves external additional triggering of part of the ectopic pacemaker unit on the basic simulator. The external triggering acts on the diastolic timer (i.e. monostable M_4 , Fig. AIV,2) in addition to the unit's own triggering of that monostable. The purpose of this is to extend the effective duration of E_A (i.e. the ectopic action potential) - this is followed by normal phase 4 depolarization. In other words, the beginning of E_4 (ectopic phase 4) is delayed by an amount equal to the extension of E_A . Most of the external circuitry used to simulate action potential extension is concerned with establishing the correct delay according to the timing of the propagated sinus QRS pulse in the ectopic cycle.

The block diagram, and voltage waveforms at various points in the additional circuitry are shown in Figs. AVI,1 and 2. The output of 'integrator 1' determines the excitability of the ectopic pacemaker - the nearer the output is to zero volts the greater is the excitability (Fig. AVI,2). The excitability at the moment of arrival of a propagated sinus QRS pulse determines the magnitude of the ensuing delay, after which the ectopic diastolic timer (M_4 , Fig. AIV,2) is re-triggered to initiate a full E_4 . As can be seen from Fig. AVI,2 (line 4), following an ectopic QT the excitability recovers to some maximum and then returns to nothing (+10 volts). A sinus QRS arriving after the completion of the loss of excitability has no effect on the ectopic pacemaker. A sinus QRS pulse which arrives while the ectopic is excitable causes re-triggering of the ectopic diastolic timer after a time interval proportional to the level of excitability. This last process is achieved by a second integrator (Fig. AVI,2, line 9) which begins to ramp down when the sinus QRS pulse arrives. A comparator detects when the two integrator outputs are equal and causes the ectopic diastolic timer to be triggered.

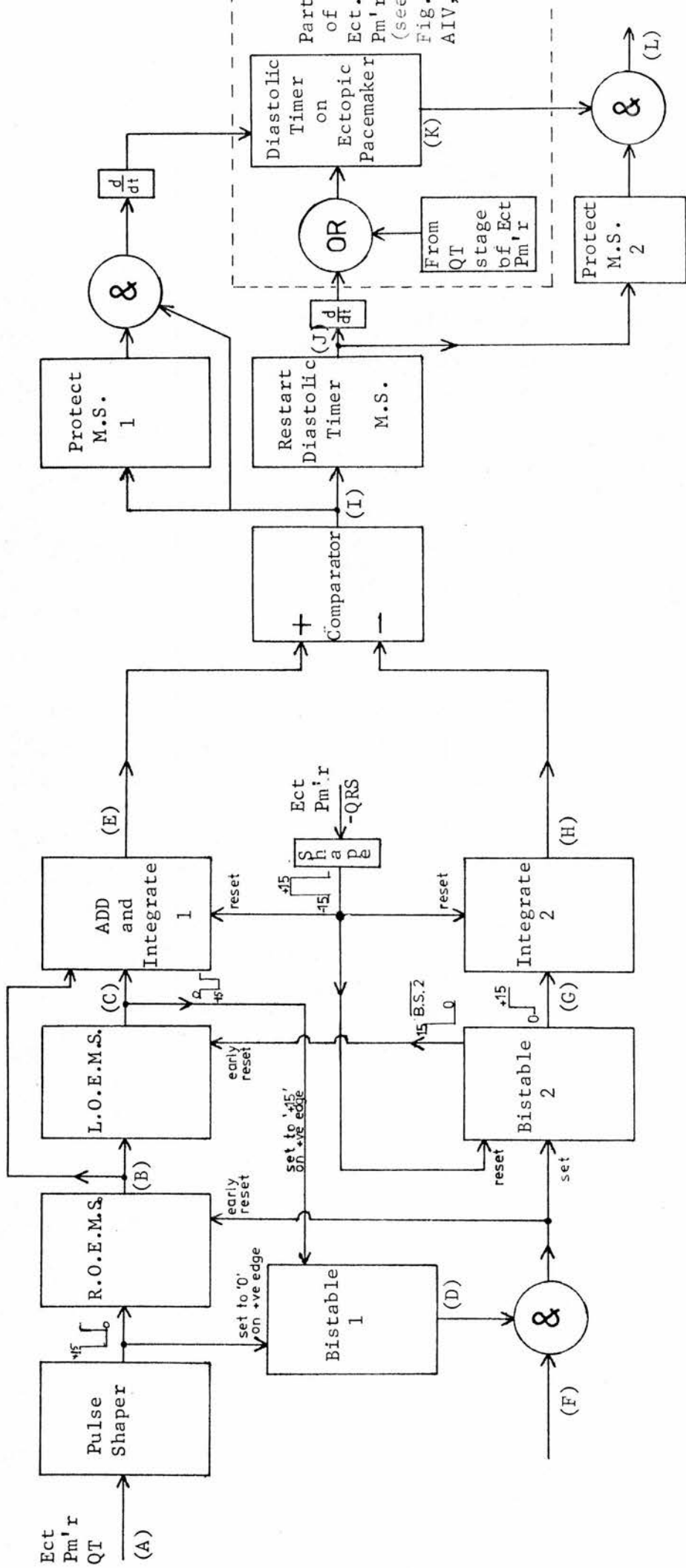


Fig. AIV, 2: Block diagram of the additional circuitry used to simulate Action Potential Extension.

The sequence of events is as follows. The last falling edge of ectopic pacemaker QT causes the recovery of excitability monostable (R.O.E.M.S.) to fire, and on completion of this pulse the loss of excitability monostable (L.O.E.M.S.) fires. While these monostables are active 'bistable 2' is switched "on" so that a sinus QRS pulse can in turn switch "on" 'bistable 1' via the AND gate shown (Fig. AVI,1). Outside of this time band sinus QRS pulses have no effect. The R.O.E. and L.O.E. pulses are integrated to give the excitability curve mentioned earlier (Fig. AVI,2, line 4). The level of excitability attained at the time of arrival of a sinus QRS pulse is held at the output of 'integrator 1'. 'Bistable 1' is also turned "on" by the sinus QRS pulse and this causes 'integrator 2' to ramp down. When this ramp reaches the level of excitability held at the output of 'integrator 1' (as detected by the comparator) the ectopic diastolic timer is triggered. Thus the total delay in the ectopic cycle consists of the time interval between the completion of ectopic QT and the start of sinus QRS, plus the time taken for the second ramp to attain the held excitability level. This latter interval represents the duration of the subthreshold response in the ectopic pacemaker fibre and is directly proportional to the level of excitability attained prior to the arrival of the sinus QRS pulse.

The last sections of the circuit (comparator onwards) ensure that no false triggering occurs. The full circuit diagram is shown in Fig. AVI,3.

The width of the R.O.E. and L.O.E. pulses are variable between 20ms and 200ms (X1) and the amplification of these are variable so that the output of 'integrator 1' always starts at +10 volts, reaches 0 volts and returns to +10 volts provided no sinus QRS pulse intervenes. The rate of the ramp output of 'integrator 2' is variable so that the maximum subthreshold response is selectable between 35ms and 400ms (X1).

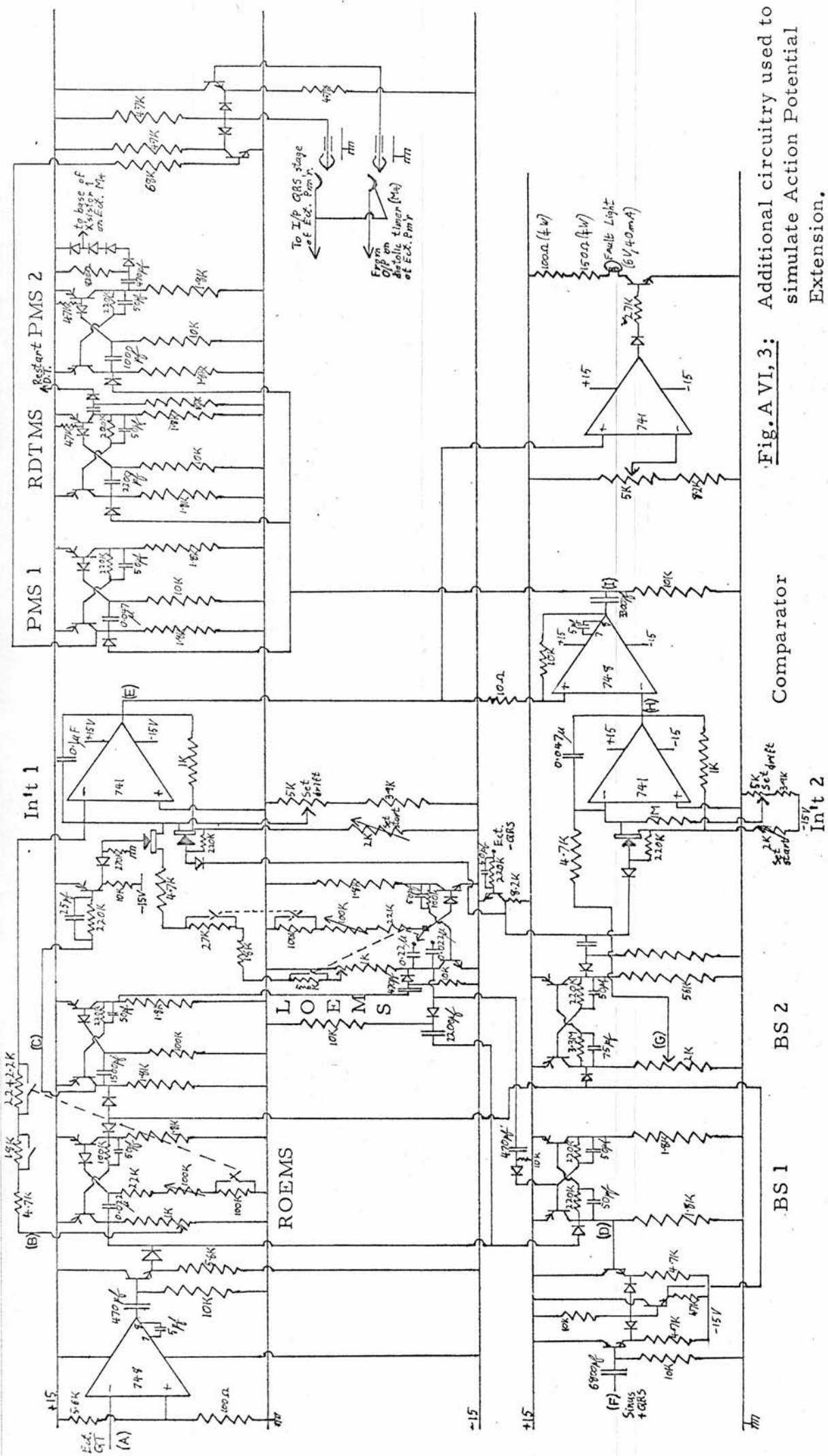


Fig. A VI, 3: Additional circuitry used to simulate Action Potential Extension.

Fig. AVII, 1: Phase 4 Cathodal Extension. To calculate T_2 from T_1 .

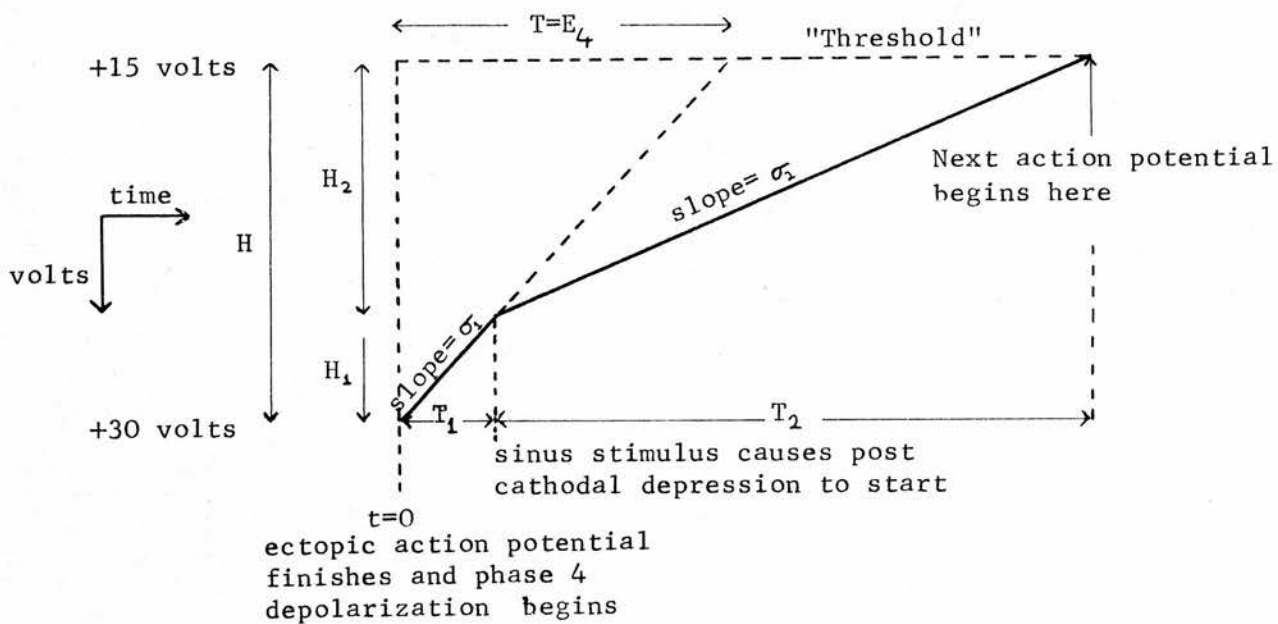
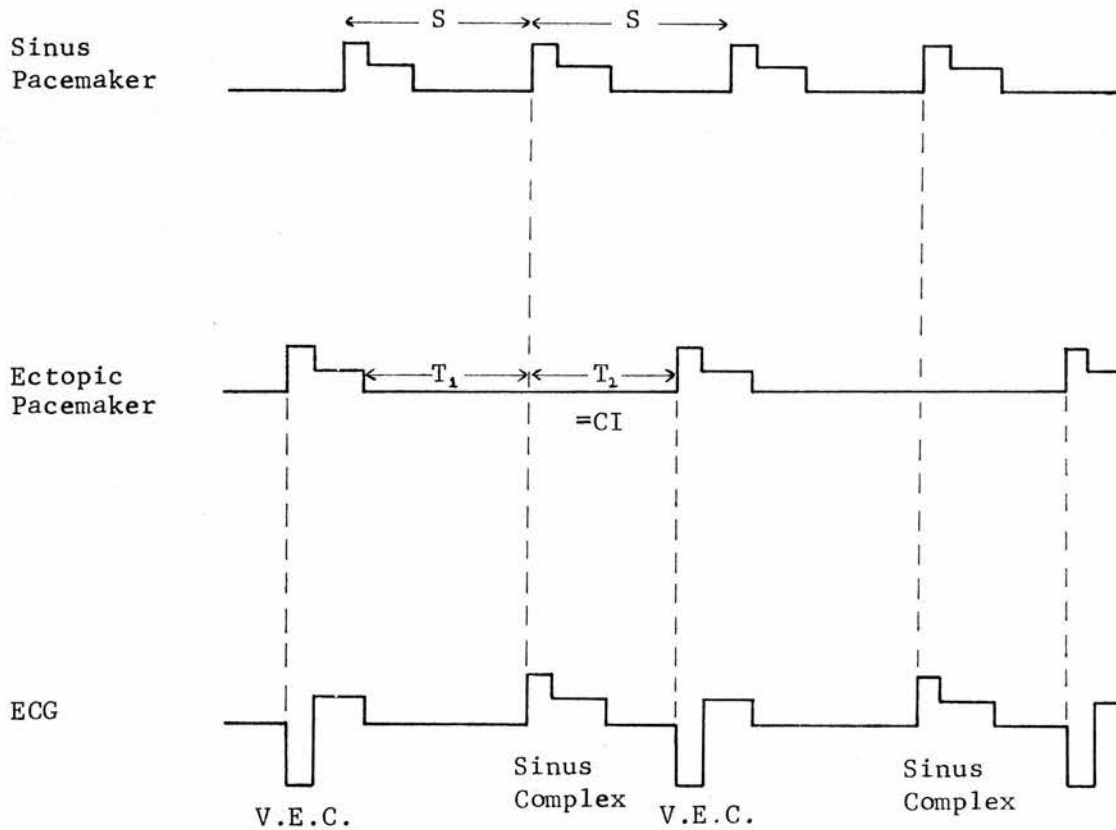


Fig. AVII, 2: Rigeminy for Phase 4 Cathodal Extension.



APPENDIX VII A Quantitative Check of the Static
Performance of the Electronic
Simulators for Phase 4 Cathodal
Extension and Action Potential
Extension

Phase 4 Cathodal Extension

Fig.A VII,1 depicts the voltage waveform that determines the length of ectopic phase 4 depolarization in the model. (Waveform taken at the collector of current controlling transistor in monostable M₄, Fig.A IV,2.) Normal depolarization begins at time t = 0 and continues for a time T₁. After this, the slope of depolarization changes from σ₁ to σ₂. The change in slope is proportional to the time interval T₁. Given the appropriate parameters, T₂ can be predicted from T₁. The relationship between T₂ and T₁ is required in order to predict the behaviour in the X-Y plot of static bigeminy.

For phase 4 cathodal extension the applied voltage, V, is proportional to T₁. We therefore put V = KT₁ volts, where K is a constant depending on the "pull input" setting. K is a measure of the effect of pulling.

Now

$$\begin{aligned} \sigma_2 &= \sigma_1 - \frac{V}{2RC \times 60 \times 1000} \text{ volts/ms} \\ &= \sigma_1 - \frac{KT_1}{2RC \times 60 \times 1000} \\ &= \sigma_1 - AT_1 \text{ volts/ms, say} \quad (1) \\ &= \frac{H}{E_4} - AT_1 \end{aligned}$$

K, and hence A, is measured by noting i) the attenuation at the pull input potentiometer to monostable M₄ (Fig.A IV,2); ii) the slope of the ramp that determines the size of the voltage applied to this input - this ramp is generated within the phase 4 cathodal extension circuitry (Appendix V).

To determine T₂, given T₁ (Fig.A VII,1):

$$T_2 = \frac{H_2}{\sigma_2}$$

Table A VII, 1: Four Cases of Static Bigeminy for Phase 4 Cathodal Extension

CONSTANTS MEASURED FROM MODEL	MEASURED				PREDICTED in X-Y plot
	from model		from X-Y plot		
	K volts/ms	A = K X 4.62 X 10 ⁻³ ms ⁻²	S ms	slope	
$E_A = 800\text{ms}$ $E_4 = 800\text{ms}$ $= \frac{H}{E_4}$ (Fig. A VII, 1) $= \frac{15}{800} \text{V/ms}$	$\frac{1}{260}$	1.78×10^{-5}	800	-0.73	-0.7
	$\frac{1}{200}$	2.31×10^{-5}	800	slope <0.01	-0.02
	$\frac{1}{160}$	2.89×10^{-5}	800	+0.42	+0.4
	$\frac{1}{120}$	3.80×10^{-5}	800	+0.75	+0.8

Substituting (1):

$$T_2 = \frac{H_2}{\sigma_1 - AT_1} \quad (2)$$

$$\begin{aligned} \text{Now } H_2 &= H - H_1 \\ &= \sigma_1 E_4 - \sigma_1 T_1 \\ &= \sigma_1 (T - T_1) \end{aligned}$$

substituting in (2):

$$T_2 = \frac{\sigma_1 (E_4 - T_1)}{\sigma_1 - AT_1}$$

$$\text{Rearranging: } T_1 = \frac{\sigma_1 (E_4 - T_2)}{\sigma_1 - AT_2} \quad (3)$$

Fig. A VII, 2 depicts bigeminy for phase 4 cathodal extension. CI = T₂, hence we require to know T₂.

$$2S = E_A + T_1 + T_2$$

Substituting (3):

$$2S = E_A + \frac{\sigma_1 (E_4 - T_2)}{\sigma_1 - AT_2} + T_2$$

$$\text{i.e. } AT_2^2 + A(E_A - 2S)T_2 + \sigma_1(2S - E) = 0$$

$$\text{where } E = E_A + E_4$$

$$\therefore \text{CI} = T_2 = \frac{-A(E_4 - 2S) \pm \sqrt{A^2(E_A - 2S)^2 - 4A\sigma_1(2S - E)}}{2A}$$

$$\therefore \frac{d(\text{CI})}{dS} = 1 \pm \frac{A(2S - E_A) - 2\sigma_1}{\sqrt{A^2(2S - E_A)^2 - 4A\sigma_1(2S - E)}} \quad (4)$$

$$\text{where } A = \frac{K}{2RC \times 60 \times 1000} = K \times 4.62 \times 10^{-3} \text{Vms}^{-2}$$

The predicted and measured slopes for four cases of bigeminy with different pulling strengths (i.e. K) are presented in Table A VII, 1. Predicted slopes are only quoted to one significant figure since the effect of errors in the estimates of the parameters in equation (4) do not justify greater accuracy. The agreement between measured and predicted slopes is good.

Fig.AVII,3: Definition of ectopic excitability (X) for Action Potential Extension.

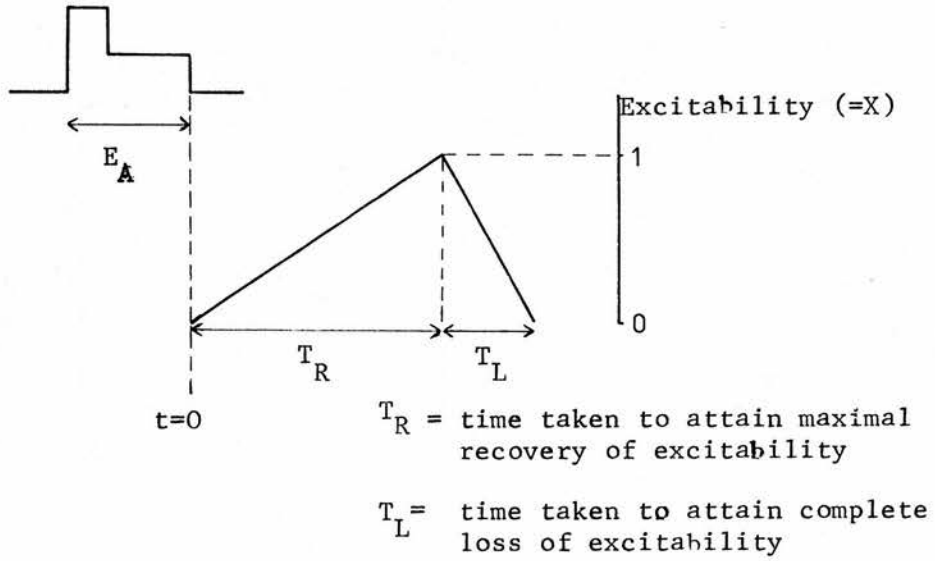
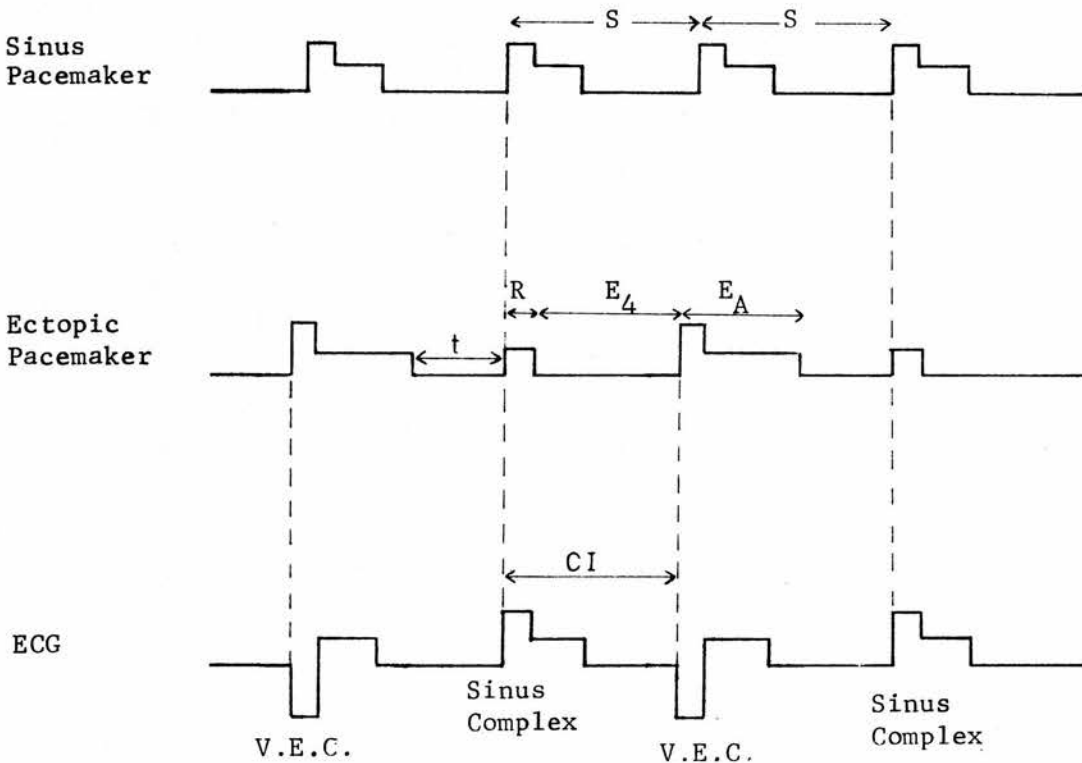


Fig.AVII,4: Bigeminy for Action Potential Extension



Action Potential Extension

The variation of ectopic excitability with time is depicted in Fig.A VII,3. If the sinus stimulus arrives when the excitability (X) is greater than zero, a response of duration Rms (X1) is initiated, where $R = MX$. Clearly when $X = 1$ the response is maximum (M) and thus M is a measure of the pulling strength. From Fig.A VII,3 it is seen that:

$$X = \frac{t}{T_R} \quad 0 < t < T_R \quad (5)$$

$$X = 1 - \frac{t - T_R}{T_L} \quad T_R < t < T_R + T_L \quad (6)$$

Bigeminy is depicted in Fig.A VII,4. Over every pair of sinus periods the following relation holds:

$$2S = R + E_4 + E_A + t \quad (7)$$

$$\text{Now } CI = R + E_4 \quad (8)$$

∴ we require R from equation (5).

There are two cases to be considered:

$$1^{\text{st}} \text{ case: } 0 < t < T_R$$

$$\text{from equation (5): } R = MX = K \frac{t}{T_R}$$

$$\therefore t = \frac{RT_R}{M}$$

Substituting for t in equation (7):

$$2S = R + E_4 + E_A + \frac{RT_R}{M}$$

$$\text{i.e. } R = \frac{2S - E_4 - E_A}{1 + T_R/M}$$

∴ from equation (8):

$$CI = \frac{2S - E_4 - E_A}{1 + T_R/M}$$

$$\therefore \frac{d(CI)}{dS} = \frac{2K}{M + T_R} \quad (9)$$

Table A VII, 2: Three Cases of Static Bigeminy Simulated on the Model of Action Potential Extension

MEASURED											PREDICTED	
from Model				from X-Y Plot							in X-Y Plot	
M ms	T _L ms	T _R ms	E ₄ ms	E _A ms	S ms	CI ms	slope	CI ms	slope	CI ms	slope	
50	500	25	800	500	900	785	-0.22	800	-0.22	800	-0.22	
50	200	25	600	500	650	630	-0.63	600	-0.63	600	-0.67	
100	200	25	600	500	670	630	-1.9	600	-1.9	600	-2.0	

2nd case: $T_R < t < T_R + T_L$

from equation (6): $R = MX = K \left(1 - \frac{t - T_R}{T_L} \right)$

i.e. $t = \left(1 - \frac{R}{M} \right) T_L + T_R$

substituting for t in equation (7):

$$2S = R + E_4 + E_A + \left(1 - \frac{R}{M} \right) T_L + T_R$$

i.e. $R = \frac{2S - E_4 - E_A - T_L - T_R}{1 - \frac{T_L}{M}}$

∴ from equation (8):

$$CI = \frac{2S - E_4 - E_A - T_L - T_R}{1 - \frac{T_L}{M}} \quad (10)$$

$$\therefore \frac{d(CI)}{dS} = \frac{2K}{M - T_L} \quad (11)$$

Table A VII,2 contains the results of three cases of simulated bigeminy. The model's performance agrees well with that predicted by equations (10) and (11).

REFERENCES

1. Anderson, G. J. and Bailey, J. C. (1973).
Conduction delay and block within the peripheral Purkinje system. In *Cardiac Arrhythmias*, 203-215. Ed. by Dreifus, L. S. and Likoff, W. Grune and Stratton, New York and London.
2. Barr, L. and Berger, W. (1964).
The role of current flow in the propagation of cardiac muscle action potentials.
Pflueger Arch. Ges. Physiol. 279, 192-194.
3. Bhéreur, P., Roberge, F. A. and Nadeau, R. A. (1971).
See also ref. no. 53.
A simulation unit for cardiac arrhythmias.
Med. and Biol. Eng. 9, 13-21.
4. Bigger, J. T. (1973).
Electrical properties of cardiac muscle and possible causes of cardiac arrhythmias. In *Cardiac Arrhythmias*, 13-34. Ed. by Dreifus, L. S. and Likoff, W. Grune and Stratton, New York and London.
5. Bolzer, E. (1942-43).
The initiation of impulses in cardiac muscle.
Am. J. Physiol. 138, 273-282.
6. Brooks, C. McC., Orias, O., Gilbert, J. L., Siebens, A. A., Hoffman, B. F. and Suckling, E. E. (1951).
Auricular fibrillation: relationship of 'vulnerable period' to 'dip' phenomenon of auricular excitability curve.
Am. J. Physiol. 164, 301-306.
7. Burchell, H. B. (1963).
Analogy of electronic pacemaker and ventricular parasystole with observations on refractory period, supernormal phase and synchronization.
Cir. 27, 878-889.
8. Castellanos, A., Lenberg, L., Johnson, D. and Berkovits, B. V. (1966).
Wedensky effect in the human heart.
Brit. Heart J. 28, 276-283.
9. Chung, E. K. Y. (1968).
Parasystole.
Progr. Card. Dis. 11, 64-81.
10. Cranefield, P. F. and Hoffman, B. F. (1958).
Propagated repolarization in heart muscle.
J. Gen. Physiol. 41, 633-649.

11. Cranefield, P. F., Klein, H. O. and Hoffman, B. F. (1971).
Conduction of the cardiac impulse I. Delay, block, and one-way block in depressed Purkinje fibres.
Cir. Res. 28, 199-219.
12. Cranefield, P. F. and Hoffman, B. F. (1971).
Conduction of the cardiac impulse II. Summation and inhibition.
Cir. Res. 28, 220-233.
13. Documenta Geigy Scientific Tables (7th edition) (1970).
Ed. by Diem, K. and Lentner, C.
J. R. Geigy S. A., Basle, Switzerland.
14. Ettinger, P. (1965).
Synchronization during electrical pacing.
Am. Heart J. 70, 110-114.
15. Fisch, C. and Knoebel, S. B. (1968).
"Wedensky facilitation" in the human heart. Report of a probable case.
Am. Heart J. 76, 90.
16. Fisch, C., Greenspan, K. and Anderson, G. J. (1971).
Exit block.
Am. J. Cardiol. 28, 402-405.
17. Han, J. (1971).
The concepts of re-entrant activity responsible for ectopic rhythms.
Am. J. Cardiol. 28, 253-262.
18. Hernandez-Pieretti, O., Morales-Rocha, J. and Barcelo, J. E. (1969).
Supernormal phase of conduction in human heart demonstrated by subthreshold pacemakers.
Brit. Heart J. 31, 553-558.
19. Hill, I. G. and Cameron, J. D. S. (1936).
A case of parasystole showing simple interference dissociation.
Am. Heart J. 11, 140-162.
20. Hodgkin, A. L. (1937).
Evidence for electrical transmission in nerve (Parts I and II).
J. Physiol. 90, 183-232.
22. Hoff, H. E. and Nahum, L. H. (1938).
The supernormal period in the mammalian ventricle.
Am. J. Physiol. 124, 591-595.
23. Hoffman, B. F., Kao, C. Y. and Suckling, E. E. (1957).
Refractoriness in cardiac muscle.
Am. J. Physiol. 190, 473-482.

24. Hoffman, B. F., De Carvalho, A. P., Mello, W. C. and Cranefield, P. F. (1959).
Electrical activity of single fibres of the A-V node.
Cir. Res. 7, 11-18.
25. Hoffman, B. F. (1966).
The genesis of cardiac arrhythmias.
Progr. Cardiovasc. Dis. 8, 319-329.
26. Julian, D. G., Valentine, P. A. and Miller, G. G. (1964).
Disturbances of rate, rhythm and conduction in acute myocardial infarction.
Am. J. Med. 37, 915-927.
27. Kao, C. Y. and Hoffman, B. F. (1958).
Graded and decremental response in heart muscle fibres.
Am. J. Physiol. 194, 187-196.
28. Langendorf, R., Pick, A. and Winternitz, M. (1955).
Mechanisms of intermittent ventricular bigeminy
I. Appearance of ectopic beats dependent on length of the ventricular cycle, the "rule of bigeminy".
Cir. 11, 422-430.
29. Langendorf, R. and Pick, A. (1955).
Mechanisms of intermittent ventricular bigeminy
II. Parasystole, and parasystole or re-entry with conduction disturbance.
Cir. 11, 431-439.
30. Levy, M. N. and Edelstein, J. (1970).
The mechanism of synchronization in isorhythmic A-V dissociation II. Clinical studies.
Cir. 42, 689-699.
31. Levy, M. N., Lee, M. H. and Zieske, H. (1972).
A feedback mechanism responsible for fixed coupling in parasystole.
Cir. Res. 31, 846-856.
32. Lown, B., Bey, S. K., Perlroth, M. and Abe, T. (1963).
Comparative studies of ventricular vulnerability to fibrillation.
J. Clin. Invest. 42, 953.
33. Lown, B. (1969).
The philosophy of coronary care.
Archiv. Für Klinische Medizin. 216(3), 201-241.
34. Mack, I. and Langendorf, R. (1950).
Factors influencing the time of appearance of premature systoles (including a demonstration of cases with ventricular premature systoles due to re-entry but exhibiting variable coupling).
Cir. 1, 910-921.

35. Marriott, H. J. L. (1956).
Atrioventricular synchronization and accrochage.
Cir. 14, 38-43.
36. Marriott, H. J. L. (1957).
Interference between atria and ventricles during
interference-dissociation and complete A-V block.
Am. Heart J. 53, 884-889.
37. Meltzer, L. E. and Kitchell, J. B. (1966).
The incidence of arrhythmias associated with acute
myocardial infarction.
Prog. Cardiovasc. Dis. 9, 50-63.
38. Mendez, C., Gruhzt, C. C. and Moe, G. K. (1956).
Influence of cycle length upon refractory period of
auricles, ventricles and A-V node in the dog.
Am. J. Physiol. 184, 287-295.
39. Mendez, C., Mueller, W. J., Meredith, J. and Moe, G. K.
(1969).
Interaction of transmembrane potentials in canine Purkinje
fibres and at Purkinje fibre muscle junctions.
Cir. Res. 24, 361-372.
40. Mines, G. R. (1913).
On dynamic equilibrium in the heart.
J. Physiol. 46, 349.
41. Mogensen, L. (1970).
Ventricular tachyarrhythmias and lignocain prophylaxis
in acute myocardial infarction.
Acta Medica Scandinavica (supplement 513).
42. Mouloupoulos, S. D., Kardaras, N. and Sideris, D. A. (1965).
Stimulus-response relationship in dog ventricle in vivo.
Am. J. Physiol. 208, 154-157.
43. Mouloupoulos, S. D. and Sideris, D. A. (1967).
Time relation between two pacemakers in atrial parasystole.
Brit. Heart J. 29, 758-760.
44. Mueller, P. and Baron, B. (1953).
Clinical studies on parasystole.
Am. Heart J. 45, 441-447.
45. Nadeau, R.A., Roberge, F. A. and Bhéreur, P. (1969).
The mechanism of the Wenkebach Phenomenon.
Israel J. Med. Sci. 5, 814-818.
46. Narula, O. S. (1973).
Conduction disorder in the AV transmission system. In
Cardiac Arrhythmias, 259-291. Ed. by Dreifus, L. S. and
Likoff, W. Grune and Stratton, New York and London.

47. Neilson, J. M. M. (1971).
Computers for analysis and control in medical and biological research.
I.E.E. Conference Publication No. 79, 151.
48. Neilson, J. M. M. and Vellani, C. W. (1972).
Computer detection and analysis of ventricular ectopic rhythms. In *Quantitation in Cardiology*, 117-125. Ed. by Snellen, H. A., Hemker, H. C., Hugenholtz, P. G. and Van Bommel, J. H. Leiden University Press.
49. Palmer, D. G. (1962).
Interruption of T waves by premature QRS complexes and the relationship of this phenomenon to ventricular fibrillation.
Am. Heart J. 63, 367-373.
50. Pick, A. (1953).
Parasyctole.
Cir. 8, 243-252.
51. Roberge, F. A. (1969).
Simulation of the phenomenon of concealed conduction.
Computers and Biomedical Research. 2, 362-372.
52. Roberge, F. A. and Nadeau, R. A. (1969).
The nature of Wenkebach cycles.
Can. J. Physiol. and Pharmacol. 47, 695-704.
53. Roberge, F. A., Bhéreur, P. and Nadeau, R. A. (1971).
See also ref. no. 3.
A cardiac pacemaker model.
Med. and Biol. Eng. 9, 3-12.
54. Rosenbaum, M. B. and Lipeschkin, E. (1955).
The effect of ventricular systole on auricular rhythm in atrioventricular block.
Cir. 11, 240-261.
55. Rosenbleuth, A. (1958).
Mechanism of the Wenkebach-Luciani cycles.
Am. J. Physiol. 194(3), 491-494.
56. Schamroth, L. (1962).
Ventricular parasystole with slow manifest ectopic discharge.
Brit. Heart J. 24, 731-737.
57. Schamroth, L. and Marriott, H. J. L. (1963).
Concealed ventricular extrasystoles.
Cir. 27, 1043-1049.
58. Schamroth, L. (1965).
Concealed extrasystoles and the rule of bigeminy.
Cardiologia 46, 51-58.

59. Schamroth, L. (1965).
Genesis and evolution of ectopic ventricular rhythm.
Brit. Heart J. 28, 244-257.
60. Schamroth, L. and Dolara, A. (1967).
Paroxysmal ventricular tachycardia with rate dependent
coupling intervals.
Cir. 36, 255-260.
61. Schamroth, L. (1971).
The Disorders of Cardiac Rhythm.
Blackwell, Oxford and Edinburgh.
62. Scherf, D. and Boyd, L. J. (1950).
Three unusual cases of parasystole.
Am. Heart J. 39, 650-663.
63. Scherf, D., Schott, A., Reid, E. C. and Chamsai, D. G.
(1957).
Intermittent parasystole.
Cardiologia 30, 217-228.
64. Scherf, D. and Bornemann, C. (1961).
Parasystole with a rapid ventricular centre.
Am. Heart J. 62, 320-331.
65. Scherf, D., Blumenfeld, S. and Yildiz, M. (1962).
Extrasystoles and parasystole.
Am. Heart J. 64, 357-363.
66. Scherf, D., Schott, A. (1973).
Extrasystoles and Allied Arrhythmias (2nd edition).
Heinemann, London.
67. Schubert, A. F., Marriott, H. J. L. and Gorten, R. J.
(1958).
Isorhythmic dissociation. A-V dissociation with
synchronization.
Am. J. Med. 24, 209.
68. Segers, M. (1946).
Les phénomènes de synchronisation au niveau du coeur.
Arch. Intern. Physiol. 54, 87-108.
69. Segers, M., Lequime, J. and Denolin, H. (1947).
Synchronization of auricular and ventricular beats during
complete heart block.
Am. Heart J. 33, 685-691.
70. Sideris, D. A. and Mouloupoulos, S. D. (1973).
Time relationship between two pacemakers in nodal
parasystole.
J. Electrocardiology 6(2), 165-169.
71. Singer, D. H., Lazzara, R. and Hoffman, B. F. (1967).
Interrelationships between automaticity and conduction
in Purkinje fibers.
Cir. Res. 21, 537-558.

72. Smirk, F. H. (1949).
R waves interrupting T waves.
Brit. Heart J. 11, 23-36.
73. Smirk, F. H. and Palmer, D. G. (1960).
A myocardial syndrome with particular reference to the
occurrence of sudden death and of premature systoles
interrupting antecedent T waves.
Am. J. Cardiol. 6, 620-629.
74. Smirk, F. H. and Ng, J. (1967).
Interruption of T waves by electrocardiographic complexes
starging before the apex of positive or the trough of
negative T waves.
New Zealand Med. J. 66, 787-794.
75. Soloff, L. A. (1973).
Parasystole. In Cardiac Arrhythmias, 409-415. Ed. by
Dreifus, L. S. and Likoff, W. Grune and Stratton, New
York and London.
76. Sperelakis, N. and Tarr, M. (1965).
Weak electrotonic interaction between neighbouring
visceral smooth muscle cells.
Am. J. Physiol. 208(4), 737-747.
77. Stock, J. P. P. (1970).
Diagnosis and treatment of Cardiac Arrhythmias (2nd
edition).
Butterworths, London.
78. Surawicz, B. and MacDonald, M. G. (1964).
Ventricular ectopic beats with fixed and variable
coupling. (Incidence, clinical significance and
factors influencing the coupling interval.)
Am. J. Cardiol. 13, 198-208.
79. Van Dam, R. T., Moore, E. N. and Hoffman, B. F. (1963).
Initiation and conduction of impulses in partially
depolarized cardiac fibres.
Am. J. Physiol. 204, 1133-1144.
80. Van Der Pol, B. and Van Der Mark, J. (1929).
The heartbeat considered as a relaxation oscillation
and an electrical model of the heart.
Arch. néerl Physiol. 14, 418-443.
81. Vellani, C. W. (1972).
Mechanisms of Ventricular Ectopic Rhythms in Myocardial
Infarction.
M.D. Thesis, University of Wales.
82. Wallace, A. G., Mignone, R. J. and Durham, N. C. (1966).
Physiologic evidence concerning the re-entry hypothesis
for ectopic beats.
Am. Heart J. 72, 60-70.

83. Watanabe, Y. and Dreifus, L. S. (1968).
Newer concepts in the genesis of cardiac arrhythmias.
Am. Heart J. 76, 114-135.
84. Watanabe, Y. (1971).
Reassessment of Parasystole.
Am. Heart J. 81, 451-466.
85. Weidmann, S. (1951).
Effect of current flow on the membrane potential of
cardiac muscle.
J. Physiol. 115, 227-236.
86. Weidmann, S. (1955).
The effect of the cardiac membrane potential on the
rapid availability of the sodium carrying system.
J. Physiol. 127, 213-224.
87. Weidmann, S. (1955).
Effects of calcium ions and local anaesthetics on
electrical properties of Purkinje fibres.
J. Physiol. 129, 568-582.
88. Wennemark, J.R., Ruesta, V. J. and Brody, D. A. (1968).
Microelectrode Study of Delayed Conduction in the canine
Right Bundle Branch.
Cir. Res. 23, 753-769.
89. Weyl, H. (1916).
Math. Annaler, 77, 313-352.
90. Bailey, N. T. J. (1959).
Statistical Methods in Biology.
The English Universities Press, London.
91. Tocher, K. D. (1963).
The Art of Simulation, 10-13.
The English Universities Press, London.